UNIVERSITEIT VAN PRETORIA
UNIVERSITY OF PRETORIA
YUNIBESITHI YA PRETORIA

Epigenetic repression of gene expression controls the initial phases of gametocytogenesis in the malaria parasite, *Plasmodium falciparum*

by

Jessica Connacher

Submitted in partial fulfilment of the requirements for the degree

Philosophiae Doctor in Biochemistry

In the Faculty of Natural and Agricultural Sciences

Department of Biochemistry

University of Pretoria

August 2021

UNIVERSITEIT VAN PRETORIA
UNIVERSITY OF PRETORIA
YUNIBESITHI YA PRETORIA

I, Jessica Connacher, declare that the thesis, which I hereby submit for the degree *Philosophiae Doctor* in the Department of Biochemistry, Genetics and Microbiology at the University of Pretoria, is my own work and has not previously been submitted by me for a degree at this or any other tertiary institution.

Signature: ……

Date: 31 August 2021……..

PLAGIARISM DECLARATION

UNIVERSITY OF PRETORIA

FACULTY OF NATURAL AND AGRICULTURAL SCIENCES

DEPARTMENT OF BIOCHEMISTRY, GENETICS AND MICROBIOLOGY

Full names of student: Jessica Connacher

Student number: 11159325

Declaration:

1. I understand what plagiarism entails and am aware of the University's policy in this regard.

2. I declare that this thesis is my own, original work. Where someone else's work was used (whether from a printed source, the internet or any other source due acknowledgement was given and reference was made according to departmental requirements.

3. I did not make use of another student's previous work and submit it as my own.

4. I did not allow and will not allow anyone to copy my work with the intention of presenting it as his or her own work.

Signature: ……

Date: 31 August 2021……..

Acknowledgements

I would like to express my utmost gratitude to each mentor, colleague, friend and family member who has supported me during the completion of this degree. I would like to acknowledge and thank my supervisor, Prof. Lyn-Marié Birkholtz for providing me with funding, opportunities to perform and present research overseas and the consistent guidance and mentorship which were integral for the completion of this thesis. I would like to thank Prof. Manuel Llinás and Gaby Josling for hosting me at Pennsylvania State University and providing me with valuable skills that were required for this project. I would also like to thank my parents, Jeff and Trudi Connacher for their unwavering support and inspiration that have been instrumental in the achievement of my goals. To my other family members and friends, specifically my husband, Alex Nepomuceno and Janie Duvenhage, thank you for the support and being there for me through all the high and low moments throughout my studies.

Summary

The renewed focus on global malaria eradication necessitates the discovery and development of novel strategies to block the transmission of the *Plasmodium* parasites that remain a burden to the health and socio-economic advancement of most developing nations to this day. A comprehensive understanding of the processes that drive the development of the transmissible gametocyte stages of the malaria parasite and the regulation thereof, is foundational for the effective development of these strategies. The tight modulation of gene expression that directs asexual parasite and gametocyte stage transitions throughout the *P. falciparum* life cycle has been extensively documented. However, the vast majority of the mechanisms responsible for this regulation, particularly for the gametocyte stage transitions, remain unknown. The contribution of epigenetic mechanisms to transcriptional regulation in asexual parasites has also been well studied. While unique histone post-translational modification landscapes have been associated with each asexual and sexual stage, the functional relevance of histone modifications for gametocyte stage transitions remained to elucidated.

In this study, the roles of H3K27me2&3 and H3K36me2&3 during early and intermediate gametocyte development were examined. As H3K27me2&3 and H3K36me2&3 peak in abundance and are present almost exclusively in the stage II gametocytes, we hypothesised that these histone modifications are crucially involved in the transcriptional reprogramming associated with the transition from early gametocyte differentiation (stage I) to intermediate development (stage III). To test this hypothesis, we employed chromatin immunoprecipitation followed by high throughput sequencing, histone methylation profiling, transcriptional fingerprint analysis of epigenetic inhibitor perturbations and molecular docking strategies. Ultimately, the data generated from these approaches and conclusions drawn make substantial contributions to the current body of knowledge regarding the epigenetic regulation in malaria parasites.

More specifically, this study advances the understanding and provides novel insights into the regulatory role of histone methylation in gametocyte differentiation and development. Firstly,

we provide comprehensive genome-wide maps of H3K27me2&3 and H3K36me2&3 during early and intermediate gametocyte development. Next, we show that these histone modifications are independently involved in stage II gametocyte-specific transcriptional regulation with key repressive roles deconvoluted for each. The independent enrichment and repression of asexual stage-specific genes, regulators of commitment and chromatin modifying enzymes demonstrates that as in other eukaryotes, H3K27me2&3 and H3K36me2&3 not only silence irrelevant genes directly but also reinforce this repression by modulating higher order epigenetic and transcriptional regulators. Lastly, the transcriptional fingerprints of histone methyltransferase and demethylase inhibition generated in this study illustrate the importance of epigenetic mechanisms for gametocyte development, link the activity and potency of these inhibitors with the disruption of normal histone modification patterns and identify candidate enzymes that may be responsible for the stage II gametocyte-specific abundance of H3K27me2&3 and H3K36me2&3.

Ultimately, this thesis presents the first description of the roles of histone modifications and importance of epigenetic regulation as a whole for the differentiation and development of the transmissible stages of the *P. falciparum* parasite.

Table of Contents

List of Figures

Chapter 1

Chapter 2

List of Tables

.

Abbreviations

ACT	Artemisinin combination therapy
APAD	3-acetyl pyridine adenine dinucleotide
ApiAP2	Apicomplexan-specific Apetala2
asRNA	Antisense RNA
BCA	Bicinchoninic acid
BDP	Bromodomain-containing protein
CBX	Chromo-box
CDR	Coding regions
ChIP-seq	Chromatin immunoprecipitation followed by high throughput sequencing
DDT	Dichlorodiphenyltrichloroethane
DE	Differentially expressed
DMSO	dimethyl sulfoxide
DOZI-CITH	DDX-6 class DEAD box RNA helicase and Sm-like factor homolog of CAR-I and Trailer Hitch
ESC	Embryonic stem cell
EZH2	Enhancer of Zeste homolog 2
GDV1	Gametocyte development protein 1
GEXP	Gametocyte exported proteins
GMQE	Global mean quality estimate
HAT	Histone acetyltransferase
HDAC	Histone deacetylase
HDM	Histone demethylase
HDMi	Histone demethylase inhibitor
HMGB	High mobility group B
HMT	Histone methyltransferase
HMTi	Histone methyltransferase inhibitor
HP1	Heterochromatin protein 1
HRP	Horseradish peroxidase
IDC	Intraerythrocytic developmental cycle
IMC	Inner membrane complex
IP	Immunoprecipitated
IRS	Indoor residual spraying
IVM	Integrated vector management
JMJC	Jumonji-C domain-containing
LSD1	Lysine-specific demethylase 1
LysoPC	Lysophosphatidylcholine
mRNP	mRNA-ribonucleoproteins
MSL	Male-specific lethal
myb	myeloblastosis
NAG	N-acetylglucosamine

NCC	Next-cycle conversion
ncRNA	non-coding RNA
NDRs	Nucleosome-depleted regions
PcG	Polycomb group of complexes
PHD	Plant homeodomain
pLDH	Parasite lactate dehydrogenase
PRC2	Polycomb repressive complex 2
PTMs	Post-translational modifications
PUF	Pumilo family proteins
SAH	S-adenosylhomocysteine
SAM	S-adenosylmethionine
SCC	Same-cycle conversion
SET	(Su(var)3-9, Enhancer of Zeste and Trithorax)
SUMO	Small ubiquitin-like modifier
TARE	Telomere-associated long non-coding RNA
TCP	Target candidate profile
TF	Transcription factor
TPP	Target product profile
TSS	Transcription start sites
UTX	Ubiquitously Transcribed tetratricopeptide repeat, X chromosome
WHO	World Health Organisation

Chapter 1

Introduction

1.1 The burden of malaria and the successes and challenges of global eradication

Malaria persists as a serious threat to human health and socio-economic advancement in most of the developing world despite being both completely preventable and treatable. This continued burden is reflected by the World Health Organisation's (WHO) global estimate of 229 million cases of malaria in 2019 (1). In an effort to combat the disease, concerted transdisciplinary endeavours by the WHO, Roll Back Malaria, Malaria Eradication Agenda and other initiatives aim to achieve the elimination goals set out for malaria-endemic regions (1-3).

Africa remains the region most severely affected by malaria, contributing 94% of the global deaths in 2019 (Figure 1.1a). The severity of the disease in Africa predominantly arises from the prevalence of the most lethal malaria parasite species, *Plasmodium falciparum* and an abundance of the highly efficient *Anopheles* mosquito vector species (4). However, the successes of elimination programs are evident both in Africa and globally as a decline in malaria deaths worldwide from 736 000 reported by 106 countries in 2000 to 409 000 across 87 countries in 2019. Furthermore, children under five years of age represent the most severely affected demographic however, in 2019 this group contributed 67% of the global malaria deaths (Figure 1.1a), down from 84% in 2000 (1).

Once zero cases of indigenous malaria have been reported for three consecutive years, a country becomes eligible to apply for a WHO certification of malaria elimination. In 2019, China and El Salvador both reached this milestone and are thus now considered to have eliminated the disease (Figure 1.1b). These successes lend themselves to the global malaria eradication strategy and are underpinned by interdisciplinary approaches for preventing and treating the disease.

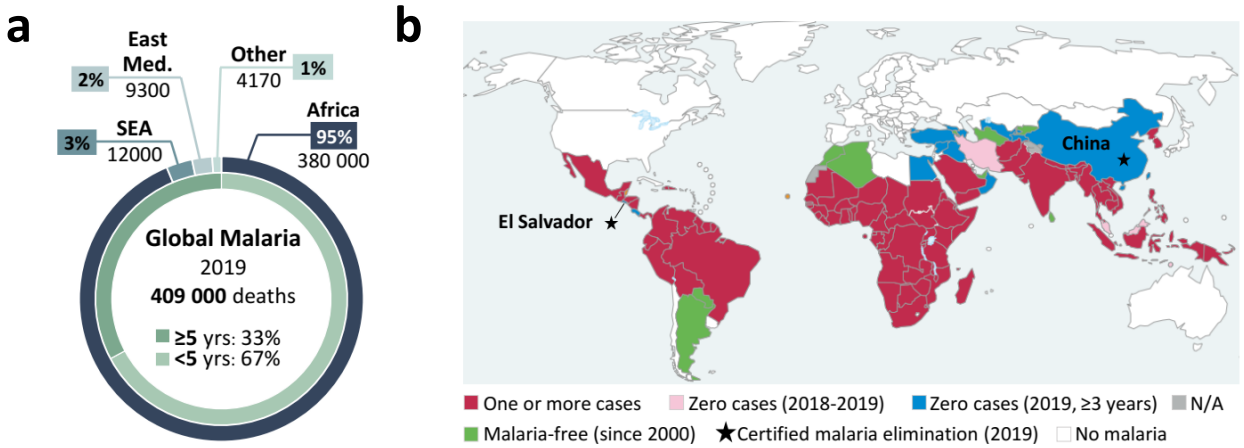

Figure 1.1: The continued global burden of malaria. **(a)** Malaria deaths per WHO 2019 global estimates categorised by region (number and % of total deaths indicated) and age group (≥5 years or below 5 years, % of total deaths). Legend: E. Med. = Eastern Mediterranean region, SEA = South-East Asian region. **(b)** Malaria case numbers per country in the context of elimination in 2019. Countries with zero cases over three or more consecutive years are certified as having eliminated malaria by the WHO (blue), with those receiving certification in 2019 highlighted with a star on the map. Image adapted from World Malaria Report, 2020 (1).

Preventative measures include vector control, primary health promotion and education and the use of chemoprophylaxis in vulnerable populations. The treatment of malaria involves the administration of chemotherapeutics that kill the parasites in infected patients (5-7).

1.1.1 Malaria prevention

Integrated vector management (IVM) strategies are widely used to target the *Anopheles* mosquitoes that transmit malaria parasites between human hosts (8). These include the use of insecticide-treated bed nets, larviciding programs that kill the immature, aquatic stages thereby reducing the adult mosquito population and indoor residual spraying (IRS) to eliminate adult mosquitoes in dwellings (9-11). South Africa's IVM program primarily focuses on IRS using dichlorodiphenyltrichloroethane (DDT) (12), an insecticide that is approved for use in countries nearing malaria elimination (13). In addition to the management of vectors, South Africa's malaria control program includes the frequent training of health workers and stock management of diagnostic tools at primary health care facilities to ensure the early detection of malaria-infected patients (14).

In 2019, programs were initiated to vaccinate African children against *P. falciparum* malaria using RTS,S, the first vaccine ever licensed for use against a human parasitic disease (15, 16). However,

the use of this vaccine is controversial due to its limited efficacy (15-50% effective in children 5-17 months of age) (17). More recently, the new candidate vaccine, R21/Matrix M was shown to be safe and highly immunogenic in Africa children (5-17 months of age) with 77% efficacy maintained for up to a year following completion of the vaccination program (18). As a relatively small number of participants (450 individuals) were included in this primary study, larger trials will be required to confirm these results prior to the approval of the vaccine for general use. Therefore, malaria vaccine research is ongoing with recent suggestions for the development of additional malaria vaccine candidates using the mRNA technology common to several of the COVID-19 vaccines (19).

Chemoprevention of malaria takes two forms: 1) the short-term administration of chemoprophylactic treatment for individuals visiting malaria endemic areas and 2) intermittent preventative treatment (IPT) for high-risk groups living in regions with malaria (20). IPT is currently recommended for pregnant women (IPTp) and infants (IPTi) with evidence supporting its use in school-age children to protect these individuals and reduce overall transmission levels (20-22).

1.1.2 Malaria treatment

Treatment of malaria-infected patients involves chemical-based parasite control interventions. In accordance with the WHO-recommended first-line treatment for malaria, South Africa uses artemisinin-based combination therapies (ACTs) to treat patients with uncomplicated malaria (14). ACTs contain a derivative of artemisinin, a compound originally isolated from *Artemisia annua* plants that reduces parasite numbers and acute symptoms within the first three days of treatment. This is combined with a longer-acting partner drug that is able to eliminate the residual parasites in circulation (1, 23). In addition to the use of ACTs to treat the symptoms of malaria, patients may also be prescribed a single dose of primaquine (24, 25). Primaquine specifically targets the transmissible stages of the parasite life cycle making it an ideal tool to prevent secondary transmission and facilitate malaria elimination (24, 26, 27).

Although ACTs are widely used to treat malaria, the emergence of ACT-resistant parasites in recent years has led to increased mortality and is cited as an important barrier to global eradication (19, 28). This is unsurprising given that *Plasmodium* parasites have developed resistance mechanisms against all historically used drugs from the major anti-malarial compound classes including the quinolines (e.g. chloroquine), antifolates (e.g. pyrimethamine) and artemisinins (e.g. dihydroartemisinin) (29-32).

1.1.3 Drug resistant malaria

Drug resistance is defined as the ability of parasites to survive and/or proliferate when exposed to drug concentrations greater or equal to those usually required to inhibit these processes in susceptible parasites (33). Drug-resistant phenotypes can be acquired by two mechanisms: 1) an increase in gene copy number and 2) mutation of genes that are associated with a compound's mode-of-action or mechanism of resistance (30, 34). For example, amplification of the multi-drug resistance 1 gene (*mdr1*) is linked to *in vitro* parasite resistance and the clinical failure of mefloquine, lumefantrine, quinine and artemisinin derivatives (35-37). The delayed parasite clearance associated with artemisinin resistance can arise from mutations in the *kelch13* gene (*k13*) (38, 39) that have been detected alongside the clinical failure of ACTs in six Asian countries. Parasites with *k13* mutations are becoming increasingly more prevalent across the Horn of Africa however, these have yet to affect the efficacy of the ACTs used in the region (1).

The spread of ACT-resistant parasites in recent years necessitates the expedited discovery and development of novel anti-malarial compounds. Furthermore, the global malaria eradication agenda requires that these compounds be pan-active, targeting multiple stages of the parasite's life cycle (40). To this end, the drug discovery community has detailed the types of molecules (target candidate profiles, TCPs) and product formulations (target product profiles, TPPs) that will be most useful as the next generation of anti-malarial medicines (40). Delineating the effects of anti-malarials on the parasite is critical given the high value of candidate molecules and products with activity against multiple life cycle stages. However, such characterisation requires a thorough understanding of malaria parasite biology which is currently incomplete. Therefore,

the renewed interest in global malaria eradication and the goals set out to achieve this necessitate a greater focus towards understanding the fundamental biology of *Plasmodium* parasites (40, 41).

1.2 The life cycle of *P. falciparum* parasites

The *P. falciparum* parasite life cycle is complex, unfolding in both the human host and mosquito vector with parasites progressing through several asexual and sexual stages (42). The asexual and sexual developmental pathways are mutually exclusive with the decision to commit to one or the other fate determined either in the current (same-cycle conversion, SCC pathway) or the preceding (next-cycle, NCC pathway) asexual proliferative cycle and stably maintained thereafter (43-45).

1.2.1 Asexual proliferation

Malaria infections are established when mature sporozoites are injected into the human during mosquito feeding (Figure 1.2). Aided by the circulatory system, the self-propelled sporozoites are then transported to the liver where they invade hepatocytes and undergo a 14-day process of exoerythrocytic development (46). Subsequently, schizogony occurs in which short-lived daughter merozoites are released into the blood stream to invade erythrocytes (47). Once inside the host erythrocyte, the intraerythrocytic developmental cycle (IDC) is established with the merozoite developing into a haploid ring-stage parasite within the first two hours after invasion. Within the next eight hours, the ring stages develop into metabolically active trophozoites that are characterised by increased cytoplasmic volume and the appearance of a hemozoin crystal, a by-product of haem detoxification (48).

Following sufficient growth, the parasite undergoes several rounds of DNA replication and nuclear division, yielding a schizont containing 16-32 daughter merozoites. The schizont ruptures, releasing these merozoites that then go on to invade new erythrocytes, re-initiating the 48-hour asexual IDC that is responsible for malaria pathology (42).

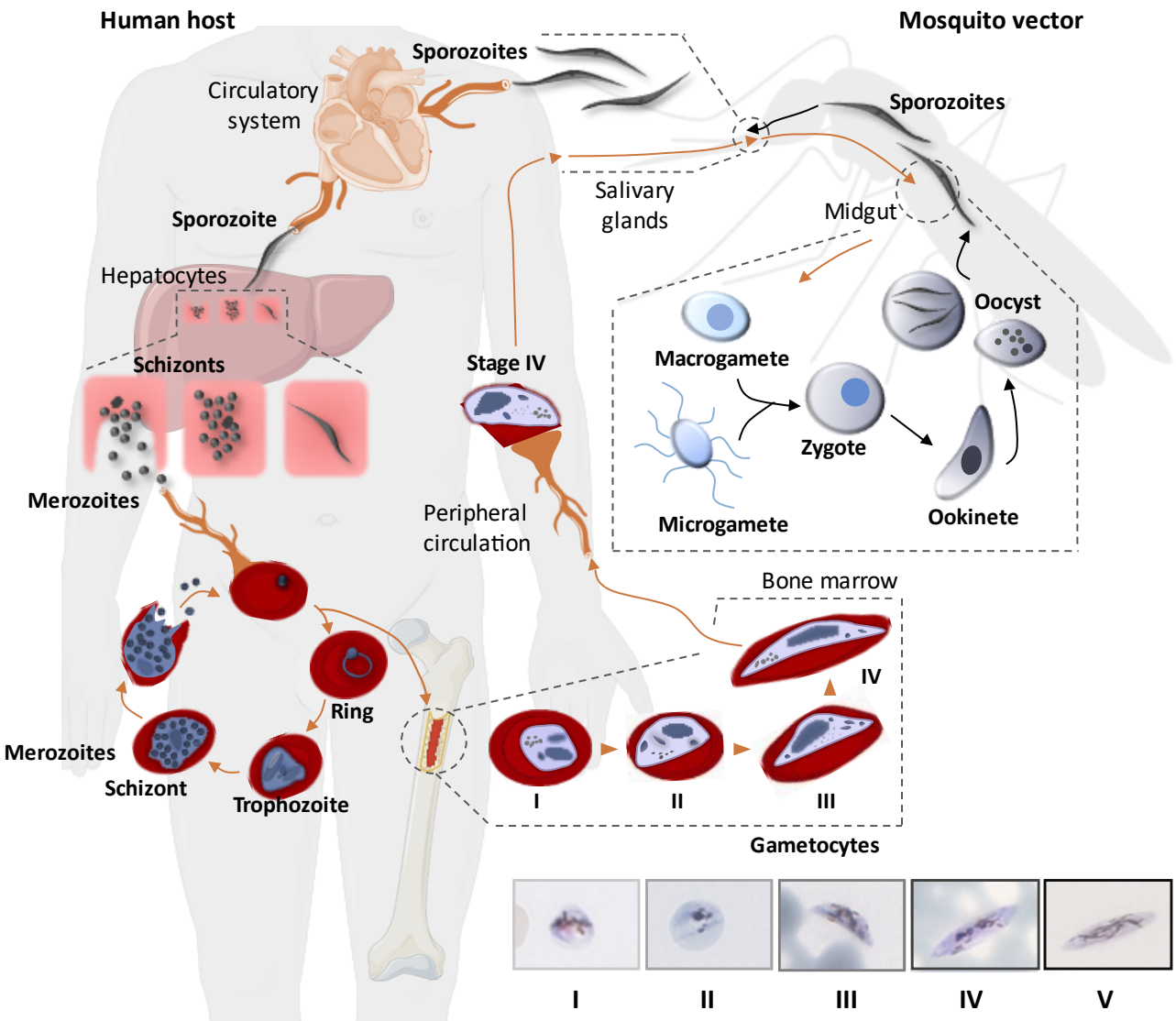

Figure 1.2: The life cycle of *P. falciparum* parasites. The life cycle begins with the injection of sporozoites by a mosquito vector into the circulatory system of a human host. The sporozoites then travel to and invade liver cells, ultimately forming hepatic schizonts that rupture, releasing merozoites into the peripheral circulation. These merozoites invade erythrocytes and initiate a cycle of asexual proliferation that involves development into ring-, trophozoite- and schizont-stage parasites. Schizonts then rupture to release new daughter merozoites that repeat this cycle once again. Within each cycle, a small proportion (≤10%) of the parasites will deviate from this fate and instead commit to sexual differentiation. Sexually committed merozoites also invade erythrocytes and form stage I gametocytes that sequester in the bone marrow where subsequent maturation into stages II-IV occurs. Gametocytogenesis yields mature stage V gametocytes that re-enter into the host's circulatory system where they are ideally situated for transmission to the mosquito during feeding. Once taken up, gametogenesis ensues in the mosquito midgut in which male microgametes fertilise female macrogametes to form diploid zygotes. Zygote development involves maturation into an ookinete and then the oocyst that contains new, maturing sporozoites. Finally, the oocyst ruptures, releasing sporozoites that travel to the mosquito's salivary glands where they will be transmitted to a new host during feeding. Images taken during the microscopic evaluation of Giemsa-stained stage I-V gametocytes are shown.

1.2.2 Sexual commitment and differentiation

In each IDC, a small subset (≤10%) of parasites commit to sexual differentiation and undergo a specialised process of cellular differentiation that secures transmission back to the mosquito (44, 49). Firstly, these sexually committed parasites complete the replicative IDC with the daughter merozoites that emerge going on to invading new erythrocytes and initiate gametocytogenesis (Figure 1.2) (50, 51). As this additional round of post-commitment replication is not obligatory, parasites may also undergo SCC in which ring-stage parasites switch directly to sexual differentiation (45). Whether parasites commit via the NCC or SCC route is determined by the temporal expression of the factors that drive sexual differentiation (45, 52). Irrespective of the route taken, gametocytogenesis entails the differentiation and development of five (stages I-V) morphologically distinguishable stages in *P. falciparum* (Figure 1.2). Unlike the gametocytes of other human malaria parasites that take between 24 and 48 hours to mature, *P. falciparum* gametocytes undergo an extended 10- to 14-day process of development (44, 53). Stage I gametocytes are morphologically similar to the asexual trophozoite stages, distinguishable only by their diffuse distribution of haemozoin crystals that contrasts with the punctate clusters that are indicative of haemoglobin digestion in trophozoites (54). Additionally *in vivo*, the stage I gametocytes are predominantly present in the bone marrow while the trophozoite stages are associated with microvasculature sequestration (55, 56). The sequestration of gametocyte-infected erythrocytes in the bone marrow persists throughout the development of stages I-IV (Figure 1.2) (55, 57). Host erythrocyte remodeling during the early steps of differentiation facilitate this sequestration and enable gametocytes to avoid splenic clearance (58, 59). Specifically, the multi-gene families encoding the STEVOR, RIFIN and gametocyte exported proteins (GEXPs) are implicated in the establishment and maintenance of bone marrow sequestration (60-62). The development of the inner membrane complex (IMC) and supporting microtubule substructure culminate in the formation of the D-shape that characterises stage II gametocytes (44). In stage III, sexual dimorphism becomes discernible and gametocytes appear elongated into an oval shape with one of the lengths curved and the other straight, supported by a completed IMC and microtubule scaffold (63). This shape further elongates in stage IV gametocytes to resemble a spindle shape with cuspated ends. The sexes of stage IV gametocytes

are more readily distinguishable from one another with haemozoin in females concentrated into punctate foci that contrast with the dispersion of these crystals in male gametocytes (64). Gametocytogenesis ultimately yields stage V gametocytes with a characteristic crescent shape with rounded ends. Stage V gametocytes enter the peripheral circulation of the human host to be taken up by a mosquito during feeding (Figure 1.2). Female stage V, or macrogametocytes, are slightly more curved and elongated compared to male microgametocytes (63). Upon ingestion, the stage V gametocytes enter a vastly different microenvironment with a lower temperature (25°C), an increased pH (8.0 compared to 7.3 in the human host) and concomitant exposure to the xanthurenic acid present in the mosquito midgut. These three environmental conditions trigger egress from erythrocytes and initiate gametogenesis (65, 66). Male gametogenesis involves rapid DNA replication followed by endomitosis and axoneme formation to yield eight microgametes within 20 minutes (67, 68). Axoneme development is critical for microgamete motility during and after exflagellation, the process in which male gametes are released into the environment for fertilisation (68, 69). The process of female gametogenesis is less conspicuous however, it entails the translation of a large pool of mRNAs that were synthesised and translationally repressed in the preceding gametocyte stages (70). The synthesis of these transcripts in advance ensures that female gametogenesis rapidly produces a macrogamete (one gamete per female gametocyte) containing the proteome required for zygote formation (71, 72). During fertilisation, the male and female gametes fuse to form a diploid zygote that subsequently develops into an ookinete and then oocyst (Figure 1.2) (73). Oocysts undergo sporogony in which asexual replication generates many haploid sporozoites. These sporozoites are then released and travel to the mosquito's salivary glands in preparation for transmission to a new human host (74).

1.3 Regulation of *P. falciparum* parasite fate

The binary fate associated with intraerythrocytic development in malaria parasites is determined by cooperating environmental and genetic factors. The earliest studies of binary fate regulation were based on identifying the genetic aberrations in parasites that had lost the ability to produce

gametocytes *in vitro* (75-77). Whole-genome sequencing of such gametocyte-deficient lines and more recently, the use of inducible expression systems, have identified the key genetic regulators that underly the decision to proliferate or differentiate (78). Here, the determinants of fate in *Plasmodium* parasites will be dissected.

1.3.1 Extrinsic determinants of fate

Several extrinsic drivers of fate have been proposed and investigated including changes in host physiology, variation in *in vitro* conditions, increased parasitaemia, anti-malarial drugs and certain toxins (79-82). For example, both chloroquine and the cholera toxin are associated with amplified gametocyte commitment while reticulocytopenia can significantly increase a host's gametocyte load (79-81). However, the mechanisms underlying these increases and their role in gametocyte conversion remain somewhat controversial (83). By contrast, the role of lysophosphatidycholines (lysoPCs) in determining *Plasmodium* parasite fate has been well demonstrated. LysoPCs are abundant in human serum with physiological concentrations of these lipids stimulating parasites to continue proliferating asexually (84). Phosphatidylcholines (PCs) are the most prolific of the phospholipids in the *Plasmodium* parasite membrane and therefore asexual proliferation requires a rapid production of PCs via the Kennedy pathway (85). Host serum LysoPCs are the precursor molecules required for the Kennedy pathway and thus, an adequate supply indicates ideal conditions for proliferation (85). By contrast, the depletion of lysoPC concentrations induces the upregulation of several intrinsic factors that drive the switch to sexual differentiation (84).

1.3.2 Intrinsic determinants of fate

Currently, the specific mechanism linking lysoPC depletion with the cessation of asexual proliferation and the concurrent switch to sexual differentiation is unclear. Nevertheless, several essential genetic factors have reproducibly been shown to be upregulated upon this cue and drive sexual differentiation in *P. falciparum*, indicating the conservation of commitment

regulatory mechanisms in malaria parasites (77, 86). Moreover, variable characteristics of gametocyte commitment may also be present and are dictated by genotypic diversity between parasite populations. For example, a recent study identified that parasites circulating in low-transmission settings have adapted to produce more gametocytes at the expense of reduced asexual proliferation compared to parasites in high-transmission areas (87). Irrespective of the number of gametocytes produced however, the commitment process is driven by AP2-G, a member of the Apicomplexan-specific Apetala2 (ApiAP2) DNA binding domain-containing protein family (88). Due to the essential nature of this transcription factor (TF) for sexual commitment, AP2-G has been heralded as the master regulator of gametocytogenesis (86). During the IDC, the *ap2-g* locus is populated with an abundance of repressive factors, including heterochromatin protein 1 (HP1) that is recruited by the histone post-translational modification (PTM), H3K9me3 to silence this gene (Figure 1.3) (89, 90). Additionally, the expression of the gametocyte development protein 1 gene (*gdv1*) is inhibited by its own antisense RNA (asRNA) during asexual proliferation (90). Upon the cue for commitment, GDV1 is upregulated and evicts H3K9me3/HP1. This complex is subsequently replaced by the activating histone PTM H3K9ac, followed by a loss of the heterochromatic environment at the *ap2-g* locus. This de-repression promotes the transcription of *ap2-g* that is subsequently maintained by a positive feedback loop (Figure 1.3) (90, 91). Sequence-specific binding of AP2-G to promoters containing the 'GTAC' motif results the transcriptional activation of hundreds of genes. These genes are predominantly involved in commitment and early gametocyte development and include those encoding invasion proteins that are co-regulated by a second AP2 TF, AP2-I during early commitment (52, 86, 91). Additionally, AP2-G2 is associated with silencing of genes that have asexual proliferation-specific functions (Figure 1.3) (92).

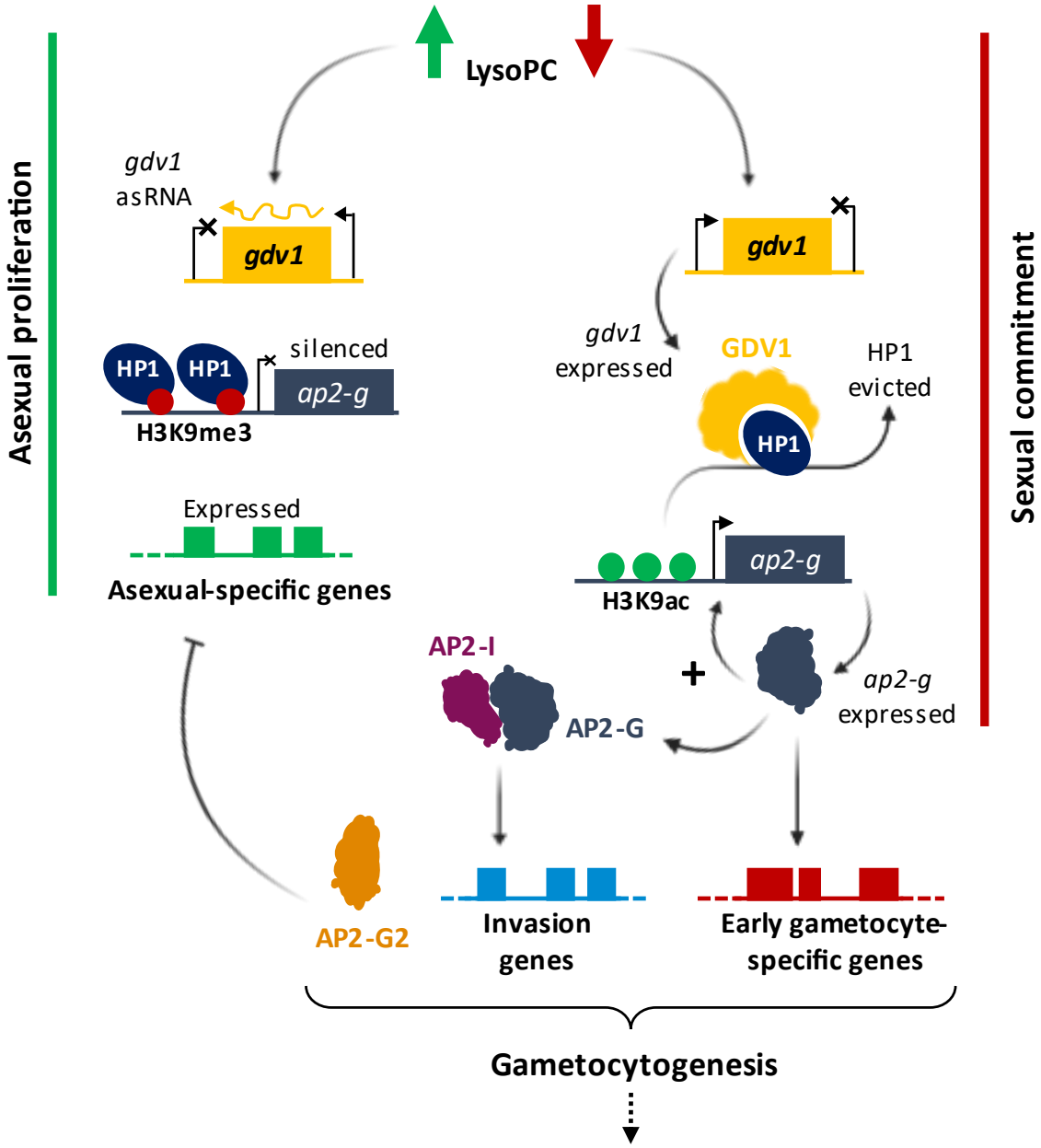

Figure 1.3: Mechanisms of binary fate decision in *Plasmodium* parasites. Under normal physiological lysophosphatidylcholine (lysoPC) levels (green arrow), *gdv1* and *ap2-g* are silenced by anti-sense RNA (asRNA) expression and H3K9me3/heterochromatin protein 1 (HP1)-mediated heterochromatin, respectively. Asexual-related genes are expressed to drive parasite proliferation. Upon lysoPC depletion (red arrow), expression of *gdv1* sense mRNA occurs. GDV1 evicts HP1 at the *ap2-g* locus which additionally becomes populated with H3K9ac. Together, these changes result in the expression of AP2-G with subsequent transcription stimulated through a positive feedback loop (+). AP2-G binds and transcribes early gametocyte-specific genes and together with AP2-I, regulates the expression of invasion genes. AP2-G2 is associated with the repression of asexual-related genes during gametocytogenesis. These mechanisms cooperatively drive the switch from asexual proliferation to sexual commitment and subsequent gametocyte differentiation.

Outside of these intrinsic determinants of fate, a vast array of other regulatory mechanisms orchestrates both asexual and sexual stage transitions and life cycle progression in *Plasmodium* parasites. These regulatory systems, including transcriptional, post-transcriptional and epigenetic mechanisms, will be discussed in greater detail below.

1.4 Regulation of *P. falciparum* life cycle progression

The complexities of the *Plasmodium* life cycle are evident from the array of developmental stages and cycles that are compartmentalised into diverse host cell types within different species. The unique biology of each stage is underpinned by precise the transcriptional regulation of stage-specific gene sets (93-95).

1.4.1 Transcriptional regulation of the *P. falciparum* genome

The *P. falciparum* genome, consisting of 23 Mb of DNA divided into 14 chromosomes, has extremely low complexity in both coding (80% A/T content) and non-coding (90% A/T content) regions (96, 97). During replication of such low complexity DNA, polymerase slippage introduces insertions and deletions that contribute to genetic diversity and promote antigen variability between parasite strains (98, 99). Each of the ~5600 *P. falciparum* genes have a typical eukaryotic gene structure consisting of a promoter sequence, an open reading frame and intergenic regions (97). Thus, gene expression also proceeds in the characteristic eukaryotic manner involving nuclear mRNA synthesis and processing followed by cytoplasmic translation (98).

Throughout asexual proliferation, ~80% of the *P. falciparum* parasite genome is expressed in a "just-in-time" manner with the cyclic nature of this process evident from >75% of the genes that have peak transcript abundance only once throughout the IDC (93, 100). Similarly in gametocytes, transcription is regulated in a hierarchical manner that dictates the processes of gametocyte differentiation and development (94). These ordered transcriptional cascades are governed by an interplay between typical eukaryotic *cis*-acting DNA regulatory elements and *trans*-acting elements (e.g. TFs) that are largely conserved in *Plasmodium* parasites (101, 102).

For example, transcription in *Plasmodium* parasites is initiated at TA dinucleotides that are present in conventional TATA-box regulatory elements (103, 104). The local G/C base composition downstream of transcriptional start sites (TSSs) guides the identification and usage of these initiation sites within the low-complexity genome (105). Additionally, the presence of promoter-proximal and distal regulatory elements, some of which have been associated with stage- or function-specific transcription, indicate that genes are also regulated by distance-independent *cis*-acting elements in *Plasmodium* parasites (106-108).

Regarding *trans*-acting regulatory elements, *Plasmodium* parasites have relatively few TFs compared to other eukaryotes, implying that other regulatory mechanisms (e.g. epigenetic regulation) may be more important for transcriptional control (109). Prior to the identification of the ApiAP2 TFs in 2005, only a few sequence-specific TF binding domains had been identified for *Plasmodium* parasites including myeloblastosis (MYB), high mobility group B (HMGB) and C2H2 zinc fingers (109-113). Indeed, MYB1 is the only non-ApiAP2 TF validated as essential for cell cycle progression in *P. falciparum* parasites (114, 115). By contrast, the 27-member ApiAP2 family has been relatively well-studied in recent years with both repressor and activator functions described for the individual TFs (52, 88, 92, 110, 116-120). The ApiAP2s are expressed throughout the asexual and sexual stages of the *Plasmodium* life cycle with certain of these linked to the expression of stage-specific gene sets (86, 92, 94, 119).

1.4.2 Post-transcriptional and post-translational regulation

mRNA transcripts in *Plasmodium* parasites are subject to many of the conventional eukaryotic post-transcriptional and -translational control mechanisms, such as alternative splicing, mRNA stabilisation and non-coding regulatory RNAs (121). Peak protein levels may be achieved as early as ten hours after the synthesis of the corresponding mRNA transcripts, highlighting the importance of immediate and subsequential translation of mRNAs for the progression of the *Plasmodium* parasite life cycle (122). Alternatively, certain transcripts may be stabilised by mRNA-ribonucleoproteins (mRNP) in a process known as translational repression (112, 123, 124). mRNPs mediate this repression in one of two ways: 1) directly blocking the translation of the

transcript, or 2) stabilising mRNAs to prevent degradation and enhance their fidelity for later use (101). mRNPs identified in *Plasmodium* parasites include the DOZI-CITH complex (DDX-6 class DEAD box RNA helicase and Sm-like factor homolog of CAR-I and Trailer Hitch) and pumilo family proteins (PUF2) with the crucial roles of these proteins clearly defined during gametocytogenesis (125-127).

Non-coding RNAs (ncRNAs) regulate various eukaryotic processes including chromosome maintenance, transcription, translation and enzyme activity (128). Although hundreds of ncRNAs have been identified in *Plasmodium* parasites, only a few of these such as the telomere-associated repeat elements (TAREs), have been functionally characterised. TAREs regulate telomere maintenance and the expression of virulence genes (129, 130). Additionally, certain small ncRNAs were recently identified to be exclusively expressed in gametocytes, suggesting stage-specific roles for these molecules (106).

In addition to the abovementioned mechanisms, chromatin status is substantially reorganised throughout the *P. falciparum* life cycle and is thought to be a strong, overarching influence on the progression of the parasite from one stage to the next (131). Accordingly, recent studies have begun to document the importance of the epigenetic landscape, encompassing three-dimensional genome organisation, histone and chromatin modifiers and nucleosome positioning (89, 132-135), in *Plasmodium* parasites. To dissect and describe the unique aspects of epigenetics in *Plasmodium*, it will first be useful to examine the contribution of epigenetic mechanisms in the broader context of eukaryotic gene regulation.

1.5 Epigenetic regulation in eukaryotes

The study of epigenetics aims to understand heritable changes in gene expression that do not involve alterations to the underlying DNA sequence (136). Epigenetic changes are predominantly non-permanent with the sum of all these modifications collectively referred to as the epigenome of a cell. By regulating cell type- and stage-specific gene sets, the epigenome is a major determinant of cellular phenotype (137). The prokaryotic epigenome consists of an extremely limited repertoire of regulatory factors. DNA methylation, the only epigenetic mechanism

described in prokaryotes thus far, influences transcription rate and directs DNA damage repair (138-141). In eukaryotes, this methylation predominantly occurs at cytosine nucleotides that are guanine-adjacent (CpG sites) and is involved in both transcriptional activation and silencing (142).

Within the nucleus, genomic DNA is tightly wrapped around nucleosomes (146 bp/unit) containing an octamer of two molecules of each of the four core histone proteins (two H2A/H2B dimers and an H3/H4 tetramer) (Figure 1.4).

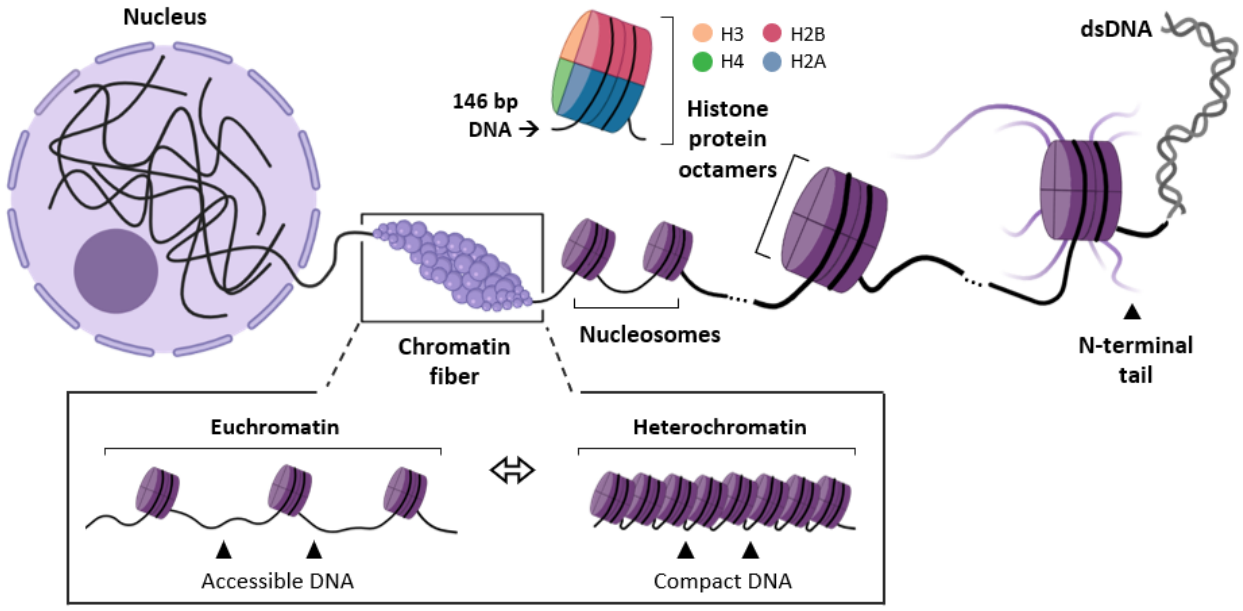

Figure 1.4: Eukaryotic chromatin structure. Within the eukaryotic nucleus, 146 bp segments of double-stranded (ds) DNA are coiled around histone octamers (two molecules of each core histones: H3, H4, H2A and H2B, with the N-terminal tails exposed for modification) proteins, forming nucleosomes. These nucleosomes, the basic structural units of chromatin are then condensed into fibers that either exist in a euchromatic state or are further condensed to form heterochromatin. Various epigenetic mechanisms alter chromatin structure and thus accessibility of the DNA to transcription factors.

Histone proteins are rich in lysine (K) and arginine (R) residues that neutralise the negative charge of DNA and allow the formation of nucleosomes. The four core histones are structurally similar: three *α*-helices form a fold that mediates associations with adjacent histones and an N-terminal tail extending outwards from the nucleosome (Figure 1.4). These nucleosomes are condensed into fibers that subsequently exist as open euchromatin or are further condensed to form compact heterochromatin (143). Euchromatin is accessible to TFs while heterochromatin

prevents these proteins from interacting with DNA and thus alterations to chromatin structure influence the level of transcription (144, 145). Further compaction of chromatin fibers is influenced by highly ionic environments and via an interaction between histone protein H1 and the linker DNA that joins adjacent nucleosomes (146). After the translation of H1, the protein may undergo modification with chemical groups that influence its DNA-binding affinity (147, 148).

Nucleosomes are modified in a variety of ways that influence chromatin structure and accessibility. Firstly, chromatin remodeling complexes promote or restrict DNA accessibility by repositioning nucleosomes at new locations or completely evicting them from the chromatin structure (Figure 1.5) (145).

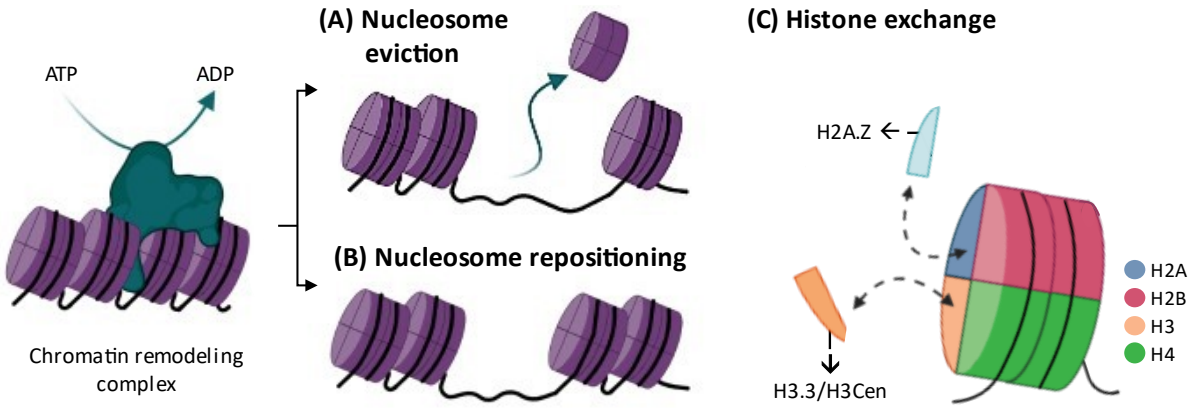

Figure 1.5: Eukaryotic chromatin remodeling mechanisms. Chromatin remodeling complexes hydrolyse ATP to drive the eviction of nucleosomes from chromatin (A), reposition nucleosomes at new locations (B) or exchange canonical histones for their variants (C). Mechanisms A-C regulate chromatin status and thereby influence the transcriptional accessibility of DNA.

Nucleosome depleted regions (NDRs) within promoters enhance DNA accessibility, thereby promoting the binding of the transcription pre-initiation complex. By contrast, at silent gene promoters this interaction is inhibited by a dense population by nucleosomes (143, 145). Eukaryotic NDRs are characterised and flanked by two strongly positioned nucleosomes: the -1 nucleosome (upstream) and +1 nucleosome (downstream). The distance between transcription start sites (TSSs) and strongly positioned +1 nucleosomes vary between species, reflecting the divergence of transcriptional regulatory mechanisms (149, 150).

Other remodeling complexes may influence the stability of nucleosomes by exchanging the canonical histones for their variants (e.g. H2A.Z and H3.3) (Figure 1.5). While less common than H3 and H2A variants, some eukaryotes encode H4 and H2B histone protein variants, such as H2B.Z in *Plasmodium* parasites (151). Finally, nucleosome and chromatin stability are regulated by the plethora of PTMs that may be present on the N-terminal histone tails (144, 152).

1.5.1 Eukaryotic histone post-translational modifications

Histone PTMs include methylation, acetylation, phosphorylation, ubiquitylation and SUMOylation with the former two modifications most commonly observed and thus, most well-studied to date (152, 153). Given their influence on gene regulation and relevance for this study, this section focuses on the transcriptional effects associated with histone PTMs. Nevertheless, it is important to note that the functions of histone PTMs are not limited to transcriptional control but also include other pertinent cellular processes such as DNA replication and repair (154, 155).

There are two mechanisms by which histone PTMs exert their effects on transcription: 1) direct perturbation of chromatin structure and 2) the regulation of effector (or "reader") protein binding (143, 156). PTMs that alter the overall charge of histones (e.g. lysine acetylation and serine phosphorylation) directly disrupt their electrostatic interactions with DNA and thereby enhance chromatin accessibility (157). The addition of large chemical groups (e.g. ubiquitin) physically induces conformational changes and thus alters the stability of nucleosomes and chromatin. Alternatively, small modifications that do not affect histone charge (e.g. lysine methylation) mediate changes by recruiting other proteins (e.g. chromatin regulators and TFs) that subsequently shape chromatin structure and accessibility (152).

Phosphorylation of serine, threonine and tyrosine residues predominantly occurs at the N-terminal of the histone tail with phosphate groups added and removed from by kinases and phosphatases, respectively (156, 158). In addition to increasing the overall negative charge of DNA, phosphorylate histones also directly recruit TFs to DNA (159). Ubiquitylation involves the covalent modification of lysine residues with one or more large (76-amino acid) ubiquitin polypeptides. Ubiquitylation is most well-characterised for histone H2A and H2B with the mono-

ubiquitylation of H2AKK119 and H2BK123 associated with transcriptional repression and activation, respectively (160-162). The modification of lysine with the small ubiquitin-like modifier (SUMO) has been detected on all four of the canonical histones (163). SUMOylation physically inhibits the accumulation of acetylation and ubiquitylation PTMs and thus is predominantly associated with repressive functions (164, 165).

Histone lysine, and to a lesser extent arginine, residues are subject to modification with up to three methyl groups, generating mono-, di- or tri-methylated states. Whether these histone PTMs functions as activators or repressors of transcription is determined by the position of the lysine within the histone tail, the degree of methylation and the position relative to gene regulatory elements (Figure 1.6a) (143, 145). For example, when associated with promoters, H3K36me3 represses transcription while the presence of this histone PTM in coding regions (CDRs) is indicative of recent transcriptional activity (166-168). Additionally, the local chromatin environment may also influence the transcriptional effects of histone PTMs (169). This has been observed for enhancers enriched with H3K4me1, a PTM that attracts or repels reader proteins depending on DNA methylation status and the presence of histone modifier enzymes (Figure 1.6a) (170-172).

Acetylation is predominantly associated with actively transcribed gene as these PTMs weaken DNA-histone electrostatic interactions, thereby generating a euchromatic environment (143, 173). The dynamic balance between acetylation and methylation at certain lysine residues (e.g. H3K4, H3K27 and H3K36) (Figure 1.6a), is of critical importance for transcriptional regulation (170, 172, 174).

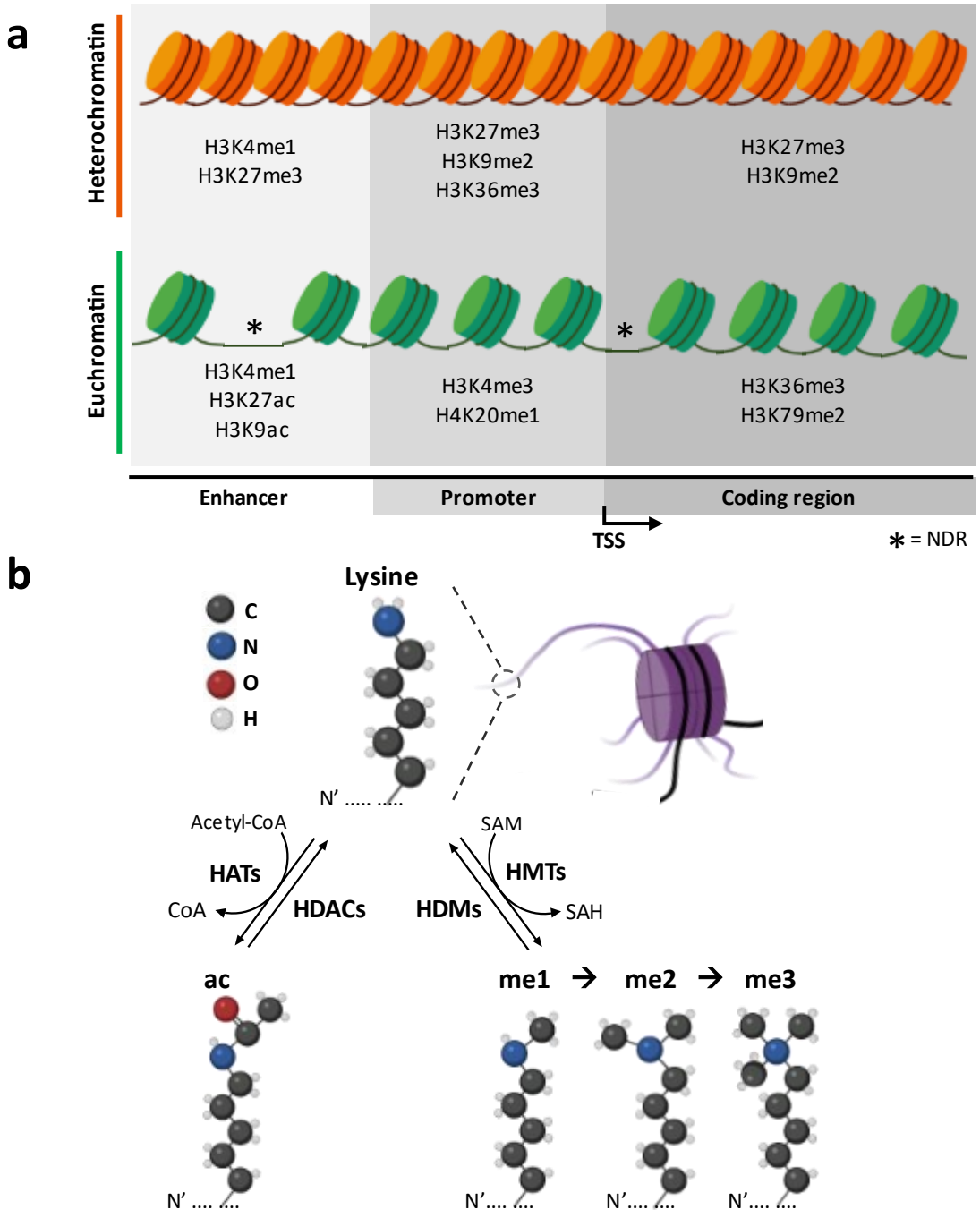

Figure 1.6: Acetylation and methylation of histone lysine residues. (a) Common repressive (orange) and activating (green) histone PTMs categorised based on their genomic position. Certain lysine residues can be acetylated or methylated with these two modifications having various effects on transcription. Nucleosome depleted regions (NDRs) are characteristic of euchromatin. **(b)** Lysine residues at the N-terminal end (N') of histone proteins are subject to acetylation by histone acetyltransferases (HATs) that require acetyl-CoA (donor) and yield CoA, the removal of acetyl groups by histone deacetylases (HDACs), mono- (me1), di- (me2) and tri-methylation (me3) catalysed by histone methyltransferases (HMTs) that require S-adenosyl methionine (SAM) as a methyl donor (yields S-adenosylhomocysteine) and the eviction of methyl groups from lysine residues by histone demethylases (HDMs).

The methylation and demethylation of histones is performed by histone methyltransferases (HMTs) and histone demethylases (HDMs), respectively (Figure 1.6b). S-adenosylmethionine (SAM) is the methyl-donating substrate of HMTs and catalyses the formation of a methylated lysine and S-adenosylhomocysteine (SAH) (175-177). As these PTMs do not alter histone charge, the transcriptional changes they mediate are predominantly carried out by the *trans*-acting reader proteins that recognise them (178). Histone acetyltransferases (HATs) catalyse the transfer of an acetyl group from acetyl-CoA to lysine, generating CoA during this process (Figure 1.6b) (145, 174). The removal of acetyl groups by histone deacetylase (HDAC) activity is associated with the cessation of transcription.

In addition to the vast array of individual histone PTMs, the combinatorial effects of co-occurring modifications are posited as an additional layer of epigenetic regulation. This "histone code" hypothesis predicts that a distinct set of histone PTMs, acting either sequentially or in combination, represent a code that specifies a unique biological outcome (179). While only a handful of histone PTM combinations have been functionally validated (157, 180, 181), the histone code hypothesis further highlights the complexity and importance of epigenetic regulation in eukaryotes (179).

Many of the abovementioned mechanisms are conserved across eukaryotic species, including *Plasmodium* parasites. The exceptional selective pressures encountered by malaria parasites have driven the evolution of a distinct epigenome encompassing both atypical and typical eukaryotic features (131, 182). These unique and shared facets of the *Plasmodium* parasite's epigenetic landscape will now be discussed in detail.

1.6 Epigenetic regulation of *P. falciparum* life cycle progression

1.6.1 The *P. falciparum* nucleosome

Compared to higher eukaryotes, *Plasmodium* chromatin structure is considerably less stable with this manifesting as a relatively accessible genome (183). Nevertheless, the ubiquitous eukaryotic

nucleosome structure is largely conserved in *Plasmodium* parasites, consisting of DNA similarly associated with an octamer of the four core histone proteins. These proteins may be exchanged for the four variant histones (H2A.Z, H2B.Z, H3.3 and H3Cen) that have particular functional characteristics in *Plasmodium* parasites (151, 184). Typically, the replacement of H3 by CenH3 or H3.3 occurs at centromeres and active gene regulatory elements, respectively (185, 186). While H2A.Z generally demarcates the 5' promoter regions of all genes irrespective of their transcriptional status, H2A/H2A.Z exchange at *var* gene promoters is involved in antigenic switching (187, 188). H2B variants are relatively uncommon in eukaryotes with Apicomplexa having independently evolved the lineage-specific H2B.Z (previously H2Bv) (189, 190). In *Plasmodium* parasites, H2B.Z is associated with the euchromatic histone PTM, H3K4me3 and is present in H2A.Z/H2B.Z double-variant nucleosomes that primarily occupy *var* gene introns and other intergenic regions across the genome (191). As in other Apicomplexans, no homologs of the linker histone H1 have been identified in *Plasmodium* parasites (192, 193). This lack of H1 is unsurprising and likely contributes to the characteristic low nucleosome stability and absence of chromatin condensation during mitosis in the parasite (194). Nucleosome density in *Plasmodium* parasites contributes to the accessibility of chromatin in a manner congruent to that occurring in higher eukaryotes. NDRs are frequently observed in promoters with a greater degree of nucleosome depletion corresponding to greater transcriptional activity. However, these NDRs are atypical in that they are not flanked by strongly-positioned +1 nucleosomes, rather these nucleosomes are present at the starts and ends of coding regions (195-199). In addition to the dynamic positioning and structure of nucleosomes, an array of histone modifying enzymes that expand the regulatory capacity of these basic chromatin units have been described for *Plasmodium* parasites.

1.6.2 Histone modifying enzymes in *P. falciparum*

As in model organisms, the writers and erasers of acetyl and methyl histone PTMs are the most extensively studied. To date, four HAT-encoding genes (*hat1*, PF3D7_0416400; *gcn5*, PF3D7_0823300; *myst*, PF3D7_1118600 and PF3D7_0809500) have been identified in *P.*

falciparum parasites (200). Although the site specificity of *P. falciparum* HAT1 remains to be elucidated, homologs in higher eukaryotes acetylate the H4K5 and H4K12 residues to distinguish newly synthesised histones (201, 202). The acetyltransferase activities of GCN5 and MYST are specific to the lysine residues of H3 and H4, respectively (203, 204).

Table 1.1. Histone methyltransferases and demethylases in *P. falciparum* parasites

Protein	Gene ID	Site of activity and function (and reference)
		Histone methyltransferases
SET1	PF3D7_0629700	Writer of H3K4me3 (200)
SET2 (SETvs)	PF3D7_1322100	Writer of H3K36me2&3, *var* gene regulation (205, 206)
SET3	PF3D7_0827800	Writer of H3K9me2&3 (207-209)
SET4	PF3D7_0910000	Writer of H3K4 PTMs (200, 208)
SET5	PF3D7_1214200	Unknown (200)
SET6	PF3D7_1355300	Writer of H3K4 PTMs (200, 208)
SET7	PF3D7_1115200	Writer of H3K4, H3K9 and H3K27 PTMs (*in vitro*) (200, 210)
SET8	PF3D7_0403900	Writer of H4K20me1&2&3 (200, 205, 207)
SET9	PF3D7_0508100	Unknown (200)
SET10	PF3D7_1221000	Writer of H3K4me3, present at expressed *var* gene (200, 211)
		Histone demethylases
JMJC1	PF3D7_0809900	Eraser of H3K9 and H3K36 PTMs (200, 205)
JMJC2	PF3D7_0602800	Unknown (200, 205)
JMJ3	PF3D7_1122200	Eraser of H3K36 PTMs (200, 212)
LSD1	PF3D7_1211600	(200, 208)

HAT activity is antagonised by the five HDACs present in *P. falciparum* parasites: HDA1 (PF3D7_1472200) HDAC1 (PF3D7_0925700), HDA2 (PF3D7_1008000), SIR2A (PF3D7_1328800) and SIR2B (PF3D7_1451400). During commitment, transcript abundance increases for *hda1* and

decreases for *hdac1,* congruent with the respective sexual and asexual stage-specific roles of these HDACs (87, 134). The *P. falciparum* genome encodes ten HMTs, all of which belong to the evolutionarily conserved SET (Su(var)3-9, Enhancer of Zeste and Trithorax) domain-containing protein family (200). The site specificities of all, except two (SET5 and SET9) of these HMTs have been determined (Table 1.1). Both SET2, SET3 and SET10 are implicated in the regulation of expression of the multi-gene families that contribute to invasion, host cell remodelling and nutrient transport (205, 206, 211). Less is known regarding the three Jumonji-C (JmjC) domain-containing HDMs and the one lysine-specific demethylase 1 (LSD1) in *P. falciparum* however, JMJC1 and JMJ3 both have H3K36-specificty (Table 1.1) (200, 212). Together, these histone modifying enzymes generate an extensive *P. falciparum* parasite histone PTM landscape that is interpreted by the reader proteins that will be discussed next.

1.6.3 Histone post-translation modification reader proteins in *P. falciparum* parasites

The deposition and removal of histone PTMs in *Plasmodium* parasites, as in other eukaryotes, may result in the physical disruption of histone-DNA interactions thereby leading to altered chromatin structure (143, 182). Alternatively, histone PTMs may be recognised by epigenetic "reader" complexes which mediate chromatin reorganisation. To date, 28 putative histone PTM reader complexes have been identified in *P. falciparum* parasites (Table 1.2) however, only a few of these have been functionally validated (213). The bromodomain (BDP)-containing and PHD (plant homeodomain) finger domain-containing protein groups are the largest of the reader protein families with eight and ten members, respectively. The importance of these families, particularly the BDP-containing proteins, is evident from the proportion of these readers that are essential or result in a growth defect when genetically disrupted (Table 1.2).

Table 1.2. Epigenetic reader protein families in *P. falciparum* parasites. Proteins and corresponding genes in bold font have confirmed histone reader-specific functions. Compiled from data in (89, 205, 211, 213).

Protein	Gene ID	*P. falciparum* asexual parasites	Curated reader-specific functions
Bromodomains – Acetylated histone binding			
SET1	**PF3D7_0629700**	Essential	Regulation of transcription
GCN5	**PF3D7_0823300**	Growth defect	Regulation of transcription
BDP1	**PF3D7_1033700**	Essential	Chromatin/histone binding
BDP2	**PF3D7_1212900**	Essential	Protein binding
BDP3	PF3D7_0110500	Dispensable	-
BDP4	PF3D7_1475600	Growth defect	-
BDP5/TAF1	PF3D7_1234100	Growth defect	-
BDP6	PF3D7_0724700	Essential	-
PHD finger – Methylated (some acetylated) histone binding			
SET1	**PF3D7_0629700**	Essential	Regulation of transcription
SET2	**PF3D7_1322100**	Dispensable	Regulation of transcription
SET10	**PF3D7_1221000**	Dispensable	Regulation of transcription
PHD1	**PF3D7_1008100**	Growth defect	Modified H3K4 binding
PHD2	PF3D7_1433400	Essential	-
PHD finger protein	PF3D7_0310200	Dispensable	-
E3 SUMO protein ligase	**PF3D7_1360700**	Essential	Histone binding
EELM2	PF3D7_1141800	Dispensable	-
Zinc finger protein	PF3D7_0420000	Dispensable	-
LSD1	PF3D7_1211600	Dispensable	-
Chromodomain-like – Methylated histone binding			
HP1	PF3D7_1220900	Essential	Modified H3K9 binding
MYST	PF3D7_1118600	Essential	Histone binding
Chromodomain protein	PF3D7_1140700	Dispensable	Histone binding

CHD1	PF3D7_1023900	Dispensable	Modified H3K9 binding
14-3-3 – Phosphorylated histone binding			
14-3-3I	**PF3D7_0818200**	Growth defect	Modified H3K28 binding
14-3-3II	PF3D7_1362100	Growth defect	-
14-3-3 protein	PF3D7_1422900	Growth defect	-

Bromodomain protein 1 (BDP1) specifically binds to acetylated lysine residues where an interaction with a second domain-containing protein (BDP2) and the AP2-I TF contribute to the mutually exclusive transcription of only the active *var* gene (119, 214, 215). In addition to a catalytic SET domain, SET10 also contains a PHD domain that has been implicated in *var* gene regulation during asexual proliferation (211). Although less widely studied to date, phosphorylated histones and specifically H3S28ph, are known to be read by the 14-3-3I protein in *P. falciparum* parasites (216). Except for these examples, the reader-specific roles of these proteins in *Plasmodium* remain largely uncharacterised. Specific functional predictions relating to modified histone binding are putatively assigned based on reader protein domain homology and function in model organisms (Table 1.2). With a few exceptions, such as recruitment of independent HP1 and PHD1 by tri-methylated H3K9 and H3K4, respectively, many *P. falciparum* reader proteins exist in complexes with other readers and/or TFs that would presumably require sequential binding occurrences for recruitment (213). Such cooperation between epigenetic regulatory proteins is exemplified in the recruitment of the GCN5/ADA2 reader complex to H3K4me3 through an interaction with PHD1 followed by the subsequent GCN5-catalysed acetylation of H3K9 (213, 217). Collectively, these histone reader proteins orchestrate chromatin and transcriptional dynamics throughout the *P. falciparum* parasite life cycle.

1.6.4 The *P. falciparum* histone post-translational modification landscape

Mass spectrometry has been widely used to quantitatively identify histone PTMs and capture their dynamic profiles across the *Plasmodium* life cycle (133, 151, 184, 218, 219). The N-terminal PTMs detected include the acetylation, methylation, phosphorylation, ubiquitylation and

SUMOylation of all the canonical and variant histone proteins (Figure 1.7) (133, 151, 184, 200, 203-205, 216, 220-224).

Figure 1.7: Histone PTMs identified in *P. falciparum* parasites. Map of histone PTMs identified to date across various asexual and sexual life cycle stages in *P. falciparum* parasites. Acetylated, phosphorylated, mono-, di- and tri-methylated methylated, sumoylated and ubiquitinated sites are shown with amino acid (K = lysine, S = serine, R = arginine, T= threonine, A = alanine, Y = tyrosine) residues numbered starting from the N-terminal end of histone tails. Each of the four canonical (H2A, H2B, H3 and H4 in bold) and four variant histones (H2A.Z, H2Bv, H3.3 and HCen) are shown. Data compiled from various published sources (133, 184, 200, 218-222, 224-226).

The most recent and comprehensive study to date identified 106 individual modifications that constitute the histone PTM landscape of the asexual and sexual intraerythrocytic stages of *P. falciparum* parasites (133). Typical euchromatic histone PTMs that have been identified and are positively correlated with transcription include H3K8ac, H3K9ac, H3K14ac, H3K56ac and H4ac

and tri-methylation of H3K4 and H4K20 (Figure 1.7) (184, 218). Notwithstanding telomeres and the interior chromosomal regions that contribute to antigenic variability, nutrient import and sexual commitment, the majority of the genome is marked by euchromatic histone PTMs that maintain transcriptional permissivity during asexual proliferation (89, 135, 209, 218, 227). For example, H3K4me3 and H3K9ac frequently and dynamically occupy intergenic regions that are stably demarcated by H2A. H3K9ac abundance strongly correlates with transcription throughout the IDC, contrasting with the stage-specific enrichment of H3K4ac (188). Furthermore, H3K9ac has a distinct regulatory role in the expression of immune evasion proteins by recruiting BDP1 to *var* gene promoters where it interacts with the TF AP2-I to regulate expression (119, 214).

By contrast, fewer histone PTMs with confirmed or postulated repressive functions have been identified in *Plasmodium* parasites and include H3K9me3 and the di- and tri-methylation of H3K27 and H3K36 (133, 218, 219). H3K9me3 was the most well-studied of these to date given the prominence and function of this histone PTM in generating and maintaining heterochromatin in the asexual and sexual stages. Specifically, H3K9me3 plays an important role in regulating clonally variant gene expression during asexual proliferation (89, 132, 135). Furthermore, H3K9me3/HP1-mediated heterochromatin expands during gametocyte development, giving rise to a chromatin state that is indicative of the transition from asexual proliferation to the more nuanced process of differentiation (133, 135, 218, 219, 228).

Each of the asexual and sexual stages of the *P. falciparum* parasite life cycle is characterised by the notable abundance of a unique subset of histone PTMs (Figure 1.8) (133). For example, gene expression becomes increasingly more active as the asexual IDC proceeds (93) with this reflected by an accumulation of activating histone PTMs such as H3K9ac in trophozoites and H3K27ac and H3K4me3 in schizonts (Figure 1.8) (133). By contrast, early (stage I-III) and late (stage IV/V) gametocytes are associated with a greater abundance of repressive histone PTMs including H3K27me2&3 and H3K9me3, respectively (133).

Aside from H3K9me3, the relevance of histone PTMs for sexual differentiation and development remains largely unknown. Nevertheless, the dynamics and plasticity described for the histone

PTM landscape in gametocytes point towards a crucial role for epigenetic regulation throughout the development of the transmissible stages of the *Plasmodium* parasite life cycle.

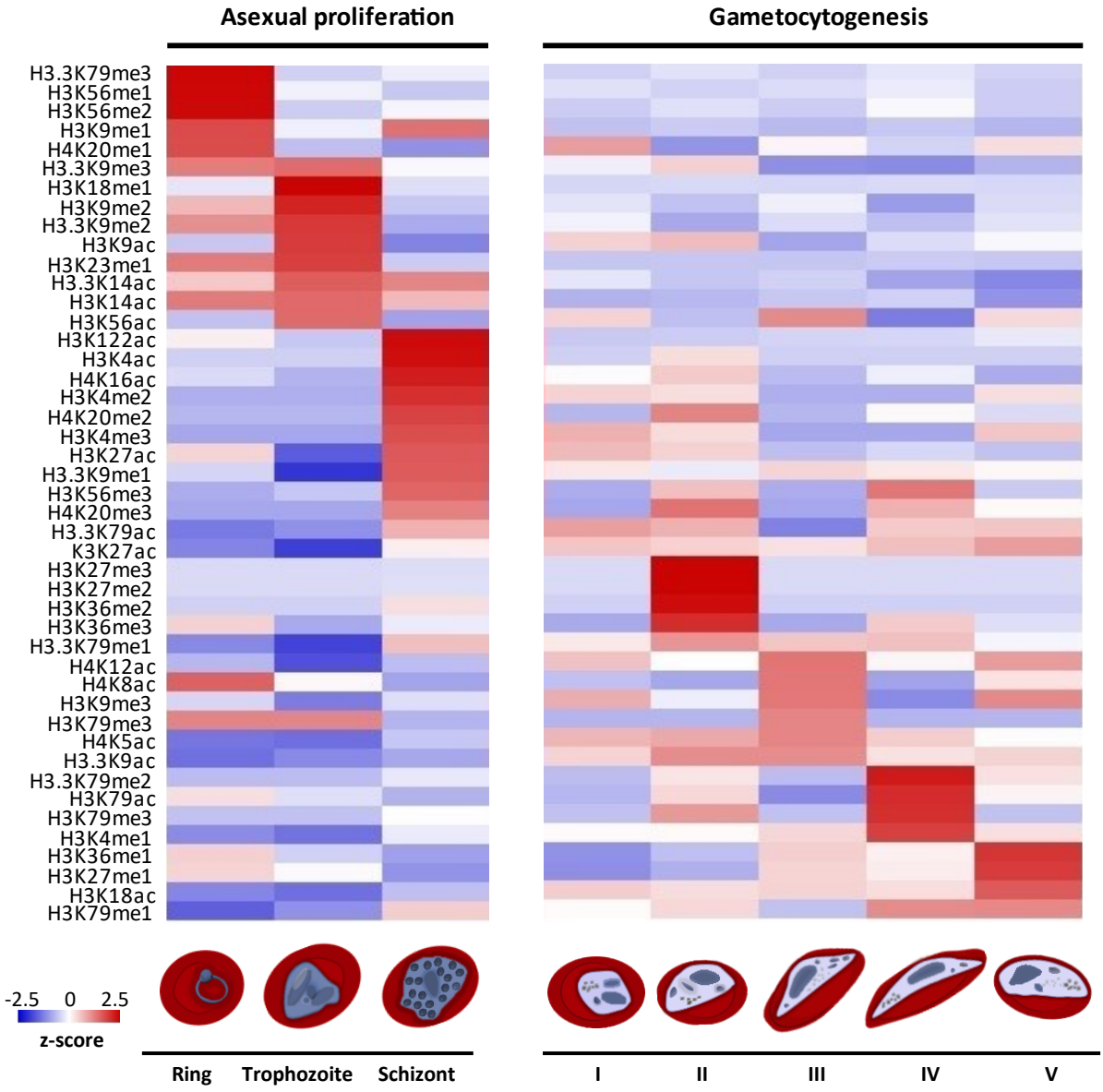

Figure 1.8: Specific histone post-translational modification sets define the asexual and sexual stages of the *P. falciparum* life cycle. The relative abundance of histone PTMs in ring, trophozoite and schizont stage parasites associated with asexual proliferation and in the stage I-IV gametocytes. Relative abundance represents z-score values for each histone PTM. Data obtained from (133).

Specifically, di- and tri-methylated H3K27 and H3K36 display a striking and intriguing increase in abundance in stage II gametocytes (Figure 1.9a) (133). Although present in the other sexual and

asexual stages, the levels of these PTMs are relatively low, suggesting a stage II gametocyte-specific function. Although the writer (SET2) and erasers (JMJC1 and JMJ3) of H3K36me2&3 have been elucidated in *P. falciparum* asexual parasites (200, 206, 212), the HMT and HDM enzymes involved in H3K27me2&3 deposition and removal remain unclear (Figure 1.9b).

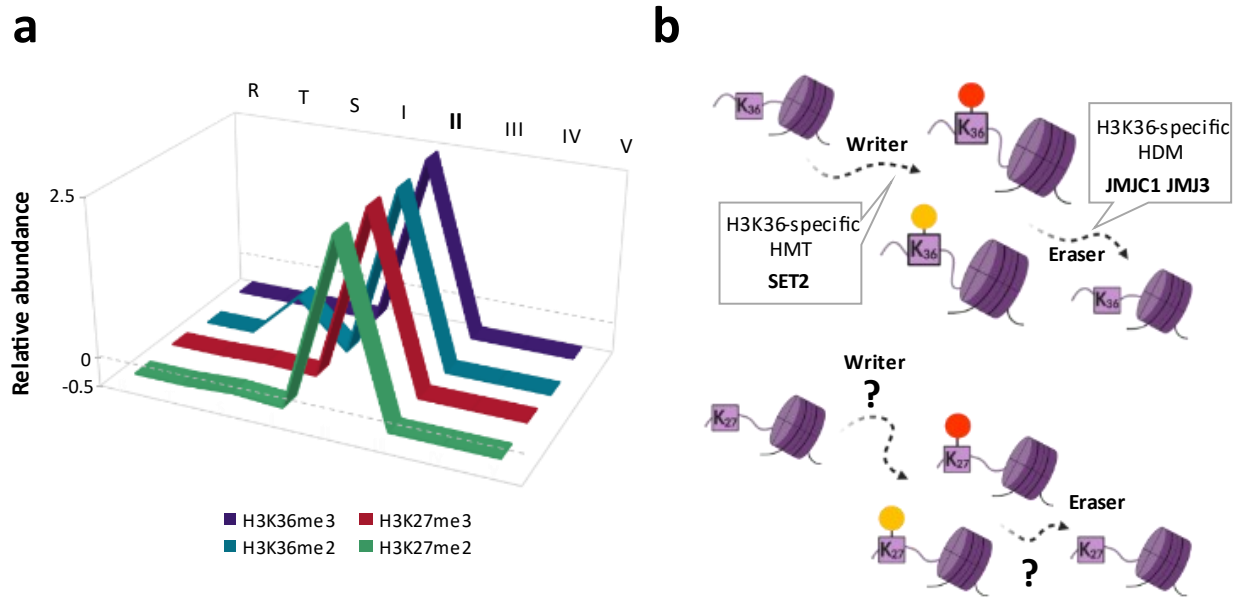

Figure 1.9: Di- and tri-methylated H3K27 and H3K36 are strikingly abundant in the *P. falciparum* stage II gametocytes. (a) The relative abundance, expressed as z-scores, of H3K27 and H3K36 di- and tri-methylation during asexual proliferation (R: ring-, T: trophozoite- and S: schizont-stage parasites) and gametocyte development (stages I-V) highlights the peak levels of these histone PTMs occur in the stage II gametocytes. **(b)** The H3K36-specific histone methyltransferase (HMT) writer protein SET2 and histone demethylase (HDM) eraser proteins JMJC1 and JMJC3 deposit and remove di- and tri-methyl modifications in *P. falciparum* asexual parasites, respectively. The writer and eraser proteins that deposit and remove methylation from H3K27 in *P. falciparum* currently remain elusive (?).

In model organisms the fate- and differentiation-specific roles of H3K27me2&3 and H3K36me2&3 have been extensively described (229-233). This raises several interesting questions: 1) Are di- and tri-methylated H3K27 and H3K36 functionally relevant for gene activation or repression in gametocytes? 2) Are H3K27me2&3 and H3K36me2&3 involved in the transcriptional reprogramming that occurs during the transition from early gametocyte differentiation (stage I) to intermediate development (stage III)? 3) Do these PTMs cooperate with or antagonise one another and/or other epigenetic regulatory mechanisms? and 4) What is the effect of disrupting these stage II gametocyte-specific histone PTM patterns? Answering

these questions would not only shed light on the specific histone PTMs but also provide a basis for understanding epigenetic regulation during gametocyte development.

The work presented in this thesis focuses on the involvement of histone methylation in transcriptional regulation at the key transition point between early gametocyte differentiation and intermediate development. The novelty of this work is underpinned by the sexual stage-specific investigation of H3K27me2&3 and H3K36me2&3, the former of which had not previously been functionally interrogated and, until recently (133), was thought to be absent in *Plasmodium* parasites. The use of chemical inhibitors as tools to highlight the crucial nature of histone methylation during sexual development provides a foundation for further studies of other histone PTMs and the epigenetic readers, writers and erasers involved in *Plasmodium* sexual development. Ultimately, this thesis contributes to a greater, more thorough understanding of the biology of the deadliest human malaria parasite.

1.7 Hypothesis

H3K27me2&3 and H3K36me2&3 independently reprogram transcription to define the transition from early differentiation to intermediate development in *P. falciparum* gametocytes.

1.8 Aim

This study aimed to elucidate the genome-wide occupancy and enrichment of H3K27me2&3 and H3K36me2&3 and investigate their functional relevance for transcriptional reprogramming during the transition from early gametocyte differentiation to intermediate development.

1.9 Objectives

1. Map the genome-wide occupancy of H3K27me2&3 in early and intermediate gametocytes using ChIP-seq and investigate the functional relevance of these histone

PTMs by integrating this data with chemical interrogation and transcriptome analyses (Chapter 2).

2. Map the genome-wide occupancy of H3K36me2&3 during early and intermediate gametocyte development with ChIP-seq and investigate the function of these histone PTMs using chemical interrogation and transcriptome analysis (Chapter 3).

3. Deconvolute and differentiate the specific regulatory roles of H3K27me27&3 and H3K36me2&3 enrichment in the stage II gametocytes by integrating ChIP-seq and transcriptional profiling analyses (Chapter 4).

1.10 Research outputs

Peer-reviewed manuscripts:

1. Connacher, J., Josling, G.A., Orchard, L.M., Reader, J., Llinás, L. and Birkholtz, L.M. H3K36 methylation reprograms gene expression to drive early gametocyte development in *Plasmodium falciparum*, Epigenetics & Chromatin, 2021;14(1):19 (Chapter 3).
2. Reader, J., van der Watt, M.E., Taylor, D., Le Manach, C., Mittal, N., Ottilie, S., Theron, A., Moyo, P., Erlank, E., Nardini, L., Venter, N., Lauterbach, S., Bezuidenhout, B., Horatscheck, A., van Heerden, A., Spillman, N.J., Cowell, A.N., Connacher, J., Opperman, D., Orchard, L.M., Llinás, M., Istvan, E.S., Boyle, G.A., Calvo, D., Mancama, D., Coetzer, T.L., Winzeler, E.A., Duffy, J., Koekemoer, L.L., Basarab, G., Chibale, K. and Birkholtz, L.M. Multistage and transmission-blocking targeted antimalarials discovered from the open-source MMV Pandemic Response Box. Nature Communications, 2021;12(1):269 (parts of Chapter 3).
3. The work presented in Chapter 2 is currently being prepared as a manuscript for submission to the Journal of Epigenetics and Chromatin.

Conference proceedings:

1. Connacher, J., Josling, G.A., Llinas, M. and Birkholtz, L.M. Epigenetic control of gametocyte development in *Plasmodium falciparum* through unique repressive markers of gene expression. Poster presentation at BioMalPar XV, Heidelberg, Germany (May 2019).
2. Connacher, J., Josling, G.A., Llinas, M. and Birkholtz, L.M. Regulation of gametocyte development in *Plasmodium falciparum* through unique repressive markers of gene expression. Oral presentation at the 5th Malaria Research Conference. Pretoria, South Africa (July 2019).
3. Connacher, J., Josling, G.A., Llinas, M. and Birkholtz, L.M. Epigenetic control of gametocyte development in *Plasmodium falciparum* through unique repressive markers of gene expression. Poster presentation at Molecular Parasitology Meeting. Woods Hole, MA, USA (September 2019).

Chapter 2

H3K27me2&3 reprogram gene expression to drive early gametocyte development in *Plasmodium falciparum*

2.1 Introduction

Epigenetics describes any alterations to genes and chromosomes that do not arise from changes in the DNA sequence (234). Histone proteins and their PTMs are key factors involved in the generation and maintenance of specific chromatin landscapes throughout the cell cycle and in terminally differentiated cells (235). Histones can be modified by an extensive array of PTMs including acetylation, methylation and phosphorylation with the distal N-terminal tail of the protein containing the greatest density of modifiable sites (144, 172). Histone lysine methylation, identified at six different sites (H3K4, H3K9, H3K27, H3K36, H3K79 and H4K20) to date in eukaryotes, is arguably one of the most complex yet interesting PTMs. Histones may undergo mono-, di- or tri-methylation, yielding one of three different states each of which specify a unique functional outcome with this additionally dependent on the position of the PTM within the N-terminal tail (144, 152). For example, H3K4me3 is associated with gene activation (236) while the presence of tri-methylated H3K27 is predictive of transcriptional repression (237).

H3K27 is one site of histone methylation that has been extensively studied in eukaryotes and each of the three methylation states has been associated unique functions. Mono-methylated H3K27 is regulated by SET2-dependent H3K36me3 and thus accumulates within active coding regions where it promotes transcription (Figure 2.1) (238). The effects of the more highly methylated states of H3K27 (i.e. H3K27me2&3) have been described previously as both dramatic and predictable (239-241) with well-defined roles in transcriptional repression, particularly during cellular differentiation and development (240-242).

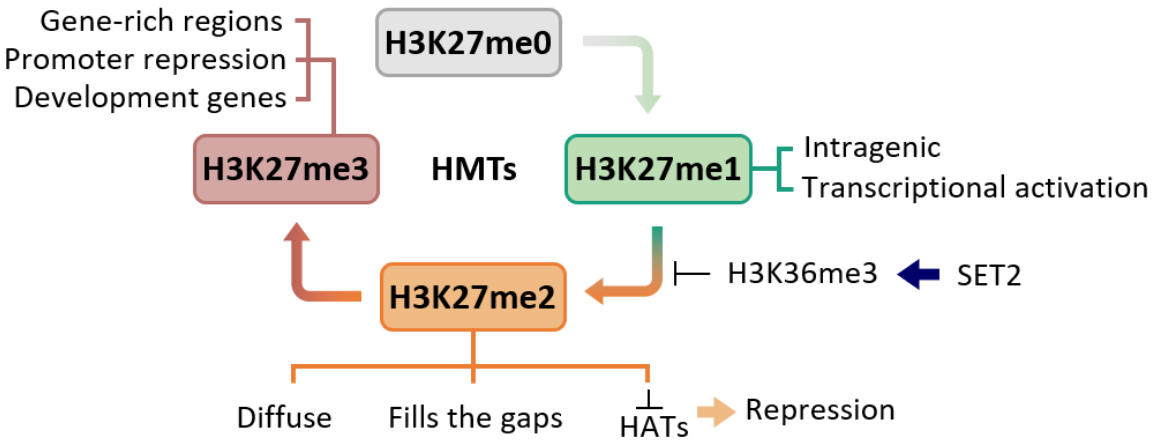

Figure 2.1: H3K27 methylation states and their unique functions in eukaryotic transcriptional regulation. H3K27 may exist unmethylated (me0) or in the mono-, di- or tri-methylated (me1, me2, and me3, respectively) states in eukaryotic cells. These methylated states are generated by histone methyltransferases (HMTs). SET2-dependent H3K36me3 antagonises the further methylation of H3K27me1. H3K27me2 mediates transcriptional repression through the inhibition of histone acetyltransferase (HAT) activity. H3K27me3 is present at the promoters of developmental genes during cellular differentiation. Figure was created using published data from various sources (238-243).

H3K27me2 has been described as widely diffuse, present on ~70% of histone H3 proteins in murine embryonic stem cells (ESCs) and is involved in silencing the regulatory regions of cell type-specific gene sets (Figure 2.1) (238). Research on other eukaryotic species indicates that di-methylation is the most abundant of the three H3K27 methylation states in ESCs with this histone PTM "filling the gaps" between regions of H3K27me3-associated chromatin (243). Additionally, H3K27me2 impedes the activity of HATs at enhancer sites that become active only during differentiation, thereby contributing to the maintenance of cell pluripotency (238, 239, 244).

Similarly, H3K27me3 is repressive with the presence of this histone PTM at promoter and enhancer regions indicative of transcriptional inactivity (239-241). H3K27me3 is typically associated with gene-rich regions of DNA in contrast to H3K9me3 that mediates the repression of non-genic regions (240, 241). In pluripotent cells, H3K27me3 is present at the promoters of developmental regulators such as the *Hox* and *Sox* gene families that are activated and drive differentiation following cell fate determination (Figure 2.1) (240, 241, 245). Thereafter, H3K27me3 silences gene sets that become irrelevant to the particular developmental pathway required by the differentiating cell (231, 246, 247). Therefore, H3K27me3 distribution and activity are highly dependent on tissue type (248).

Histone methylation and demethylation are regulated by site-specific writer HMTs and eraser HDMs, respectively (101). The multimeric Polycomb repressive complex 2 (PRC2) is assembled from the evolutionarily conserved Polycomb group (PcG) of protein subunits and is the ubiquitous writer of H3K27 methyl PTMs in eukaryotes (249-251). Eukaryotic H3K27-specific HDMs belong to the Jumonji-C domaining-containing UTX (Ubiquitously Transcribed tetratricopeptide repeat, X chromosome) and JMJD3 HDM families (229, 252, 253). A broad array of reader proteins and complexes that recognise site-specific histone methylation and subsequently effect changes in gene expression and chromatin state have been described (254, 255). While the readers of methylated H3K27 are less well-conserved compared to the HMTs and HDMs that deposit and remove these histone PTMs, these recognition complexes typically all contain the conserved site-specific methyl lysine chromo-domains that are present in mammalian chromo-box (CBX) protein complexes (256, 257).

Until recently, H3K27me2&3 were thought to be absent in *Plasmodium* parasites however, these studies focused solely on the asexual parasite stages (218, 219, 221, 258). Moreover, this was supported by the absence of PRC2 subunit homologs in *Plasmodium* species (200). Since then, however, both H3K27me2&3 have been detected almost exclusively in the *P. falciparum* stage II gametocyte stages through stringent quantitative mass spectrometry (133). Supporting this, *P. falciparum* SET7 is able to further methylate H3K27me2 forming the tri-methylated state of H3K27 *in vitro* (210). H3K27me2&3 occupancy is dynamic in the gametocytes with enrichment in the stage II gametocytes (133) suggesting the typical eukaryotic link between these histone PTMs and cellular differentiation (238, 240, 242, 243, 245, 246, 249, 251, 252, 257) is conserved in *P. falciparum* gametocytes. While the transcriptional transitions in gametocytes have been delineated (94, 259), the mechanisms driving these shifts remain largely unknown. Nevertheless, one mechanism that has been relatively well-studied across all the stages of the *P. falciparum* life cycle is H3K9me3 (135, 184, 188, 209, 221, 227, 260). In addition to regulating virulence gene expression, H3K9me3 also recruits the heterochromatin protein1 (HP1) that silences sexual commitment-specific genes during the asexual proliferative cycle (227, 260). Following the induction of gametocytogenesis, H3K9me3/HP1 is displaced, allowing for the expression of proteins that drive the commitment and early differentiation of gametocytes (89, 90).

Thereafter, H3K9me3/HP1 patterns are regenerated, bringing about heterochromatin organisation that supports subsequent developmental steps (135).

During cellular differentiation in model eukaryotes, H3K9me3 and H3K27me2/3 are non-redundantly associated with transcriptional silencing as a result of their variable genomic distributions, temporality and mechanisms of repression (261). H3K9me3 domains are more prominent during late differentiation and are associated with constitutive heterochromatin that inhibits transcription factor binding (262-266). By contrast, H3K27me2&3 are typically found in facultative heterochromatin that is indicative of silenced but poised genes and is more commonly involved in transcriptional reprogramming during the early and intermediate stages of differentiation (232, 240, 266-270). As H3K27me2&3 are highly abundant in stage II gametocytes, we therefore postulated that these histone PTMs may have similar repressive functions in *P. falciparum* gametocytes and complement the H3K9me3-associated silencing that, as in other organisms, becomes increasingly prevalent in the later stages of gametocyte differentiation (132, 135).

To investigate this, ChIP-seq was performed on three distinct *P. falciparum* gametocyte populations spanning stage II gametocyte development. This approach enabled the profiling of the H3K27me2&3 occupancy dynamics during the early and intermediate gametocyte stages and confirmed the enrichment of H3K27me2&3 in the stage II gametocytes. By leveraging existing data sets from other ChIP-seq and gene expression studies (94, 135), H3K27me2&3 are shown to be associated with the transcriptional repression of stage-specific gene sets during *P. falciparum* gametocyte differentiation. Furthermore, the variation between these histone PTMs and H3K9me3 was examined, revealing largely independent positioning and function for H3K27me2&3 during early gametocyte development. Finally, profiling the transcriptional perturbations arising from the treatment of early gametocytes with HMT inhibitors (HMTi) demonstrated the crucial importance of normal histone PTM patterns during *P. falciparum* gametocyte differentiation and development. The novelty of the results presented in this chapter are evident as the first description of the functional relevance of H3K27me2&3 in *Plasmodium* parasites. Ultimately, the findings presented here extend the current knowledge relating to *P. falciparum* epigenetic mechanisms and contribute to a greater understanding of

the foundational biology of the gametocytes that are essential for the continued transmission of malaria.

2.2 Materials and methods

2.2.1 *In vitro* parasite culturing

P. falciparum NF54 asexual parasite cultures were maintained *in vitro* at 37°C in human erythrocytes at a 5% haematocrit (ethics approval obtained from the University of Pretoria Research Ethics Committee, Health Sciences Faculty 506/2018) and synchronised using 5% (w/v) D-sorbitol as described elsewhere (271, 272). *P. falciparum* gametocytes were induced as described (273-275) via a combination of nutrient starvation and a drop in haematocrit from synchronous asexual parasite cultures (≥95% ring stages, 0.5% parasitaemia at 6% haematocrit). Culture media (RPMI-1640, 23.8 mM Na_2CO_3, 0.024 mg/ml gentamycin, 25 mM HEPES, 0.2 mM hypoxanthine and 0.5% (w/v) Albumax II) was replaced 48 h after initiation. The haematocrit was reduced to 4% 72 h after initiation (day 0) and maintained as such throughout gametocyte development with daily replacement of glucose-enriched (20 mM) media. Residual asexual parasites were removed by supplementing media with 50 mM *N*-acetylglucosamine (NAG, Sigma-Aldrich) from day 1 of development. Gametocytes were sampled on days 2, 4 and 7 post-induction as the pre-stage II, stage II and post-stage II samples, respectively. Two independent cultures were prepared as biological replicates for each of the ChIP-seq and ChIP-qPCR experiments. Independent cultures were generated for microarrays and the histone methylation analyses with each sample for these experiments having a single biological replicate. Gametocytaemia and gametocyte stage composition was determined by microscopically evaluating Giemsa-stained smears of the cultures.

2.2.2 H3K27me2&3 ChIP antibody validation

The ability of commercially obtained ChIP-grade rabbit α-H3K27me2 (Millipore, 07-449) and α-H3K27me3 (Millipore, 07-421) antibodies to detect modified histone H3 in *Plasmodium* was

determined using modified and unmodified synthetic peptides (Genscript) designed to contain the *P. falciparum* histone H3 sequence (Appendix: Table S1). Modified peptides were designed and synthesised to contain di- or tri-methyl modifications at K9, K27 or K36 and corresponding unmodified peptides for K9 (ARTKQTARKSTAGKAPRKQ), K27 (ARKSAPISAGIKKPHRYRPG) and K36 (ARKSAPISAGIKKPHRYRPG) were included to test a broader range of specificities. Nitrocellulose membranes were spotted with each peptide (25 ng) and then blocked for 30 min in blocking buffer (5% milk powder in TBS-t [50 mM Tris (pH 7.5), 150 mM NaCl and 0.1% (v/v) tween-20]). Membranes were then incubated overnight in a 1:5000 dilution of the respective primary antibodies (α-H3K27me2 or α-H3K27me3 in TBS-t) followed 1 h incubation with horse radish peroxidase (HRP)-conjugated rabbit α-IgG (Abcam, ab6721) secondary antibody (1:10000) in TBS-t. Thereafter, signal intensity obtained from Super Signal West Pico PLUS Substrate (Pierce) was quantified using densitometry and ImageJ analysis software (276).

2.2.3 H3K27me2&3 chromatin immunoprecipitation

ChIP was performed as described previously (52) with modifications. Gametocytes (1-3% gametocytaemia, fixed in 1% formaldehyde for 10 min at 37°C followed by 0.125 mM glycine quenching) were released from erythrocytes using 0.1% (w/v) saponin. Thereafter, the gametocytes were resuspended in lysis buffer (10 mM Hepes (pH 7.9), 10 mM KCl, 0.1 mM EDTA (pH 8.0), 0.1 mM EGTA (pH 8.0)) and lysed with 0.25% Nonidet P-40 by douncing. Nuclei were then resuspended in Covaris shearing buffer (0.1% sodium dodecyl sulfate (SDS), 10 mM Tris (pH 8.1), 1 mM EDTA) and sonicated using a 5% duty cycle at 75 W peak incident power; 200 cycles per burst for a total treatment time of 300 s using a M220 ultrasonicator (Covaris). The sonicated chromatin was then pre-cleared using Protein A/G magnetic beads (Millipore 16-663) and aside from a small quantity kept separately as input material, chromatin was incubated overnight with 3 µg of α-H3K27me2 or α-H3K27me3. Reversal of cross-linking was achieved by adding 0.2 M NaCl followed by a 30 min RNAseA (12 µg, Promega) and 2 h Proteinase K (12 µg, Sigma) treatment carried out at 37°C and 45°C, respectively. DNA was purified using the Qiagen MinElute kit and used to prepare DNA libraries for sequencing and qPCR validation.

2.2.4 DNA library preparation and sequencing

DNA libraries were prepared for sequencing as described elsewhere (52). End-repair and A-tailing of DNA fragments were achieved using NEBNext End Repair Enzyme Mix (#E6051A) with 30 min incubation at 20°C and NEBNext 3'-5' exo Klenow fragment (#E6054A) for 30 min at 37°C, respectively. Indexed adaptors (NEXTflex DNA-Seq barcoded adaptors) were ligated (NEB Quick Ligase, #M2200L) to fragments (10 min at 20°C) that were then size selected (250 bp) using 0.7x AMPure XP beads (Beckman Coulter). The selected fragments were amplified using KAPA HiFi with dNTPs and NEXTflex primer mix (#NOVA-514107-96) with 12 cycles of the following program: 98°C for 1 min; 98°C for 10 sec; 65°C for 1 min followed by a final extension step at 65°C for 5 min. The PCR products were purified (0.9x AMPure XP beads) and quantified using the Qubit fluorometer HS (high sensitivity) DNA kit. DNA quality and purity were assessed by means of the DNA 1000 Bioanalyser kit prior to sequencing using a Illumina HiSeq 2500.

2.2.5 ChIP-qPCR

ChIP-qPCR was performed to validate ChIP-seq data using several randomly selected genomic loci. Firstly, to determine primer efficiency and specificity a 4-point serial dilution (10x) of *P. falciparum* NF54 genomic DNA and 6 µM of the primer pairs (equal concentrations of each individual primer) were prepared in a MicroAMP optical 96-well reaction plate (Applied Biosystems) containing Power SYBR Green PCR Master Mix (Life Technologies) and the passive reference dye, ROX (Applied Biosystems). Thereafter, the DNA was subjected to a 2 min dissociation step (56°C), a 10 min hold at 95°C and then 40 cycles of 95°C for 15 sec; 56°C for 1 min using the Applied Biosystems 7500 Real-Time PCR machine. Only the primer pairs with ≥90% efficiency and specificity, evidenced by single peaks (indicative of single amplicons) on the melting curves, were used for ChIP-qPCR. using same input and immunoprecipitated samples (two biological replicates for each) that were prepared for ChIP-seq. Amplification of each sample (two biological replicates for each input and immunoprecipitated), standard and negative control was performed in technical triplicate under the same conditions used to generate the primer melting curves using the 7500 R-T PCR machine and SDS v1.4. The ΔΔCt method (i.e. cycle

threshold at which the signal of sample (reporter dye, SYBR green) becomes detectable above background (ROX reference dye) was used to determine fold enrichment for H3K27me2&3 at the amplified sites. Values are expressed as fold enrichment of immunoprecipitated to input DNA, averaged for two biological replicates.

2.2.6 Epigenetic inhibitor assays

The parasite lactate dehydrogenase (pLDH) assay (277) was used to evaluate the *in vitro* activity of nine histone methyltransferase inhibitors from the Cayman Epigenetic Screening Library (Cayman Chemicals, #11076, batch 0498084-1) against early gametocytes as previously described (274). The pLDH assay leverages the spectrophotometric detection of the *P. falciparum* parasite's utilisation of 3-acetyl pyridine adenine dinucleotide (APAD) as a coenzyme for LDH during lactate to pyruvate conversion (277, 278). The epigenetic inhibitor compounds were dissolved in dimethyl sulfoxide (DMSO) and culture media to obtain <0.5% final DMSO concentration (non-toxic to gametocytes) (274) and final drug concentrations of 5 µM. Additionally, methylene blue (5 µM) was included as a treatment control for inhibition. These drug dilutions were screened in technical triplicate against pre-stage II (days 2 and 3 cultures for two replicate data sets spanning pre-stage II development) and II gametocytes (days 4 and 5 for stage II gametocyte replicates) for 72 h along with an untreated 100% growth control. Following this, media was replaced and gametocytes were incubated for an additional 72 h after which the assay plates were placed at -20°C for ≥24 h. Thereafter, the contents of the plates were thawed, resuspended and 20 µL from each well was added to 100 µL of Malstat reagent (0.21% v/v Triton-100, 222 mM L-(+)-lactic acid, 54.5 mM Tris, 0.166 mM APAD (Sigma Aldrich), pH 9) in a new 96-well plate. To this, 25 µL of PES/NBT (0.239 mM phenazine ethosulphate/1.96 mM nitro blue tetrazoliumchloride) was added followed by the measurement of absorbance at 620 nm using a Multiskan Ascent 354 multi-plate reader (Thermo Labsystems). Gametocyte viability (%) was determined using the equation:

$$Gametocyte\ viability = \frac{Mean_{compound} - Mean_{background}}{Mean_{+\ growth\ control} - Mean_{background}}$$

Data are reported as the % gametocyte inhibition:

$$Gametocyte\ inhibition\ (\%) = 100 - gametocyte\ viability$$

2.2.7 Detection of changes in global H3K27me2&3

Stage II gametocytes (days 3, 4 and 5) were treated with 5 µM of the mammalian G9a inhibitor UNC0224 or the EZH2 inhibitor GSK343 (Cayman Chemicals) and sampled 24 h later. Histones were extracted as described before (184) with minor modifications. Nuclei were extracted by Dounce homogenisation in hypotonic lysis buffer (10 mM Tris-HCl (pH 8), 0.25 M sucrose, 3 mM $MgCl_2$, 0.2% (v/v) Nonidet P-40) and protease inhibitors (Roche)). Histones were isolated from nuclei resuspended in Tris buffer (10 mM Tris (pH 8.0), 0.8 M NaCl, 1 mM EDTA and protease inhibitors) by overnight acid-extraction (0.25 M HCl, with rotation at 4°C) and subsequent precipitated with 20% TCA. Histone pellets were washed with acetone and reconstituted in $dddH_2O$. Protein quantity in each sample was ascertained using the BCA Protein Assay Kit (Pierce). This highly sensitive assay features colourimetric detection of the chelation of bicinchoninic acid (BCA) chelating with cuprous cations (Cu^+). Cu^+ is formed by the reduction of Cu^{2+} when exposed to an alkaline environment (279). Thereafter, histones were spotted quantitatively (100 ng per sample) on nitrocellulose membranes. Membranes were submerged in blocking buffer for 30 min followed by 1 h incubation with α-H3K27me2 and α-H3K27me3 (same as used for ChIP-seq) primary antibody dilutions (1:5000 in TBS-t). Membranes were washed three times in TBS-t and then incubated with HRP-conjugated rabbit α-IgG secondary antibody (1:10000 in TBS-t) for 1 h. Chemiluminescent signal was quantified with ImageJ analysis software (276).

2.2.8 DNA microarrays

DNA microarrays containing 12 468 60-mer oligonucleotide probes (Agilent Technologies, USA) based on the full *P. falciparum* genome (280) were used to assess global transcriptomic changes in stage II gametocytes following 24 h treatment with 5 µM UNC0224 or GSK343. The design of

these custom arrays have an average of <3 individual oligonucleotide probes for each *P. falciparum* coding gene (280). Following treatment, gametocyte cultures (1-3% gametocytaemia, 4% haematocrit) were isolated from host erythrocytes using 0.1% (w/v) saponin. Total RNA was extracted using a combination of TRIzol (Sigma Aldrich, USA) and phenol-chloroform extraction. For each untreated and treated sample, between 5 and 13 µg of the total RNA was reverse transcribed to synthesise cDNA as described previously (280). The RNA was incubated with oligo-DT (2 µg/µL) and random nonamers (2 µg/µL) at 70°C for 10 min to allow annealing between the RNA and primers. In the presence of 0.2 mM each of dATP and amino-allyl dUTP, 0.1 mM each of dCTP, dTTP and dGTP and 100 mM DTT (all from Invitrogen), cDNA was synthesised using Superscript IV (200 U/µg, Invitrogen) for 16 h at 42°C. Thereafter, remaining RNA template was hydrolysed using 1 M NaOH and 0.5 M EDTA for 15 min at 65°. The cDNA was purified using Wizard SV Gel and PCR Clean-UP system (Promega) according to the manufacturer's instructions and eluted into 0.1 M Na_2CO_3 (pH 9). Treated and untreated sample cDNA was labelled with Cy5 dye (GE Healthcare) prior to array hybridisation with an equal amount (350-500 ng) of Cy3-labelled (GE Healthcare) reference pool containing equal amounts of cDNA from each gametocyte sample and mixed stage NF54 asexual parasites. Dye coupling was performed in dark conditions for 2 h at pH of 9 followed by purification of the labelled cDNA per the Zymo DNA 25 Clean and Concentrator Kit (Zymo Research) instructions. Slides were hybridised overnight at 65 °C followed by washing and scanning using an Agilent G2600D microarray scanner (Agilent Technologies). Normalised signal intensities for each oligo were extracted using the GE2_1100_Jul11_no_spikein protocol and Agilent Feature Extractor Software (v 11.5.1.1) as described before (280).

2.2.9 Molecular docking of epigenetic inhibitors

Molecular docking was performed to predict the interaction between epigenetic inhibitors and potential target HMTs. The structure of GSK343 was obtained from the ZINC database (281) while the canonical SMILES for UNC0224 was used to generate a ligand structure in UCSF Chimera (282). Amino acid sequences of *P. falciparum* SET3 and SET7 from PlasmoDB (v39, plasmodb.org)

were used to prepare structures with SwissModel (283). The SET3 and SET7 models selected for docking were obtained from AlphaFold 2.0 (284). Residues with low quality prediction scores (AlphaFold's per-residue score <70, indicating low confidence) were trimmed to obtain high confidence core models that were subsequently prepared using Dock Prep (282). Molecular docking calculations were performed for GSK343-SET3 and UNC0224-SET7 by SwissDock (285). The scoring function for free-energy was used to evaluate the most stable binding modes with the ViewDock utility in UCSF Chimera (282).

2.2.10 Data analyses

2.2.10.1 ChIP-seq

ChIP-seq data analysis was performed according to ENCODE guidelines (www.encodeproject.org) (24) and as described previously (52, 92). Sequence read quality was determined using FastQC (286) prior to analysis and adapter sequences were removed using Trimmomatic (v0.32.3) (287). Reads were mapped to the *P. falciparum* 3D7 genome (v39 obtained from PlasmoDB, www.plasmodb.org) and duplicate and low-quality reads filtered and removed using BWA-MEM (v0.4.1) (288) and SAMtools (v1.1.2) (289), respectively. Correlations between corresponding biological replicates were determined prior to subsequent analysis. The deepTools suite (v3.1.2.0.0) (290) was used to plot the average occupancy of H3K27me2&3 (plotProfile and plotHeatmap tools) and to generate bigwig files that were viewed in IGV (291). Genome track images that are presented in results sections were exported from the IGV viewer. Genome-wide occupancy was calculated and is reported as $\log_2$-transformed ChIP/input ratios averaged for 1 kb bins. Occupancy upstream of transcription start sites (TSSs as defined previously by Adjalley *et al.,* 2016) (105) and within the CDR was calculated from $\log_2$ChIP/input ratios over 50 bp bins averaged across these regions. MACS2 (292) was used with the broad peak option (q-value ≤0.05; '-broad—cutoff 0.1') to call peaks as described by others (52, 92, 293). As two biological replicates were used for each experiment, only regions enriched in both biological replicates were used for all subsequent analyses. These were identified and annotated using the Multiple Intersect function and ClosestBED, respectively from the BEDtools suite (294). All results are

representative of data averaged for two biological replicates unless otherwise stated. GO enrichment analyses were performed with PlasmoDB using a *P*-value cut-off ≤0.05. Differential binding analyses to identify sites uniquely enriched with H3K27me2&3 in the different gametocyte stages was performed using the BEDtools Multiple Intersect function (294).

2.2.10.2 Microarrays

The microarray red and green signal intensities that passed the standard background filters (*P* <0.01) were normalised with Robust-spline for within-array and G-quantile for between slide normalisation in R (v3.2.3, www.r-project.org) using the limma and MArray packages, respectively (295, 296). The fit of a linear model was used to obtain $\log_2$-transformed expression values ($\log_2$Cy5/Cy3). Differential expression values were calculated for each gene as the $\log_2$-transformed fold change ($\log_2$FC) of treated over untreated with genes having $\log_2$FC ≥0.5 in either direction defined as differentially expressed in the UNC0224- or GSK343-treated gametocytes. Visualisation of differentially expressed genes was performed using TIGR MeV with functional classification of genes to significantly associated biological processes (*P*-values ≤0.05) performed using PlasmoDB (v39, www.plasmodb.org).

2.3 Results

2.3.1 Application of a ChIP-seq strategy to identify *Plasmodium* histone PTM occupancy

ChIP-seq is a core functional genomics approach used for whole-genome mapping of modified histones and DNA binding proteins (297). In this study, ChIP-seq was used to identify the genomic distribution of H3K27me2&3 in early-stage gametocytes. The first step of this approach involves stabilising the DNA-histone interaction using formaldehyde as a cross-linker (Figure 2.2). Additional cross-linking using disuccinimidyl glutarate may be used however, this is preferable only for transiently bound factors (e.g. chromatin modifying enzymes) and not for histones (298).

Next, the cross-linked DNA was sheared using ultrasonication to generate fragments of an ideal length (200-300 bp) for sequencing. Thereafter, the fragmented DNA was subjected to immunoprecipitation (IP) using an antibody specific to the protein of interest (297, 299). Prior to IP, small amounts of the DNA were separated from each sample and kept as input that is then sequenced in parallel with the DNA from IP samples and serves as a crucial control to identify and normalise sequencing biases during analysis. Sample IP allows for DNA fragments bound to H3K27me2&3-modified nucleosomes to be isolated or "pulled out" from those not associated with the histone PTMs and then prepared as sequencing libraries (Figure 2.2). The reads obtained from sequencing were extensively filtered to ensure only high-quality reads were included in the mapping of sequences to the *P. falciparum* reference genome. In addition to the use of two biological replicates for each population, statistical tools including MACS2 peak calling (292) and differential binding analyses (294) were used to identify regions enriched with H3K27me2&3. This stringent mapping and quantification of histone PTM enrichment provides confidence that the data accurately reflects the patterns of H3K27me2&3 in early-stage gametocytes (24, 297). The ChIP-seq experiment performed therefore included all the required controls to meet the standards outlined by ENCODE (encodeproject.org), a consortium that provides practical guidelines for the generation of high-quality functional genomic data to the scientific community (24).

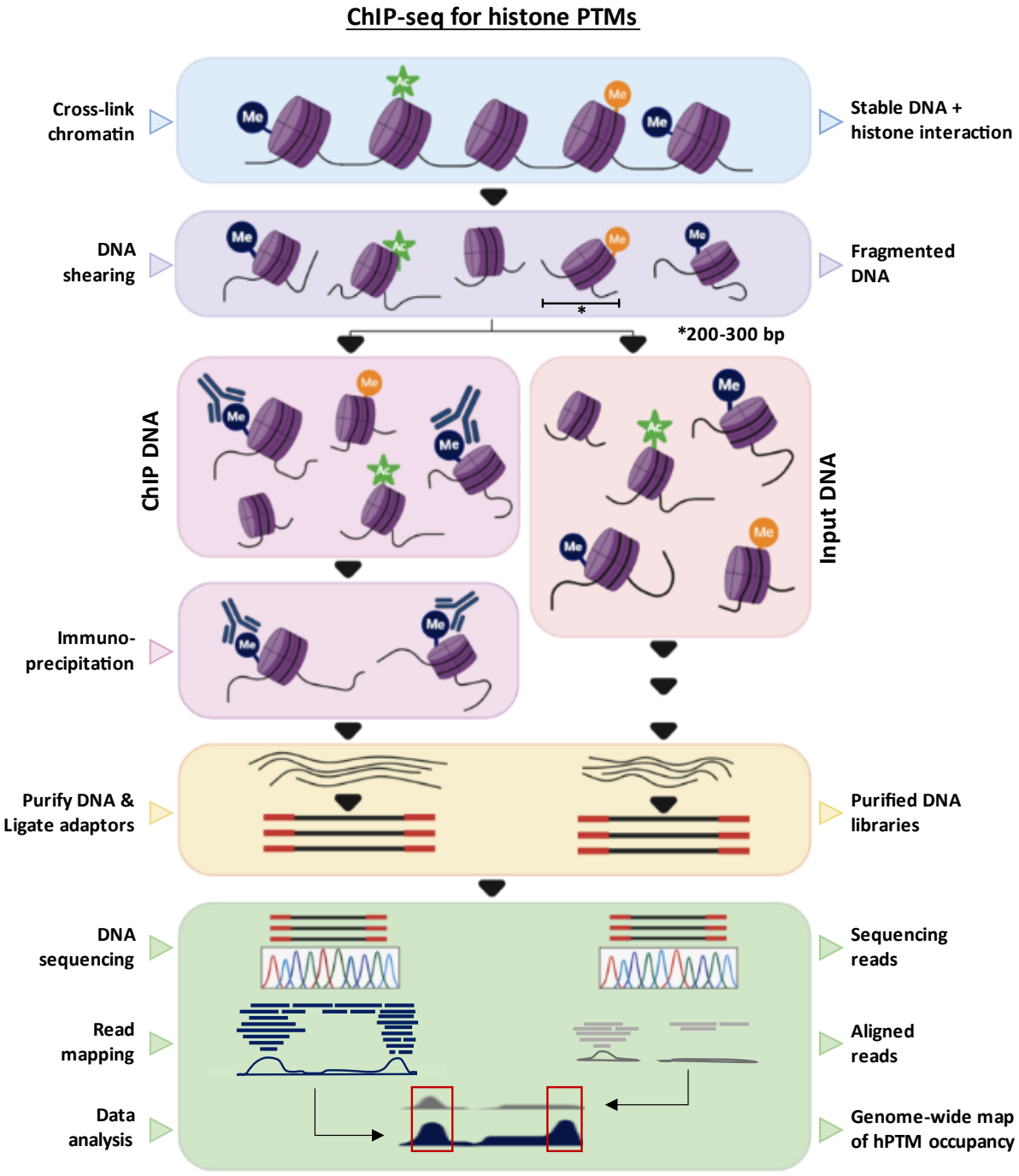

Figure 2.2: ChIP-seq approach for the study of histone post-translational modification patterns in *P. falciparum* gametocytes. Gametocyte chromatin in each of the two biological replicates was chemically cross-linked using formaldehyde, yielding a stable interaction between DNA and histone proteins. Fragmented DNA was generated by ultrasonication. Except for small amounts that were separated to serve as input samples, DNA was subjected to immunoprecipitation (IP) with either α-H3K27me2 or α-H3K27me3 antibodies to select DNA fragments bound to histones with the PTMs of interest. The IP and input DNA samples were then purified and ligated to adaptors to generate DNA libraries for sequencing. Sequencing reads were mapped to the reference genome with the data subsequently analysed to generate genome-wide maps of H3K27me2&3 in early gametocytes.

2.3.2 Sampling of *P. falciparum* gametocytes for ChIP-seq

In order to capture snapshots of the dynamic H3K27me2&3 patterns in early-stage gametocytes, distinct gametocyte populations spanning stage II development were obtained and classified as "pre-stage II", "stage II" and "post-stage II" gametocytes. Gametocytes were initiated (day -3) from synchronised, ring-stage (≥95%) cultures with 0.5% parasitaemia and 6% haematocrit (Figure 2.3) as described by others (274). The haematocrit was reduced to 4% to induce gametocyte production on day 0 and from day 1 onwards, NAG-supplemented media was replaced daily to eliminate residual asexual parasites from the cultures. Pre-stage II, stage II and post-stage II gametocytes were isolated from host erythrocytes using saponin treatment on days 2, 4 and 7, respectively (Figure 2.3).

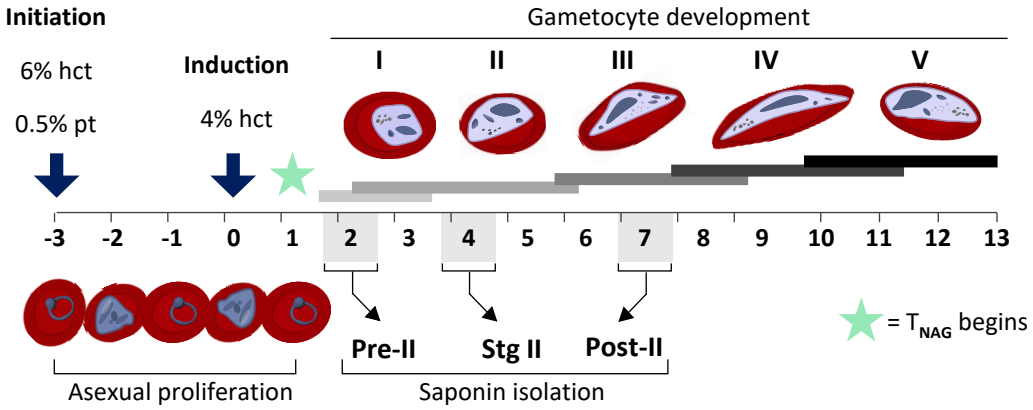

Figure 2.3: Gametocyte culture generation and sampling strategy for ChIP-seq. Gametocyte production was initiated from synchronised (≥95% ring-stages) asexual parasite cultures at a 6% haematocrit (hct) and 0.5% parasitaemia (pt) on day -3. After 72 h, the haematocrit was reduced to 4% (day 0) to induce gametocytogenesis. N-acetylglucosamine (NAG) supplemented media was replaced daily from day 1 to day 4 to remove residual asexual parasites from culture. Morphology was monitored daily by microscopic evaluation of Giemsa-stained parasite samples. Pre-stage II (pre-II), stage II (stg II) and post-stage II (post-II) gametocyte populations were isolated using saponin treatment on days 2, 4 and 7 of gametocyte (GC) development, respectively.

Classification of these populations was based on the stage compositions (determined by microscopic evaluation of Giemsa-stained parasites) for each set of two biological replicates at the time of sampling. Pre-stage II populations consisted mostly of asexual parasites (60 ± 4%) with some stage I (40 ± 4%) and stage II gametocytes (0.3 ± 0.4%; Figure 2.4). Typically, asexual parasites were distinguished from stage I gametocytes by their pycnotic appearance arising from

growth arrest due to NAG treatment. Stage II populations were enriched for stage II gametocytes (74 ± 3.2%) with minor proportions of stage I (9 ± 6%) and stage III (17 ± 2.5%) gametocytes present but no asexual parasites. Post-stage II populations predominantly contained stage III/IV gametocytes (90 ± 6%) and only a small proportion (10 ± 6%) of stage II gametocytes (Figure 2.4). These populations were deemed sufficiently divergent to detect the changes in histone PTM levels across early gametocyte development and were thus for chromatin-immunoprecipitation followed by high-throughput sequencing (ChIP-seq) to map the genome-wide occupancy of H3K27me2&3.

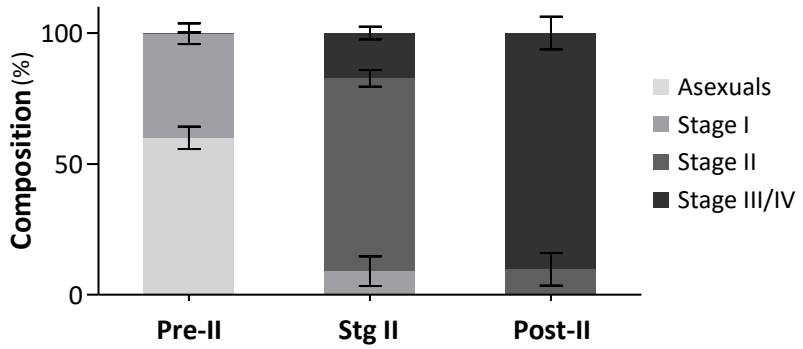

Figure 2.4: Stage composition of gametocyte samples used for ChIP-seq. The stage compositions (%) of gametocyte populations generated to capture snapshots of the dynamic occupancy of histone PTMs in early gametocytes. Compositions were determined by counting ≥100 parasites or gametocytes. Data are representative of the two independent biological repeats, ± S.E.

2.3.3 Validation of antibody specificity and ChIP-seq data quality

The use of highly specific and good quality antibodies against the proteins of interest is critical for successful ChIP-seq experiments (24). As *Plasmodium* parasite-specific antibodies were not available, commercial ChIP-grade antibodies against rabbit H3K27me2 and H3K27me3 were selected and verified for cross-reactivity. ChIP-seq has been performed successfully by others using the selected antibodies in organisms that have high (>99%) sequence similarity to *P. falciparum* histone H3, suggesting the suitability of both the α-H3K27me2 (300, 301) and α-H3K27me3 (302-304) antibodies for this study. Secondary validation was performed to demonstrate antibody specificity in *P. falciparum* parasites. The antibodies were indeed able to

detect the respective modified H3 histone sequence with high specificity; ≥27 times greater specificity towards the *P. falciparum* histone H3 peptides modified with H3K27me2 or H3K27me3 compared to methylated H3K9 and H3K36 or unmodified H3K27 peptides that were included as controls (Figure 2.5).

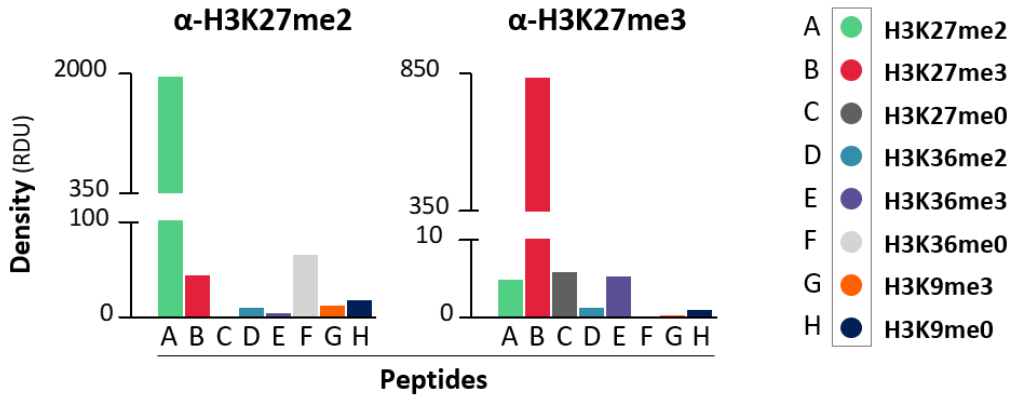

Figure 2.5: Validation of antibody specificity against *P. falciparum* H3K27me2&3. The selected α-H3K27me2 and α-H3K27me3 antibodies were used to detect peptides containing the *P. falciparum* H3 sequence without modification or with di- or tri-methylation on K9, K27 or K36 using dot blot analysis. Blot images were quantified to obtain the relative density units (RDU) shown here for each peptide. Data are representative of a single replicate experiment.

Importantly, the antibodies were specific to their modification, with negligible cross-reactivity between the di- and tri-methylated modification. Therefore, these antibodies were used to IP H3K27me2&3-associated DNA fragments in the pre-stage II, stage II and post-stage II gametocyte samples. ChIP-seq data belonging to corresponding replicates were highly correlated with Pearson correlation coefficients between H3K27me2-IP replicates of r^2= 0.89, r^2= 0.93 and r^2= 0.95 for pre-stage II, stage II and post-stage II gametocytes, respectively (Appendix: Table S2). Additionally, the occupancies of H3K27me2&3 were highly correlated with one another in the stage II gametocytes with a Pearson correlation coefficient of r^2= 0.95 (Figure 2.6a), an observation that was less prominent for the pre- and post-stage II gametocyte samples (Pearson correlation, r^2= 0.68 and r^2= 0.5, respectively). Since a single histone cannot simultaneously contain di- and tri-methylated forms of H3K27, the apparent presence of both histone PTMs at the same site is most likely indicative of one of the PTMs present as an intermediate of the other with the populations containing a mixed pool of histones in either state of methylation or the presence of asymmetrically modified nucleosomes (i.e. one H3 with K27 di-methylated and the

other tri-methylated) (305, 306). Finally, the presence of H3K27me2&3 in the stage II gametocytes was weakly or completely anti-correlated with that in pre- and post-stage II gametocytes (e.g. Pearson correlation, r^2= -0.44 and r^2= -0.1, respectively for H3K27me3; Figure 2.6a).

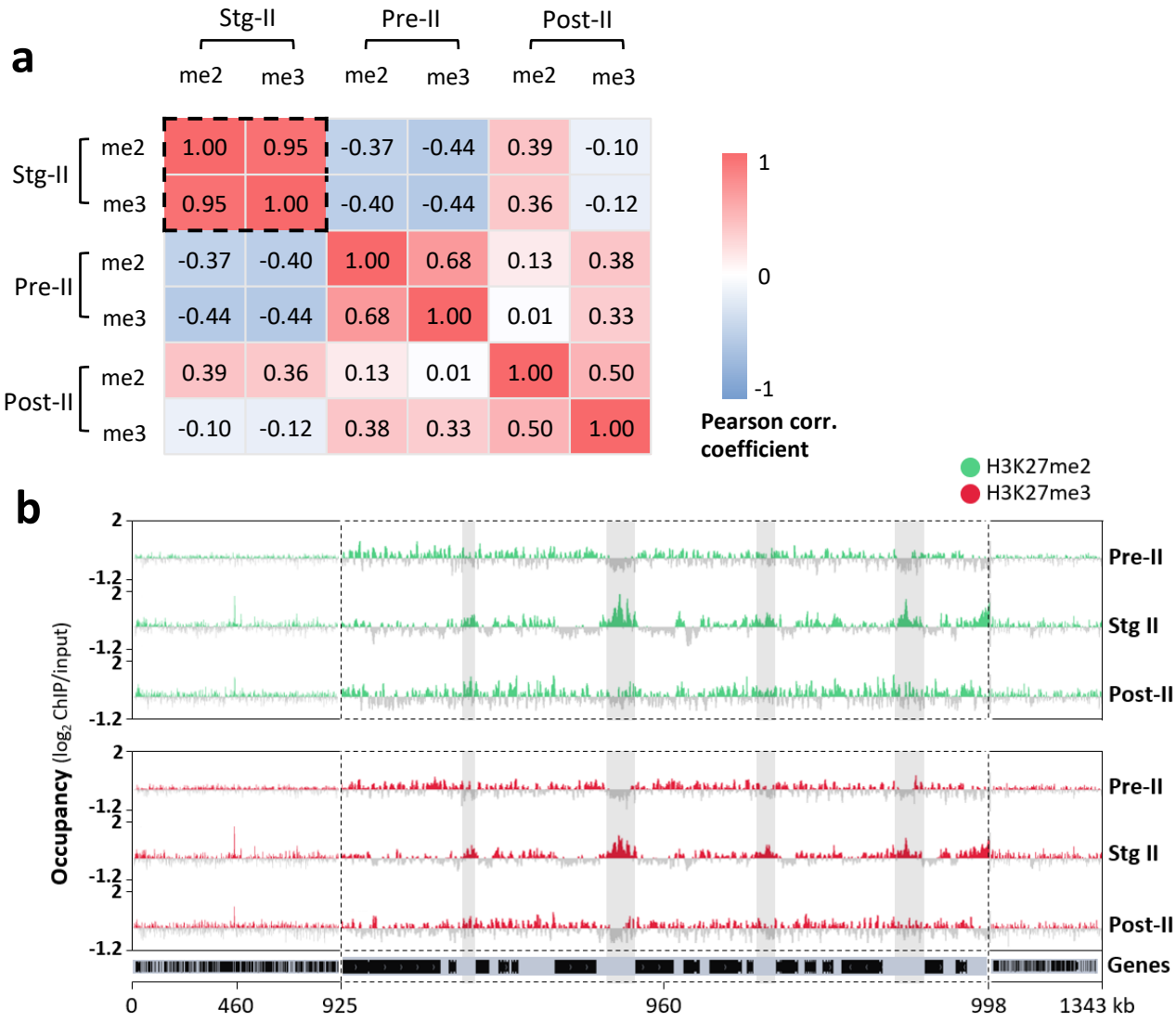

Figure 2.6: Dynamic distribution of H3K27me2&3 occupancy is dynamic during *P. falciparum* early and intermediate gametocyte development. (a) Pearson correlation coefficient plot of the genome-wide occupancy of H3K27me2&3 (me2 and me3) obtained for pre-stage II (pre-II), stage II (stg II) and post-stage II (post-II) gametocytes using ChIP-seq. Data are representative of the two independent biological replicates for each stage and histone PTM. The dashed box highlights the increased positive correlation between H3K27me2&3 in the stage II gametocytes. **(b)** H3K27me2&3 occupancy (average log_2-transformed ChIP/input) over chromosome 14 for each of the gametocyte stages with all data representative of two biological replicates. Green and red regions on the tracks indicate occupancy (log_2ChIP/input ratios >0) and grey regions represent depletion (log_2ChIP/input ratios ≤0) of the modifications. Shadowed regions highlight regions exhibiting an increased abundance of H3K27me2&3 t in the stage II gametocytes with positions of genes indicated below genome tracks.

The use of ChIP-seq allowed for the detection of H3K27me2&3 in all the gametocyte populations and for the delineation of the unique occupancy patterns associated with each. In pre-stage II gametocytes, very low levels of H3K27me2&3 are present, contrasting with a strong increase in the occupancy of both histone PTMs in the stage II gametocytes (Figure 2.6b). This stage II gametocyte-specific abundance manifests as concentration of H3K27me2&3 upstream of transcriptional start sites (TSSs) as previously defined by Adjalley *et al.,* 2016, (105). In post-stage II gametocytes, reduced levels of the histone PTMs are evident with the patterns of residual H3K27me2&3 exhibiting a similar intergenic distribution. These stage-specific trends, specifically the consistently greater levels of H3K27me2&3 in the stage II gametocytes, were confirmed with ChIP-qPCR (Figure 2.7) using several randomly selected loci and the primers listed in Appendix: Table S3.

These observations are congruent with the gametocyte stage-specific dynamics of H3K27me2&3 described previously (133). In view of the preferential H3K27me2&3 occupancy within intergenic regions, particularly in the stage II gametocytes, this bias towards non-coding regions was further interrogated.

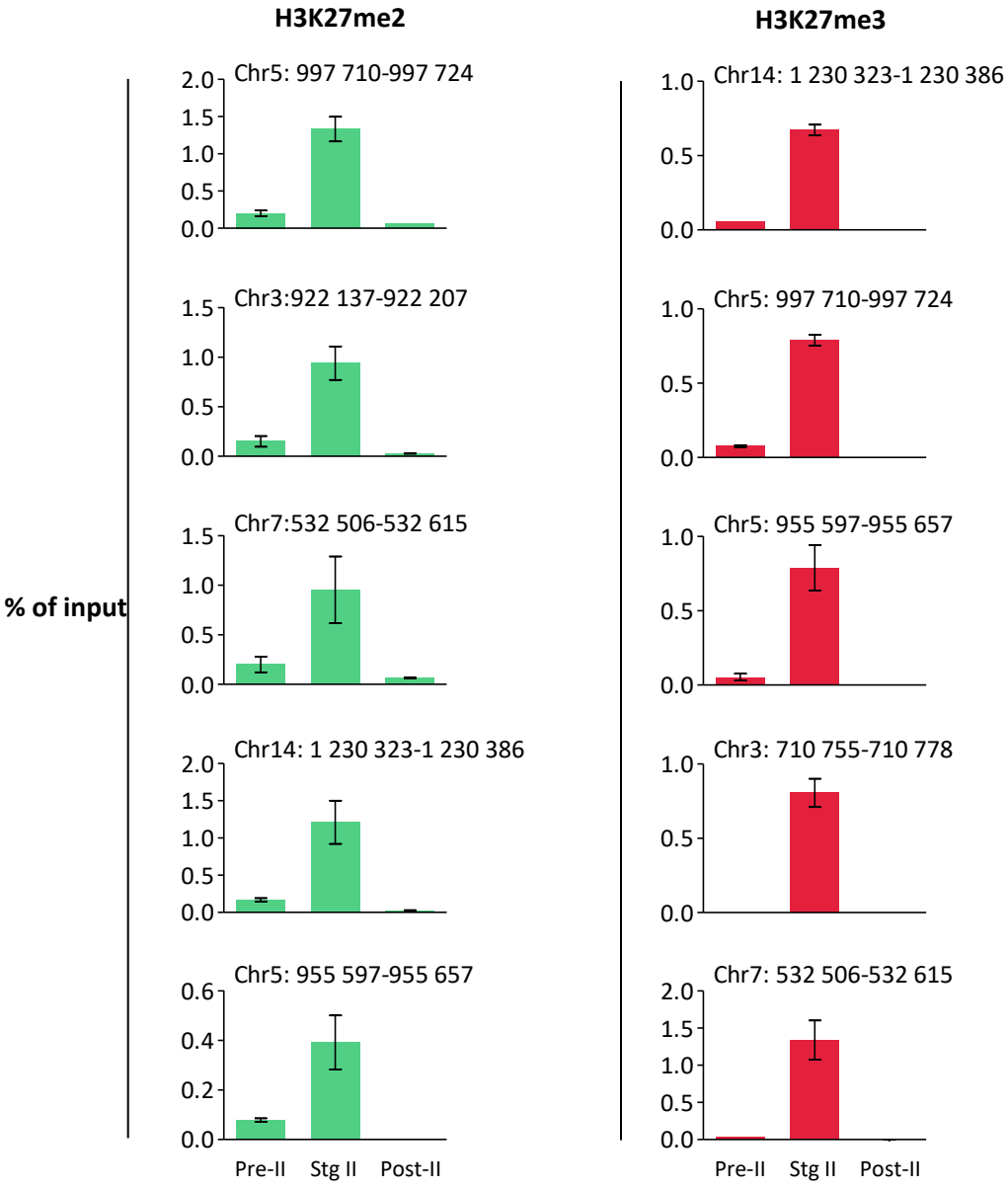

Figure 2.7: Validation of the gametocyte stage-specific patterns of H3K27me2&3 occupancy. ChIP-qPCR was performed to validate H3K27me2&3 ChIP-seq data for the pre-stage II (pre-II), stage II (stg II) and post-stage II (post-II) gametocyte samples. The amplification of each the samples (input and immunoprecipitated) and controls were performed in technical triplicate. Data were analysed using the ΔΔCt method (cycle threshold at which signal becomes detectable above background). H3K27me2&3 occupancies are expressed as the % of input at each chromosome region indicated with data points representative of two independent biological replicates, ±SD. Sequences of each primer pair used are detailed in Appendix: Table S3.

2.3.4 Stage II gametocytes have a unique pattern of H3K27me2&3 occupancy

To examine the preferentially intergenic occupancy of H3K27me2&3 during early gametocyte development, the presence of each histone PTM spanning the 5602 *P. falciparum* genes for which sequencing data were obtained was assessed. The occupancies of H3K27me2&3 were found to be extremely similar upstream and within the coding regions of genes in stage II gametocytes compared to more divergent patterns of occupancy in the pre- and post-stage II gametocytes (Figure 2.8a). The average H3K27me2&3 profiles indicate that in stage II gametocytes, these histone PTMs are distinctly concentrated 750 bp upstream of TSSs with the occupancy scores (log_2ChIP/input) across this region peaking at 0.24 and 0.23 (average of 0.21 and 0.2), respectively (Figure 2.8a). Within the coding regions (CDRs) however, there is a notable absence (average CDR occupancy scores of -0.13 for both histone PTMs) of H3K27me2&3 in the stage II gametocytes. Conversely, in both the pre- and post-stage II gametocytes, the CDRs are on average associated with some H3K27me2&3 occupancy (e.g. H3K27me3 occupancy scores of 0.07 and 0.02, respectively) with an inverse depletion of the histone PTMs upstream of TSSs (e.g. H3K27me2 occupancy scores of -0.1 and -0.05, respectively) (Figure 2.8a). The contrasting patterns associated with these gametocyte stages highlight the prominent abundance of H3K27me2&3 upstream of genes in the stage II gametocytes.

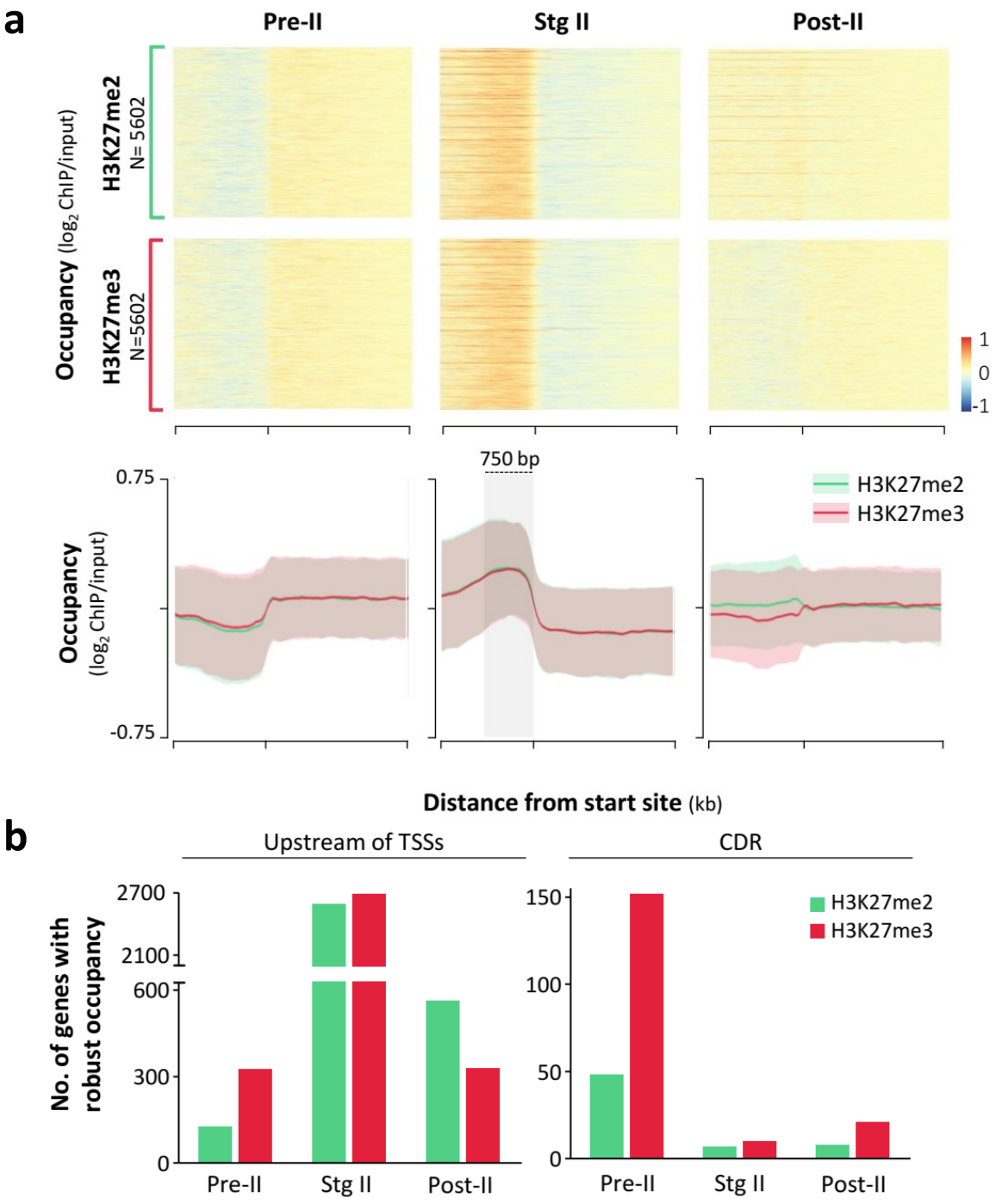

Figure 2.8: H3K27me2&3 robustly occupy the regions upstream of transcriptional start sites in *P. falciparum* stage II gametocytes. **(a)** The occupancy of H3K27me2&3 (average $\log_2$ ChIP/input over 50 bp bins) spanning a 1.7 kb region upstream and 2.5 kb region downstream of TSSs for all *P. falciparum* genes (PlasmoDB genome annotation, v39) in pre-stage II, stage II and post-stage II gametocytes. Data are representative of two independent biological repeats. In the individual heatmaps, genes were rank-ordered based on occupancy values. Summary plots of the average occupancy for H3K27me2&3 (green and red, respectively) across all genes present in the heatmaps. The peak enrichment in stage II gametocytes is highlighted in the light grey shadowed region 750 bp upstream of transcriptional start sites (TSS). Ribbons represent average occupancy of the region ± SD. **(b)** The number of genes with robust H3K27me2&3 occupancy (i.e. $\log_2$ ChIP/input ≥0.21 and ≥0.2, respectively) upstream of TSS and in the CDRs for each gametocyte stage.

Next, the numbers of H3K27me2&3-occupied genes were quantified for each gametocyte stage with these subsequently classified based on the location of this occupancy either exclusively upstream of the TSSs, within CDRs or both. Of all the genes for which sequencing data was obtained in stage II gametocytes, 90% (5044) and 87% (4856) were associated with some degree of H3K27me2&3 occupancy (i.e. $\log_2$ChIP/input > 0) (Appendix: Table S4) upstream of TSSs. Of these genes, 2590 and 2688 were associated with a robust level (i.e. have $\log_2$ChIP/input scores above the average values of 0.21 and 0.2 in stage II gametocytes) of H3K27me2&3 occupancy, respectively (Figure 2.8b). Although ~20% of these robustly occupied genes also had the respective histone PTM present within CDRs in stage II gametocytes, few of these (7 and 10, respectively) had H3K27me2&3 occupancy exclusively limited to CDRs. Combined with the greater proportion of robust occupancy that is present exclusively upstream of genes (2583 and 2678, respectively), this indicates that H3K27me2&3 are predominantly associated with the intergenic regions upstream of TSSs in the stage II gametocytes. Similarly for pre- and post-stage II gametocytes, H3K27me2&3 are more frequently associated with the regions upstream of TSSs (e.g. 125 upstream of TSS *vs.* 48 CDRs with robust H3K27me2 occupancy) however, far fewer genes have robust H3K27me2&3 occupancy in these stages overall (Figure 2.8b).

2.3.5 H3K27me2&3 are associated with transcriptional repression in early gametocytes

With the aim of investigating the functional relevance of the H3K27me2&3 occupancy upstream of genes in the stage II gametocytes, transcription profiles obtained from previous work in our lab (94) were compared with the levels of histone PTM occupancy for genes. For the H3K27me2&3 robustly occupied genes in stage II gametocytes, corresponding transcript levels were available for 96% and 97% of the two sets, respectively (Appendix: Table S5). A genome-wide comparison of the histone PTM and transcript levels (average $\log_2$Cy5/Cy3) in stage II gametocytes (i.e. days 4 and 5 of gametocyte development) indicates H3K27me2&3 occupancy upstream of TSSs is anti-correlated with transcription (Pearson correlation coefficients of r^2= -0.19 and r^2= -0.16 for H3K27me2&3, respectively) (Figure 2.9). Large proportions of genes with robust occupancy for H3K27me2 (99%) and H3K27me3 (98%) showed reduced transcript levels

on the days (2-6) associated with stage II gametocyte development (Appendix: Table S5). Furthermore, these genes differentiate into three clusters according to changes in expression patterns in the stage II gametocytes with each cluster significantly associated (*P*-value <0.05) with various biological categories (Figure 2.9) (Appendix: Table S6).

Although the transcript levels do oscillate throughout early and intermediate gametocyte development, the H3K27me2&3 robustly occupied genes are typically repressed in stage II gametocytes and encode protein products involved asexual parasite-specific processes such as schizogony (P = 0.004), haemoglobin catabolism (P = 0.014), transcription (P = $5.7e^{-4}$), host cell entry (P = 0.001) and exit P = 0.038), DNA replication (P = 0.011) and cell gliding (P = 0.041) (Figure 2.9). Other genes that are robustly occupied are associated with critical processes that function during proliferation, sexual commitment and early gametocyte differentiation. These include antigenic variation (P = $1.2e^{-21}$), multi-organism transport (P = $2.2e^{-4}$) and chromatin organisation for both H3K27me2 (P = 0.028) and H3K27me3 (P = 0.007). These significant links with critical asexual- and commitment-specific processes suggest that H3K27me2&3 are associated with the generation of gametocyte development-specific transcriptional programs.

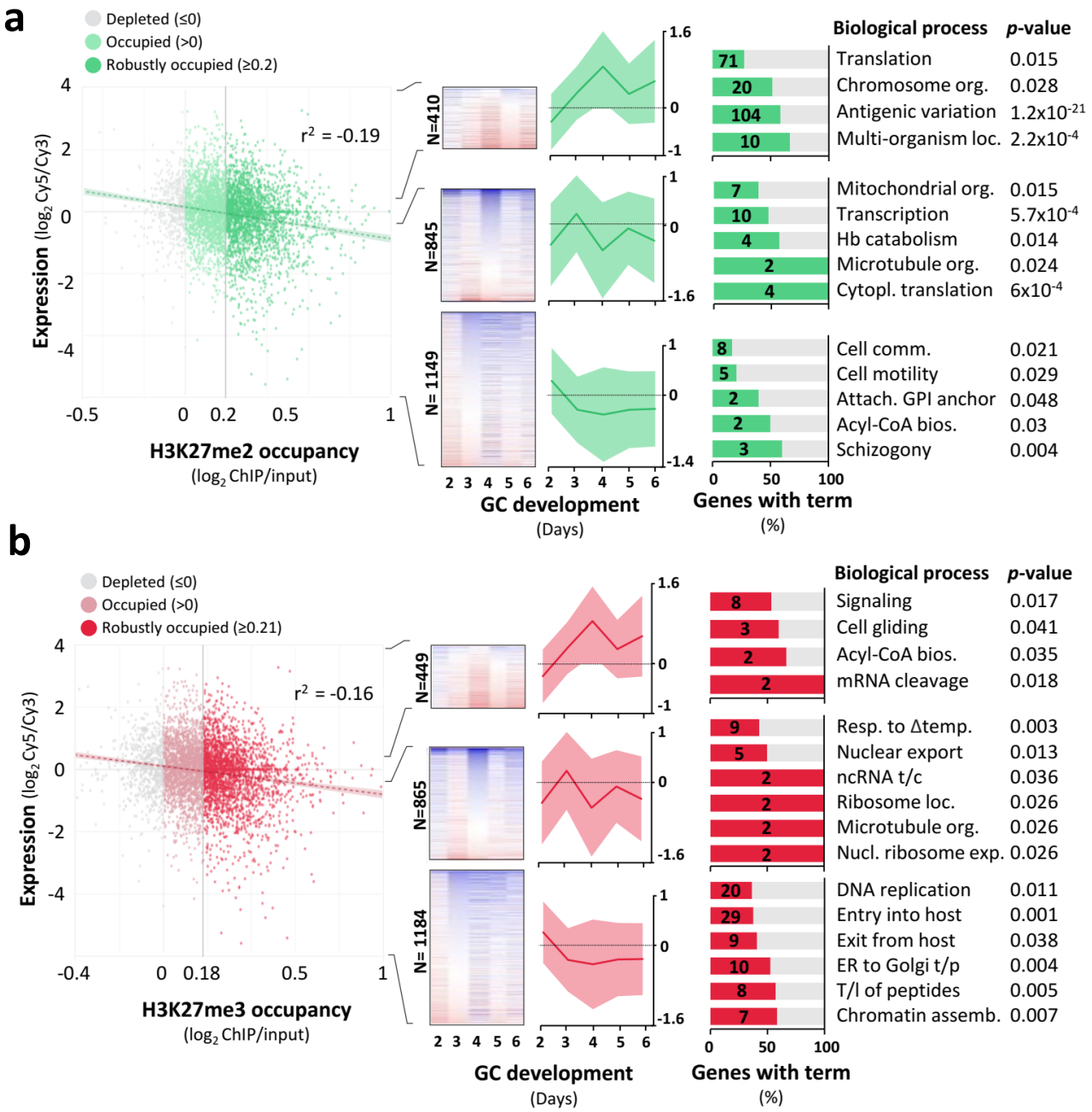

Figure 2.9: H3K27me2&3 occupancy in *P. falciparum* stage II gametocytes is associated with transcriptional repression. **(a)** Average expression values (log_2Cy5/Cy3 on day 4 and 5 of gametocyte (GC) development (94) plotted against H3K72me2 (green) occupancy 750 bp upstream of genes in stage II gametocytes for all 5602 *P. falciparum* genes. Genes are colour-coded based on the level of H3K27me2 occupancy as indicated. **(b)** Average expression levels plotted against H3K27me3 occupancy in stage II gametocytes (750 bp upstream of TSSs). Genes are categorised based on occupancy score as indicated by colour. For both **(a)** and **(b)**, linear regression is represented by dashed lines with 95% confidence interval indicated by ribbons; r^2 values represent Pearson correlation coefficients. All histone PTM data points are representative of two independent biological repeats. Robustly occupied genes were clustered based on transcript abundance patterns over days 2-6 of GC development and the number of genes in each cluster (N) is shown. The expression profiles of individual genes shown in the heatmaps for each cluster were then averaged to obtain expression line plots with ribbons indicating log_2Cy5/Cy3 ± SD. Each cluster is significantly (*P*-value ≤0.05) associated with the biological processes indicated. The value on each bar indicates the number of H3K27me2&3 robustly occupied genes and is presented as a % of all background genes that are associated with the biological process in *P. falciparum* parasites. Legend: org. = organisation; loc. = localisation; Hb. = haemoglobin; cytopl. = cytoplasmic; comm = communication; attach. = attachment; bios. = biosynthesis; resp = response; Δtemp. = change in temperature; t/c = transcription; nucl. = nuclear; exp. = export; t/p =transport; t/l = translocation; assemb. = assembly.

Although H3K27me2&3 are most highly abundant during the stage II gametocytes, the detection of these histone PTMs in the pre- and post-stage II gametocytes here and previously (133), is still of interest and thus was also examined. The 124 genes that are robustly occupied and repressed by H3K27me2&3 in both the pre-stage II and stage II gametocytes are significantly associated with H3K9 methylation (P = 0.023) and cell gliding processes (P = 0.020) (Figure 2.10a). These processes become increasingly active in subsequent gametocyte developmental stages (135, 307, 308) and this is reflected by the absence of repressive H3K27me2&3 at these genes in post-stage II gametocytes. In both the stage II and post-stage II gametocytes, genes significantly associated with the early gametocyte differentiation-specific processes of protein export (P = $2.93e^{-4}$), host erythrocyte aggregation (P = $2.77e^{-55}$) and sex determination (P = 0.023) (57, 58, 76, 309) are robustly occupied and repressed by H3K27me2&3 (Figure 2.10a). This indicates that the H3K27me2&3-associated suppression of these processes, established in the stage II gametocytes, is maintained in subsequent developmental stages.

Interestingly, 62% and 31% of robustly occupied genes in the pre- and post-stage II gametocytes are associated with this level of H3K27me2&3 only in these gametocyte stages, respectively (Figure 2.10a). These stage-specific robustly occupied gene sets are significantly associated (P <0.05) with processes predominantly related to metabolism which undergoes substantial remodelling during gametocyte development (310-312). Similar to the stage II gametocytes, the repression of these gene sets corresponds with the presence of robust occupancy of H3K27me2&3 in the pre- and post-stage II gametocytes (Figure 2.10b). This suggests that while in lower abundance in the pre- and post-stage II gametocytes, these histone PTM are likely still relevant for transcriptional regulation in these stages. These results further demonstrate the repressive association between H3K27me2&3 and gene expression during early and intermediate gametocyte development. As this is strikingly more notable for the stage II gametocytes, further analyses were focussed on this stage.

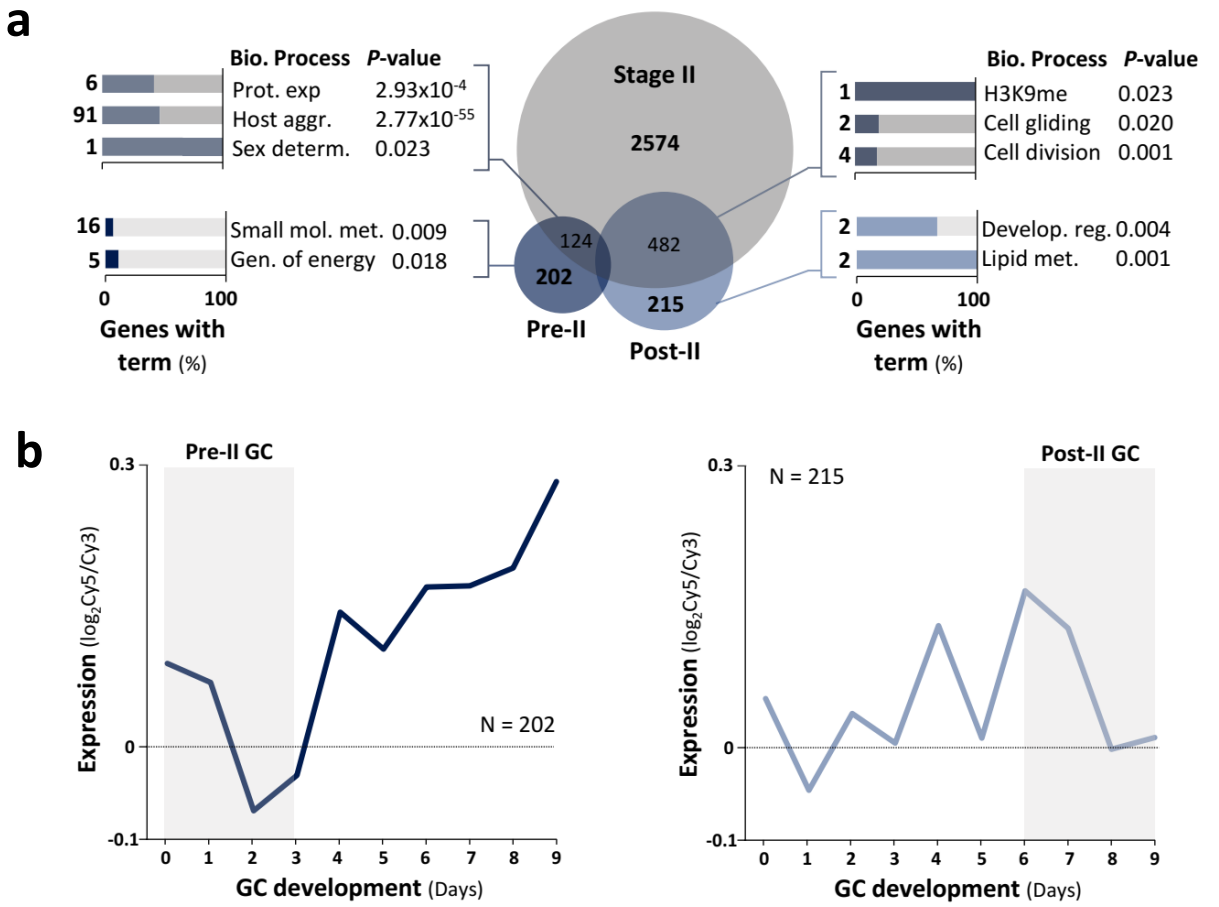

Figure 2.10: H3K27me2&3 are associated with transcriptional repression of stage-related processes during early and intermediate gametocyte development. **(a)** Comparison of the numbers of genes with robust levels of H3K27me2&3 occupancy (log_2ChIP/input ≥0.21 and ≥0.2, respectively) upstream of TSSs in the pre-stage II, stage II and post-stage II gametocytes. Sets of genes with robust occupancy only in the pre-stage II or post-stage II gametocytes and those sharing robust occupancy with stage II gametocytes are significantly associated (P <0.05) with unique biological (bio.) processes that are less/not active during these respective stages. The number of robustly occupied genes associated with the biological process is indicated to the left of each bar and is expressed a % of all background genes associated with the term in *P. falciparum* parasites. Legend: Prot. exp. = protein export into host erythrocyte; aggr. = aggregation; determ. = determination; mol. = molecule; met. = metabolism; gen. = generation; H3K9me = methylation of H3K9; develop. = development; reg. = regulation. **(b)** Average expression values (log_2Cy5/Cy3) (94) on days 0-9 of gametocyte (GC) development for genes with robust occupancy in the pre-stage II and post-stage II gametocytes with grey shadowed boxes indicating days on which the respective gametocyte stages are present in culture.

2.3.6 H3K27me2&3 are significantly enriched in stage II gametocytes

The transcriptional repression associated with H3K27me2&3 has been described previously in model eukaryotes (229-232, 270, 303). However, as these histone PTMs were only recently described in *P. falciparum* parasites, we sought to provide additional support for the repressive

roles of H3K27me2&3 in *Plasmodium*, particularly in the stage II gametocytes in which these histone PTMs are highly abundant (133). To do so, the stage-dynamic nature and quantitative potential of the ChIP-seq data was leveraged using a peak calling approach to complement the qualitative assessment of histone PTM occupancy and define genomic regions significantly enriched (q-value ≤0.05, present in both biological replicates) with H3K27me2&3.

Congruent with the observations of robust occupancy, peak calling indicated that chromatin in stage II gametocytes is far more enriched with H3K27me2&3 (848 and 947 sites, respectively) (Appendix: Table S7) compared to the pre-stage II (231 and 262 sites, respectively) and post-stage II gametocytes (5 sites each) (Figure 2.11a). In the stage II gametocytes, these H3K27me2&3 levels correspond to the significant enrichment of 603 and 738 genes (Figure 2.11a) with these numbers equating to 23% and 27% of the H3K27me2&3 robustly occupied gene sets, respectively. Less enrichment in the pre- and post-stage II gametocytes translates to fewer genes that are significantly associated with H3K27me2&3 (185 and 195 in pre-stage II and 4 and 5 in the post-stage II gametocytes). Furthermore, in the stage II gametocytes, enrichment of the histone PTMs was predominantly associated with the regions upstream of the TSSs (61% and 70% of the H3K27me2&3 enriched sites, respectively (Figure 2.11a) and therefore, subsequent analyses were focused on these regions.

All *P. falciparum* genes were stratified into one of four categories based on H3K27me2&3 levels upstream of TSSs in the stage II gametocytes: 1) those completely depleted of the histone PTMs (log_2ChIP/input ≤0: 559 and 474 genes for H3K27me2&3, respectively), 2) those with occupancy (log_2ChIP/input >0: 2454 and 2168 genes), 3) robustly occupied genes (log_2ChIP/input ≥0.21: 2225 genes and log_2ChIP/input ≥0.18: 2187 genes) or 4) enriched genes (365 and 501 genes with significant enrichment) (Figure 2.11b).

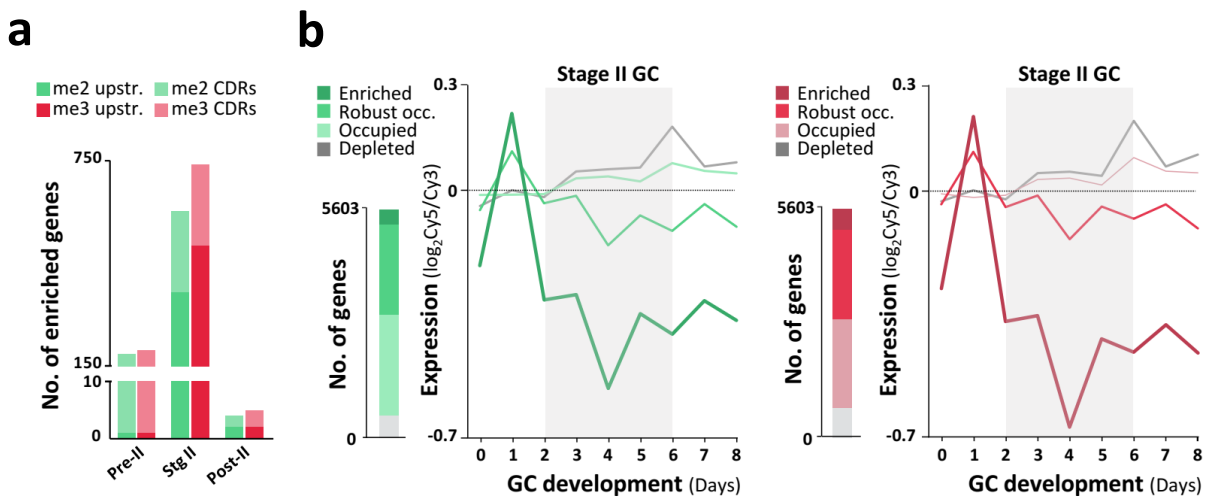

Figure 2.11: H3K27me2&3 enrichment is associated with transcriptional repression in *P. falciparum* stage II gametocytes. (a) Clustered column graphs specifying the number of genes significantly enriched (i.e. called peaks with q-value ≤0.05 and present in both biological replicates) with H3K27me2&3 (green and red, respectively) upstream of TSSs (darker shading) or within CDRs (lighter shading) in the pre-stage II, stage II and post-stage II gametocytes. **(b)** All 5602 *P. falciparum* genes were stratified into one of four categories based on the level of H3K27me2 (green) and H3K27me3 (red) levels present 750 bp upstream of TSSs in stage II gametocytes: depleted (log_2ChIP/input ≤0), occupied (log_2ChIP/input >0), robustly occupied (log_2ChIP/input ≥0.21 and ≥0.2 for H3K27me2&3, respectively) or enriched. For each of these categories, average transcript abundance (log_2Cy5/Cy3) (94) is plotted on days 0-8 of gametocyte (GC) development. The presence of stage II gametocytes in culture is highlighted by the grey shadowed regions across days 2-6.

For each category, the levels of H3K27me2&3 are inversely proportional to transcript abundance (e.g. no repression associated with depletion and enriched genes with the greatest reduction in transcript levels, Figure 2.11b), a relationship that confirms H3K27me2&3 are indeed associated with transcriptional repression in the stage II gametocytes. In addition to providing significance to the data, the trends associated with these significantly enriched sites validate the qualitative analysis used to determine robust occupancy. However, as the peak calling analyses were superior at filtering out background, only the significantly enriched gene sets identified in this way were employed in downstream analyses.

The transcriptional signatures associated with H3K27me2&3 in stage II gametocytes appear notably similar (Figure 2.11b) and to quantify these similarities, a differential binding analysis of the histone PTM-enriched sites identified during peak calling was performed. This differential analysis indicated extremely little divergence in the positioning of these two histone PTMs with only 7% independently enriched with H3K27me2 and 2% with H3K27me3 (Figure 2.12). This is

even more pronounced for the other gametocyte stages with only a single gene independently enriched with H3K27me3 in the post-stage II gametocytes and none in pre-stage II.

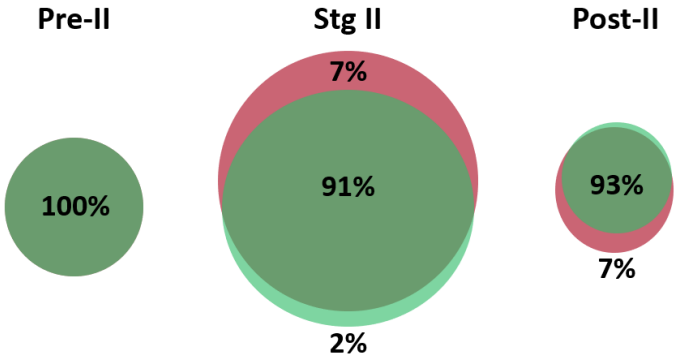

Figure 2.12: Extremely low divergence in the distribution of H3K27me2&3 enrichment in early gametocytes. Differential binding analysis was performed between the H3K27me2- and H3K27me3-enriched gene sets in the pre-stage II, stage II and post-stage II gametocyte stages with the percentages indicating the proportions of genes that are shared or independently enriched with either of the histone PTMs.

As the di- and tri-methylation of individual H3K27 residues are mutually exclusive (143), this confirms that one of these states of H3K27 methylation is an intermediary product in the generation of the other. In other eukaryotes, H3K27me2&3 are also have overlapping enrichment and functions (231, 233, 238). Therefore, downstream analyses were conducted using a consolidated list of all the H3K27me2&3-enriched sites in each stage.

2.3.7 H3K27me2&3 regulate transcription independently of other epigenetic mechanisms

In other eukaryotes dual regulation by co-existing H3K9me3 and H3K27me2&3 has been described (313), however, these histone PTMs are more frequently associated with discrete functions (314, 315). We therefore sought investigate the potential association between H3K9me3 and H3K27me2&3 in *P. falciparum* gametocytes. The interaction between H3K9me3 and HP1 is well-established as an important regulator of gene expression in the sexual stages of the *P. falciparum* life cycle (135). A few individual genes within internal chromosome regions are repressed via this mechanism, contrasting with the extensive domains of sub-telomeric heterochromatin. These sub-telomeric regions, organised into discrete clusters within the

nuclear periphery, consist largely of multi-gene families encoding erythrocyte invasion and immune evasion proteins and nutrient transporters that are subject clonally variant expression involving H3K9me3/HP1 (135, 209, 227, 316).

An evaluation of the consolidated set of 786 H3K27me2&3-enriched genes in the stage II gametocytes revealed a significant association with antigenic variation ($P = 4.87e^{-37}$) and modulation of host erythrocyte processes ($P = 1.18e^{-42}$), arising from the proportion (14%) of the enriched genes that are members of the *rif, stevor* and *var* multi-gene families. Although the precise role of the expression of these genes during commitment remains unclear, they are released from heterochromatin and upregulated by AP2-G at this point and subsequently re-repressed post-commitment (52, 94). Congruent with the repressive nature of H3K27me2&3 described here, both H3K27me2&3 are depleted (average occupancy of -0.01 and -0.06, respectively) upstream of the members of these multi-gene families in pre-stage II gametocytes. In the proceeding stage II gametocytes, these loci then become populated with H3K27me2&3 in addition to the re-association of these genes with H3K9me3/HP1 in the stage II/III gametocytes (135). Crucially, H3K27me2&3 enrichment is present at the proximal end of chromosome 2 and distal end of chromosome 14 (Figure 2.13), the two regions that show notable H3K9me3/HP1-mediated heterochromatin expansion in post-commitment gametocytes (135). These regions contain the gene clusters associated with the erythrocyte remodelling that occurs during early gametocyte differentiation including *kahrp* (PF3D7_0202000), *kahsp40* (PF3D7_0201800) and *emp3* (PF3D7_0201900) on chromosome 2 and on chromosome 14, several exported proteins (*phist,* PF3D7_1477300, PF3D7_1477400, 1477700, PF3D7_1478000) (58, 76, 317).

Interestingly, while both H3K9me3/HP1 and H3K27me2&3 populate these broad genomic areas in stage II gametocytes, the enrichment of particular gene regions by these histone PTMs is predominantly independent. Similarly in other eukaryotes, H3K9me3 and H3K27me2&3 may be present across the same broad genomic domains but have independent and non-redundant functions (318-323). For example, we find that the broad abundance of H3K9me3/HP1 in the CDRs of PF3D7_1476600, PF3D7_1477300 and PF3D7_1477400 contrasts with the depletion or lower levels of diffused H3K27me2&3 at these sites (Figure 2.13).

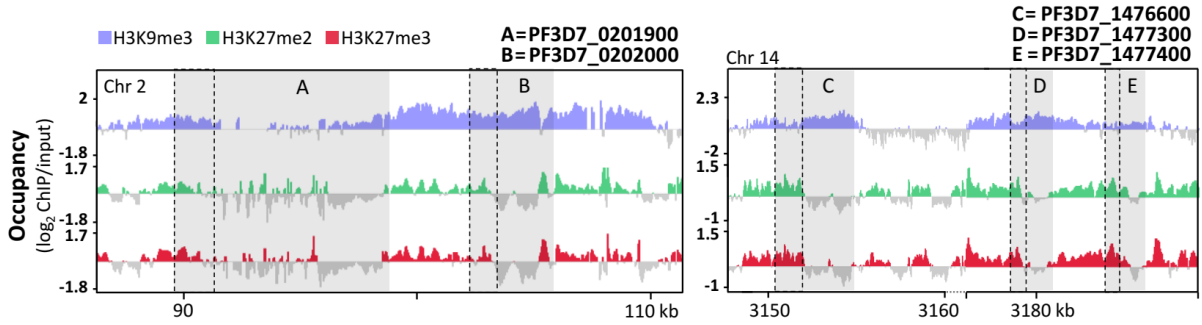

Figure 2.13: Independent H3K27me2&3 and H3K9me3/HP1 enrichment is characteristic of repressed genes during early gametocyte development. H3K27me2&3 occupancy (average log_2-transformed ChIP/input) across the broad genomic regions (ends of chromosomes 2 and 14) previously identified as preferentially occupied by H3K9me3/HP1 (blue) in stage II/III gametocytes (135). Genes encoding proteins of the cytoadherance complex (PF3D7_0201900, *emp3* and PF3D7_0202000, *kahrp*) and early gametocyte makers (PF3D7_1476600; PF3D7_1477300, *pfg14-744*; PF3D7_1477400, *phist*) are highlighted by the grey shadowed regions with all data representative of two biological replicates.

In CDRs enriched with both H3K9me3/HP1 and H3K27me2&3 (e.g. *kahrp* and *emp3),* these epigenetic factors occur in independent patterns. This suggests that while H3K9me3 and H3K27me2&3 are present in close genomic proximity, they do not co-exist on the same histone in stage II gametocytes. While H3K27me1 co-exists with H3R17me1 and H3K14ac in early-stage and with H3K4me3 and H3K14ac in late-stage gametocytes, no combinations of mono-, di- or tri-methylated H3K9 and H3K27 have been detected by either bottom-up (shorter peptides) (324) or middle-down proteomics (longer peptides) (325). Taken together, this indicates that the stage II gametocyte-specific H3K27me2&3 enrichment occurs and functions independently of the re-establishment of H3K9me3/HP1-mediated heterochromatin once post-commitment gametocyte development begins.

While H3K9m3/HP1-mediated heterochromatin is reorganised throughout the *P. falciparum* parasite life cycle (135), H3K9me3 is predominantly restricted to sub-telomeric regions (132, 227). No such bias towards certain chromosomal regions is present for H3K27me2&3 in the stage II gametocytes with the sites of enrichment relatively equally distributed across the lengths of both the positive and negative strands of each of the 14 *P. falciparum* chromosomes (Figure 2.14).

H3K27me2&3-enriched			
Chr	Total genes	Enriched Genes	Chromosome view
14	804	117	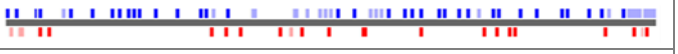
13	732	76	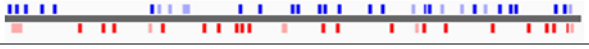
12	550	67	
11	505	70	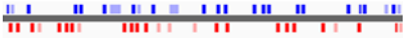
10	411	64	
9	379	50	
8	339	48	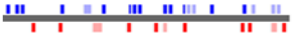
7	332	57	
6	332	30	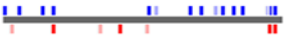
5	331	41	
4	260	56	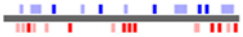
3	252	30	
2	236	49	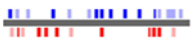
1	157	30	

Figure 2.14: H3K27me2&3-enriched genes are uniformly distributed across the genome in stage II gametocytes. Genome-wide chromosome maps of H3K27me2 and H3K27me3 enrichment in stage II gametocytes. The total number of genes and genes with enrichment is indicated for each chromosome. Chromosome maps were generated using the JBrowse genome viewer in PlasmoDB (326).

Furthermore, there is no evidence of preferential enrichment of certain chromosomes by H3K27me2&3 as has been demonstrated to be the case for H3K9me3 (135). This linear distribution of H3K27me2&3 enrichment in stage II gametocytes therefore further supports the independent nature of theses repressive mechanism. Finally, in contrast to H3K9me3, H3K27me2&3-associated repression reflects the broad genome-wide re-setting of gene expression that generates a transcriptional environment optimal for subsequent gametocyte development.

2.3.8 Chemical interrogation of histone methylation highlights the importance of histone PTMs in *P. falciparum* gametocytes

The enrichment of H3K27me2&3 in stage II gametocytes remains intriguing given the absence of PRC2 subunit homologs in *Plasmodium* parasites (200). Nevertheless, genetic disruption studies have alluded to the existence of alternative H3K27-specific methyltransferases (327-329). To begin the process of elucidating the writers of H3K27me2&3 in *P. falciparum*, epigenetic complex inhibitors (epidrugs) were used as tools to interrogate HMT activity based on the epidrugs' confirmed targets in other organisms. From a commercial epidrug library, nine histone methyltransferase inhibitors (HMTi) were selected and screened at 5 µM for 24 h against pre-stage II and stage II gametocyte populations. Pre-stage II gametocyte samples contained a large proportion of asexual-stage parasites (91%), some stage I gametocytes (8 ± 3%) and few stage II gametocytes (1 ± 1%). The stage II samples (day 4 and 5) predominantly consisted of stage II gametocytes (77 ± 11%) with smaller proportions of asexual parasites (10 ± 12%) and stage I (5 ± 3%) and stage III (8 ± 4%) gametocytes.

GSK343 was the most potent inhibitor (96%) of stage II gametocyte viability among the four epidrugs that target EZH2 (Enhancer of Zeste homolog 2), the major catalytic subunit of PRC2 (330, 331) (Table 2.1). Despite sharing a target, GSK343, 3-Deazaneoplanocin (DZNep) and UNC1999 have distinct transcriptional fingerprints and disrupt different pathways in cancer cell lines (332, 333). These differences in the downstream effects of target inhibition could explain the lower potency of DZNep (52%) and UNC1999 (78%) compared to GSK343 specifically in *P. falciparum* stage II gametocytes in which transcriptional reprogramming and differential pathway regulation drive the transition from early gametocyte differentiation to intermediate development (94). This postulation is supported by relatively similar levels of activity of these four epidrugs in the pre-stage II gametocytes (Table 2.1). Additionally, the lower potency of GSK126 (58%) compared to GSK343 in stage II gametocytes aligns with previous observations in cancer cell lines where increased potency has been attributed to GSK343's enhanced membrane permeability (334-336).

Likewise, one of the G9a inhibitors, UNC0224 was more active compared to the others, inhibiting 83% of stage II gametocyte viability compared to only 72% and 62% for UNC0638 and BIX-01294, respectively (Table 2.1). This is not unexpected since UNC0224 was obtained from the derivatisation of BIX-01294 in order to improve activity (337). Although more potent in cell-free assays, the poorer pharmacokinetic properties of UNC0638 compared to the UNC0224 parent inhibitor provides a possible explanation this epidrug's lower activity in the stage II gametocytes (338). The *s*-adenosyl-homocysteine (SAH) hydrolase inhibitor neplanocin A (339) and chaetocin (inhibitor of SUV39H1) (340) were not particularly potent, inhibiting 61% and 64% of the stage II gametocytes, respectively (Table 2.1).

Table 2.1: Selected histone methyltransferase inhibitors screened against early gametocytes. Pre-stage II (91% asexual parasites, 8 ± 3% stage I and 1 ± 1% stage II gametocytes) and stage II (77 ± 11% stage II, 5 ± 3% stage I and 8 ± 4% stage III gametocytes and 10 ± 12% asexual parasites) gametocytes were subject to treatment with HMT inhibitors (5 µM) for 24 hours with the % of gametocyte inhibition determined thereafter. Results represent the average of two biological data points for each stage with drug assays performed in technical triplicate for each. The mammalian target and possible target in *P. falciparum* are provided. The two epidrugs with the greatest degree of activity against stage II gametocytes are highlighted by bold text.

Inhibitor	Mammalian target	Possible target in *P. falciparum*	Gametocyte inhibition (%)	
			Pre-stage II	Stage II
GSK343	**SUV39H1**	**SET3**	**49**	**96**
UNC1999	EZH2		**56**	**78**
GSK126	EZH2		**62**	**58**
3-Deazaneoplanocin	EZH2		**63**	**52**
Chaetocin	SUV39H1	SET3	**64**	**64**
UNC0224	**G9a**		**37**	**83**
UNC0638	G9a	**SET7**	**65**	**72**
BIX-1294	G9a		**70**	**62**
Neplanocin A	SAHH	SAHH	**51**	**61**

The reduced transcript abundance of the possible target of neplanocin A, *sahh* (PF3D7_0520900) in the stage II gametocytes (Figure 2.15) is congruent with the lower potency of this epidrug.

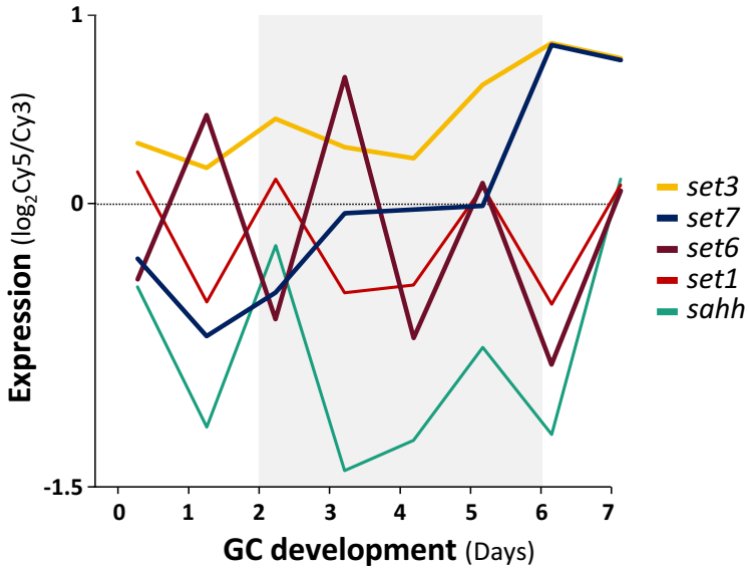

Figure 2.15: Transcription profiles of the potential targets of histone methyltransferase inhibitors during early and intermediate gametocyte development. Expression profiles (log_2Cy5/Cy3) of genes encoding the *P. falciparum* histone methyltransferases *set1* (PF3D7_0629700), *set3* (PF3D7_0827800), *set6* (PF3D7_1355300), *set7* (PF3D7_1115200) and *sahh* (PF3D7_0520900) on days 0 to 7 of gametocyte (GC) development (94). The grey shadowed region represents days on which stage II gametocytes were present in culture.

The expression levels of *set3* and *set7* in the stage II gametocytes (Figure 2.15) suggest that these HMTs may be involved in the deposition of H3K27me2&3 in *P. falciparum* parasites. During eukaryotic cellular differentiation, G9a-mediated H3K9 methylation predominantly silences previously euchromatic genes (341), similar to the activities of H3K27me2&3 in stage II gametocytes. In addition to its characteristic H3K9 methyltransferase activity, G9a is also able to methylate H3K27 *in vitro* (342) and *in vivo* (327). While H3K9 is the major substrate of SET7 (homologous to G9a), *in vitro* this HMT also methylates H3K27 (200), supporting the involvement of SET7 in generating the enrichment of H3K27me2&3 in stage II gametocytes.

In light of these considerations and the potency of GSK343 and UNC0224 towards the stage II gametocytes, these two epidrugs were further evaluated using the same treatment conditions used in the primary drug screen (5µM, 24h) to determine if their activity is linked to the inhibition of H3K27 di- and tri-methylation. Untreated stage II gametocytes showed 5- and 7-fold greater levels of H3K27me2 compared to those treated with GSK343 and UNC0224, respectively (Figure 2.16). Furthermore, both epidrugs almost completely abolished the presence of H3K27me3 (19- and 15-fold lower for GSK343 and UNC0224, respectively) compared to the untreated control

gametocytes (Figure 2.16). The greater effect of these HMTi epidrugs on H3K27me3 supports the intermediary nature of H3K27me2 and demonstrates that histone methylation is specifically affected by HMTi in *Plasmodium* parasites.

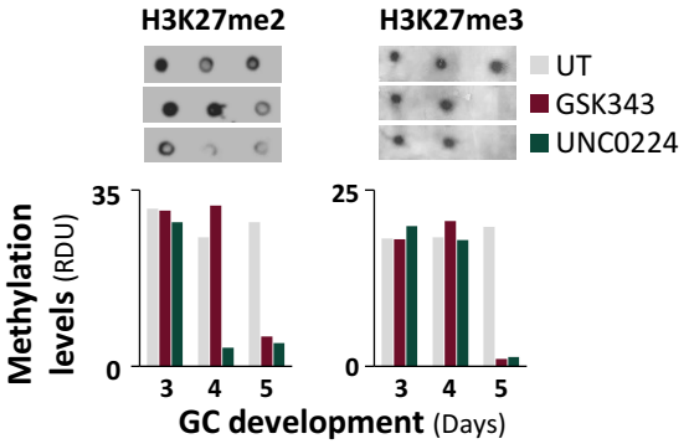

Figure 2.16: The activity of the histone methyltransferase inhibitors, GSK343 and UNC0224, is associated with H3K27 hypomethylation in stage II gametocytes. (a) Detection of changes in H3K27me2&3 levels by dot blot analysis of stage II (days 3-5) gametocytes treated for 24 h with 5 µM GSK343 (maroon) or UNC0224 (green) compared to untreated (UT, gray) control gametocytes prepared in parallel. Data are representative of a single biological replicate for each day of treatment. Methylation levels are expressed as the relative density units (RDU) for each sample above background.

These findings support UNC0224 and GSK343 as inhibitors of HMT activity in *P. falciparum* parasites. Next we sought to predict whether UNC0224 (G9a) and GSK343 (EZH2) specifically inhibit SET7 and SET3 in *P. falciparum* gametocytes, respectively using a computational molecular docking approach. Models were obtained from the AlphaFold 2.0 database that contains high-quality structural predictions for 5187 *P. falciparum* proteins including SET3 and SET7. AlphaFold 2.0 uses a novel machine learning approach to predict protein structures with atomic accuracy even in the absence of homologous structures (284), making it ideal for predicting protein folding in *Plasmodium* parasites. Indeed the confidence levels for the SET domain-containing regions of the SET3 and SET7 models obtained from AlphaFold 2.0 were substantially higher (per-residue score >70, indicating high to very high confidence models) compared to those generated within SwissModel (283) (global mean quality estimate (GMQE) = 0.25 and 0.35 for SET3 and SET7, respectively). Thus, UNC0224 and GSK343 were docked into the SET7 and SET3 models predicted by AlphaFold 2.0 using SwissDock (285).

Predicted binding sites for SET7-UNC0224 were represented by 35 clusters with populations of between three and eight members. Of these, 13 clusters demonstrate binding within the SET-domain (Glu^{353}-Tyr^{551}) with one of these clusters corresponding to the direct occlusion of residues (Asn^{495}, Ala^{496}, Ser^{513}, Met^{514} and Leu^{515}) predicted to be critical for the active site of SET7. The third member of this cluster represents a binding mode between UNC0224 and SET7 with Gibbs' free energy, ΔG = -11.7 kcal/mol (Figure 2.17a).

The docking of GSK343 into SET3 resulted in 34 clusters consisting of between two and nine members. Eight of these clusters represent a favourable interaction between GSK343 and the SET domain-containing region (Tyr^{2252}-Ile^{2385}) with ΔG values for individual binding modes ranging from -8.26 to -10.26 kcal/mol. Unfortunately, no predictions of the critical amino acid residues are currently availble for the active site of SET3.

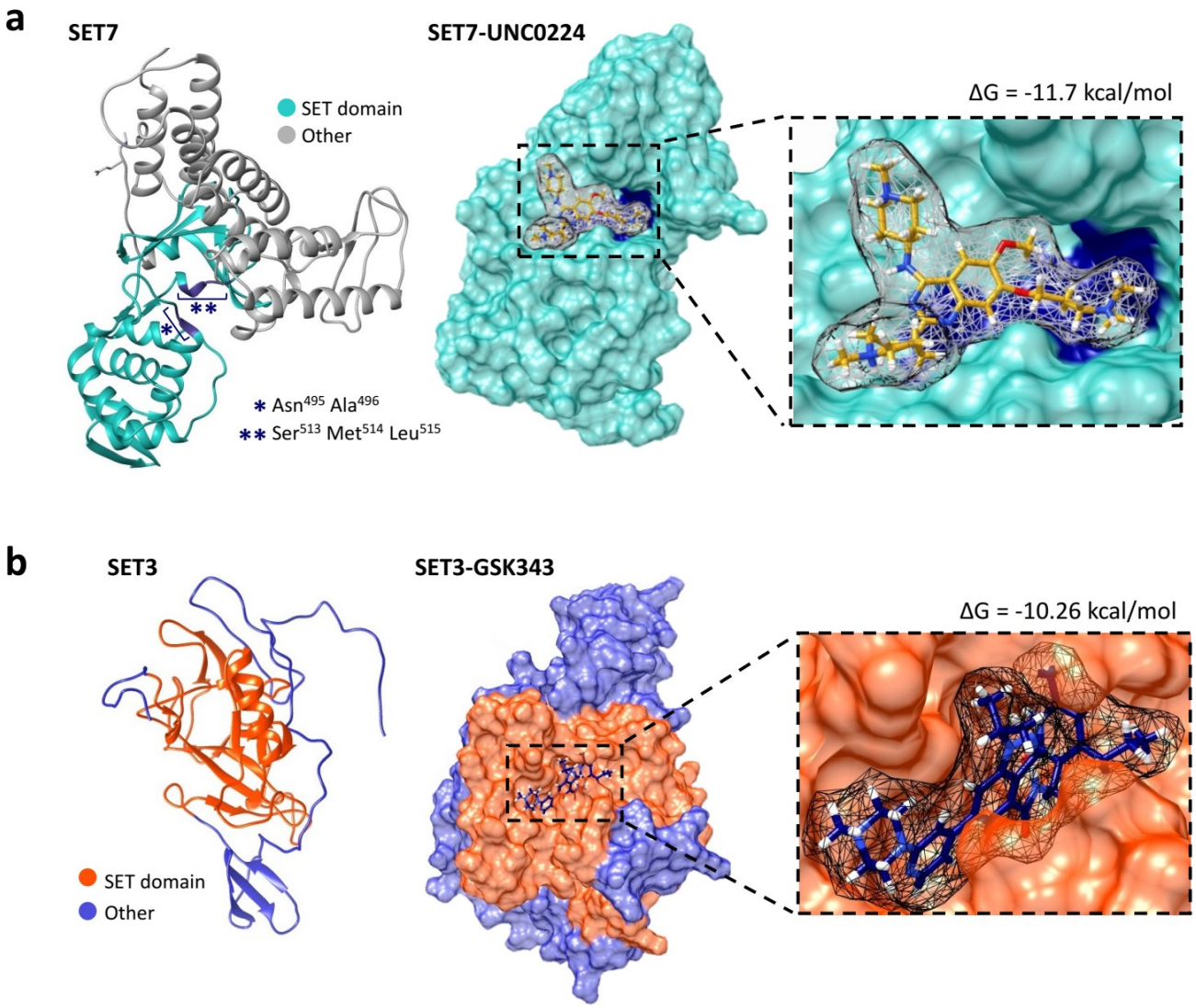

Figure 2.17: Molecular docking predicts the favourable binding of HMTi into *P.falciparum* SET7 and SET3. Predicted models for SET7 and SET3 were obtained from AlphaFold (www.alphafold.ebi.ac.uk) (284). Ligand structures for were generated using the canonical SMILES in UCSF Chimera (282) and obtained from the ZINC database (281) for UNC0224 and GSK343, respectively. Protein and ligand structures were prepared with Dock Prep (282) followed by docking with SwissDock (285). Visualisation of the docking results was performed using UCSF Chimera (282). **(a)** The SET domain of SET7 is coloured light blue with critical amino acid residues within the active site indicated by dark blue to distinguish these regions from the rest of the protein (grey). The most favourable binding mode from the cluster corresponding to a direct occlusion of critical amino acid residues is shown with free energy value. **(b)** The SET domain is coloured orange to distinguish the region from the rest of the predicted structure for SET3. The most favourable binding mode from the eight clusters representing SET domain-specific binding is shown with corresponding free energy (ΔG) value.

The binding mode with the most favourable interaction for SET3-GSK343 has predicted binding energy of ΔG = -10.26 kcal/mol (Figure 2.17b). These molecular docking predictions provide evidence supporting that the activities of GSK343 and UNC0224 may arise from SET3 and SET7

inhibition, respectively, the postulated targets for these inhibitors in *P. falciparum* gametocytes. However, it is important to note that this does not exclude the possiblity of other targets that may also be inhibited by these epidrugs.

Next, to investigate the transcriptional perturbations underlying the gametocytocidal activity and H3K27 hypomethylation induced by UNC0224 and GSK343 in the stage II gametocytes, genome-wide expression profiling was performed using the same treatment conditions (24 h, 5 µM) used in previous experiments.

Treatment of stage II gametocytes with GSK343 induced differential expression ($log_2FC \geq 0.5$ in either direction) of 1192 genes, equating to ~22% of the genome (Appendix: Table S8). Large proportions of the 563 differentially expressed (DE) genes with increased transcript abundance belong to the broad functional categories of host erythrocyte remodelling (6%), invasion (8%) and gene expression (15%) or not classified (28%, owing to the current lack of functional annotation) (Figure 2.18). The genes not falling into any of these categories (43%) are significantly associated with ncRNA processing ($P = 0.044$), mRNA splicing ($P = 0.024$), cell motility ($P = 0.029$) and DNA replication ($P = 0.01$; Appendix: Table S9), each of which were also significantly linked with H3K27me2&3-enriched gene sets in stage II gametocytes (see section 2.3.7).

Accordingly, 59% of the genes with increased expression have robust H3K27me2&3 occupancy in stage II gametocytes (Figure 2.18). This suggests that the activity of GSK343 does indeed lead to abnormal expression of genes that are associated with H3K27me2&3-associated repression in the stage II gametocytes. A slightly greater number of genes (629) had reduced transcript abundance downstream of GSK343 treatment however, a similar proportion (57%) of these were associated with robust H3K27me2&3 occupancy in stage II gametocytes (Figure 2.18). Genes with decreased transcript abundance could be similarly categorised based on the functional annotations of host erythrocyte remodelling (6%), invasion (12%), gene expression (15%) or a lack thereof (31%).

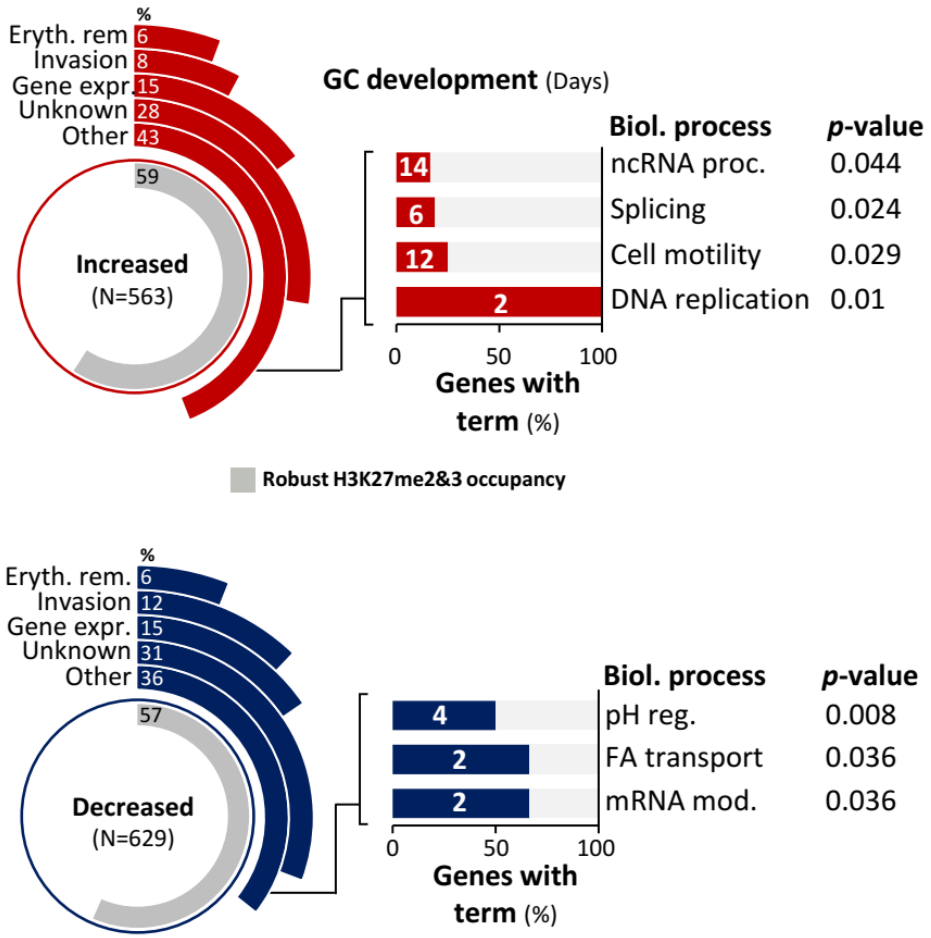

Figure 2.18: GSK343 induces abnormal transcription patterns in stage II gametocytes. Functional classification of DE genes (with increased (red) or decreased (blue) expression) in response to GSK343 in stage II gametocytes. The number of DE genes assigned to each biological category is shown and expressed as a proportion (%) of the full DE gene set. The proportion of genes that is robustly occupied by H3K27me2&3 (log_2ChIP/input ≥0.21 and ≥0.2, respectively) in the stage II gametocytes is shown on the inner most segment with data representative of two independent biological repeats.

The set of genes assigned to the category "other" (36%) is significantly associated with pH regulation (P = 0.008), fatty acid transport (P = 0.036) and mRNA modification (P = 0.036, Figure 2.18). As fatty acid metabolism is extensively remodelled during sexual development to supply a sufficient source of lipids for energy and membrane formation (310, 312), the disruption of this process by GSK343 during gametocyte development would be particularly detrimental.

Interestingly, UNC0224 perturbed the expression of a larger fraction (36%) of the stage II gametocyte genome compared to GSK343. This UNC0224-mediated disruption is underpinned by 919 and 1041 genes with increased and decreased transcript levels, respectively. Relatively

similar proportions of genes with increased and decreased transcript abundance could be functionally categorised into the invasion (8 and 9%, respectively) and gene expression (17 and 18%, respectively) classes (Figure 2.19). However, the number of genes with increased transcript abundance that are functionally associated with erythrocyte remodelling (6%) was double that of genes with reduced transcript levels (3%).

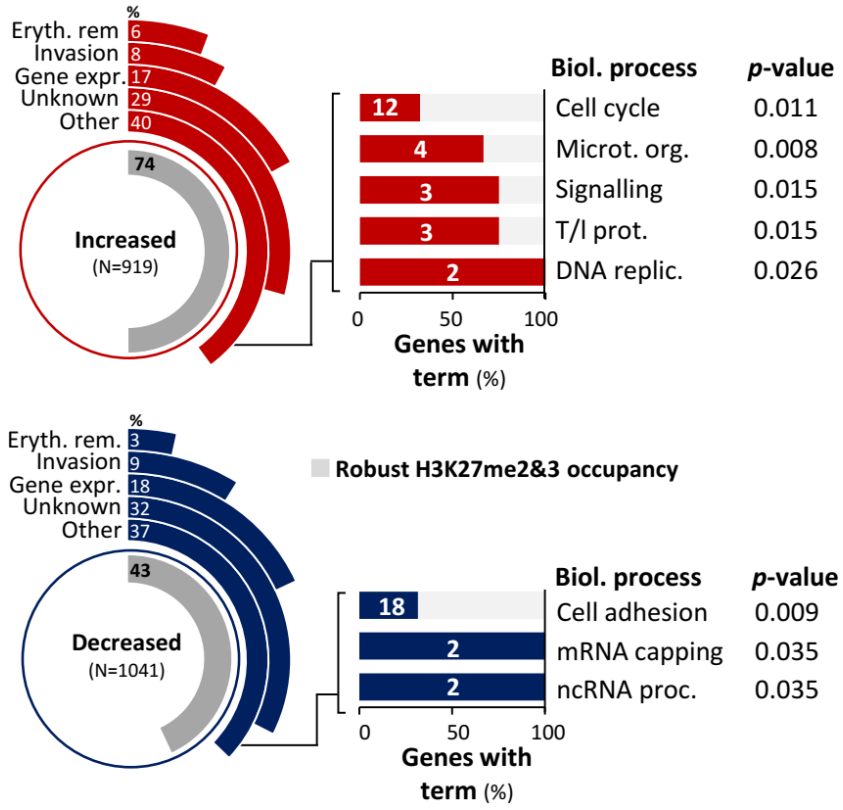

Figure 2.19: Genome-wide fingerprint of the transcriptional disruption induced by UNC0224 in early gametocytes. Classification of DE genes (with increased (red) or decreased (blue) transcript abundance) based on function with the number of genes within each biological process shown and expressed as a proportion (%) of the entire set of DE genes. The inner-most grey segment indicates the proportion of DE genes with robust H3K27me2&3 occupancy in the stage II gametocytes with data representative of two biological replicates.

Genes with increased transcript abundance are of particular interest since inhibiting the methylation of H3K9 and H3K27 would lead to the loss of normal transcriptional repression. The genes in the category "other" (40%) (Figure 2.19) are significantly associated with processes that are suppressed during early gametocyte development including the asexual parasite-specific processes of cell cycle regulation (P = 0.011), DNA replication (P = 0.026), microtubule

organisation (*P* = 0.008) and translation (*P* = 0.015; Appendix) (Table S9) and become active in the late gametocyte and gamete stages (93, 343). Fewer UNC0224-specific DE genes are associated with robust levels of H3K27me2&3 occupancy (43% of genes with decreased transcript abundance) compared to GSK343. This combined with the broader transcriptional disruption by UNC0224 compared to GSK343 (36% *vs.* 22% of the genome) could arise from the aberrant methylation of both H3K9 and H3K27 as a result of SET7 inhibition by UNC0224.

A comparison of the transcriptional signatures associated with the epidrugs in stage II gametocytes indicated that 52% and 32% of the GSK343 and UNC0224 DE genes overlap (Figure 2.20). This set of 624 commonly dysregulated genes is significantly associated with the molecular functions of lipase activity (*P* = 0.029) and carboxylic acid transmembrane transport (*P* = 0.047), highlighting the link between gametocyte metabolism and the potency of GSK343 and UNC0224 (Appendix: Table S9). Furthermore, these shared genes encode protein products involved in DNA binding activity (*P* = 0.024) and H3K4 methylation (*P* = 0.012) (Figure 2.20) both of which underpin the effect of the inhibitors on epigenetic genome regulation. The DE genes that are unique to each inhibitor reflect the differential target inhibition by GSK343 (SET3) and UNC0224 (SET7) as determined by molecular docking.

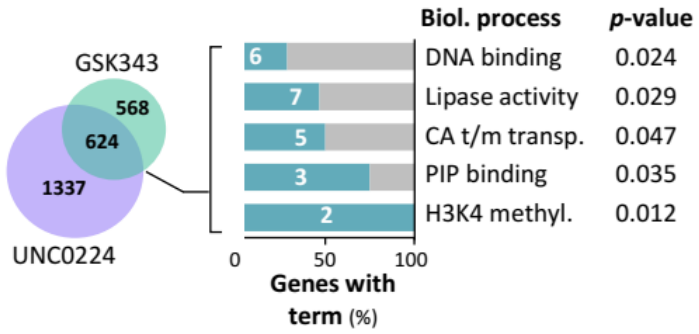

Figure 2.20: Comparison of the transcription fingerprints associated with GSK343- and UNC0224-treated early gametocytes. Genes with differential expression ($log_2FC \geq 0.5$ in either direction) induced by GSK343 and UNC0224 in the stage II gametocytes were compared and the biological (biol.) processes significantly associated (*P*-value ≤0.05) with both inhibitors are shown.

2.4 Discussion

Deciphering the intricate life cycle of *Plasmodium* parasites and the regulation thereof is foundational to accelerate the discovery and development of novel chemotherapeutics for malaria eradication (344-346). To date, only a handful of epigenetic mechanisms had been examined in the context of gametocyte development (89, 135, 347). However, the extensive transcriptional reprogramming that occurs during gametocytogenesis and the limited genomic distribution of the constitutive heterochromatin regulator, H3K9me3 (135, 262, 264) strongly implied contributions by additional epigenetic mechanisms. In this chapter, the stage II gametocyte-specific abundance of H3K27me2&3 was studied through a combination of ChIP-seq and transcriptional profiling following chemical perturbation of histone methyltransferase activity. This integrated approach provides a thorough demonstration of the link between H3K27me2&3 and transcriptional regulation, thereby lending evidence to the existence of functional H3K27me2&3 in *Plasmodium* parasites which until recently (133), was not clear. Specifically, H3K27me2&3 contribute to gene regulation during the transition from early (stage I) to intermediate (stage III/IV) gametocyte development. The stage II gametocyte has previously been postulated as a key transition point at which non-essential processes are "switched off" to allow subsequent development (94). Indeed, we find that H3K27me2&3 enrichment and repression of asexual stage-related genes is prolific in stage II gametocytes.

H3K27me2&3 are typically indicative of gene repression and are more commonly involved in transcriptional reprogramming during the early and intermediate stages of eukaryotic cellular differentiation (232, 240, 266-270). Notably, we observe that these characteristic eukaryotic trends of H3K27me2&3 distribution and function are conserved in *Plasmodium* parasites. In stage II gametocytes, intragenic regions are most highly enriched with H3K27me2&3, congruent with the distribution of these histone PTMs when functioning in a repressive capacity in higher organisms (241, 242, 348). Additionally, the H3K27me2&3-associated repression of genes that become obsolete during gametocytogenesis emphasises that the cellular differentiation-specific roles of these histone PTMs are preserved in *Plasmodium* parasites. The pre- and post-stage II gametocyte populations used in this study not only served as controls to define stage II gametocyte-specific trends but also further implicate H3K27me2&3 as a repressive mechanism

in *P. falciparum* parasites. Although considerably fewer, the presence of H3K27me2&3-enriched genes in pre- and post-stage II gametocytes implies that these histone PTMs may function in a less prominent capacity in the other life cycle stages similar to the maintenance functions of H3K27me2&3 in differentiated cells in higher organisms (349-351). In this study due to the significant overlap between H3K27me2 and H3K27me3 enrichment, we predominantly evaluated these histone PTMs as a single entity. We note that this overlapping enrichment reflects one of two possible scenarios: 1) one of these histone PTMs is present as an intermediate in the formation of the other or, 2) the presence of nucleosomes that have an asymmetrically modified histone H3 pair. To date, little is known regarding their functional relevance and how common asymmetrically modified nucleosomes are among eukaryotes however, H3K27me2&3 have been reported to asymmetrically modify nucleosomes in embryonic stem cells (306). Therefore, our findings facilitate future investigations into the possible presence of asymmetrically modified nucleosomes in *Plasmodium* parasites.

The diffuse distribution of H3K27me2&3 and lack of bias towards the enrichment of certain chromosomal regions or multi-gene clusters in *P. falciparum* parasites reflects the typical nature of these histone PTMs in differentiating cells (238, 239, 244). Furthermore, we find H3K27me2&3 enrichment is predominantly independent from the restricted distribution of H3K9me3 (135) in the stage II gametocytes, indicating that the mechanisms of H3K27me2&3 enrichment and repression are independent of other epigenetic regulators. Similarly in model eukaryotes, the deposition and removal, genomic distributions and functions of H3K9me3 and H3K27me2&3 are largely independent with these histone PTMs rarely present on the same histone (261, 267, 270). Congruent with this, studies employing bottom-up (133) and middle-down (325) mass spectrometry did not identify combinations of H3K27me2&3 with H3K9me3 on the same histone throughout the *P. falciparum* life cycle. Together, these data support the largely independent distribution and non-redundant function described here for H3K27me2&3 in stage II gametocytes.

HDACs are responsible for the removal of acetyl PTMs from histones with this enabling and promoting the subsequent methylation of lysine residues (352). This is particularly prominent following eukaryotic stem cell fate decision where enhanced HDAC activity leads to H3K27

deacetylation in favour of the tri-methylation of these residues. This H3K27me3 is subsequently involved in repressing genes that are irrelevant for the differentiation of a particular cell type (243, 353). Similarly, in *P. falciparum* stage II gametocytes, H3K27me2&3 enrich and repress genes that are not required for gametocyte differentiation. In stage I gametocytes, acetylation is more abundant at certain sites, including H3K27 and H3K9, compared to the subsequent developmental stages (133). Interestingly, the HDAC inhibitor, JX21108 has stage-specific efficacy towards *P. falciparum* stage II gametocytes (354), suggesting that chromatin deacetylation may be critically important at this stage. These findings provide an interesting question for future investigation as to whether regions associated with H3K27ac in stage I gametocytes overlap with H3K27me2&3-enriched sites identified in this study. If so, this would suggest that as in higher eukaryotes (243, 353), the deacetylation of H3K27 is a prerequisite for the H3K27me2&3 accumulation that subsequently drives gametocyte development.

Following fertilisation in mice, H3K4 is tri-methylated leading to the activation of master transcriptional regulators with this followed by a genome-wide increase in H3K27me3 levels. Thereafter, the distinct H3K4me3- and H3K27me3-associated chromatin domains independently drive the transition from the two-cell stage to a blastocyst (236). H3K4me3 abundance also increases in the stage I gametocytes (133) however, the functional relevance of this for transcriptional regulation remains unknown. Thus, it will be interesting to examine whether H3K4me3 similarly activates sexual commitment master regulators prior to their enrichment and repression by H3K27me2&3 once gametocytogenesis has been established.

This conservation of eukaryotic epigenetic mechanisms for regulating sexual differentiation in *Plasmodium* parasites is underscored by the cross-species potency and induction of H3K27 hypomethylation in stage II gametocytes by the mammalian HMTi, GSK343 and UNC0224. It could be argued that the use of epidrugs to probe HMT activity was not ideal to identify the enzymes responsible for H3K27me2&3 in *Plasmodium* parasites, particularly in the case of inhibitors of G9a (UNC0224), an HMT with site-specificity towards both H3K9 and H3K27 (327, 342). However, as the *Plasmodium* parasite genome lacks the ubiquitous H3K27-specific modifying complexes (200), there were no clear candidate HMTs that could be targeted in genetic manipulation experiments. Thus, the use of epidrugs that have been well-studied in mammals

(337, 355, 356) was a logical starting point in the effort to understand histone methylation in *Plasmodium* parasites. This chemical interrogation emphasised the importance of histone PTMs and epigenetic regulation as a whole for the transmissible stages of the malaria parasite. Despite their efficacy against gametocytes, UNC0224 and GSK343 could not be developed as anti-malarial medications due to the evolutionary conservation of epigenetic mechanisms in eukaryotes. Nevertheless, this study shows that these and other similar inhibitors are invaluable tools for studying epigenetic regulatory mechanisms. Indeed, the use of GSK343 and UNC0224 provided novel insights into the mechanisms regulating *P. falciparum* gametocytogenesis and illuminated SET3 and SET7 as clear candidates for the further investigation of H3K27-specific HMTs

Together, these findings provide substantial evidence that epigenetic regulation and in particular, histone PTMs, are crucial transcriptional regulators in gametocytes. Although the morphological stage transitions and associated transcriptional shifts during gametocytogenesis have been well-studied (94), the mechanisms regulating these broad changes remained elusive. This study provides the first examination of specific factors that contribute to the transcriptional reprogramming during early gametocyte differentiation. As in other eukaryotes (229, 231, 236, 243), H3K27me2&3 play an integral part in directing the transcriptional program required for gametocyte differentiation. Ultimately, this chapter contributes to a greater understanding of epigenetic regulatory mechanisms in the transmissible stages of the human malaria parasite.

Chapter 3

H3K36me2&3 reprogram gene expression to drive early gametocyte development in *Plasmodium falciparum*

The work in this chapter has been published as follows:

> Connacher J., Josling G.A., Orchard L.M., Reader J., Llinás M., Birkholtz LM. H3K36 methylation reprograms gene expression to drive early gametocyte development in *Plasmodium falciparum*. Epigenetics Chromatin. 2021 Apr 1;14(1):19 (347).

Drug microarrays presented in this chapter were published as follows:

> Reader, J., van der Watt, M.E., Taylor, D., Le Manach, C., Mittal, N., Ottilie, S., Theron, A., Moyo, P., Erlank, E., Nardini, L., Venter, N., Lauterbach, S., Bezuidenhout, B., Horatscheck, A., van Heerden, A., Spillman, N.J., Cowell, A.N., Connacher, J., Opperman, D., Orchard, L.M., Llinás, M., Istvan, E.S., Boyle, G.A., Calvo, D., Mancama, D., Coetzer, T.L., Winzeler, E.A., Duffy, J., Koekemoer, L.L., Basarab, G., Chibale, K. and Birkholtz, L.M. Multistage and transmission-blocking targeted antimalarials discovered from the open-source MMV Pandemic Response Box. Nature Communications, 2021;12(1):269 (357).

3.1 Introduction

Malaria remains a serious threat to public health in most of the developing world and is responsible for millions of deaths annually (1). Nevertheless, progress is being made toward the global eradication of the disease (358). Malaria eradication relies on preventing the transmission of *Plasmodium* parasites between human hosts, facilitated by the mosquito vector. In the human host, malaria parasites exist either as the asexual proliferative stages, responsible for the symptoms of malaria, or as sexually differentiated and transmissible gametocytes (43, 51). The extended 10-12 day process of gametocyte development is characterised by morphologically distinct stages (I-V) and is unique to the human malaria parasite, *Plasmodium falciparum.* Mature gametocytes are the only stage within the life cycle that can be transmitted to a new human host and as such, the mechanisms and processes underlying gametocyte differentiation and development are ideal targets for transmission-blocking interventions (40, 45, 359).

The transition from one stage to the next in the *P. falciparum* life cycle is driven by global gene expression reprogramming that is tightly regulated by complex transcriptional and post-transcriptional control mechanisms (104, 343, 360). Additionally, epigenetic factors are known to establish and maintain the transcriptional programs that support proliferation in asexual parasites and are postulated to do the same during gametocyte development (183). The histone PTM landscape in *P. falciparum* parasites is dynamic with each life cycle stage associated with a unique subset of PTMs that have been postulated as fundamental for generating the specialised transcriptional program for the stage (133). Accordingly, several histone PTMs have shown to be functionally relevant for asexual parasite processes (361). For example, H3K4me3, H3K8ac and H3K9ac are involved in the transcriptional activation of stage-specific genes encoding products that drive proliferation and the maintenance of the euchromatic genome that is characteristic of the asexual parasite stages (184, 188, 203, 218, 260). By contrast, H3K36me2 is anti-correlated with global transcript abundance in asexual parasites and as such, is likely to be repressive in these stags (258). While more often linked to broad maintenance functions such as the conservation of genomic integrity, H3K36me2 also directs gene repression in model eukaryotes (362-364). H3K36me3 is also associated with transcriptional silencing and regulates the mutually exclusive expression of single members belonging to the multi-gene invasion, immune evasion and export protein families, thereby contributing to the parasite's extensive capacity for phenotypic plasticity (205, 209, 365). H3K36me2&3 are both well-documented regulators of eukaryotic cellular differentiation and development (269, 362, 366).

During proliferation, sexual stage-specific genes are silenced either by the lack of expression of their transcription factors or by their localisation within H3K9me3/HP1-mediated heterochromatin (89, 227). Sexual differentiation involves the release of the commitment master switch, *ap2-g* from this repressive chromatin structure, resulting in a transcriptional environment that drives sexual commitment (52, 77, 86, 135). However, only a handful of studies have examined the epigenetic mechanisms that are associated with post-commitment gametocyte development (89, 135, 195). Aside from the demonstrated role of H3K9me3/HP1 in heterochromatin rearrangement for stage-specific gene sets during gametocytogenesis (359),

the functions of histone PTMs in generating gametocyte-relevant transcriptional programs have not been studied.

The dynamic nature of the histone PTM landscape during gametocyte development and departure from the patterns observed during asexual proliferation are predictive of roles for these histone PTMs in directing gametocyte stage-specific transcription in a way similar to that in the asexual parasites (89, 132, 135, 183, 218, 361, 367). In line with this, the shifts in the histone PTM and transcriptomic landscapes occur in parallel with morphological stage transitions in gametocytes (94, 133). The striking peak abundance of H3K36me2&3 occurring uniquely in the stage II gametocytes is intriguing, particularly given the corresponding changes in the transcriptome and morphology associated with the transition from early differentiation (stage I) to intermediate (stage III) development (94, 133). Therefore, we set out to examine the functional consequences of this increase in histone PTM abundance during the early stages of gametocytogenesis (133). To do so, chromatin immunoprecipitation followed by high-throughput sequencing (ChIP-seq) performed using three distinct gametocyte populations and the results integrated with published data from other ChIP-seq and transcriptome profiling studies. This chapter provides a comprehensive map of H3K36me2&3 occupancy during early and intermediate gametocyte development and documents the role of these histone PTMs in the transcriptional reprogramming underlying the transition from early gametocyte differentiation to intermediate development (94). Furthermore, through the chemical interrogation of HDM activity, this work highlights the importance of histone methylation for sexual differentiation in *P. falciparum* parasites and in particular, the role of H3K36me2&3 for gene expression in early gametocyte development. The combined use of histone methylation profiling and whole transcriptome analysis revealed a link between histone demethylation and the enhanced gametocytocidal activity of the mammalian Jumonji-C HDM inhibitors, JIB-04 and ML324 (212, 368). The inherent novelty of the work presented here is embedded in the first association between H3K36me2&3 and gene regulation in gametocytes. Furthermore, this work provides evidence to support the postulation that the dynamic deposition and removal of histone PTMs drives gene expression reprogramming during *P. falciparum* sexual differentiation and development.

3.2 Materials and methods

3.2.1 *In vitro* parasite culturing

The *P. falciparum* NF54 parasite cultures used here for the ChIP-seq and microarray experiments were the same as those used for the experiments in Chapter 2 (section 2.2.1) and thus the *in vitro* cultivation methodology is identical to that followed previously. For histone methylation profiling and DNA microarray experiments, single biological replicates were generated. Two independent cultures were prepared as biological replicates for each of the ChIP-seq and ChIP-qPCR experiments.

3.2.2 H3K36me2&3 ChIP antibody validation

The commercial antibodies selected for the ChIP-seq study were previously demonstrated (same batch numbers) to be specific towards H3K36me2&3 in *P. falciparum* and other eukaryotes (205, 233, 367, 369-371). Nevertheless, the specificity of the ChIP-grade rabbit α-H3K36me2 (Abcam, ab9049) and α-H3K36me3 (Abcam, ab9050) antibodies was validated using modified and unmodified synthetic peptides (Genscript) of the *P. falciparum* 3D7 histone H3 sequence as per ENCODE standards (www.encodeproject.org) and using the same methodology outlined in Chapter 2 (section 2.2.2 and Appendix: Table S1). Briefly, the modified peptides were di- or tri-methylated on K9, K27 or K36 each with a corresponding unmodified peptide. Nitrocellulose membranes containing 25 ng spots of each peptide were blocked for 30 min in blocking buffer and incubated with primary antibodies (1:5000) against H3K36me2 or H3K36me3 overnight followed 1 h incubation with HRP-conjugated rabbit α-IgG secondary antibody (1:10000). Chemiluminescent signal intensity was subsequently quantified using densitometry in ImageJ analysis software (276).

3.2.3 H3K36me2&3 chromatin immunoprecipitation

ChIP was performed as previously described (52) with modifications as described in section 2.2.3. Briefly gametocytes (1-3% gametocytaemia, fixed in 1% formaldehyde for 10 min at 37°C followed by 0.125 mM glycine quenching) were released from erythrocytes using 0.1% (w/v) saponin. Thereafter, chromatin was sonicated and then pre-cleared using Protein A/G magnetic beads (Millipore 16-663). Aside from a small quantity set aside to serve as input material, the pre-cleared chromatin was incubated overnight with 3 µg of α-H3K36me2 or α-H3K36me3 antibodies. Cross-linking was reversed, the DNA was treated with RNAseA and Proteinase K and subsequently purified.

3.2.4 DNA library preparation and sequencing

DNA libraries were prepared for sequencing as in Chapter 2 (section 2.2.4) and as described elsewhere (52). In brief, DNA fragments were end-repaired and A-tailed followed by the ligation of indexed adaptors. The size (250 bp) selected fragments were then PCR amplified and the resulting DNA products were purified with integrity and concentration determined by Qubit fluorometry. Sequencing of the DNA libraries was carried out on an Illumina HiSeq 2500.

3.2.5 ChIP-qPCR

ChIP-qPCR was performed on the same material used for ChIP-seq and as described in section 2.2.5. Using 10x serial dilutions of NF54 genomic DNA all primers were determined to be ≥90% efficient and specific, evidenced by single peaks on the melting curves. ChIP-qPCR data were analysed using the ΔΔCt method and values are expressed as fold enrichment of IP to input DNA, averaged for two biological replicates for H3K36me2&3 in stage II and post-stage II gametocytes. Pre-stage II gametocyte data represents only one replicate as insufficient DNA was obtained for the second replicate samples.

3.2.6 Epigenetic inhibitor assays

The *in vitro* activity of five histone demethylase inhibitors from the Cayman Epigenetic Screening Library (Cayman Chemicals, #11076, batch 0498084-1) was screened in early gametocytes with the pLDH assay as described previously in section 2.2.6 (274). The inhibitors were dissolved in DMSO and prepared in culture media to obtain final drug concentrations of 5 µM with these dilutions screened against pre-stage II (days 2 and 3 cultures for two replicate data sets spanning pre-stage II development) and II gametocytes (days 4 and 5 for stage II gametocyte replicates) in technical triplicate. Malstat reagent and PES/NBT were added prior to the measurement of absorbance (620 nm) to determine gametocyte viability (%).

3.2.7 Detection of global changes in H3K36me2&3 patterns

Stage II gametocytes (day 3, 4 and 5) were treated with either ML324 or JIB-04 (5 µM) and sampled 24 h thereafter. Histones were extracted as described before (184) with minor modifications as outlined in Chapter 2 (section 2.2.7). Briefly, dounce homogenisation was used to extract nuclei in a hypotonic lysis buffer supplemented with protease inhibitors. Histones were extracted overnight using HCl, precipitated with TCA, washed with acetone and finally reconstituted in dddH_2O. Protein concentration was determined using the BCA Protein Assay Kit prior to the quantitative spotting of histones (100 ng) on nitrocellulose membranes. Membranes were submerged in blocking buffer for 30 min followed by 1 h incubation with α-H3K36me2 (Abcam, ab9049) or α-H3K36me3 (Abcam, ab9050) primary antibody dilutions (1:5000 in TBS-t). Membranes were washed three times in TBS-t and then incubated with HRP-conjugated rabbit α-IgG antibody (1:10000) for 1 h. Chemiluminescent signal was quantified with ImageJ analysis software (276).

3.2.8 DNA microarrays

DNA microarrays (60-mer, Agilent Technologies, USA) based on the full *P. falciparum* genome (280) were used to assess global transcriptomic changes (as described in section 2.2.8) in stage II

gametocytes treated with 5 µM ML324 or JIB-04. Gametocyte cultures (1-3% gametocytaemia, 4% haematocrit) were treated with 5 µM ML324 or JIB-04 (Cayman Chemicals) for 24 h followed by isolation of gametocytes using 0.1% (w/v) saponin. The isolation of RNA, cDNA synthesis and labelling and hybridisation was performed in a manner identical to that described in section 2.2.8 and previously by others (280).

3.2.9 Data analysis

ChIP-seq and microarrays data analyses were performed as in Chapter 2 sections 2.2.10.1 and 2.2.10.2, respectively and as described elsewhere (52, 92). All results are representative of data averaged for two biological replicates unless otherwise stated. GO enrichment analyses were performed with PlasmoDB using a *P*-value cut-off ≤0.05.

3.3 Results

3.3.1 H3K36me2&3 occupancy is dynamic in *P. falciparum* gametocytes

To investigate the functional role of the H3K36me2&3 in *P. falciparum* early gametocytes, ChIP-seq was performed on the same discrete gametocyte populations (pre-stage II, stage II and post-stage II gametocytes) that were used for the H3K27me2&3 ChIP-seq. As such, the gametocyte-stage compositions of these populations were identical to those described previously for H3K27me2&3 in Chapter 2 (see section 2.3.2 and Figure 2.4). Briefly, the stage II samples consisted mostly of stage II gametocytes (74 ± 3.2%) while pre- and post-stage II gametocytes contained minor proportions of stage II gametocytes (0.3 ± 0.4% and 10 ± 6%, respectively).

As H3K36me2&3 peak in abundance in stage II gametocytes (133), the compositions of the samples were considered adequately divergent to detect the variation in H3K36me2&3 occupancy using ChIP-seq. Thus, ChIP-seq was performed for each of the two independent biological replicates for each population using commercially available ChIP-grade antibodies against either H3K36me2 or H3K36me3. These selected antibodies have demonstrated specificity towards histone variants from various organisms (233, 369-372). Conservation of histone sequences and the use of these antibodies in *P. falciparum* parasites by others (200, 205) indicated suitable specificity for H3K36me2&3. Nevertheless, an independent validation of the selected antibodies was performed with the results demonstrating specific detection of *P. falciparum* histone H3 with either H3K36me2 or H3K36me3 (Figure 3.1).

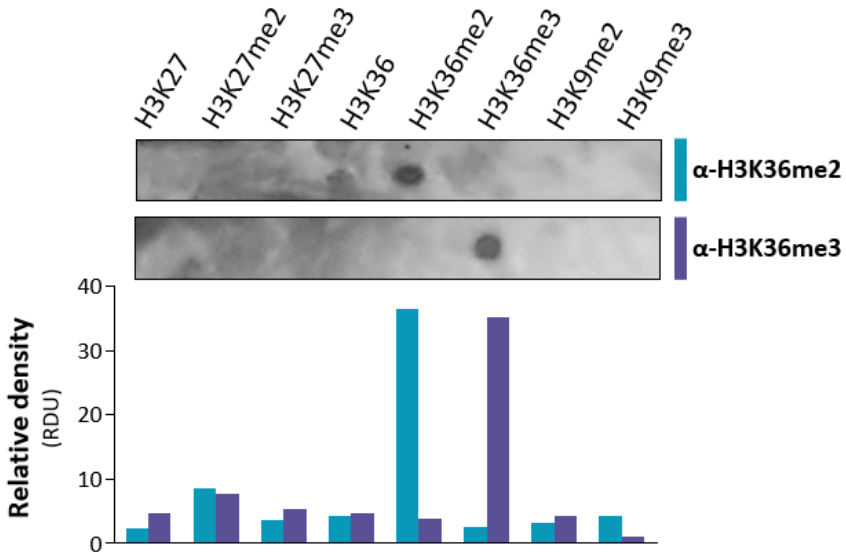

Figure 3.1: Determination of antibody specificity towards *P. falciparum* H3K36me2&3. Validation of α-H3K36me2 and α-H3K36me3 antibodies to be used in ChIP-seq experiments. The ability of the antibodies to detect unmodified or modified (di- or tri-methylated K9, K27 and K36) *P. falciparum* H3 peptides was determined using dot blot analysis. Graph represents the relative optical density units obtained for each peptide.

ChIP-seq sequencing data were obtained for each of the two independent biological replicates except for the pre-stage II gametocytes that only had one due to insufficient DNA obtained for the second replicate. Data for corresponding replicate samples were well correlated for example, Pearson correlation coefficients of r^2= 0.93 and r^2= 0.94 between the two H3K36me2 biological replicates in stage II and post-stage II samples, respectively (Appendix: Table S10). H3K36me2 and H3K36me3 were detected individually in each of the sampled gametocyte populations with a strong positive correlation (Pearson correlation coefficient, r^2= 0.9) present for the two histone PTMs in the stage II gametocytes (Figure 3.2a). Histones would not have a single residue (H3K36) di- and trimethylated concurrently (145). Therefore, it is likely that the gametocyte samples consisted of a combination of histones, some modified with the intermediate histone PTM and others with the final product or asymmetrically modified nucleosomes. Such robust correlations between H3K36me2&3 were absent for the pre- and post-stage II gametocytes with each of these stages additionally weakly correlated with the stage II samples (e.g. between stage II and post-stage II gametocytes, r^2= 0.22 for H3K36me2 and r^2= 0.26 for H3K36me3) (Figure 3.2a).

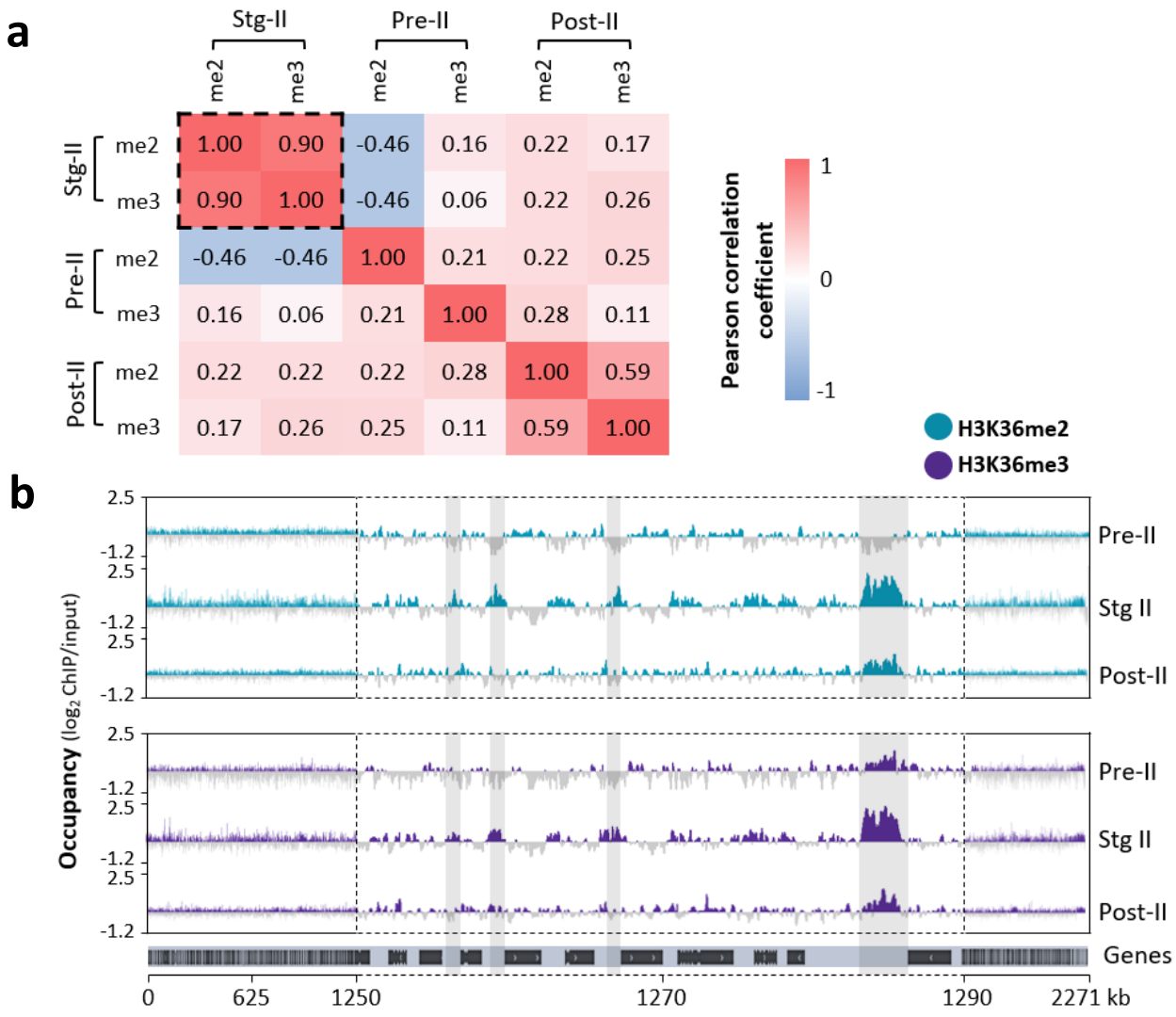

Figure 3.2: H3K36me2&3 patterns are dynamic during *P. falciparum* early and intermediate gametocyte development. (a) Plot of Pearson correlation coefficients for the genome-wide occupancy of H3K36me2&3 (me2 and me3) obtained for pre-stage II (pre-II), stage II (stg II) and post-stage II (post-II) gametocyte populations. The black box highlights the increased positive correlation between H3K36me2&3 in stage II gametocytes. H3K36me2&3 occupancy (average log_2-transformed ChIP/input) over chromosome 12 for each gametocyte population. Data are representative of two independent biological replicates except for the pre-II gametocytes with a single replicate. **(b)** H3K36me2&3 occupancy (average log_2-transformed ChIP/input) over chromosome 12 for each gametocyte population. Data are representative of two independent biological replicates except for the pre-II gametocytes with a single replicate. Turquoise and purple represent regions where the histone PTMs are present (log_2ChIP/input ratios >0) and dark grey represents regions of depletion (log_2ChIP/input ratios ≤0). The light grey shadowed areas indicate increased occupancy of H3K36me2&3 in the stage II gametocytes, exemplified in a central region of the chromosome 12 (1250-1290 kb) with the positions of genes indicated below the occupancy tracks.

As highlighted in a central region of chromosome 12 (1250-1290 kb), both H3K36me2&3 were detected at low levels in pre-stage II gametocytes (Figure 3.2b). However, this contrasts sharply with an abundance of both histone PTMs in the stage II gametocytes in which occupancy is

evident and found preferentially in intergenic regions and upstream of gene coding sequences. In post-stage II gametocytes, the levels of the histone PTMs dissipate, as evidenced by only residual H3K36me2&3 occupancy (Figure 3.2b). These dynamic patterns of "low-high-low" H3K36me2&3 abundance associated with pre-stage II, stage II and post-stage II gametocyte populations, respectively were independently validated through ChIP-qPCR (Figure 3.3) with the same gametocyte samples that were used for ChIP-seq.

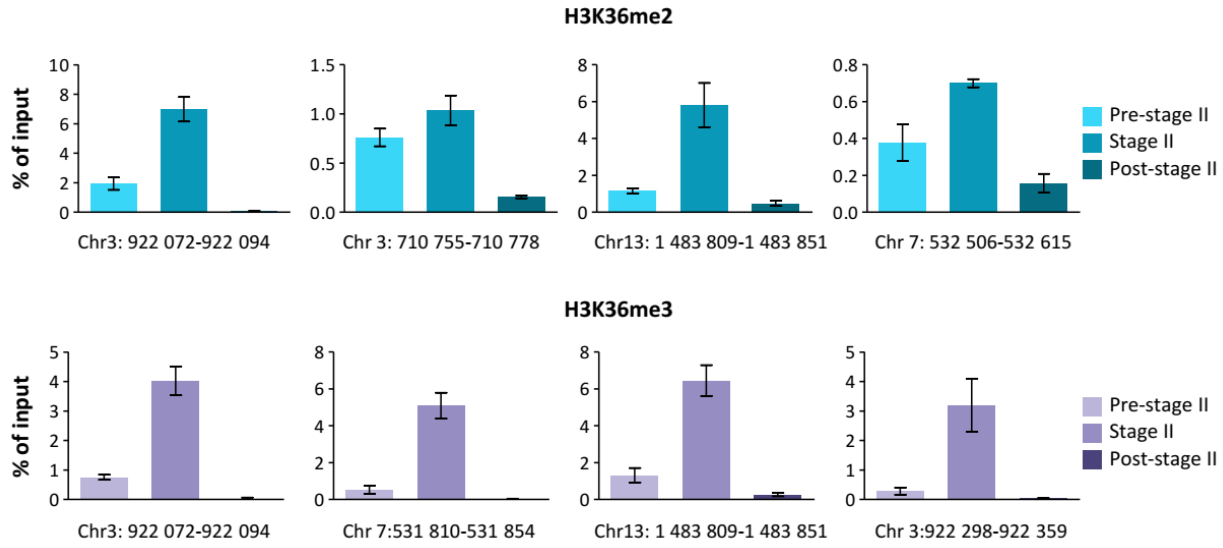

Figure 3.3: Validation of the stage II gametocyte-specific increase in H3K36me2&3 levels. The levels of H3K36me2&3 are expressed as a % of input (non-immunoprecipitated control) for each of the chromosome regions indicated. With the exception of pre-stage II gametocytes, all data are representative of two independent biological replicates, ±SD. Sequences of each primer pair used are detailed in chapter 2 (see section 2.3.3).

Consistent with the stage-specific dynamics reported previously for *P. falciparum* H3K36me2&3 (133), these results validate the experimental strategy used to detect changes in the histone PTM landscape during gametocyte development. Given the unique abundance of H3K36me2&3 in the stage II gametocytes, subsequent analyses focussed on the preferential association of these histone PTMs with the regions upstream of genes in this gametocyte stage.

3.3.2 Stage II gametocytes have a unique pattern of H3K36me2&3 occupancy

To determine the genome-wide positioning of H3K36me2&3, the histone PTM occupancy spanning each of *P. falciparum* genes for which sequencing data were obtained (Appendix: Table

S11) was interrogated. The occupancy profiles of H3K36me2&3 are distinctly uniform across the non-coding intergenic regions in stage II gametocytes, contrasting with more variable patterns in the pre- and post-stage II gametocytes. In stage II gametocytes, both H3K36me2&3 are concentrated 1.5 kb upstream of TSSs (105). Occupancy values (log_2ChIP/input) across this upstream region peak at 0.24 and 0.2 (average of 0.2 and 0.15) for H3K36me2&3, respectively, contrasting with a depletion of the histone PTMs (average occupancy values of -0.095 and -0.089, respectively) in CDRs (Figure 3.4a). In the pre- and post-stage II gametocytes, both histone PTMs are on average depleted upstream of TSSs (e.g. average H3K36me3 occupancy of -0.26 and -0.02 over this region in pre- and post-stage II gametocytes, respectively), emphasising the prominent abundance of H3K36me2&3 upstream of genes that is exclusive to the stage II gametocytes.

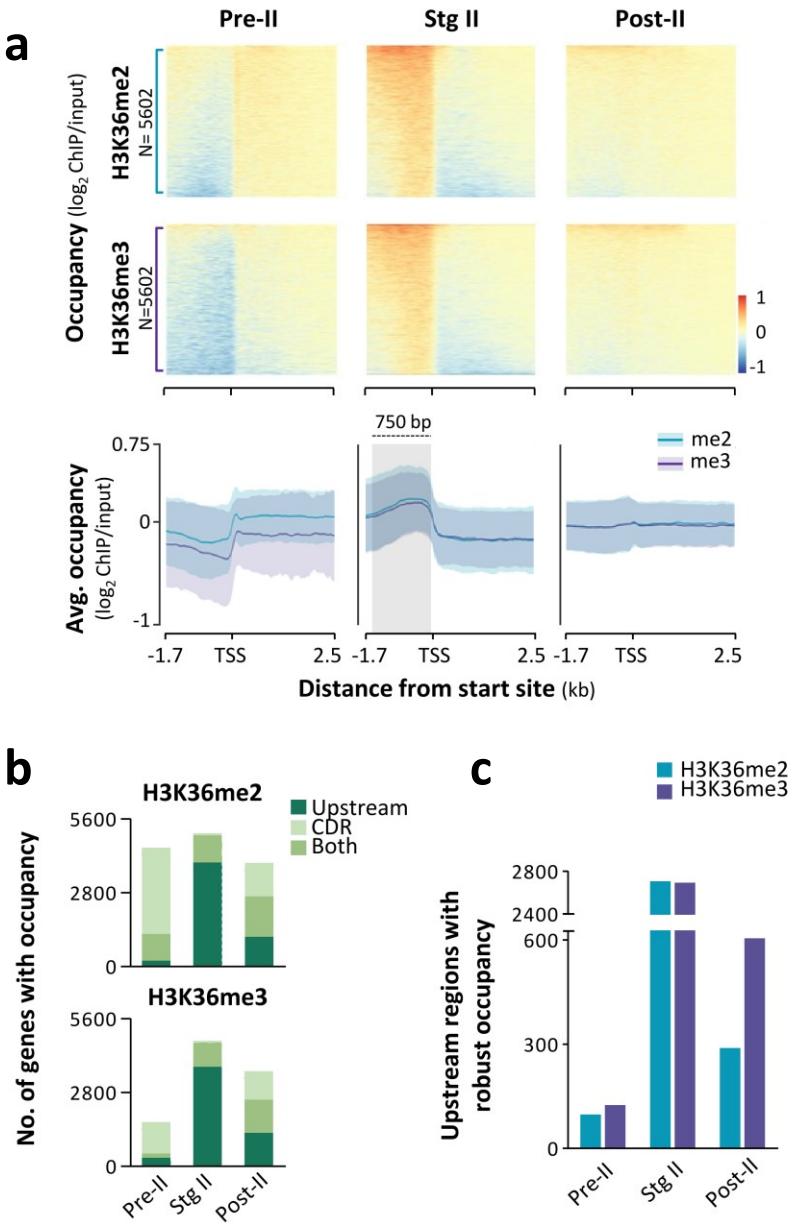

Figure 3.4: Stage II gametocytes have unique patterns of H3K36me2&3 occupancy associated with genes. (a) H3K36me2&3 occupancy (average $\log_2$ ChIP/input binned into 50 bp regions) spanning 1.7 kb upstream and 2.5 kb downstream of transcriptional start sites (TSS) of 5206 *P. falciparum* genes (PlasmoDB genome annotation, v39) in pre-stage II, stage II and post-stage II gametocyte populations. Data are representative of the average occupancy obtained for two independent biological repeats, except for pre-stage II gametocytes with only one. Genes were rank ordered individually in each heatmap. Summary plots of the H3K36me2&3 (turquoise and purple, respectively) occupancy in each of the gametocyte stages with ribbons representing ± SE. The light grey shadowed region highlights the stage II gametocyte-specific increase in occupancy 750 bp upstream of TSSs. **(b)** Numbers of genes occupied by H3K36me2&3 (i.e. $\log_2$ ChIP/input >0) only upstream of TSSs (dark green), only in the coding region (CDRs, light green) or both (intermediate green) for each gametocyte stage. **(c)** Clustered column plots specifying the number of genes robustly occupied by H3K36me2&3 (ie. with $\log_2$ChIP/input above average, ≥0.2 and ≥0.15 for H3K36me2&3, respectively).

Next, the numbers of H3K36me2&3 occupied genes were quantified and stratified according to location. In stage II gametocytes, H3K36me2&3 were detected (log_2ChIP/input >0) upstream of 89% (4969) and 83% (4677) of the occupied genes, respectively (Figure 3.4b). Of these, 3942 and 3776 genes had H3K36me2&3 exclusively present upstream of TSSs while only a minor proportion (85 and 75 genes) had H3K36me2&3 exclusively present in the CDRs, respectively. This contrasts sharply with the distribution of the histone PTMs in pre- and post-stage II gametocytes, where CDR occupancy is evident. In post-stage II gametocytes, both H3K36me2&3 were distributed relatively equally upstream of TSSs and within the CDRs of genes. Unexpectedly, low level H3K36me2 occupancy (average log_2ChIP/input = 0.07) was pervasive (4292 genes) in the CDRs of pre-stage II gametocytes (Figure 3.4b). Since the pre-stage II gametocyte samples used for ChIP-seq still contained a relatively large subpopulation of asexual parasites, this occupancy likely results from the detection of H3K36me2 in these stages where CDR occupancy has previously been linked with transcriptional repression (206, 258). The wide-spread patterns of intergenic H3K36me2&3 occupancy that are predominantly exclusive to the stage II gametocytes each translate to a number of genes that are robustly occupied (i.e. above average log_2ChIP/input value in stage II gametocytes by these histone PTMs. H3K36me2 robustly occupies the regions upstream of TSSs of 2480 genes while H3K36me3 is present upstream of 2691 genes in stage II gametocytes (Figure 3.4c).

3.3.3 H3K36me2&3 are associated with post-commitment transcriptional regulation

To explore the functional roles of H3K36me2&3 in stage II gametocytes, the level of occupancy of each histone PTM was compared with gene expression levels from the same gene expression time course data set (94) used in Chapter 2 (see section 2.3). Corresponding expression profiles were obtained for days 2-6 of gametocyte development (days on which stage II gametocytes were present) for 96% and 95% (2594 and 2545 genes) of the genes robustly occupied with H3K36me2&3, respectively. A global analysis of the presence of H3K36me2&3 upstream of genes and the transcript levels in stage II gametocytes (average log_2Cy5/Cy3 on days 4 and 5 of development associated with the greatest proportion of stage II gametocytes) indicated that the degree of occupancy of the histone PTMs is anti-correlated with the expression (Pearson

correlations, r^2= -0.12 and r^2= -0.1 for H3K36me2&3, respectively, Figure 3.5). The contrasting depletion of H3K36me2&3 upstream of TSSs in the other stages, particularly in pre-stage II gametocytes suggests that in the stage II gametocytes, these histone PTMs are involved in the active repression of genes that are not required for gametocyte development. Consistent with this finding, 63% of these H3K36me2&3-enriched and repressed genes have been shown to be indispensable for asexual proliferation previously (373). The genes occupied by H3K36me2&3 in the stage II gametocytes clustered into three groups based on expression profiles over days 2-6 of gametocyte development (Figure 3.5a) with ~98% (2548 genes) of the genes showing reduced transcript abundance. A similar pattern was present for H3K36me3 with ~98% (2545 genes) of the genes occupied by this histone PTM repressed in the stage II gametocytes (Figure 3.5b).

The H3K36me2&3-occupied and repressed gene sets are significantly (*P*-value ≤0.05) associated with shared and unique biological processes (Figure 3.5 and Appendix: Table S12), reflecting the large proportion of genes in the stage II gametocytes that were associated with robust levels of both H3K36me2&3 (2012 genes, i.e. 80%) and 20% of each set independently associated with these histone PTMs (695 and 680 genes for H3K36me2&3, respectively). This overlap supports one of the H3K36 methylation states as a transient intermediate in the generation of the other (205).

The biological processes associated with genes robustly occupied with H3K36me2&3 include those that are well established to be essential in the proliferative parasite stages such as antigenic variation and DNA replication (93, 94) and include genes coding for Maurer's cleft proteins (e.g. *rex1* and *rex4*), members belonging to the major multi-gene families *rhs*, *ebas, vars, rifs* and *msps* and the *kahsp40* and *kahrp* components of the cytoadherence complex (Figure 3.5). Similar to the role previously ascribed to H3K36me3 as a repressor of multi-gene families when associated with regions upstream of genes in asexual parasites (205, 258), the majority of the erythrocyte membrane proteins (*emp1s*, 75%), *stevors* (94%) and *rifins* (70%) are robustly occupied with H3K36me3 in stage II gametocytes, suggesting the control of variant gene expression by H3K36me3 is not limited to asexual parasites but is conserved across multiple life cycle stages. Additionally, most of these genes were also occupied by H3K36me2 as an intermediate as in the asexual stages (205).

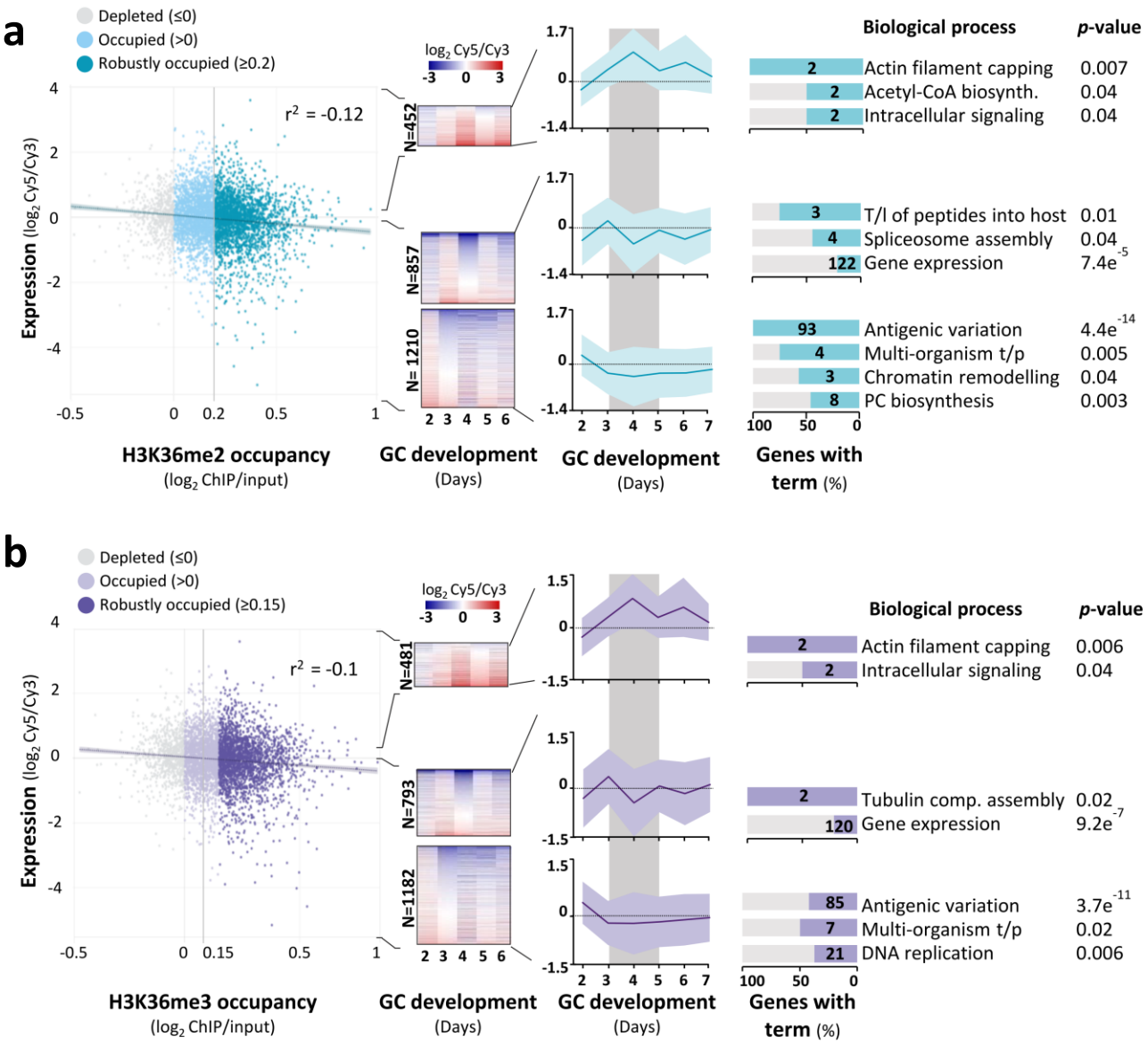

Figure 3.5: H3K36me2&3 are involved in the repression of genes encoding protein products that drive proliferation and sexual commitment. (a) Expression values (log_2Cy5/Cy3) averaged for day 4 and 5 of gametocyte development plotted against H3K36me2 (blue) occupancy in stage II gametocytes for all *P. falciparum* genes. Genes are stratified by colour based on occupancy scores (log_2ChIP/input): depleted ≤0 = grey, occupied >0 = blue, robustly occupied ≥0.2 = turquoise. Data are representative of two independent biological replicates. **(b)** Expression values (log_2Cy5/Cy3) averaged for day 4 and 5 of gametocyte development plotted against H3K36me3 occupancy in stage II gametocytes, genes are stratified by colour based on occupancy scores (log_2ChIP/input): depleted ≤0 = grey, occupied >0 = lavender, robustly occupied ≥0.15 = dark purple. For both **(a)** and **(b)** linear regression is represented by dashed lines with 95% confidence interval indicated by ribbons; r^2 values represent Pearson correlation coefficients. Robustly occupied genes were divided into clusters based on patterns of expression on days 2-6 of gametocyte (GC) development. Average expression profiles for each cluster are shown for days 2-7 of development (ribbons represent ± SD). Each cluster is significantly (*P*-value ≤0.05) associated with biological processes. The number of robustly occupied genes (value on each bar) is represented as a % of all the background genes associated with each term. Biosynth = biosynthesis; t/l = translocation; t/p = transport; PC = phosphatidylcholine; comp. = complex.

Interestingly, within the process of chromatin remodelling, all four *P. falciparum* histone acetyltransferase (HAT) -encoding genes (151, 203) that generate transcriptionally active chromatin structures (184, 362) were occupied by a robust level of H3K36me2&3 and repressed in the stage II gametocytes. Various process that are documented to be functionally important during sexual commitment and early gametocyte differentiation, including protein translocation and phospholipid metabolism (52, 76, 84, 90, 135, 317, 374) are significantly associated with the robustly occupied H3K36me2&3 gene sets (Figure 3.5). Interestingly, the only processes where H3K36me2&3 occupancy was not associated with a definitive reduction in transcript abundance were actin filament capping, acetyl-CoA biosynthesis and intracellular signalling. Overall, these results indicate that H3K36me2&3 are associated with an active repression of genes that encode protein products involved in proliferation and sexual commitment when they become obsolete in the developing gametocyte.

This is further supported by an increasing anti-correlation (r^2= -0.026 and -0.02 on day 2 and r^2= -0.13 and -0.14 on day 6 for H3K36me2&3, respectively) between H3K36me2&3 abundance and transcript levels for robustly occupied genes in stage II gametocytes (Figure 3.6). Additionally, for genes depleted of H3K36me2&3, this relationship was weakened or reversed (corresponding r^2= 0.03 and 0.02 on day 2 and r^2= -0.03 and -0.01 on day 6).

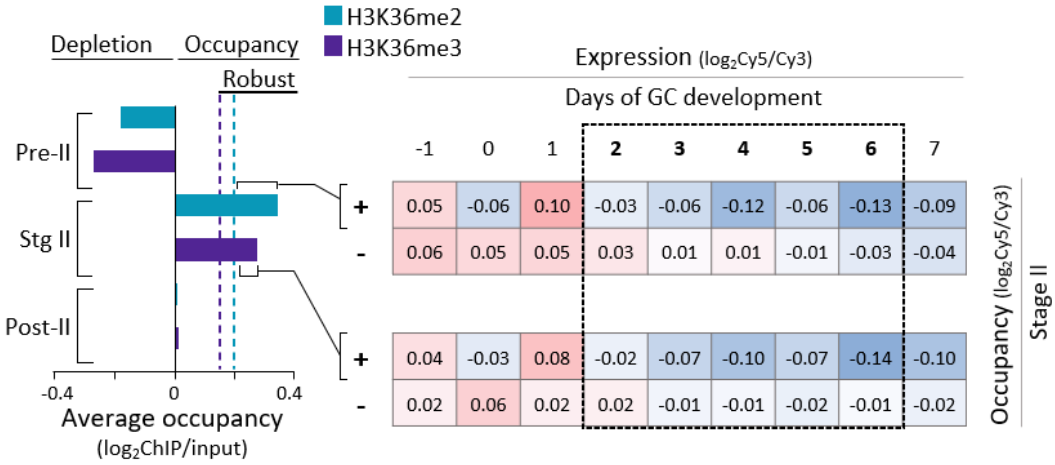

Figure 3.6: H3K36me2&3 occupancy levels are anti-correlated with transcript abundance in stage II gametocytes. Average occupancy (log_2 ChIP/input) levels in pre-stage II, stage II and post-stage II gametocytes for the sets of genes occupied by H3K36me2&3 in stage II gametocytes. Depletion refers to the absence of H3K36me2&3 (average occupancy ≤0) while the cut-off values for robust occupancy (log_2 ChIP/input ≥0.2 and ≥0.15 for H3K36me2&3, respectively) are indicated by the dashed lines. Pearson correlation between gene expression (log_2Cy5/Cy3) on days -1 to 10 of gametocyte (GC) development and level of occupancy of histone PTMs in stage II gametocytes for occupied (+) genes and those depleted of H3K36me2&3 (-). Dashed box indicates the days on which stage II gametocytes were present in cultures and where H3K36me2&3 occupancy is associated with a reduced transcript abundance.

3.3.4 Commitment- and asexual-related gene sets are enriched with H3K36me2&3

To validate the quantitative observations of H3K36me2&3 occupancy, peak enrichment analysis was performed to identify regions of the genome with significant levels (i.e. significant MACS2 peaks, q-value ≤0.05, present in both biological replicates) of the histone PTMs. By virtue of their broad nature, distinct regions of enrichment of certain histone PTMs, including methylated H3K36, may consistently be eliminated by regular peak calling algorithms since these were originally developed to identify narrow transcription factor binding domains (292, 293, 370, 375). Therefore, for this analysis parameters within the peak calling algorithm were set to identify broad peaks. This method is exceedingly more stringent compared to that used to determine robust occupancy (Figure 3.7a) with only 17% of robustly occupied genes identified as significantly enriched with H3K36me2&3 in the stage II gametocytes. For H3K36me2, 734 peaks were identified, corresponding to 327 genes with enrichment 1.5 kb upstream of TSSs and 233 genes with this histone PTM enriched in CDRs (Figure 3.7b and Appendix: Table S13). Similarly, significant H3K36me3 enrichment was identified at 569 sites across the genome in stage II

gametocytes, equating to the enrichment upstream and in the CDRs of 252 and 154 genes, respectively. With <100 genes similarly enriched at each of these sites in post-stage II (Figure 3.7b) and none in pre-stage II gametocytes, these peak calling results confirm the stage II gametocyte-specific abundance of H3K36me2&3 (133) and indicate that these histone PTMs occur in a pattern that is unique to and characteristic of this stage of gametocyte development. Furthermore, the concentration of the histone PTMs upstream of TSSs, where they would be ideally situated to influence expression by virtue of their proximity to promoters (143), suggests functional roles for the significant enrichment of H3K36me2&3 that is exclusive to stage II gametocytes.

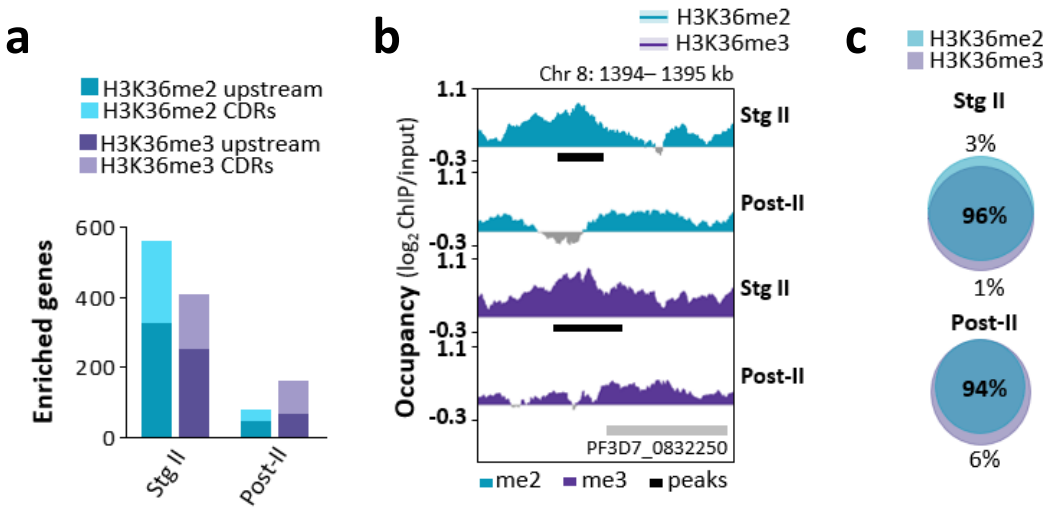

Figure 3.7: Stage II gametocytes have unique patterns of H3K36me2&3 occupancy and enrichment associated with genes. (a) Log_2-transformed ChIP/input ratio tracks for H3K36me2&3 in stage II and post-stage II gametocytes for a region on chromosome 8 to exemplify significant enrichment (MACS2 peaks with q-value ≤0.05 and present in both biological replicates) in stage II gametocytes. Called peaks are indicated by the horizontal black bars. Grey dashed lines indicate cut-off values used for the qualitative analysis of robust H3K36me2&3 occupancy. **(b)** Numbers of genes with H3K36me2&3 enrichment in stage II and post-stage II gametocytes. No peaks were detected for pre-stage II gametocytes. The proportion of genes with enrichment 1.5 kb upstream of TSSs is represented by the darker shade compared to the proportion of genes with enrichment in the coding regions (CDRs). **(c)** Common and unique H3K36me2&3 peaks determined using Multiple Intersect (BEDtools) of MACS2 peak files in stage II and post-stage II gametocytes.

Given the strong correlation between the presence of these histone PTMs in stage II gametocytes, the large number (96%) of overlapping H3K36me2&3 (Figure 3.7c) and the presence of H3K36me2 as a transient intermediate in the formation of H3K36me3 reported

elsewhere (205, 376-378), downstream analyses were performed using a combined set of enriched genes without distinguishing between the di- and tri-methylated state.

Next, H3K36me2&3-enriched genes were categorised based on the location of the histone PTMs (i.e. exclusively upstream of TSSs, exclusively in CDR or both) and the transcription profiles of each were compared using the same gene expression time-course data set (34) used in the qualitative analysis of H3K36me2&3 occupancy. Once again, corresponding expression profiles were obtained for days 2-6 of development for the majority (94%) of the H3K36me2&3 robustly occupied genes. Congruent with the location-dependant functions described for H3K36me2&3 in other organisms (167, 205, 369, 379-382), the expression profiles of the genes vary based on the site of H3K36me2&3 enrichment. Genes with H3K36me2&3 exclusively present in CDRs (37% of H3K36me2&3-enriched genes) exhibit a slight increase in transcript abundance on day 4 (Figure 3.8a). However, these levels of transcription are not as prominent as in asexual parasites (94, 205), suggesting the activation of these genes may be less relevant for gametocyte differentiation.

The majority of H3K36me2&3-enriched genes (63%) are strongly repressed during stage II gametocytes, with the histone PTMs present exclusively upstream of the TSSs in 342 of the 417 repressed genes (Figure 3.8a). Of these repressed genes, 42% are typically involved in asexual proliferative processes including translation ($P = 3.35e^{-5}$), haemoglobin metabolism ($P = 0.003$), cell cycle arrest ($P = 0.033$) and DNA replication ($P = 0.041$) (Figure 3.8b and Appendix: Table S14). Moreover, more than half of these are essential for asexual parasite development. Only 6% of the genes that are regulated by H3K36me2&3 in asexual parasites (205, 258) are significantly enriched with these histone PTMs in stage II gametocytes. This indicates that the H3K36me2&3 enrichment identified here is predominantly targeted towards a distinct subset of asexual parasite-related genes that are specifically repressed in the stage II gametocytes. Furthermore, this suggests that H3K36me2&3-associated repression of genes is involved in key transcriptional shifts that accompany the transition from early gametocyte differentiation to intermediate development (94).

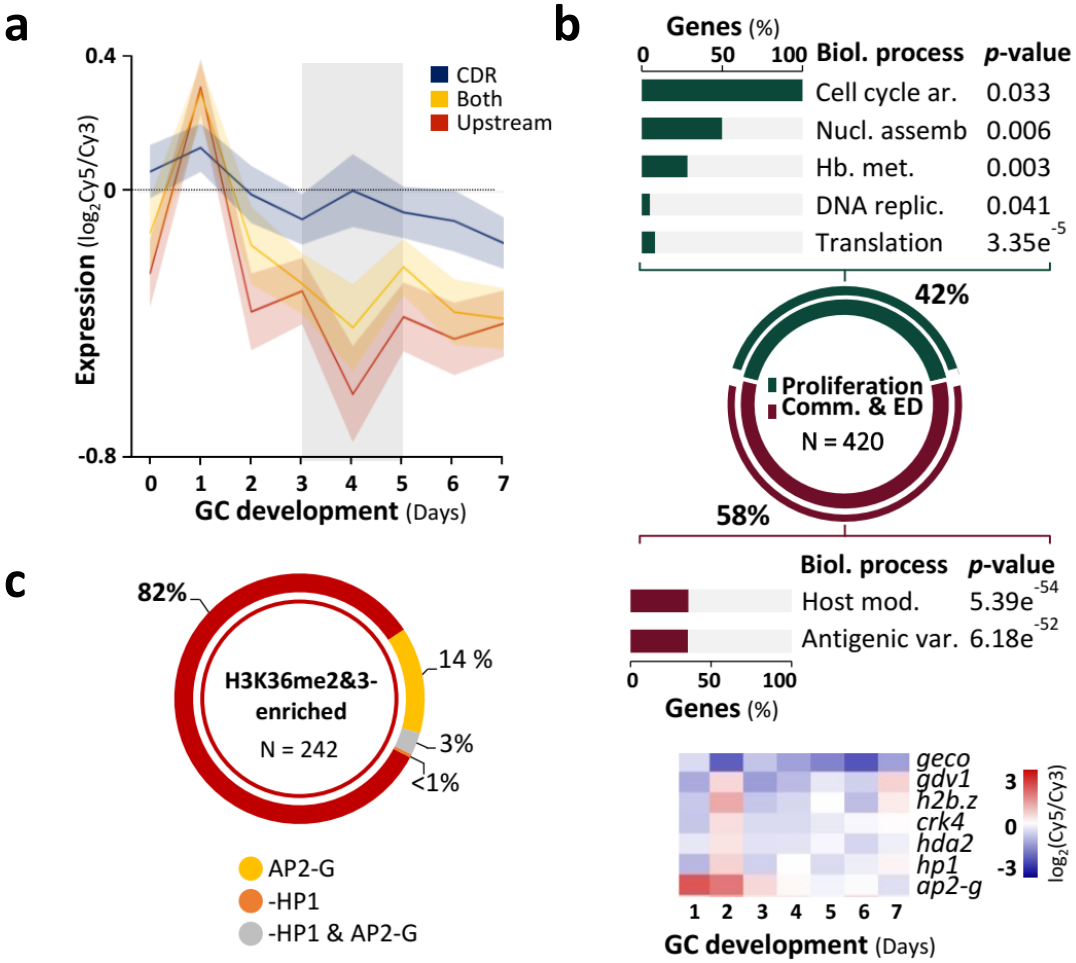

Figure 3.8: H3K36me2&3 are associated with transcriptional regulation in stage II gametocytes. (a) Average transcript abundance (log_2Cy5/Cy3) on days 0-7 of gametocyte (GC) development (94) for genes with H3K36me2&3 enrichment in coding regions (CDR, blue), 1.5 kb upstream of TSSs (upstream, red) or both (gold) with ribbons representing ± S.D. They grey shadowed region highlights days on which H3K36me2&3-associated transcriptional changes are most prominent. **(b)** The 420 H3K36me2&3-enriched and repressed genes were grouped into those associated with proliferation (178 genes, green) that are significantly associated (*P*-value <0 .05) with the biological processes indicated. The number of enriched genes is represented as a % of all background genes associated with the biological processes. The other 242 (58%) of the H3K36me2&3-enriched and repressed genes are directly involved or have increased transcript abundance during commitment and/or early differentiation (comm. & ED, maroon). This set is significantly associated with the biological processes indicated and includes the important regulators highlighted in the gene expression heatmap. Legend: ar. = arrest; nucl. = nucleosome; assemb. = assembly; replic. = replication; mod. = modification; var. = variation. **c.** H3K36me2&3-enriched and repressed genes that are associated with commitment and early differentiation were compared to gene sets that become depleted of HP1 (-HP1, orange) (135), are targets of AP2-G (gold) (52) or both (grey) during these steps.

In addition to the above, a comparison of H3K36me2&3-enriched genes in stage II gametocytes with genes previously described to be related to the processes of sexual commitment and early gametocyte differentiation (52, 76, 84, 90, 94, 135, 227, 317, 374). A large proportion (58%, 242 genes) of the H3K36me2&3-enriched and repressed genes are linked to these processes (Figure

3.8b). These include genes significantly associated with antigenic variation ($P = 6.18e^{-52}$) and host cell modification processes ($P = 5.39e^{-54}$). H3K36me2&3 enrichment is present for the *var, rifin, stevor, phist* and *hyp* multi-gene families. Interestingly, in contrast to the *vars* in asexual parasites (365), H3K36me2&3 are associated with stronger repression of the *stevors* in stage II gametocytes. This indicates that the control of multi-gene families is nuanced to meet stage-specific requirements. Additionally, H3K36me2&3-associated repression is present for early gametocyte markers (e.g. *geco,* PF3D7_1253000; *pfg14-744,* PF3D7_1477300 and *pfg14-748,* PF3D7_1477700) (58, 76, 317, 383) and key regulators of commitment and gametocytogenesis: *hp1* (PF3D7_1220900), histone deacetylase 2 (*hda2*, PF3D7_1008000), gametocyte development protein 1 (*gdv1*, PF3D7_0935400) as well as the AP2 transcription factor, *ap2-g* (Figure 3.8b) (86, 89, 90, 134, 374).

Following the cue for commitment, HP1 is displaced from 15 heterochromatic loci that would otherwise remain silenced by this interaction throughout asexual proliferation (135). This results in the expression of *ap2-g,* leading to the transcriptional cascade that drives sexual commitment (77, 86, 89, 134). Therefore, the proportion of the H3K36me2&3-enriched and repressed genes were (242 genes involved in commitment) compared to the targets of AP2-G (52) or those that become active following the displacement of HP1 (135). Only 18% of the H3K36me2&3-enriched genes are activated by AP2-G or HP1 depletion during commitment while the mechanisms of activation for the majority (82%) of these genes are unclear (Figure 3.8c). This implies that in the stage II gametocytes, H3K36me2&3-associated transcriptional repression occurs for commitment-related genes irrespective of mechanisms by which they were activated in the preceding commitment steps.

Notably, H3K36me2&3 robustly occupy the regions upstream of all 15 HP1 depleted genes that are specifically expressed and drive commitment, with 53% of these enriched for the histone PTMs in stage II gametocytes. As all of these genes remain depleted of HP1 (135) yet are associated with a sharp reduction in transcript abundance in the stage II gametocytes (94), their repression can be attributed to an association with H3K36me2&3. Ultimately, these results indicate that in the stage II gametocytes, H3K36me2&3 are involved in the active transcriptional

repression of genes that drive commitment and early differentiation once their products become obsolete in post-commitment, developing gametocytes.

3.3.5 H3K36me2&3-associated repression is largely independent of other mechanisms

Next, the H3K36me2&3 enrichment in stage II gametocytes was compared to data from previous studies describing other gene regulatory mechanisms that function during gametocytogenesis (92, 135). For instance, HP1-mediated heterochromatin has been shown to expand throughout gametocyte development, resulting in the silencing of stage-specific gene sets (135). Interestingly, only 9% of the H3K36me2&3-enriched and repressed genes are also occupied by HP1 in the stage II/III gametocytes (Figure 3.9). This small proportion of genes, including those associated with knob-formation (e.g. *kahsp40* and *emp3*) and protein export (e.g. *hyp),* may therefore be regulated cooperatively by the two mechanisms. However, the repression of the majority (91%) of the H3K36me2&3-enriched gene set in stage II gametocytes is exclusively associated with these histone PTMs.

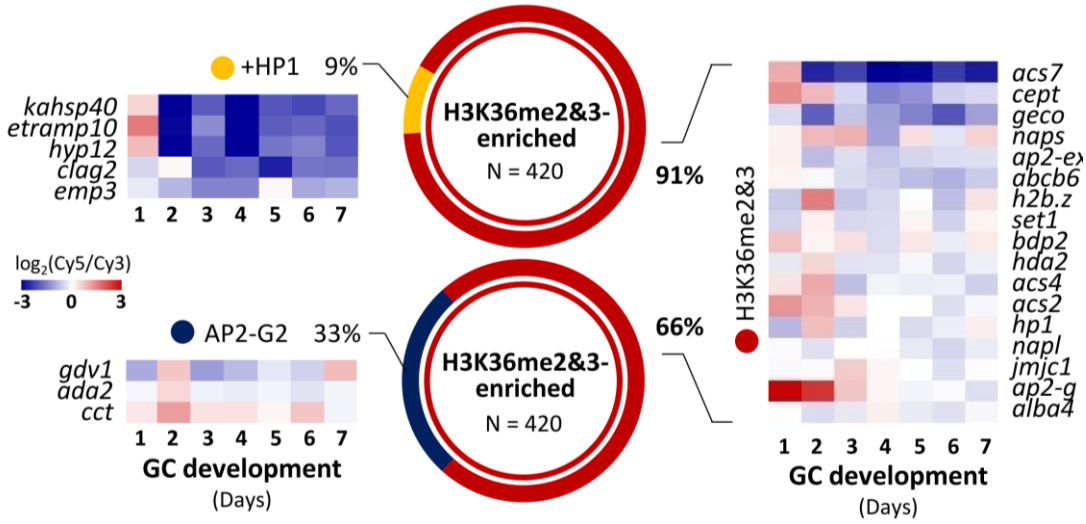

Figure 3.9: H3K36me2&3-associated transcriptional repression is largely independent of other regulatory mechanisms. The H3K36me2&3-enriched and repressed genes in stage II gametocytes were compared to genes that are regulated by HP1-mediated heterochromatin formation (+HP1, gold) (135) or by AP2-G2 (blue) (92) in the stage II/III gametocytes. Certain genes from each of these categories are exemplified in the gene expression heatmaps.

Recently, a second AP2 transcription factor, AP2-G2 was shown to be essential for gametocyte development beyond stage III and in asexual parasites, AP2-G2 represses a subset of genes by associating with H3K36me3 (92). Thus, the overlap between the AP2-G2 occupied genes and H3K36me2&3-enriched and repressed gene set in stage II gametocytes was evaluated (92). Interestingly, only 33% of the H3K36me2&3-enriched genes in stage II gametocytes are also bound by AP2-G2 during intermediate gametocyte development (Figure 3.9), indicating that the transcriptional repression associated with the H3K36me3-AP2-G2 interaction also occurs in the early gametocytes. Of note, genes include those encoding GDV1 that evicts HP1 from heterochromatic loci prior to commitment (90) and CCT (CTP:phosphocholine cytidylyltransferase, PF3D7_1316600), involved in the synthesis of PC from an alternative substrate under the lysoPC depleted conditions that cue commitment (84, 384). This indicates that an interaction between H3K36me2&3 and AP2-G2 may repress these important commitment-related genes once gametocytogenesis has been established.

The remaining 251 (60%) H3K36me2&3-enriched genes in stage II gametocytes have not been associated with any other regulatory mechanisms to date (Figure 3.9). As such, this set that includes the lysoPC synthesis-associated genes *acs2* (PF3D7_0301000), *acs4* (PF3D7_1372400), *acs7* (PF3D7_1200700) and *cept* (PF3D7_0628300) (84, 374, 385-387) and the epigenetic and transcriptional regulators *hda2, set1,* PF3D7_0629700 and *alba4* (PF3D7_1347500) (Figure 3.9) are likely regulated by a novel repressive mechanism involving the stage II gametocyte-specific enrichment of H3K36me2&3.

Furthermore, *ap2-g, hp1,* the lysine-specific demethylase, and *jmjc1* (PF3D7_0809900) are enriched for H3K36me2&3 upstream of TSSs in the stage II, but not in pre- and post-stage II gametocytes (Figure 3.10). This provides the first insights into the mechanism by which these genes are “switched off” after commitment to allow gametocyte development to proceed. Although the reason for the differentiation in CDR occupancy for *hp1* and *ap2-g* is unclear, H3K36 methylation within CDRs is indicative of recently transcribed genes (206, 388) and this may therefore reflect residual histone PTMs that were deposited during the transcription of *ap2-g* in the preceding stages.

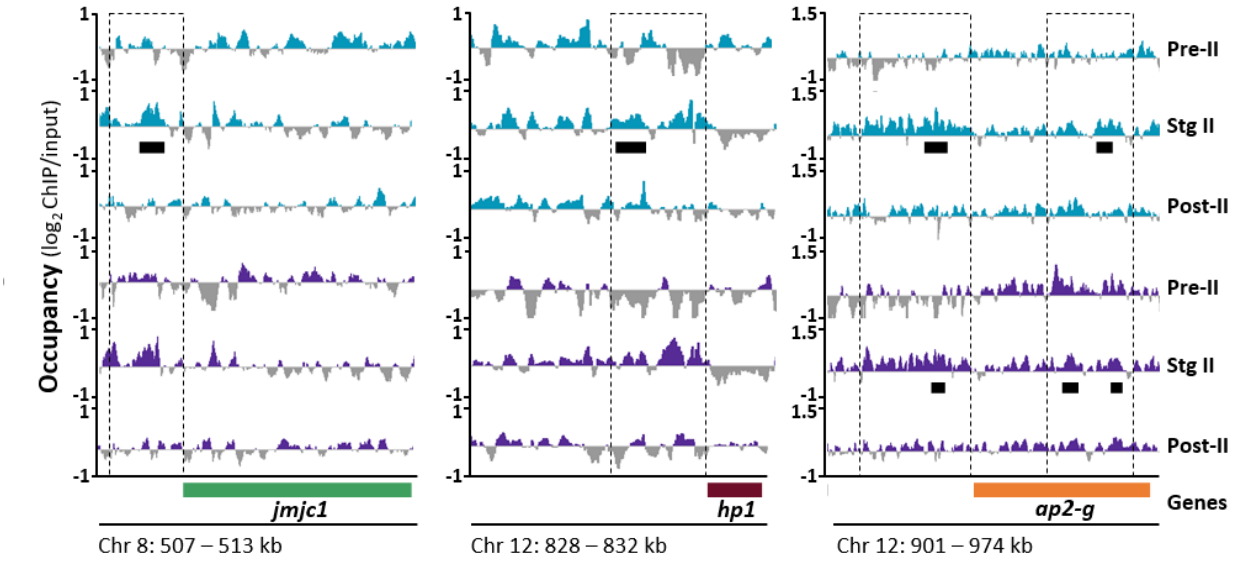

Figure 3.10: H3K36me2&3-associated transcriptional repression occurs for key regulators of sexual commitment and gametocytogenesis in stage II gametocytes. Log_2-transformed ChIP/input tracks of H3K36me2 (turquoise) and H3K36me3 (purple) occupancy for *jmjc1, hp1* and *ap2-g* in pre-stage II, stage II and post-stage II gametocytes with the CDRs of each represented by the green, maroon and orange horizontal blocks, respectively. Dashed grey boxes represent regions of differential occupancy between the three stages and horizontal black bars indicate called peaks of enrichment in stage II gametocytes.

In accordance with this, H3K36me2&3 are present in the CDRs of both *ap2-g* and *hp1* in the pre-stage II gametocytes (Figure 3.10), stages in which these genes would presumably have been transcribed. Furthermore, the H3K36me2&3 enrichment and repression of *jmjc1* is of interest given its homology with the mammalian H3K36-specific, lysine demethylase 2 (*kdm2*) family (200). As such, the repression of *jmjc1* may be present as means of safeguarding the integrity of H3K36me2&3 enrichment in the stage II gametocytes. Taken together, these results implicate H3K36me2&3 as a novel mechanism of transcriptional repression in stage II gametocytes that is largely independent of other mechanisms described to date.

3.3.6 Inhibition of H3K36 demethylation confirms the importance of histone PTMs for gene regulation in *P. falciparum* gametocytes

Finally, the potential enzymes that generate the unique stage II gametocyte-specific enrichment of H3K36me2&3 described here and previously (133) were investigated. In asexual parasites,

SET2 (PF3D7_1322100) is responsible for the methylation of H3K36 (200, 206). The transcript levels of *set2* increase on day 1 of gametocytogenesis and subsequently decline thereafter (Figure 3.11), suggesting that the H3K36-specific HMT activity of SET2 is extended to early gametocyte stages. Viable parasite lines have been obtained following the genetic disruption of *set2*, indicating that this HMT is not essential for asexual proliferation (205, 206). However, it was not possible to leverage these existing systems to evaluate the importance of *set2* during gametocytogenesis since the parental strains used to generate these mutant parasite lines do not produce gametocytes. Regarding the demethylation of H3K36, the transcript levels (94) of the three Jumonji-C HDMs in *P. falciparum, jmjc1, jmjc2 (*PF3D7_0602800) and *jmj3* (PF3D7_1122200), spanning stage II gametocyte development (Figure 3.11) strongly suggests that at least one of these enzymes is likely involved in the removal of methyl PTMs from H3K36.

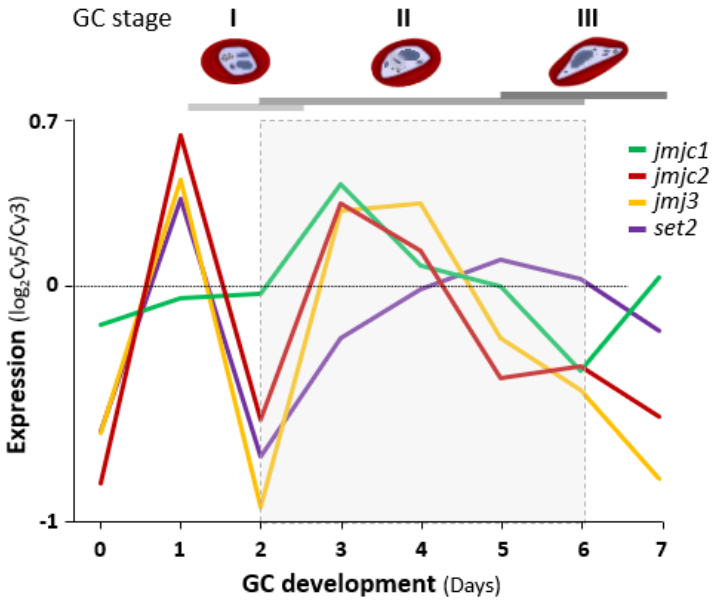

Figure 3.11: Expression of histone methyltransferases and demethylases in *P. falciparum* gametocytes. Expression profiles (log_2Cy5/Cy3) of genes encoding the *P. falciparum* Jumonji-C domain-containing HDMs (*jmjc1, jmjc2* and *jmj3)* and the H3K36-specific methyltransferase, *set2* on days 0 to 7 of gametocyte (GC) development (94) with grey shadowed region representing days of increased transcript abundance of the HDMs and the presence of stage II gametocytes.

In order to investigate the functional relevance of these enzymes for H3K36me2&3, a chemical interrogation of HDM activity was performed in early gametocytes. From a library of 96 epidrugs, five histone demethylase inhibitors (HDMi) were screened against pre-stage II and stage II

gametocytes. As these assays were performed in parallel with the HMTi epidrug screens in Chapter 2 (see section 2.3.8), the same gametocytes cultures with identical stage compositions were used. Briefly, the pre-stage II gametocyte samples contained mostly asexual parasites (91%) and stage I (8 ± 3%) with a minor proportion of stage II gametocytes (1 ± 1%). The stage II cultures were enriched with stage II gametocytes (77 ± 11%) with few asexual parasites (10 ± 12%), stage I (5 ± 3%) and stage III (8 ± 4%) gametocytes present. With the exception of the LSD1 inhibitor, 2-PCPA which was equally active (94%) against the pre-stage II and stage II gametocytes, all the HDMi were more potent towards the stage II gametocytes (Table 3.1). In the stage II gametocytes, JIB-04 (pan-selective JMJD inhibitor) and ML324 (mammalian JMJD2 inhibitor) were the more potent, inhibiting 88% and 85% of gametocytes, respectively, compared to GSK-J4 (mammalian UTX and JMJD3 inhibitor) and methylstat (inhibitor of JMJD2 and JMJD3) exhibiting 68% and 41% gametocyte inhibition, respectively (Table 3.1). These findings correspond with previous data showing that both JIB-04 and ML324 are highly active against gametocytes (212, 357, 389).

Table 3.1: Selected inhibitors of mammalian histone demethylases screened against *P. falciparum* early gametocytes. Pre-stage II (91% asexual parasites, 8 ± 3% stage I and 1 ± 1% stage II gametocytes) and stage II (77 ± 11% stage II gametocytes, 10 ± 12% asexual parasites, 5 ± 3% stage I and 8 ± 4% stage III gametocytes) gametocytes were subject to treatment with HDM inhibitors (5 µM) for 24 hours with the % of gametocyte inhibition determined thereafter. The mammalian targets and possible or confirmed targets (underlined) in *P. falciparum* are provided.

Inhibitor	Mammalian target	Possible target in *P. falciparum*	Gametocyte inhibition (%)	
			Pre-stage II	Stage II
JIB-04	**pan-JMJC**	**JMJ3**	**70**	**88**
ML324	**JMJD2**	**JMJ3**	**73**	**85**
GSK-J4	JMJD3 and UTX	JMJC1, JMJC2	**41**	**68**
Methylstat	JMJD2, JMJD3	JMJC1/JMJC2	*	**41**
2-PCPA	LSD1	LSD1	**94**	**94**

Next, the four most active epidrugs were further investigated to determine their effect on the levels of H3K36me2&3 in stage II gametocytes under the same treatment conditions (5 µM, 24 h) used in the primary drug screen. Only JIB-04 and ML324 were associated with the

hypermethylation of H3K36 relative to the untreated controls (~13-fold) (Figure 3.12). Such effects on methylation were not present for 2-PCPA or GSK-J4 as evidenced the depletion of H3K36me2&3 (15-93 times lower abundance compared to JIB-04 or ML324). The normal H3K36 methylation patterns in treated stage II gametocytes suggest that the pan-stage potency of 2-PCPA arises from the inhibition of LSD1 (demethylase of H3K4, H3K9 and non-histone targets) as in other eukaryotes (390, 391). Previous studies of JIB-04 and ML324 in asexual parasites directly attributed the activity of these epidrugs to the inhibition of the primary catalytic step (conversion of 2-oxoglutarate to succinate) of *Pf*JMJ3 HMT activity (212). By contrast, GSK-J4 has no effect on the activity of JMJ3 (212), in line with the lower activity of this inhibitor compared to ML324 and JIB- 04 in the stage II gametocytes.

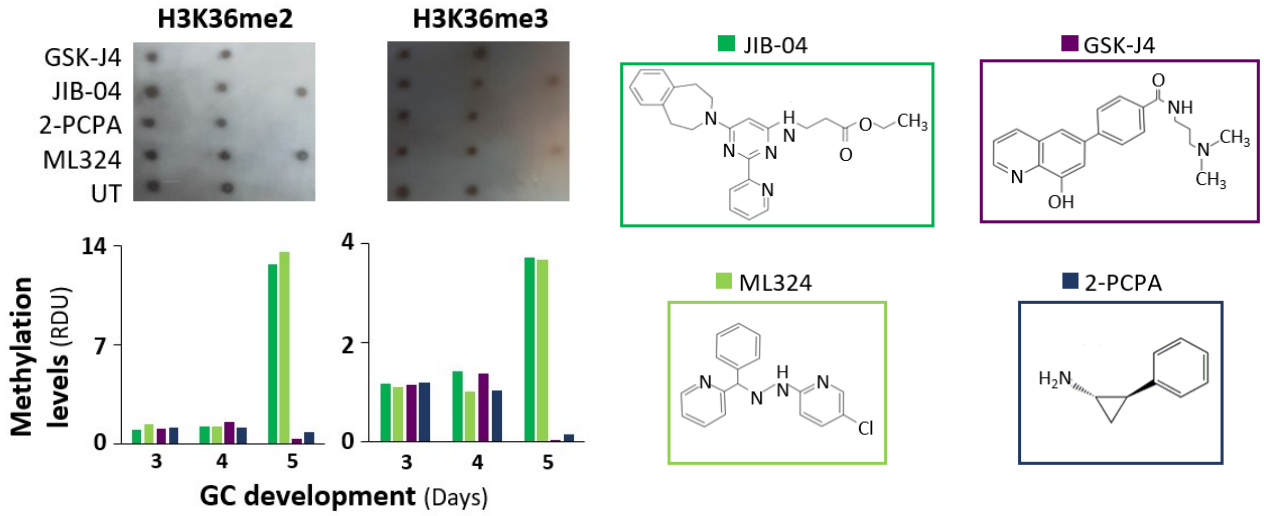

Figure 3.12: The effect of histone methyltransferase and demethylase inhibition on H3K36me2&3 levels in *P. falciparum* gametocytes. Detection of changes in H3K36me2&3 abundance (methylation levels) using dot blot analysis of stage II gametocytes treated with the Jumonji-C HDM inhibitors JIB-04 (dark green), ML324 (light green) or GSK-J4 (purple) or the lysine-specific demethylase 1 (LSD1) inhibitor 2-PCPA (dark blue) for 24 h (5 µM) compared with parallel untreated (UT) control gametocyte populations. Results of densitometry analysis are provided as fold changes (signal/background) of the relative density units (RDU). The chemical structures of the four epidrugs are shown.

These results confirm that at least one of the *P. falciparum* Jumonji-C HDMs demethylate H3K36me2&3 following the peak in abundance in stage II gametocytes and in particular, support the proposed involvement of JMJ3.

Interestingly, the hypermethylation induced by these HDMi epidrugs is similar to that observed for H3K4me3 and H3K9me3 by JIB-04 in asexual parasites (212). In the asexual parasites, the direct inhibition of *Pf*JMJ3 by JIB-04 results in transcriptional de-regulation (212) and since this inhibitor is significantly more potent towards the sexual stages (212, 357), transcriptional effects of JIB-04 in gametocytes were of particular interest. As such, genome-wide transcriptional profiling of JIB-04 activity was performed on stage II gametocytes following 24 h of treatment (5 µM) (Appendix: Table S15). Similar to the restricted transcriptional effect of JIB-04 in asexual parasites (212), treatment with JIB-04 resulted in the differential expression ($log_2FC \geq 0.5$ in either direction) of ~13% of the genome (710 and 696 genes with decreased and increased transcript abundance, respectively) in stage II gametocytes (Figure 3.13a).

Genes with reduced transcript abundance are involved in chromatin organisation (3%), gene expression (12%), lipid metabolism (1%) and transport (6%). Each of these processes have confirmed roles in gametocyte differentiation and development (58, 59, 90, 94, 119, 135, 211, 317, 374) and thus transcriptional disruption of these genes likely contributes to JIB-04's potency in gametocytes. Interestingly, the transcript levels of *jmjc2* and the HAT-encoding genes, *gcn5* (PF3D7_0823300) and *myst* (PF3D7_1118600) (151, 203) also increase, which may reflect an attempt by the gametocytes to counteract the abnormal histone methylation patterns induced by JIB-04. Combined with the abundance of H3K36me2&3 compared to other histone PTMs in the stage II gametocytes, these results indicate abnormal H3K36me2&3 levels may pose a barrier to further development. In line with this, the shift from early (stage I) to intermediate (stage III/IV) gametocyte development is a key transition period (94) with a regulatory role for histone PTMs at this point previously alluded to (133).

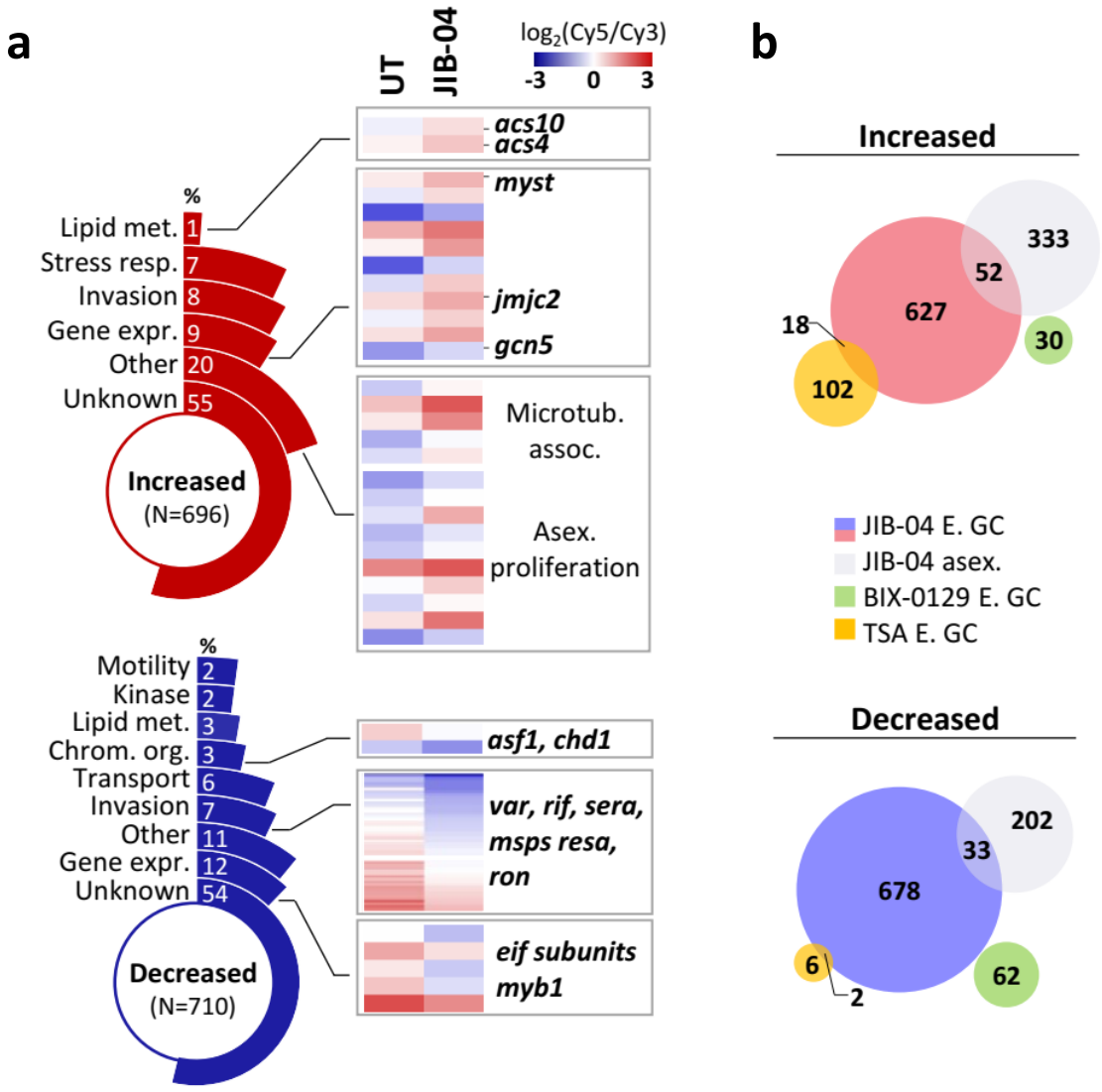

Figure 3.13: Chemical inhibition of histone demethylase activity by JIB-04 leads to the disruption of normal gene expression in gametocytes (a) Functional classification of differentially expressed genes (log_2 fold change ≥0.5 in either direction) with decreased or increased transcript abundance in response to the inhibition of histone demethylase activity by JIB-04. The % of differentially expressed genes assigned to each biological category is shown. Transcript levels in the untreated and JIB-04 treated gametocytes are exemplified for certain differentially expressed genes and categories that were enriched for H3K36me2&3 in stage II gametocytes. **(b)** Comparison of DE genes in stage II gametocytes treated with JIB-04 in this study with those for in JIB-04-treated asexual parasites (shown in grey) (212), early gametocytes (E. GC) treated with the G9a-specific inhibitor BIX-01294 (392) (green) and early gametocytes treated with the HDAC inhibitor TSA (393) (gold).

Certainly, the use of this general Jumonji-C HDMi highlights the importance of normal histone methylation patterns for transcriptional reprogramming during gametocyte differentiation and development. However, given the pan-selectivity of JIB-04, it is not expected that the inhibition of H3K36 demethylation is solely responsible for the observed transcriptional disruption and

enhanced potency of the inhibitor in gametocytes. A comparison of JIB-04-associated transcriptional disruption in asexual parasites (212) *vs.* gametocytes reveals a common interference in certain biological processes, including chromatin organisation, cell motility and kinase/phosphatase activity (Figure 3.13b). Although gametocytes treated with JIB-04 do not share common DE genes with those treated with BIX-01294, an inhibitor of the G9a-specific HMT (392), some overlap is present with HDAC inhibition by TSA (393). These results are congruent with findings for cancer cell lines that show similar gene expression signatures are associated with JIB-04 and TSA treatment (394).

In order to interrogate the downstream transcriptional effects associated with the aberrant histone methylation induced by ML324 in stage II gametocytes, a similar transcriptome analysis was performed. Interestingly, in addition to H3K36, ML324-treated stage II gametocytes also exhibit hypermethylation of H3K9 (Figure 3.14a) with this also occurring for H3K9 in asexual parasites treated with this HDMi (212). The disruption of H3K9me3 patterns has been reported as an important factor contributing to potency of this compound in gametocytes (357). ML324 treatment of stage II gametocytes resulted in the differential expression of 1507 genes, equating to ~27% of the genome.

Of the 745 DE genes with decreased transcript abundance in response to ML324 treatment, 4%, 10% and 12% are associated with erythrocyte remodelling, invasion and gene expression, respectively (Figure 3.14b). Genes belonging to the category “other” are significantly associated with lipid homeostasis (P = 0.014), acetyl-CoA biosynthesis (P = 0.009) and cytoskeleton organisation (P = 0.005) (Appendix: Table S16).

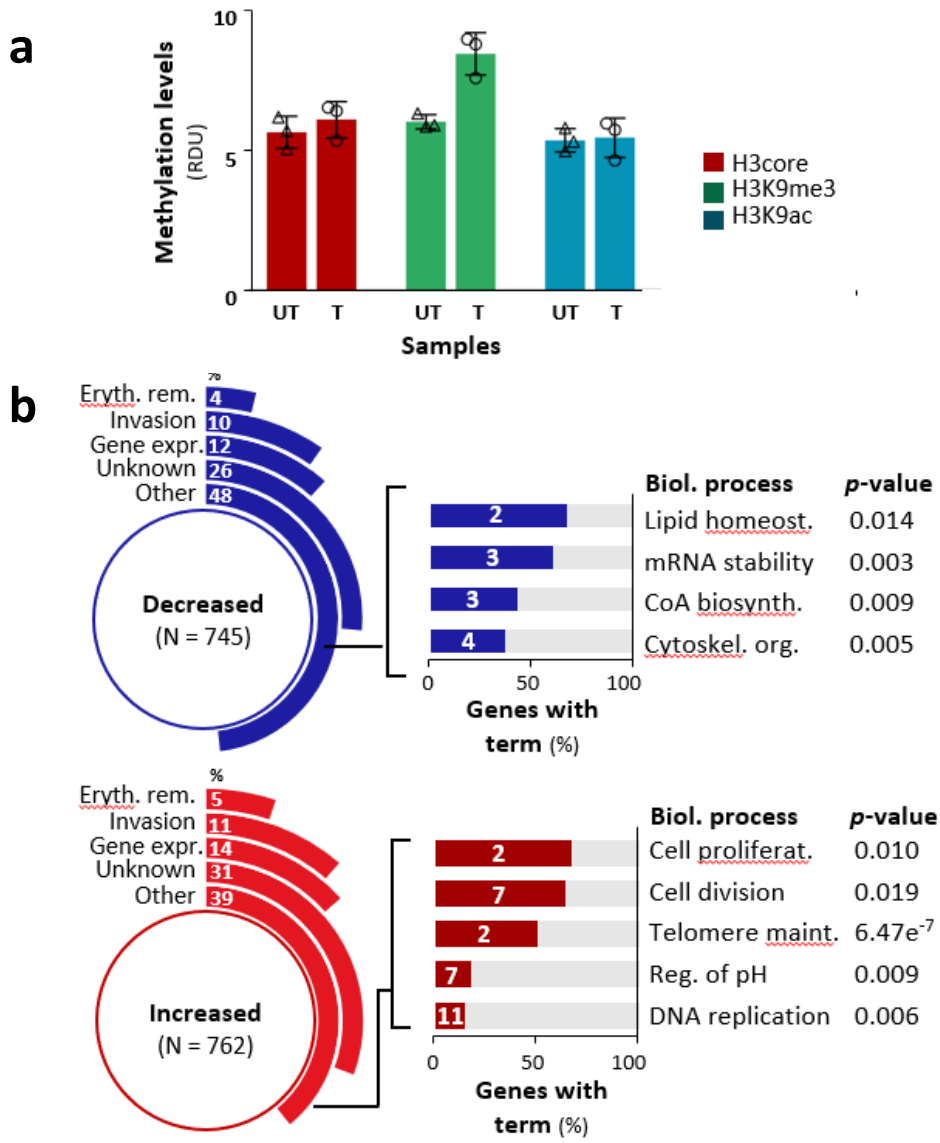

Figure 3.14: Chemical inhibition of histone demethylases with ML324 highlights the importance of histone modifications for transcriptional regulation in gametocytes (a) Comparison of the relative abundances (expressed as fold change of relative density units; RDU) of the unmodified H3 core histone, H3K9me3 and H3K9ac in gametocytes treated with ML324 (5 µM) for 24 h. Data are representative of three independent biological replicates (n = 3) performed in technical triplicates with mean ± S.E. **(b)** Transcriptome analysis of stage II gametocytes treated with ML324 (5 µM) for 24 h. Genes with differential decreased or increased transcript abundance (log_2fold change ≥0.5) were functionally classified with the number expressed as a proportion of all differentially expressed genes. Genes in the category, "Other" were subjected to GO enrichment (Appendix: Table S16) analysis with certain of the significantly (P <0.05) associated processes shown. For each, the number of genes is expressed as a % of all *P. falciparum* genes involved in the process.

These processes are regulated during early gametocyte development to enhance gametocyte-specific metabolic and development programs (84, 310-312). By contrast, the genes with increased transcript abundance are significantly associated with cell proliferation (P = 0.01) and DNA replication (P = 0.006) which may reflect an attempt by the early gametocyte to escape

sexual differentiation in favour of returning to asexual proliferation. Taken together, these results highlight the importance of the epigenetic landscape and more specifically, histone PTMs during sexual development in *P. falciparum* parasites.

3.4 Discussion

Understanding the gene regulatory mechanisms that drive differentiation and development in *P. falciparum* gametocytes is essential for the discovery and advancement of novel malaria transmission-blocking strategies (346). Here, the dynamic yet stage-specific nature of H3K36me2&3 (133) is confirmed and the association of these histone PTMs with the transcriptional reprogramming occurring post-commitment in the sexual stage of *P. falciparum* blood-stage development (94) is delineated. The chemical interrogation of *P. falciparum* HDMs supports these conclusions, highlights the importance of the dynamics of histone methylation for transcriptional control and links aberrant H3K36me2&3 patterns, at least in part, with the increased potency of Jumonji-C HDM inhibitors towards gametocytes reported before (212, 389).

The experimental strategy entailed the prior validation of antibody specificities for di- and tri-methylated *P. falciparum* H3K36. Although sequence conservation of *P. falciparum* H3 and the use of the selected antibodies previously indicated suitable specificity (205, 233, 369-372), additional validation was performed ensure that the ChIP-seq data would accurately reflect the status of H3K36me2&3 in *P. falciparum* gametocytes. While the focus of this paper is H3K36me2&3 enrichment in the stage II gametocytes, it is important to highlight that despite comparatively lower levels of enrichment, both H3K36me2&3 were detected in the post-stage II gametocyte samples and as such the possibility of these histone PTMs being functionally relevant in other gametocyte stages cannot be excluded.

The approach allowed for the delineation of the genomic regions that are dynamically occupied by H3K36me2&3 during early and intermediate gametocytogenesis. The data generated here shows that the stage II gametocyte-specific abundance (133) of H3K36me2&3 manifests as a wide-spread, yet largely intergenic enrichment that is involved transcriptional repression and is congruent with the characteristic patterns of these histone PTMs when functioning repressively in other organisms, particularly during cellular differentiation (379, 395-402). In other eukaryotes, enrichment of CDRs with H3K36me2&3 is indicative of transcriptionally permissive genes (205, 380, 403), similar to our observations for CDR enrichment in *P. falciparum* gametocytes. The distribution of H3K36me2&3 enrichment and the associated transcriptional

effects in the stage II gametocytes aligns with findings from other studies which show that in asexual parasites, the deposition of H3K36me2&3 is present in the CDRs of the active *var* gene while enrichment of the histone PTM upstream of the TSSs of silenced *var* genes is directly involved in their repression (205, 206). These similar patterns of H3K36me2&3-associated transcriptional repression in stage II gametocytes and the increased transcript levels of *set2* during early development (94), suggests this HMT is a likely candidate enzyme of H3K36 methylation in gametocytes. Nevertheless, these findings do not exclude the possibility of additional HMTs since low levels of H3K36me2&3 have been observed in *set2* deficient parasite lines (205). In addition to the likelihood of at least one shared H3K36 HMT, the similarities in the mode-of-action of JIB-04 in gametocytes and that described elsewhere for asexual parasites (212), suggests a common enzyme demethylates H3K36 in the asexual and sexual life cycle stages.

Accumulating evidence demonstrates that such epigenetic regulators are essential drivers of the transcriptional reprogramming necessary for cellular differentiation (230, 348, 395, 404). Accordingly, for *P. falciparum* gametocyte differentiation, the role of H3K36me2&3 in governing the transcriptional shifts coinciding with the transition from early differentiation to intermediate gametocyte development that was previously alluded to (94, 133) was confirmed here. The H3K36me2&3-associated repression of genes involved in asexual proliferation-related processes (e.g. DNA replication), does indeed attest to the influential role of H3K36me2&3 at this transition point. Additionally, the enrichment of genes that are upregulated under conditions of lysoPC depletion links H3K36me2&3 with the parasite's earliest responses to the environmental cue for sexual commitment (84). Specifically, an exclusive association is distinguished between H3K36me2&3 and the post-commitment repression identified previously for *hp1* and *ap2-g* (94, 117) and as such, the data presented here provide the first insights into the mechanisms that govern the regulation of these genes in differentiated gametocytes (94, 117).

While H3K36me2&3 were identified as functionally independently of other regulatory mechanisms in this study, an association was detected between these histone PTMs and AP2-G2 regulation in gametocytes as reported previously for asexual parasites (92). Additionally, a link was identified between H3K36me2&3 and the formation of heterochromatin in early

gametocytes in accordance with similar observations in other organisms (379, 405, 406). Accordingly, ML324 is shown to disrupt the normal methylation of H3K36 and H3K9 with the increased activity of ML324 in late gametocytes previously associated with the hypermethylation of the latter of these two histone PTMs (212, 357, 389).

Ultimately, this chapter documents the transcriptional repression associated with H3K36me2&3 enrichment that occurs largely independently of other mechanisms described to date for *P. falciparum* parasites. Importantly, an exclusive association between H3K36me2&3 enrichment and *hp1* and *ap2*-g was identified, thereby providing the first insights into the mechanisms governing the regulation of these genes in the post-commitment, terminally differentiated gametocytes.

Chapter 4

Comparative investigation of histone methylation patterns during *Plasmodium falciparum* gametocyte development

4.1 Introduction

Histone PTMs have been the subject of great interest and extensive research since the very first postulation of a possible transcriptional role for histone methylation and acetylation in 1964 (407). In the years proceeding this initial discovery, a large body of evidence has accumulated showing that histone PTMs do indeed regulate gene expression and also influence chromatin organisation and the repair and replication of DNA (408). Furthermore, dysregulation of the deposition and removal of histone PTMs or the disruption of the interactions with reader proteins are associated with cancer, psychiatric conditions and autoimmune and neurodegenerative diseases, attesting to the crucial nature of these epigenetic regulators for normal cellular function (352, 409, 410). Nevertheless, most studies of epigenetic regulation are accompanied by the acknowledgement of the improbability that the factor of interest functions in isolation or even with only a few interacting partners (411). Rather, epigenetic regulation is thought to be an immensely complex, interactive network of histones and their variants, PTMs and reader complexes. Histone reader complexes consist of combinations of chromatin modifying enzymes, transcription factors and even other histone PTM writers and erasers (412). Thus, while it is important to study each epigenetic factor in isolation, performing comparative investigations to examine the networks in which the factor functions are essential (412).

The idea of combinatorial epigenetic modifications and regulators was first proposed as the histone code hypothesis in the early 1900s. However, due to challenges associated with proving histone PTM co-existence and the functional relevance of this, the hypothesis lacks the same degree of experimental support that is available for individual histone PTMs (411, 413). Antibodies used in combinatorial histone PTM analysis can also be problematic for two reasons: 1) recognisable epitopes usually consist of single modifications and 2) neighbouring histone PTMs

may hinder the interaction between the antibody and epitope of interest (414, 415). Despite these challenges, some progress has been made towards understanding the co-functioning of histone PTMs and their effector proteins. For example, in embryonic stem cells, mono-methylated H3K27 and H3K36 have been shown to coexist on the same histone (H3K27me1K36me1 combination) and exhibit bidirectional crosstalk (416). Additionally, H3K36me3 is known to antagonise the subsequent methylation of H3K27me1 by reducing the efficiency of the writers that synthesise the H3K27me2&3 states (238, 417). Although all four of the possible combinations of di- and tri-methylated H3K27K36 have been observed in mouse embryonic stem cells (418), these combinations are rarely detected in other organisms. Rather, several reports indicate H3K27K36 with higher states of methylation do not co-exist on the same histone (405, 406) and furthermore have confirmed that, the presence of these di- and tri-methylated residues inhibits the writer/s of the other (417, 419, 420). In addition to this and similar to what we observed for the stage II gametocytes (see Chapter 2 section 2.3.4), many studies in other eukaryotic organisms have identified the independent patterns and networks of H3K9me3 and H3K27me2&3 enrichment (237, 421-423) with these both particularly important for defining appropriate chromatin states during cellular differentiation (424, 425). In this way, these histone PTMs create negative feedback loops that sustain the discrete chromatin environments and thereby promote appropriate gene expression patterns that are required for normal cellular differentiation and function (425, 426). Similarly, in multiple myeloma, the over-expression of an H3K36-specific HMT leads to a global increase in H3K36me2 levels and reduction of H3K27me3 followed by aberrant cell proliferation and invasion (427). This supports independent functions and the requirement for consistently maintained levels of the highly methylated states of H3K27 and H3K36 for cellular homeostasis

In addition to a role in determining cellular identity, histone methylation is also involved in driving sex determination in eukaryotes (428, 429). Both H3K27me2&3 and H3K36me2&3 are known to be important determinants in sexual differentiation in a variety or organisms (429-432). For example, the temperature-dependent and sexually dimorphic demethylation of H3K27me3 promotes the transcription of genes required for male development in the turtle species *T. scripta* with the genetic disruption of the responsible H3K27-specific HDM sufficient to induce

male-to-female reversal (432). Sexual differentiation in *Drosophila* is heavily dependent on H3K36me3 to recruit the male-specific lethal (MSL) complex that enhances the expression of genes required for male development (430, 431).

In *Plasmodium* parasites, histone PTM combinations have been identified with certain of these implicated as important regulators of transcription. As for individual modifications, histone PTM combinations are dynamic with characteristic subsets of these defining each asexual and sexual life cycle stage (219, 324, 325). For example, H3K9me1/2/3K14ac and H4K8acK12acK16ac are among several validated combinations that are present in the asexual parasites and gametocytes, respectively (219, 324, 325). For combinations identified and validated by stringent mass spectrometry profiling in *P. falciparum* parasites, the greater proportion (61%) is associated with increased abundance in the gametocyte stages compared to asexual parasites (324). This suggests that these combinations may be involved in generating distinct differentiation-specific programs in gametocytes. Of note, is the presence of H3K27me1K36me1, detected by both quantitative bottom-up (shorter peptides) (324) and middle-down (longer peptides) (325) proteomics approaches. This particular combination is distinctly abundant in the late gametocyte stages and exhibits a strong positive crosstalk, contrasting with the absence of this combination in the early gametocyte stages (324, 325). As H3K27me1 is associated with transcriptional activation both individually (238) and when in combination with H3K36me1 (433) in higher eukaryotes, the increased abundance of H3K27me1K36me1 in late gametocyte stages may be involved in the activation of genes required for transmission to the vector. Interestingly however, the synchronous increases in H3K27me2&3 and H3K36me2&3 abundance in the stage II gametocytes do not correspond with the presence of these histone PTMs in combination (324, 325). Aside from the detection of H3K27me3K36me2 exclusively in the schizont stages by bottom-up proteomics, other combinations consisting of the higher methylated states of H3K27K36 have not been identified in *Plasmodium* parasites (325), in line with the scarcity of these combinations in other eukaryotes (420, 433). This therefore suggests that H3K27me2&3 and H3K36me2&3 are unlikely to be present on the same histone and is predictive of discrete, exclusive regulatory roles for each of these histone PTMs in the stage II gametocytes. It was

therefore of interest to examine the similarities and contrasts in the genome-wide enrichment and functional relevance of H3K27me2&3 and H3K36me2&3.

In this chapter, the individual functional roles of H3K27me2&3 and H3K36me2&3 are delineated through integrative genome-wide analyses that indicate these histone PTMs are independent and predominantly repress unique subsets of asexual stage-related genes, thereby each contributing to the silencing of obsolete processes in gametocyte differentiation. The smaller subset of genes that are associated with both H3K27me2&3 and H3K36me2&3 enrichment exhibit a greater degree of transcriptional repression compared to either of the histone PTMs alone. Since a single histone is unlikely to be highly methylated at both H3K27 and H3K36 simultaneously, the apparent presence of these histone PTMs at the same genomic region may reflect their mutually exclusive existence on adjacent nucleosomes or asymmetrically modified nucleosomes with these specifying a unique biological outcome. Finally, sex-related biases in histone PTM enrichment are identified and are proposed to be linked to sex-related transcriptional regulation in stage II gametocytes.

4.2 Materials and methods

4.2.1 ChIP-seq data meta-analysis and integration

For this comparative analysis, the ChIP-seq data sets generated in Chapters 2 (section 2.3.3) and 3 (section 3.3.1) for H3K27me2&3 and H3K36me2&3 were used. Only those genes with significant enrichment (MACS2 peaks identified with q-value ≤0.05 in both biological replicates) of the histone PTMs identified in Chapter 2 (sections 2.2.9 and 2.3.3) and 3 (sections 3.2.9 and 3.3.4) were included with all data from both biological replicates included in analyses.

4.2.2 Integration of histone PTM, gene expression and functional enrichment data

In order to identify unique gene expression trends associated with the histone PTMs of interest, ChIP-seq data were integrated with the same microarray gene expression time course data set (94) used throughout Chapters 2 (section 2.3) and 3 (section 3.3). These DNA microarrays were performed using the same clonal strain of NF54 *P. falciparum* parasites that was used for ChIP-seq experiments. For gametocyte sex-specific analyses, differential transcriptomes were obtained from a publicly available gene expression set with this data also generated using a parasite strain from an NF54 background (125). Gene ontology (biological process) and metabolic pathway enrichment analyses were performed in PlasmoDB using a *P*-value cut-off ≤0.05.

4.3 Results

4.3.1 H3K27me2&3 and H3K36me2&3 are independently enriched in stage II gametocytes

To compare the patterns of H3K27me2&3 and H3K26me2&3 in *P. falciparum* gametocytes, only those sites identified in Chapters 2 (section 2.2.9) and 3 (section 3.2.9) to have significant enrichment (MACS2 peaks with q-value ≤0.05 present in both biological replicates) for H3K27me2&3 and H3K26me2&3 in the pre-stage II, stage II and post-stage II gametocytes (isolated on days 2, 4 and 7 of gametocyte development, respectively, see section 2.3.1) were assessed. As the pre-stage II gametocytes had only a single biological replicate for H3K36me2&3, the enrichment of these histone PTMs could not be determined for this stage. However, H3K27me2&3 enrichment was identified in the pre-stage II gametocytes and is present across a larger number of sites (231 and 262, respectively) compared to these histone PTMs in post-stage II gametocytes (5 and 5, respectively) (Figure 4.1). This depletion of H3K27me2&3 in the post-stage II gametocytes contrasts with a number of sites that are enriched with H3K36me2&3 (105 and 214, respectively). Comparatively, in the stage II gametocytes, H3K27me2&3 are more frequently enriched compared to H3K36me2&3 (1795 *vs.* 1302 sites, respectively) (Figure 4.1). Together, these results suggest greater functional relevance for H3K27me2&3 in earlier stages of gametocyte development.

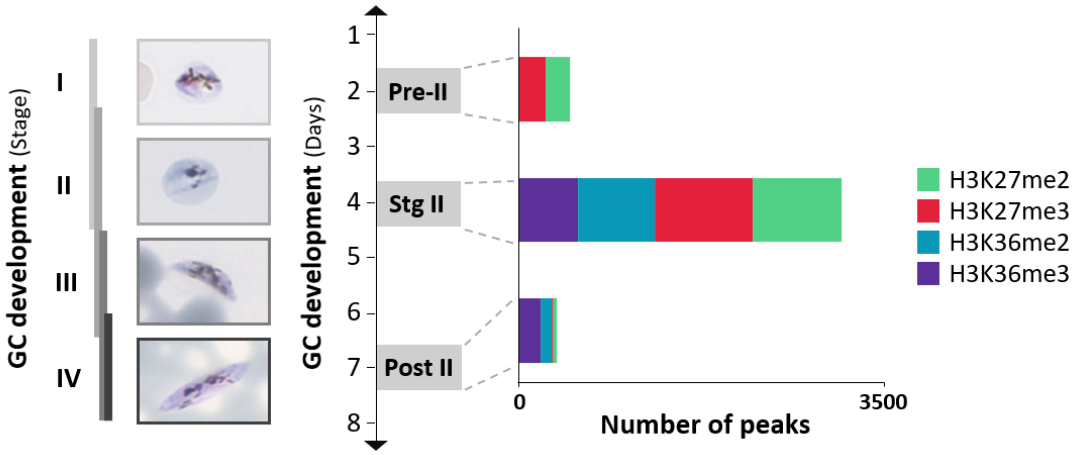

Figure 4.1: Comparative analysis of H3K27me2&3 and H3K36me2&3 enrichment during early and intermediate gametocyte development. (a) Pre-stage II (pre-II), stage II (stg II) and post-stage II (post-II) gametocyte samples were harvested on days 2, 4 and 7 of gametocyte (GC) development, respectively. ChIP-seq was performed to identify the numbers of sites significantly enriched (q-value ≤0.05) with H3K27me2&3 or H3K36me2&3 in each population. Significant sites are associated with MACS2 peaks that were present in both biological replicates.

4.3.2 Independent regulation by H3K27me2&3 and H3K36me2&3 in stage II gametocytes

Next, the identities of the H3K27me2&3- and H3K36me2&3-enriched gene sets were compared following the classification of genes based on the position of the histone PTM enrichment as before. In the stage II gametocytes, H3K27me2&3 and H3K36me2&3 enrichment have distinct distributions across the genome (Figure 4.2a). This exclusivity is more prominent for genes with enrichment concentrated upstream of TSSs with 80% and 71% of the H3K27me2&3- and H3K36me2&3-enriched sites (compared to 55% and 51% of CDRs, respectively) independently associated with the respective histone PTM. Nevertheless, small proportions genes (27% of CDRs and 13% of upstream regions) are associated with enrichment for both H3K27me2&3 and H3K36me2&3. An independent validation by differential binding analysis of the peaks used to derive the enriched gene sets confirm these results and indicate an overlap of only 19% of H3K27me2&3 and H3K36me2&3 peaks in the stage II gametocytes. As these PTMs are unlikely to co-exist on the same histone, this overlap may arise from the presence of H3K27me2&3 and H3K36me2&3 on nearby or adjacent nucleosomes in the chromatin of stage II gametocytes with

these loci referred to as “bivalently enriched” hereafter. Although the histone PTMs of interest enrich far fewer genes in the post-stage II gametocytes, the lack of overlap between the H3K27me2&3- and H3K36me2&3-enriched sets (Figure 4.2a) suggests that such bivalent enrichment of genomic loci is a stage II gametocyte-specific trend.

Next, the transcriptional fingerprints of genes with bivalent enrichment were compared to those only enriched with either H3K27me2&3 or H3K36me2&3. For this, the same publicly available gene expression data set (94) that was used throughout Chapters 2 and 3 was leveraged and contained corresponding expression values for the vast majority (98%) of the histone PTM enriched gene sets. The stage II gametocyte-specific transcriptional repression of genes with H3K27me2&3 enrichment upstream of TSSs (see section 2.3.3) is exceptionally similar to that associated with H3K36me2&3 (see section 3.3.2). Specifically, the transcription profiles of genes independently enriched with H3K27me2&3 or H3K36me2&3 are almost indistinguishable from one another on days 2 to 6 development (Figure 4.2b) on which stage II gametocytes are present in culture and exhibit a peak abundance of these histone PTMs (133).

Interestingly, bivalent enrichment of genes with H3K27me2&3 and H3K36me2&3 corresponds to a greater, cumulative degree of transcriptional repression (average $\log_2$FC = -0.9) than either of the two histone PTMs alone (average $\log_2$FC = -0.45 and -0.48 for H3K27me2&3 and H3K36me2&3, respectively) (Figure 4.2b). Additionally, the transcriptional repression associated with both the independently and bivalently enriched gene sets continues beyond day 6 of development when stage II gametocytes are no longer present. Most genes with independent (100% and 95%, respectively) or bivalent (91%) enrichment for H3K27me2&3 and H3K36me2&3 in the stage II gametocytes do not preserve this association into the post-stage II gametocytes, suggesting that these histone PTMs are involved in the primary establishment, but not maintenance, of the longer-term transcriptional repression of these genes.

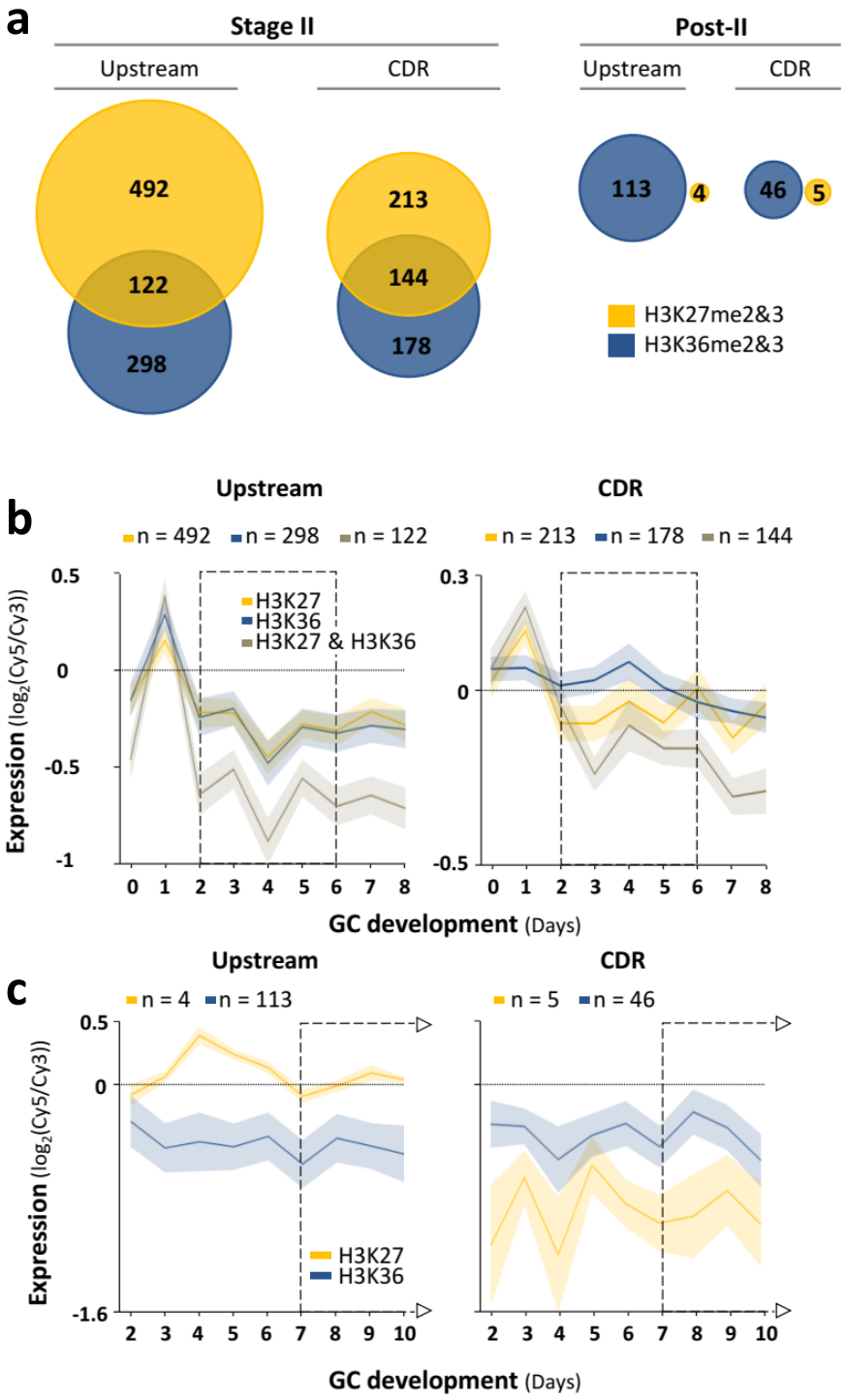

Figure 4.2: Independent transcriptional regulation by H3K27me2&3 and H3K36me2&3 in stage II gametocytes. (a) Comparison of H3K27me2&3- and H3K36me2&3-enriched (significant peaks, q-value ≤0.05 present in both biological replicates) coding regions (CDRs) and regions upstream of TSSs in the stage II and post-stage II gametocytes with values represting the number of genes per category. **(b)** Average gene expression (log_2Cy5/Cy3) levels on days 0 to 8 of gametocyte (GC) development for genes that are independently enriched with either H3K27me2&3 (yellow) or H3K36me2&3 (blue) or bivalently enriched (grey) either upstream of their TSSs or within the CDRs in stage II gametocytes. **(c)** Average gene expression (log_2Cy5/Cy3) levels on days 0 to 8 of gametocyte (GC) development for genes that have enrichment of H3K27me2&3 only (yellow) or H3K36me2&3 only (blue) either upstream of their TSSs or within the CDRs in the post-stage II gametocytes.

CDRs enriched with H3K27me2&3 in stage II gametocyte are generally not expressed during early and intermediate gametocyte development in contrast to the H3K36me2&3-enriched CDRs that have low levels of transcription across this timeframe (Figure 4.2b). This is congruent with the transcriptional permissivity or expression of CDRs enriched with H3K36me2&3 and a lack of such non-repressive functions for H3K27me2&3 in both *Plasmodium* and other eukaryotes (205, 206, 434). Interestingly however, the bivalently enriched CDRs are repressed, and to a greater degree than those exclusively enriched with H3K27me2&3, from day 2 of development and onwards (Figure 4.2b). Ultimately, this indicates that in *Plasmodium* parasites, as in other organisms (377, 418, 420), the regulatory effects of histone methylation are additionally dependent on their proximity relative to other independent histone PTMs.

In the post-stage II gametocytes, H3K27me2&3 and H3K36me2&3 are both independently associated with transcriptional repression, irrespective of whether the CDRs or regions upstream of the genes are enriched (Figure 4.2c). Genes with upstream enrichment of H3K27me2&3 in the post-stage II gametocytes are repressed following a peak in transcript abundance on day 4. As none of these genes are associated with histone PTM enrichment in the preceding stage II gametocytes, this may reflect a functional relevance for H3K27me2&3-associated transcriptional regulation in post-stage II gametocytes. Nevertheless, the small number of genes (four) for which this trend is observed suggests a negligible effect on the transcriptional environment compared to the extensive repression associated with H3K27me2&3 enrichment in the stage II gametocytes.

Taken together, these results suggest that although H3K27me2&3 and H3K36me2&3 are both repressive, they function non-redundantly and predominantly regulate unique subsets of genes in stage II gametocytes. Furthermore, at a small subset of loci in the stage II gametocytes, H3K27me2&3 and H3K36me2&3 enrich nucleosomes in close proximity, generating a bivalent state of enrichment that is associated with enhanced transcriptional repression.

4.3.3 H3K27me2&3 and H3K36me2&3 independently regulate discrete biological pathways during gametocyte development

As H3K27me2&3 and H3K36me2&3 are largely associated with the transcriptional regulation of independent gene sets in stage II gametocytes, we sought to determine if this translates to the regulation of discrete biological processes and pathways. To do so, gene ontology and metabolic pathway enrichment analyses were performed for genes independently enriched with H3K27me2&3 and H3K36me2&3 or bivalently enriched for these histone PTMs. The minor proportion (13%) of bivalently enriched genes are significantly associated with the asexual parasite-related processes of cytoadhesion ($P = 8.73e^{-15}$), polyamine biosynthesis ($P = 1.29e^{-4}$) and haem metabolism ($P = 0.038$) (Figure 4.3 and Appendix: Table S17), indicating a role for bivalent H3K27me2&3 and H3K36me2&3 enrichment during the switch from early gametocyte differentiation to intermediate development.

By deconvoluting the gene sets that are independently enriched with either H3K27me2&3 or H3K36me2&3 in the stage II gametocytes, the individual functional relevance of each histone PTM could be assigned with greater clarity and certainty. Genes enriched only with H3K27me2&3 in the stage II gametocytes were significantly associated with fatty acid oxidation ($P = 0.001$), choline biosynthesis I ($P = 0.006$), glycolipid metabolism ($P = 0.028$) and glycolysis ($P = 0.038$) (Figure 4.3 and Appendix: Table S17), indicating an important regulatory role for H3K27me2&3 early-stage gametocyte metabolism.

By contrast, processes with significant links to H3K36me2&3-enrichment are less biased toward metabolism (only choline biosynthesis III, $P = 0.002$) and more towards the early differentiation-related processes (58) such as the translocation of proteins into the host erythrocyte ($P = 5.79^{-4}$). Finally, both H3K27me2&3 and H3K36me2&3 are independently and significantly ($P = 0.027$ and $P = 0.017$, respectively) associated with chromatin organisation (Figure 4.3 and Appendix: Table S17) in the stage II gametocytes with this further dissected in the next section. Together, these results indicate that the transcriptional repression associated with genes independently enriched with H3K27me2&3 and H3K36me2&3 does indeed translate into different biological pathways and processes.

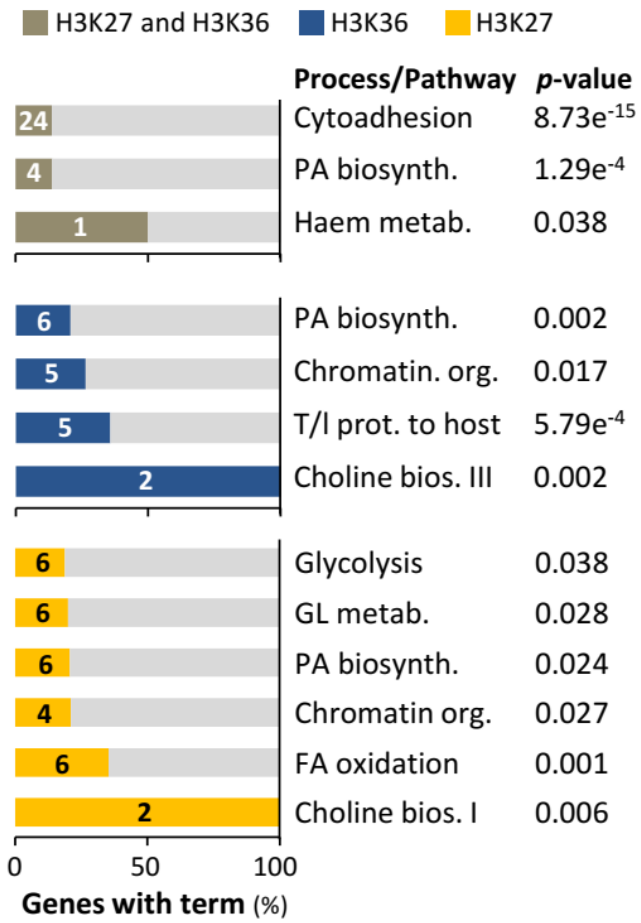

Figure 4.3: Functional classification of genes enriched with H3K27me2&3 and H3K36me2&3 in stage II gametocytes. Genes independently enriched with H3K27me2&3 or H3K36me2&3 or bivalently enriched with these histone PTMs in stage II gametocytes are significantly associated (*P*-value ≤0.05) with the biological processes and metabolic pathways as indicated. The number of enriched genes is shown on each bar and is expressed as a percentage of all genes associated with the term or pathway in *P. falciparum* parasites. Legend: PA = polyamine; biosynth/bios.. = biosynthesis; org. = organisation; t/l prot. = translocation of protein; GL = glycolipid; metab. = metabolism; FA = fatty acid.

4.3.4 Independent transcriptional repression of chromatin modifying factors by H3K27me2&3 and H3K36me2&3 in stage II gametocytes

Given the well-documented importance of chromatin organisation for eukaryotic cellular differentiation (435-437), the significant links between H3K27me2&3 and H3K36me2&3 enrichment and chromatin regulation in the stage II gametocytes were evaluated in greater detail. In stage II gametocytes, this association between H3K27me2&3 and chromatin regulation

arises from the independent enrichment and repression of several important chromatin factors including three lysine-specific HMT-encoding genes: *set2* (methylates H3K36), *set7* (methylates H3K4, H3K9 and H3K27) and *set10* (deposits H3K9me3) and two DNA helicases: *iswi* and *snf2l* (Table 4.1). Furthermore, chromatin regulators that function during asexual parasite proliferation (e.g. 14-3-3I interacts with CDPK1 to regulate asexual parasite growth) (438) and sexual commitment (e.g. HDA1) (134) are also independently enriched and repressed by H3K27me2&3 (Table 4.1). The link between H3K27me2&3 and such high-order regulators of life cycle progression illuminate the extensive importance of H3K27me2&3 for gametocyte development.

Key components of four out of the five quantitatively identified epigenetic reader complexes in *P. falciparum* parasites are enriched and repressed by H3K27me2&3 in the stage II gametocytes (Table 4.1). These include BDP2 (PF3D7_1212900) and PF3D7_1124300, both components of the BDP1/2 reader complex as well as PF3D7_1402800 of the GCN5/ADA2 complex that closely resembles the core module of eukaryotic HAT/SAGA-like complexes (213). The gene encoding PHD1 (PF3D7_1008100) is similarly enriched with H3K27me2&3 (Table 4.1) with this protein likely involved in recruiting reader complexes that positively influence transcription (213).

Likewise, independent H3K27me2&3 enrichment and repression occurs for several genes encoding components of two other *P. falciparum* reader complexes while others show this association exclusively with H3K36me2&3. The BDP4 reader protein complex contains a core module of several proteins including PF3D7_1128000 and PF3D7_0306100, both H3K27me2&3-enriched and SWIB (PF3D7_0611400) and CHD1 (PF3D7_1023900) that exhibit independent enrichment with H3K36me2&3 in the stage II gametocytes (Table 4.1). The essential components, PF3D7_0817300 and NAPS belonging to PHD2/SAGA, a second SAGA-like reader complex described in *P. falciparum* (213), are independently enriched with H3K27me2&3 and H3K36me2&3, respectively. Functional data available for GCN5/ADA2 and BDP1/2 indicate these complexes are recruited to positively influence transcription at H3K4me2&3-enriched sites (213, 439), suggesting that the repressive actions of H3K27me2&3 and H3K36me2&3 are compounded through the enrichment and repression of transcriptional activators in the stage II gametocytes

Table 4.1: Chromatin regulators independently enriched and repressed by either H3K27me2&3 or H3K36me2&3 in stage II gametocytes

Gene	Protein product	Function	References
		H3K27me2&3	
PF3D7_0818200	14-3-3I	H3S28ph reader, CDPK1 binding	(216)
PF3D7_1472200	HDA1	HDAC	(52, 86)
PF3D7_0624600	ISWI	DNA helicase	(440, 441)
PF3D7_1104200	SNF2L	DNA helicase	(52, 200)
PF3D7_1322100	SET2	HMT (H3K36me2&3)	(200, 205, 442)
PF3D7_1115200	SET7	HMT (H3K4 and H3K9)	(200, 210)
PF3D7_1221000	SET10	HMT (H3K4me3)	(200, 211)
PF3D7_1212900	BDP2	BDP1/2	(213, 214, 443, 444)
PF3D7_1124300	-	H3K4me2&3 binding; BDP1/2	(213, 444)
PF3D7_1008100	PHD1	Recruit BDP1/2 and GCN5/ADA2 to ac histones	(213, 443)
PF3D7_1402800	-	GCN5/ADA2	(213, 443)
PF3D7_1128000	-	BDP4	(213, 443)
PF3D7_0306100	-	BDP4	(213, 443)
		H3K36me2&3	
PF3D7_1014600	ADA2	Transcriptional co-activator; GCN5/ADA2	(213, 439)
PF3D7_1220900	HP1	Heterochromatin formation	(89, 209, 227)
PF3D7_1203700	NAPL	Histone chaperone	(192, 445)
PF3D7_0919000	NAPS	Histone chaperone; PHD2/SAGA	(192, 213, 445)
PF3D7_0817300	-	PHD2/SAGA	(213, 443)
PF3D7_1023900	CHD1	DNA helicase; BDP4	(200, 443)
Pf3D7_0611400	SWIB	Chromatin remodelling at *var* genes; BDP4	(446)

H3K36me2&3 also independently enrich and repress the histone chaperones, *naps* and *napl* (PF3D7_1203700) (Table 4.1) that have been described as the nucleosome assembly motors of the parasite (192, 445), indicating the involvement of the histone PTMs in suppressing nucleosome formation in stage II gametocytes. Furthermore, H3K36me2&3 enrich the gene encoding ADA2 (PF3D7_1014600), a transcriptional co-activator that potentiates acetyltransferase activity within the GCN5/ADA2 reader complex at sites modified with H3K4me3 (213, 439). In addition to being a core component of the BDP4 reader complex, SWIB is also a known regulator of *var* gene expression (213, 446). This enrichment of *swib* aligns with the repression of other immune evasion-related processes by H3K36me2&3 in the stage II gametocytes (446). Finally, the independent enrichment of *hp1* (Table 4.1) indicates that H3K36me2&3 not only antagonise transcriptional activation but also play a role in regulating additional repressive mechanisms.

4.3.5 Differential enrichment of sex-specific genes with H3K27me2&3 and H3K36me2&3 in stage II gametocytes

Previous studies have identified significant differences between the transcriptomes and proteomes of male and female gametocytes that dichotomise the sexes in *Plasmodium* parasites (125, 447-449). Given the peak enrichment of H3K27me2&3 and H3K36me2&3 in stage II gametocytes and the first appearance of male and female morphologies in stage II gametocytes (450), we questioned if these histone PTMs may be differentially associated sex-specific transcriptomes. To investigate this, the stage II gametocyte-specific H3K27me2&3- and H3K36me2&3-enriched gene sets were compared with previous transcriptome data that indicated ~66% of the gametocyte genome is differentially expressed between male and females (125). Of the genes independently enriched for H3K27me2&3 or H3K36me2&3, 43% and 37% have sex-dependent transcription in the gametocyte stages (Figure 4.4a). Irrespective of whether the enrichment is present in the CDRs or upstream of TSSs, relatively small proportions (16% CDRs and 18% upstream) of bivalently enriched genes have sex-specific expression in gametocytes (Figure 4.4a). Of the sex-specific genes that are independently enriched with

H3K27me2&3, relatively similar proportions are differentially expressed in female (46%) and male (54%) gametocytes. By contrast, the H3K36me2&3 enrichment of sex-specific genes is male-biased (67%), suggesting a link may exist between H3K36me2&3 enrichment and sex determination in gametocytes.

Further evaluation of the 174 H3K36me2&3-enriched sex-specific genes revealed a bias in the position of enrichment and the effect on transcription between gametocyte sexes. Of the 57 female-specific genes, H3K36me2&3 predominantly enrich regions upstream of TSSs (75%) with this yielding a greater transcriptional repression in stage II gametocytes compared genes with enrichment in the CDRs (Figure 4.4b). All H3K36me2&3-enriched and repressed female genes exhibit a contrasting increased transcript abundance during subsequent development. Such activation contrasts with the expression patterns of the entire set of H3K36me2&3-enriched genes for which alternative mechanisms maintain the repression into subsequent development following the initial enrichment with H3K36me2&3 in the stage II gametocytes. The distribution of H3K36me2&3 across male-specific genes is relatively equal with 56 and 61 genes showing enrichment upstream of TSSs and in CDRs, respectively (Figure 4.4b). Genes with H3K36me2&3 upstream of TSSs exhibit the decreased transcript abundance that is characteristic of genes with such H3K36me2&3 enrichment at this site (Chapter 3). Crucially however, H3K36me2&3 enrichment in male-specific CDRs is associated with a dramatic increase in transcript abundance in the stage II gametocytes (Figure 4.4b). Although a slight increase in average transcript levels also occurs for the entire set of H3K36me2&3-enriched CDRs (Chapter 3, Figure 3.8), this was only present for day 4 gametocytes and is substantially less notable when compared to the male-specific genes only (average $\log_2$FC on day 4 of 0.08 compared to 0.44) (Figure 4.4b). Taken together, these results elucidate independent sex-specific enrichment of H3K27me2&3 and H3K36me2&3 in *P. falciparum* stage II gametocytes. Furthermore, similar to previous observations of H3K36me2&3 in asexual parasites, this analysis identifies a link between transcriptional activation and H3K36me2&3 CDR enrichment with results suggesting a potential bias toward male-specific genes in the stage II gametocytes.

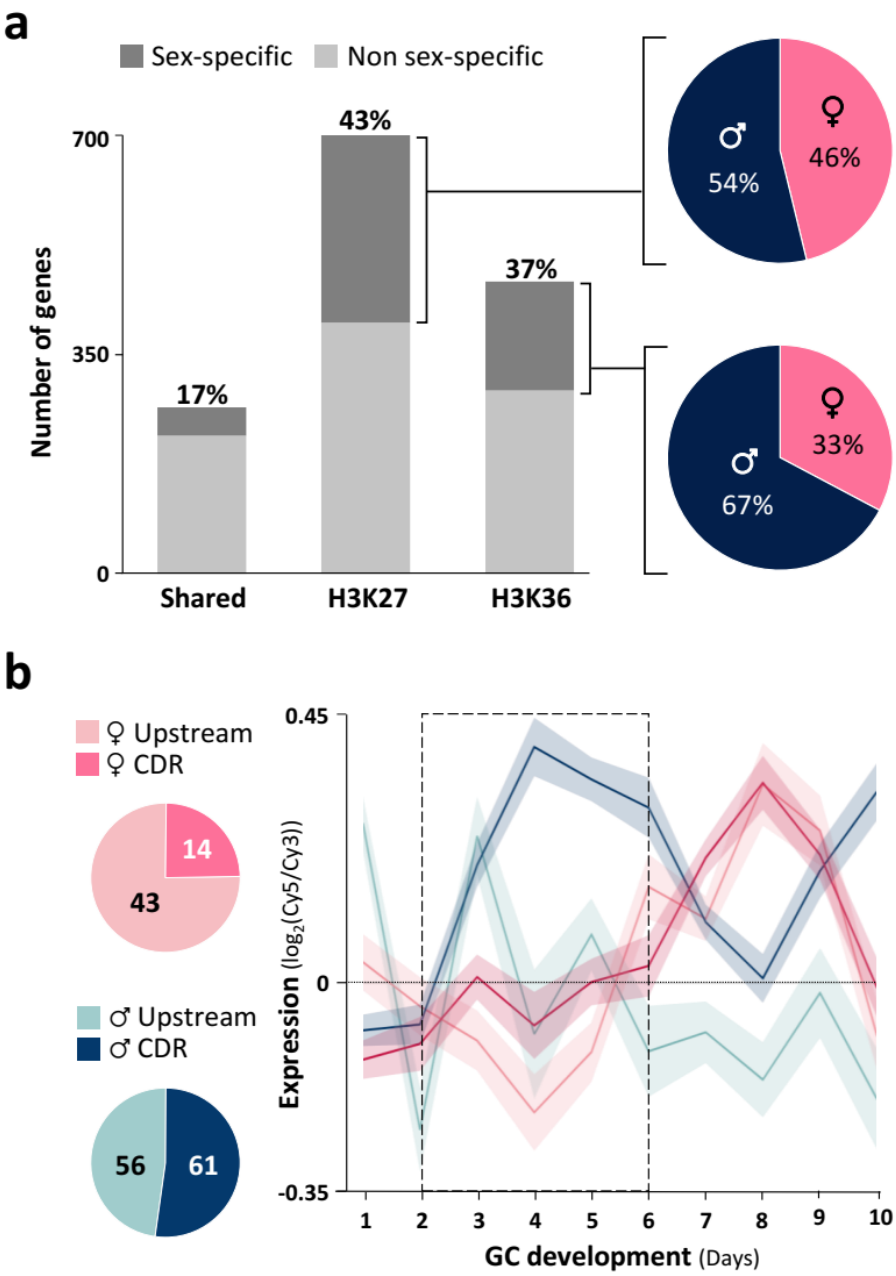

Figure 4.4: Independent H3K27me2&3 and H3K36me2&3 enrichment sex-specific genes in stage II gametocytes. **(a)** Genes were first classified based on enrichment as either independently enriched with H3K27me2&3 or H3K36me2&3 or bivalently enriched with these histone PTMs and then on the position of the enrichment either upstream of TSSs or in CDRs. For each category, the proportions of sex-specific (differentially expressed in female or male gametocytes) and non-sex-specific genes (125) are shown. The number of sex-specific genes is shown as a % of the total number of enriched genes in each category. Pie charts indicate the proportions of independently di- and tri-methylated H3K27 or H3K36 gene sets that are male- and female-specific. **(b)** H3K36me2&3-enriched male (blue) and female (pink) genes were stratified based on the position of enrichment, either upstream of TSSs or within CDRs with pie charts indicating the number of genes in each category. The expression profiles (log_2Cy5/Cy3) (94) of each category are shown for days 1 to 10 of gametocyte (GC) development. Black dashed box indicates days on which stage II gametocytes were present in culture, corresponding with days on which H3K36me2&3 were enriched.

4.4 Discussion

Many individual epigenetic factors that are involved in transcriptional regulation, DNA replication and repair and chromatin organisation have been discovered and characterised. However, it is widely accepted in the field of epigenetic research that these individual components function within expansive and interconnected networks (142, 149, 185, 189, 314, 315, 451). Thus, while primary studies usually focus on distilling the individual functionality of epigenetic factors, it is essential to advance this understanding to include the factor's contribution within the larger regulatory network. In this chapter, the functions and networks associated with H3K27me2&3 and H3K36me2&3 were contrasted. This examination indicated that these histone PTMs predominantly function independently from one another, each contributing non-redundantly to the transition from early gametocyte differentiation to intermediate development. Specifically, the independent repression of individual gene sets and epigenetic networks by these histone PTMs is documented. Together the findings in this chapter demonstrate the conservation of the characteristic eukaryotic functions of H3K27me2&3 and H3K36me2&3 for gene regulation, chromatin organisation and ultimately the differentiation of the transmissible stages of the human malaria parasite.

In *Plasmodium* parasites, functionally relevant combinations of histone PTMs have been described previously (133, 219). For example, H3K27me1K36me1 is abundant in the late gametocyte stages (325) and has been postulated to be involved in the activation of genes necessary for the subsequent transmission stages. Despite the peak abundance of the individual histone PTMs in the stage II gametocytes, combinations consisting of the higher methylation states of H3K27 and H3K36 are limited to the presence of H3K27me3K36me2 exclusively in the schizont stages (324). Accordingly, the vast majority of enriched genes identified here are independently associated with either H3K27me2&3 or H3K36me2&3, indicating that in stage II gametocytes, both of these repressive mechanisms are employed to independently regulate specific genes and processes and thereby drive subsequent development. Similarly in model organisms, combinations of H3K27me2&3 and H3K36me2&3 are rarely observed in line with reports of antagonism between these histone PTMs and the writer protein/s of the other

modification (417, 419, 420). Furthermore, this indicates that epigenetic regulation of differentiation in *Plasmodium* parasites is similarly complex to that in higher eukaryotes (240, 267, 402).

Interestingly, chromatin regulation in the stage II gametocytes is significantly associated with both H3K27me2&3 and H3K36me2&3, with these links arising from independently enriched gene sets. In model eukaryotes, similar observations have been made, with each of these histone PTMs autonomously contributing to chromatin regulation (349, 418, 452, 453). Indeed, we find H3K27me2&3 and H3K36me2&3 independently repress components of several key epigenetic reader complexes in *P. falciparum* parasites. These include enrichment and repression of components of the GCN5/ADA2 complex which resembles the HAT/SAGA complexes (213) that play central roles in eukaryotic transcriptional regulation (454, 455). Additionally, H3K27me2&3 enrich and repress the genes encoding PHD1 and the DNA helicases, ISWI and SNF2L. Based on its frequent and strong association with reader complexes and the presence of critical residues for modified histone binding, PHD1 presents the most likely candidate involved in recruiting BDP1/2 and ADA2/GCN5 to their sites of activity in *Plasmodium* parasites (213). In higher organisms, PHD domain-containing enzymes recognise unmodified and methylated histones (456) with PHD1 specifically characterised as a reader of H3K4me3 (457, 458). Likewise, H3K4me3 has been predicted to be the site of recognition for PHD1 in *P. falciparum* (213). Regarding *iswi* and *snf2l*, the expression levels of these genes are highly correlated with lysoPC depletion and the de-repression of *ap2-g* during commitment (84, 91). In model organisms the SWItch/Sucrose Non-Fermentable (SWI/SNF) complexes, containing subunits homologous to the *Plasmodium iswi* and *snf2l*, antagonise transcriptional repression by directing HATs to this site (459, 460). This shows the independent involvement of H3K27me2&3 in the subsequent silencing of these drivers of commitment once gametocytogenesis ensues. The repression of such transcription enhancing proteins and complexes (211, 439) demonstrate that H3K27me2&3 and H3K36me2&3 are not only associated with the direct silencing of genes but also augment their genome-wide effects through the enrichment and repression of gene expression activators. Interestingly, the mammalian α-HP1 and γ-HP1 isoforms influence the levels of H3K27me3 and H3K36me3, respectively (461) while in *Neurospora crassa,* fluctuations in HP1 distribution alter the ratio of

H3K27me2:H3K27me3 (462). Therefore, if HP1 also influences histone methylation in *Plasmodium* parasites, the independent enrichment and repression of this protein by H3K36me2&3 in the stage II gametocytes would be critical to ensure the correct balances of the highly methylated H3K27 and H3K36 that are required for the transition to intermediate gametocyte development. The results presented here show that similar to other eukaryotes (349, 418, 452, 453), H3K27me2&3 and H3K36me2&3 contribute to the optimisation of transcriptional environments required for differentiation.

Similar to the variation that is present between male and female gametocyte transcriptomes and proteomes (125, 447-449), sex-specific differences in the histone PTM landscapes were identified here. This was particularly prominent for the H3K36me2&3 enrichment bias towards male gametocyte-specific genes. In higher eukaryotes H3K36me2&3 levels have been demonstrated to determine sex-specific transcription and drive male differentiation (430, 431). It is therefore tempting to speculate that by regulating sex-specific transcription, H3K36me2&3 dictate the bifurcation of male and female gametocyte development. However, it is equally plausible that the differential H3K36me2&3 enrichment patterns between male and female gametocytes arise after sex differentiation has been established with this an interesting point for future investigation. Notably, male-specific H3K36me2&3-enriched CDRs enriched show a marked increase in gene expression levels. This is the only set of genes that link H3K36me2&3 in the gametocyte stages with the transcriptional activation, the more common function associated with these histone PTMs that has been extensively described in model organisms (179, 403) and *P. falciparum* asexual parasites (206). Ultimately, these finding suggest that in *Plasmodium* gametocytes as in other eukaryotes (463-465), H3K36me2&3 are associated with both the activation and repression of sex-specific gene expression.

Taken together, the data presented here underscore the importance of histone methylation in repressing transcriptional activation of irrelevant genes, regulating chromatin structure and sex-specific transcription in *P. falciparum* gametocytes. Specifically, this chapter delineates the independent functions of H3K27me2&3 and H3K36me2&3 for the regulation these processes and thus for directing gametocyte development in a manner that is characteristic of eukaryotic cellular differentiation. Ultimately, this study presents the first description of the molecular

regulators that direct the transition from early gametocyte differentiation to intermediate development, thereby contributing to a better understanding of the biology of the transmissible stages of the human malaria parasite.

Chapter 5

Concluding discussion

Malaria parasites have existed alongside humans for hundreds of years with current evidence indicating that deaths from *P. falciparum* infections date as far back as 1324 BCE during the reign of the ancient Egyptian king, Tutankhamen (466). This affliction remains largely unchanged to this day with malaria responsible for 409 000 deaths in 2019 (1). Difficulties associated with preventing and treating malaria include poverty, the rapid development of anti-malarial drug resistance and an incomplete understanding of the complexities of the *Plasmodium* parasites that cause the disease (32, 467). For many years, research focused predominantly on understanding and identifying weak points in the asexual parasite life cycle that could be used for the treatment of malaria symptoms (32, 358). More recently however, the focus on global malaria eradication has invigorated and renewed interest in the asymptomatic yet transmissible stages of the malaria parasite life cycle, the gametocytes (3, 5, 345).

As a result, great strides have been made towards understanding the fundamental biology underlying *Plamsodium* gametocyte differentiation and development. For instance, the factors determining whether parasites continue to proliferate asexually or exit this cycle in favour of sexual commitment (84, 89, 90) and the mechanisms that drive these fates (52, 86, 92, 116, 117) have been relatively well studied. Furthermore, genome-wide transcriptional shifts have been associated with the morphological stage transitions during gametocyte development (94). These studies lay the groundwork for elucidating the mechanisms responsible for such transitions. Without a clear grasp of the overarching networks and factors that regulate the *Plasmodium* genome and transcriptome, our understanding of fundamental gametocyte biology is undoubtedly incomplete.

Prior to this study, few epigenetic mechanisms had been examined in the context of gametocyte development (89, 135, 347). However, the dynamic and extensive transcriptional reprogramming that occurs throughout gametocyte development alluded to the existence of

additional epigenetic regulatory mechanisms. Correspondingly, the histone PTM landscape has been described as plastic with each gametocyte stage characterised by a unique set of histone PTMs (133). Outside of H3K9me3 (135), neither the spatial distribution nor functional relevance of these histone PTMs for gene regulation had been explored.

This study sought to examine the spatial dynamics of H3K27me2&3 and H3K36me2&3, histone PTMs that are almost exclusively present in the stage II gametocytes (133). We hypothesised that their abundance in the stage II gametocytes points to similar functional relevance and importance for H3K27me2&3 and H3K36me2&3 during *P. falciparum* gametocytogenesis as in higher eukaryotic cellular differentiation (233, 293, 370, 376, 381, 468). The stage II gametocyte has been identified as a tightly regulated key transition point between early gametocyte differentiation to intermediate development (94) with the current study providing the first insights into the mechanisms responsible for this regulation.

In order to generate genome-wide maps of H3K27me2&3 and H3K36me2&3 and identify regions of genomic enrichment in the stage II gametocytes, chromatin-immunoprecipitation followed by high-throughput sequencing was applied. This methodology provides superior resolution, a wider range of detection and fewer artefacts compared to ChIP-ChIP, the predecessor technology to ChIP-seq that used microarrays rather than DNA sequencing to map DNA-bound proteins (297, 469). Additionally, the application of DNA library preparation and sequencing protocols that are optimised for the low-complexity genome of *P. falciparum* ensured the limitation of amplification biases and uneven genomic representation thereby providing sufficient sequencing coverage to correctly map reads to the genome (470, 471).

The successful use of this methodology was contingent upon obtaining gametocyte samples that span stage II development. This ensured the brief window of H3K27me2&3 and H3K36me2&3 abundance was captured while obtaining samples that were still sufficiently divergent to differentiate the stage II gametocyte-specific trends. Integrating this ChIP-seq data with gene expression profiles from the same parasite strain (94) allowed us to, for the very first time, elucidate the functional relevance of H3K27me2&3 and H3K36me2&3 for *P. falciparum* gametocyte development. Specifically, this approach provided nucleosome-level enrichment

data that were used to generate catalogues of the specific gene sets and biological pathways that are independently associated with each histone PTM. Such a detailed interrogation of gene-specific enrichment has distinct advantages over the genome-wide correlation-based method that have previously been used to assign functional relevance to H3K36me2 in asexual parasites (258). Unlike in the asexual parasites, H3K36me3-associated repression is not restricted to the clonally variant regulation of multi-gene families in gametocytes. Rather, we identify a novel association between H3K36me2&3 enrichment and the repression of a multitude of asexual and commitment specific genes and processes in stage II.

Crucially, our ChIP-seq analyses provide evidence for the existence of functional H3K27me2&3 in *Plasmodium* parasites which, until recently was debated (258, 367). These data reflect the previous detection of H3K27me2&3 almost exclusively in the *P. falciparum* stage II gametocytes by independent quantitative mass-spectrometry methods (133). Furthermore, this supports our hypothesis of a transcriptional regulatory role for H3K27me2&3 during the transition from early gametocyte differentiation to intermediate development in a manner that reflects the dynamics and functions of these histone PTMs in higher eukaryotes (229, 230, 236-238, 243).

We show H3K27me2&3 and H3K36me2&3 are non-redundant and predominantly function independently from one another and H3K9me3 in *Plasmodium* parasites further highlighting the conservation of typical eukaryotic functions. Typically, H3K27me2&3 function is isolation in other organisms with these histone PTMs predominantly functioning in the early stages of eukaryotic cellular differentiation (232, 240, 263, 265, 266). By contrast, H3K9me3 is associated with transcriptional silencing in the later stages of differentiation (262, 263, 266). Interestingly, we find that the demethylation of H3K27 and H3K36 in the post-stage II gametocytes does not lead to increased transcription, rather these genes remain repressed. Therefore, it is reasonable to postulate that other mechanisms, such as H3K9me3/HP1, that becomes increasingly more prevalent in the late gametocyte stages (135), are also involved in maintaining the repressive environment into subsequent development following its primary establishment by H3K27me2&3 and H3K36me2&3 in the stage II gametocytes.

Our particular interest in the independently H3K27me2&3 and H3K36me2&3 enriched genes revealed an intriguing bias towards the enrichment of sex-specific genes in the stage II gametocytes. Crucially, we identified a novel link between H3K36me2&3 and male gametocyte-specific gene expression that is congruent with the sex-specific transcriptional roles that have described for these histone PTMs in higher eukaryotes (429-431). As such, these data provide the first association between gametocyte sex-specific gene expression and histone PTMs in *P. falciparum.* Furthermore, our postulation that H3K27me2&3 and H3K36me2&3 play pivotal roles in shaping gametocyte sex-specific biology provides exciting avenues for further research.

The unusual biology of the malaria parasite brings about substantial challenges in applying and adapting techniques that have been developed in model organisms. Furthermore, even within the field of *Plasmodium* research, findings for one species or strain cannot necessarily be extrapolated to others. Therefore, while the implementation of existing technologies to address a biological question may be preferable, extensive resources need to be set aside to optimise these techniques within the organism of interest and laboratory where experiments will be performed. Unfortunately, the SET2 mutant parasite line generated previously (206) would not have been useful for this study due to its inability to produce gametocytes. Therefore, the use of chemical inhibitors was the most effective starting point to investigate histone modifying enzymes in *P. falciparum*. The potency and conserved modes-of-action that we identified for these inhibitors in *P. falciparum* gametocytes underscores the fundamental nature of epigenetics and more specifically histone PTMs across multiple kingdoms of life. Through a combination of global histone methylation and transcriptional profiling of epidrug perturbations, we were able provide an explanation for the the increased potency of ML324 and JIB-04 against early gametocytes (212, 472), in addition to providing further support for the functional relevance for histone PTMs in gametocyte development. By computationally demonstrating the ability of mammalian epidrugs to inhibit *Plasmodium* histone modifying enzymes, our application of molecular docking provided a description of potential novel H3K27-specific HDMs in *P. falciparum.* Together with the potency of epidrugs and effect on H3K27 methylation, this provides additional evidence to support a crucial role for H3K27me2&3 for gene regulation in *Plasmodium*. Furthermore, since SET3 does not have substantial homology with other eukaryotic

HMTs, the identification of this potential writer of H3K27me2&3 provides an exciting starting point for future investigation that could ultimately lead to the development of transmission-blocking inhibitors that specifically target *P. falciparum* H3K27 methylation. Finally, the use of mammalian epigenetic inhibitors demonstrates the potential of such molecules for use as tools to examine epigenetic regulation in all organisms. As such, we note that future investigations will benefit from combining epidrug transcriptional signatures, like those generated here, with genetic disruption studies to provide greater confidence in the results compared to either of these two methods alone.

In conclusion, this work demonstrates the functional relevance of H3K27me2&3 and H3K36me2&3 for transcriptional reprogramming during gametocyte development. In so doing, we provide the first insights into the regulatory mechanisms that contribute to the transcriptional shifts during the transition from early gametocyte differentiation to intermediate development. The findings in this study contribute extensively to a more thorough understanding of fundamental gametocyte biology which is undoubtedly an essential foundation required for the discovery and development of novel transmission blocking strategies for malaria. The epigenome has previously been suggested to be the Achilles' heel of the *Plasmodium* parasite with epigenetic factors proposed to be excellent targets (131, 324). In line with this, we show the importance of histone methylation and in particular, H3K27me2&3 for the development of gametocytes and identify a possible H3K27-specific writer that, due to low homology with human HDMs, may present such a target. Taken together, the data and findings presented in this thesis substantially advance the current understanding of the mechanisms that regulate gene expression in *P. falciparum* parasites and in particular, the epigenetic mechanisms that influence the development of the transmissible forms of the human malaria parasite.

References

1. World malaria report 2020: 20 years of global progress and challenges. Geneva: World Health Organization; 2020.
2. The Global Malaria Action Plan. Geneva: Roll Back Malaria Partnership; 2008.
3. Rabinovich RN, Drakeley C, Djimde AA, Hall BF, Hay SI, Hemingway J, et al. malERA: An updated research agenda for malaria elimination and eradication. PLoS Med. 2017;14(11):e1002456.
4. Malaria's Impact Worldwide Centers for Disease Control and Prevention; 2021 [updated 26 January 2021. Available from: https://www.cdc.gov/malaria/malaria_worldwide/impact.html#:~:text=Africa%20is%20the%20most%20affected,cause%20severe%20malaria%20and%20death.
5. Alonso PL, Brown G, Arevalo-Herrera M, Binka F, Chitnis C, Collins F, et al. A research agenda to underpin malaria eradication. PLoS Med. 2011;8(1):e1000406.
6. Radeva-Petrova D, Kayentao K, ter Kuile FO, Sinclair D, Garner P. Drugs for preventing malaria in pregnant women in endemic areas: any drug regimen versus placebo or no treatment. Cochrane Database Syst Rev. 2014(10):CD000169.
7. Desai M, Gutman J, L'Lanziva A, Otieno K, Juma E, Kariuki S, et al. Intermittent screening and treatment or intermittent preventive treatment with dihydroartemisinin-piperaquine versus intermittent preventive treatment with sulfadoxine-pyrimethamine for the control of malaria during pregnancy in western Kenya: an open-label, three-group, randomised controlled superiority trial. Lancet. 2015;386(10012):2507-19.
8. Beier JC, Keating J, Githure JI, Macdonald MB, Impoinvil DE, Novak RJ. Integrated vector management for malaria control. Malar J. 2008;7 Suppl 1:S4.
9. Challet GL. Elements of a vector control program. J Am Mosq Control Assoc. 1991;7(1):103-6.
10. Nevill CG, Some ES, Mung'ala VO, Mutemi W, New L, Marsh K, et al. Insecticide-treated bednets reduce mortality and severe morbidity from malaria among children on the Kenyan coast. Trop Med Int Health. 1996;1(2):139-46.
11. Pluess B, Tanser FC, Lengeler C, Sharp BL. Indoor residual spraying for preventing malaria. Cochrane Database Syst Rev. 2010(4):CD006657.
12. Brooke B, Koekemoer L, Kruger P, Urbach J, Misiani E, Coetzee M. Malaria vector control in South Africa. S Afr Med J. 2013;103(10 Pt 2):784-8.
13. The use of DDT in malaria vector control. Geneva: World Health Organization; 2011.
14. Malaria elimination strategic plan for South Africa 2019-2023. Pretoria: South African Department of Health; 2019.
15. MVIP update - 1 million doses administered, Kenya 1st anniversary, cooperation for vaccine access. World Health Organisation; 2020.
16. Wilby KJ, Lau TT, Gilchrist SE, Ensom MH. Mosquirix (RTS,S): a novel vaccine for the prevention of *Plasmodium falciparum* malaria. Ann Pharmacother. 2012;46(3):384-93.
17. Mahmoudi S, Keshavarz H. Efficacy of phase 3 trial of RTS, S/AS01 malaria vaccine: The need for an alternative development plan. Hum Vaccin Immunother. 2017;13(9):2098-101.
18. Datoo MS, Natama MH, Some A, Traore O, Rouamba T, Bellamy D, et al. Efficacy of a low-dose candidate malaria vaccine, R21 in adjuvant Matrix-M, with seasonal administration to children in Burkina Faso: a randomised controlled trial. Lancet. 2021;397(10287):1809-18.
19. Lowe D. A malaria vaccine candidate. A malaria vaccine candidate2021.
20. Gosling RD, Cairns ME, Chico RM, Chandramohan D. Intermittent preventive treatment against malaria: an update. Expert Rev Anti Infect Ther. 2010;8(5):589-606.
21. Walldorf JA, Cohee LM, Coalson JE, Bauleni A, Nkanaunena K, Kapito-Tembo A, et al. School-Age Children Are a Reservoir of Malaria Infection in Malawi. PLoS One. 2015;10(7):e0134061.

22. Nankabirwa J, Brooker SJ, Clarke SE, Fernando D, Gitonga CW, Schellenberg D, et al. Malaria in school-age children in Africa: an increasingly important challenge. Trop Med Int Health. 2014;19(11):1294-309.
23. Ashley EA, Pyae Phyo A, Woodrow CJ. Malaria. Lancet. 2018;391(10130):1608-21.
24. Landt SG, Marinov GK, Kundaje A, Kheradpour P, Pauli F, Batzoglou S, et al. ChIP-seq guidelines and practices of the ENCODE and modENCODE consortia. Genome Res. 2012;22(9):1813-31.
25. Raman J, Allen E, Workman L, Mabuza A, Swanepoel H, Malatje G, et al. Safety and tolerability of single low-dose primaquine in a low-intensity transmission area in South Africa: an open-label, randomized controlled trial. Malar J. 2019;18(1):209.
26. Pukrittayakamee S, Chotivanich K, Chantra A, Clemens R, Looareesuwan S, White NJ. Activities of artesunate and primaquine against asexual- and sexual-stage parasites in *falciparum* malaria. Antimicrob Agents Chemother. 2004;48(4):1329-34.
27. White NJ. Primaquine to prevent transmission of *falciparum* malaria. Lancet Infect Dis. 2013;13(2):175-81.
28. Rosenthal PJ. Antimalarial drug discovery: old and new approaches. J Exp Biol. 2003;206(Pt 21):3735-44.
29. Price RN, von Seidlein L, Valecha N, Nosten F, Baird JK, White NJ. Global extent of chloroquine-resistant *Plasmodium vivax*: a systematic review and meta-analysis. Lancet Infect Dis. 2014;14(10):982-91.
30. Haldar K, Bhattacharjee S, Safeukui I. Drug resistance in *Plasmodium*. Nat Rev Microbiol. 2018;16(3):156-70.
31. Bansal D, Acharya A, Bharti PK, Abdelraheem MH, Elmalik A, Abosalah S, et al. Distribution of Mutations Associated with Antifolate and Chloroquine Resistance among Imported *Plasmodium vivax* in the State of Qatar. Am J Trop Med Hyg. 2017;97(6):1797-803.
32. malERA: An updated research agenda for insecticide and drug resistance in malaria elimination and eradication. malERA; 2017.
33. Technical Report Series. Chemotherapy of Malaria. World Health Organisation; 1967.
34. Menard D, Dondorp A. Antimalarial Drug Resistance: A Threat to Malaria Elimination. Cold Spring Harb Perspect Med. 2017;7(7).
35. Lim P, Alker AP, Khim N, Shah NK, Incardona S, Doung S, et al. *Pfmdr1* copy number and arteminisin derivatives combination therapy failure in *falciparum* malaria in Cambodia. Malar J. 2009;8:11.
36. Sidhu AB, Uhlemann AC, Valderramos SG, Valderramos JC, Krishna S, Fidock DA. Decreasing *pfmdr1* copy number in *Plasmodium falciparum* malaria heightens susceptibility to mefloquine, lumefantrine, halofantrine, quinine, and artemisinin. J Infect Dis. 2006;194(4):528-35.
37. Price RN, Uhlemann AC, Brockman A, McGready R, Ashley E, Phaipun L, et al. Mefloquine resistance in *Plasmodium falciparum* and increased *pfmdr1* gene copy number. Lancet. 2004;364(9432):438-47.
38. Straimer J, Gnadig NF, Witkowski B, Amaratunga C, Duru V, Ramadani AP, et al. Drug resistance. K13-propeller mutations confer artemisinin resistance in *Plasmodium falciparum* clinical isolates. Science. 2015;347(6220):428-31.
39. Ariey F, Witkowski B, Amaratunga C, Beghain J, Langlois AC, Khim N, et al. A molecular marker of artemisinin-resistant *Plasmodium falciparum* malaria. Nature. 2014;505(7481):50-5.
40. Burrows JN, Duparc S, Gutteridge WE, Hooft van Huijsduijnen R, Kaszubska W, Macintyre F, et al. New developments in anti-malarial target candidate and product profiles. Malar J. 2017;16(1):26.
41. Birkholtz LM, Coetzer TL, Mancama D, Leroy D, Alano P. Discovering New Transmission-Blocking Antimalarial Compounds: Challenges and Opportunities. Trends Parasitol. 2016;32(9):669-81.

42. Sherman IW. Biochemistry of *Plasmodium* (malarial parasites). Microbiol Rev. 1979;43(4):453-95.
43. Bruce MC, Alano P, Duthie S, Carter R. Commitment of the malaria parasite *Plasmodium falciparum* to sexual and asexual development. Parasitology. 1990;100 Pt 2:191-200.
44. Sinden RE, Canning EU, Bray RS, Smalley ME. Gametocyte and gamete development in *Plasmodium falciparum*. Proc R Soc Lond B Biol Sci. 1978;201(1145):375-99.
45. Bancells C, Llora-Batlle O, Poran A, Notzel C, Rovira-Graells N, Elemento O, et al. Revisiting the initial steps of sexual development in the malaria parasite *Plasmodium falciparum*. Nat Microbiol. 2019;4(1):144-54.
46. Kappe SH, Buscaglia CA, Nussenzweig V. *Plasmodium* sporozoite molecular cell biology. Annu Rev Cell Dev Biol. 2004;20:29-59.
47. Dvorak JA, Miller LH, Whitehouse WC, Shiroishi T. Invasion of erythrocytes by malaria merozoites. Science. 1975;187(4178):748-50.
48. Field JA. The microscopic diagnosis of human malaria: A morphological study of erythrocytic parasites. Kuala Lampur: Govt. Press; 1956.
49. Dixon MW, Dearnley MK, Hanssen E, Gilberger T, Tilley L. Shape-shifting gametocytes: how and why does *P. falciparum* go banana-shaped? Trends Parasitol. 2012;28(11):471-8.
50. Meibalan E, Marti M. Biology of Malaria Transmission. Cold Spring Harb Perspect Med. 2017;7(3).
51. Josling GA, Llinas M. Sexual development in *Plasmodium* parasites: knowing when it's time to commit. Nat Rev Microbiol. 2015;13(9):573-87.
52. Josling GA, Russell TJ, Venezia J, Orchard L, van Biljon R, Painter HJ, et al. Dissecting the role of PfAP2-G in malaria gametocytogenesis. Nat Commun. 2020;11(1):1503.
53. Carter R, Graves PM. Gametocytes. In: H. WW, McGregor I, editors. Malaria: Principles and Practice of Malariology. London: Churchill Livingstone; 1988. p. 253-305.
54. Alano P. *Plasmodium falciparum* gametocytes: still many secrets of a hidden life. Mol Microbiol. 2007;66(2):291-302.
55. Joice R, Nilsson SK, Montgomery J, Dankwa S, Egan E, Morahan B, et al. *Plasmodium falciparum* transmission stages accumulate in the human bone marrow. Sci Transl Med. 2014;6(244):244re5.
56. Pelle KG, Oh K, Buchholz K, Narasimhan V, Joice R, Milner DA, et al. Transcriptional profiling defines dynamics of parasite tissue sequestration during malaria infection. Genome Med. 2015;7(1):19.
57. Farfour E, Charlotte F, Settegrana C, Miyara M, Buffet P. The extravascular compartment of the bone marrow: a niche for *Plasmodium falciparum* gametocyte maturation? Malar J. 2012;11:285.
58. Silvestrini F, Lasonder E, Olivieri A, Camarda G, van Schaijk B, Sanchez M, et al. Protein export marks the early phase of gametocytogenesis of the human malaria parasite *Plasmodium falciparum*. Mol Cell Proteomics. 2010;9(7):1437-48.
59. Tiburcio M, Silvestrini F, Bertuccini L, Sander AF, Turner L, Lavstsen T, et al. Early gametocytes of the malaria parasite *Plasmodium falciparum* specifically remodel the adhesive properties of infected erythrocyte surface. Cell Microbiol. 2013;15(4):647-59.
60. Aguilar R, Magallon-Tejada A, Achtman AH, Moraleda C, Joice R, Cistero P, et al. Molecular evidence for the localization of *Plasmodium falciparum* immature gametocytes in bone marrow. Blood. 2014;123(7):959-66.
61. McRobert L, Preiser P, Sharp S, Jarra W, Kaviratne M, Taylor MC, et al. Distinct trafficking and localization of STEVOR proteins in three stages of the *Plasmodium falciparum* life cycle. Infect Immun. 2004;72(11):6597-602.
62. Tiburcio M, Sauerwein R, Lavazec C, Alano P. Erythrocyte remodeling by *Plasmodium falciparum* gametocytes in the human host interplay. Trends Parasitol. 2015;31(6):270-8.

63. Sinden RE. Gametocytogenesis of Plasmodium falciparum in vitro: an electron microscopic study. Parasitology. 1982;84(1):1-11.
64. Hawking F, Wilson ME, Gammage K. Evidence for cyclic development and short-lived maturity in the gametocytes of *Plasmodium falciparum*. Trans R Soc Trop Med Hyg. 1971;65(5):549-59.
65. Billker O, Lindo V, Panico M, Etienne AE, Paxton T, Dell A, et al. Identification of xanthurenic acid as the putative inducer of malaria development in the mosquito. Nature. 1998;392(6673):289-92.
66. Billker O, Shaw MK, Margos G, Sinden RE. The roles of temperature, pH and mosquito factors as triggers of male and female gametogenesis of *Plasmodium berghei* in vitro. Parasitology. 1997;115 (Pt 1):1-7.
67. Billker O, Dechamps S, Tewari R, Wenig G, Franke-Fayard B, Brinkmann V. Calcium and a calcium-dependent protein kinase regulate gamete formation and mosquito transmission in a malaria parasite. Cell. 2004;117(4):503-14.
68. Ponzi M, Siden-Kiamos I, Bertuccini L, Curra C, Kroeze H, Camarda G, et al. Egress of *Plasmodium berghei* gametes from their host erythrocyte is mediated by the MDV-1/PEG3 protein. Cell Microbiol. 2009;11(8):1272-88.
69. Kuehn A, Pradel G. The coming-out of malaria gametocytes. J Biomed Biotechnol. 2010;2010:976827.
70. Mair GR, Braks JA, Garver LS, Wiegant JC, Hall N, Dirks RW, et al. Regulation of sexual development of *Plasmodium* by translational repression. Science. 2006;313(5787):667-9.
71. Mair GR, Braks JA, Garver LS, Dimopoulos G, Hall N, Wiegant JC, et al. Translational Repression is essential for *Plasmodium* sexual development and mediated by a DDX6-type RNA helicase. Science. 2006;42(1):84-94.
72. Guerreiro A, Deligianni E, Santos JM, Silva PA, Louis C, Pain A, et al. Genome-wide RIP-Chip analysis of translational repressor-bound mRNAs in the *Plasmodium* gametocyte. Genome Biol. 2014;15(11):493.
73. Waters AP. Epigenetic Roulette in Blood Stream *Plasmodium*: Gambling on Sex. PLoS Pathog. 2016;12(2):e1005353.
74. Sinden RE. *Plasmodium* differentiation in the mosquito. Parassitologia. 1999;41(1-3):139-48.
75. Alano P, Roca L, Smith D, Read D, Carter R, Day K. *Plasmodium falciparum:* parasites defective in early stages of gametocytogenesis. Exp Parasitol. 1995;81(2):227-35.
76. Eksi S, Morahan BJ, Haile Y, Furuya T, Jiang H, Ali O, et al. *Plasmodium falciparum* gametocyte development 1 (*Pfgdv1*) and gametocytogenesis early gene identification and commitment to sexual development. PLoS Pathog. 2012;8(10):e1002964.
77. Sinha A, Hughes KR, Modrzynska KK, Otto TD, Pfander C, Dickens NJ, et al. A cascade of DNA-binding proteins for sexual commitment and development in *Plasmodium*. Nature. 2014;507(7491):253-7.
78. Ngotho P, Soares AB, Hentzschel F, Achcar F, Bertuccini L, Marti M. Revisiting gametocyte biology in malaria parasites. FEMS Microbiol Rev. 2019;43(4):401-14.
79. Dyer M, Day K. Expression of *Plasmodium falciparum* trimeric G proteins and their involvement in switching to sexual development. Mol Biochem Parasitol. 2000;110(2):437-48.
80. Buckling A, Ranford-Cartwright LC, Miles A, Read AF. Chloroquine increases *Plasmodium falciparum* gametocytogenesis *in vitro*. Parasitology. 1999;118 (Pt 4):339-46.
81. Trager W, Gill GS. Enhanced gametocyte formation in young erythrocytes by *Plasmodium falciparum in vitro*. J Protozool. 1992;39(3):429-32.
82. Williams JL. Stimulation of *Plasmodium falciparum* gametocytogenesis by conditioned medium from parasite cultures. Am J Trop Med Hyg. 1999;60(1):7-13.
83. Peatey CL, Dixon MW, Gardiner DL, Trenholme KR. Temporal evaluation of commitment to sexual development in *Plasmodium falciparum*. Malar J. 2013;12:134.

84. Brancucci NMB, Gerdt JP, Wang C, De Niz M, Philip N, Adapa SR, et al. Lysophosphatidylcholine Regulates Sexual Stage Differentiation in the Human Malaria Parasite *Plasmodium falciparum*. Cell. 2017;171(7):1532-44 e15.
85. Pessi G, Kociubinski G, Mamoun CB. A pathway for phosphatidylcholine biosynthesis in *Plasmodium falciparum* involving phosphoethanolamine methylation. Proc Natl Acad Sci U S A. 2004;101(16):6206-11.
86. Kafsack BF, Rovira-Graells N, Clark TG, Bancells C, Crowley VM, Campino SG, et al. A transcriptional switch underlies commitment to sexual development in malaria parasites. Nature. 2014;507(7491):248-52.
87. Rono MK, Nyonda MA, Simam JJ, Ngoi JM, Mok S, Kortok MM, et al. Adaptation of *Plasmodium falciparum* to its transmission environment. Nat Ecol Evol. 2018;2(2):377-87.
88. Balaji S, Babu MM, Iyer LM, Aravind L. Discovery of the principal specific transcription factors of Apicomplexa and their implication for the evolution of the AP2-integrase DNA binding domains. Nucleic Acids Res. 2005;33(13):3994-4006.
89. Brancucci NMB, Bertschi NL, Zhu L, Niederwieser I, Chin WH, Wampfler R, et al. Heterochromatin protein 1 secures survival and transmission of malaria parasites. Cell Host Microbe. 2014;16(2):165-76.
90. Filarsky M, Fraschka SA, Niederwieser I, Brancucci NMB, Carrington E, Carrio E, et al. GDV1 induces sexual commitment of malaria parasites by antagonizing HP1-dependent gene silencing. Science. 2018;359(6381):1259-63.
91. Poran A, Notzel C, Aly O, Mencia-Trinchant N, Harris CT, Guzman ML, et al. Single-cell RNA sequencing reveals a signature of sexual commitment in malaria parasites. Nature. 2017;551(7678):95-9.
92. Singh S, Santos JM, Orchard LM, Yamada N, van Biljon R, Painter HJ, et al. The PfAP2-G2 transcription factor is a critical regulator of gametocyte maturation. Mol Microbiol. 2020;00:1-20.
93. Bozdech Z, Llinas M, Pulliam BL, Wong ED, Zhu J, DeRisi JL. The transcriptome of the intraerythrocytic developmental cycle of *Plasmodium falciparum*. PLoS Biol. 2003;1(1):E5.
94. van Biljon R, van Wyk R, Painter HJ, Orchard L, Reader J, Niemand J, et al. Hierarchical transcriptional control regulates *Plasmodium falciparum* sexual differentiation. BMC Genomics. 2019;20(1):920.
95. Young JA, Fivelman QL, Blair PL, de la Vega P, Le Roch KG, Zhou Y, et al. The *Plasmodium falciparum* sexual development transcriptome: a microarray analysis using ontology-based pattern identification. Mol Biochem Parasitol. 2005;143(1):67-79.
96. Hamilton WL, Claessens A, Otto TD, Kekre M, Fairhurst RM, Rayner JC, et al. Extreme mutation bias and high AT content in *Plasmodium falciparum*. Nucleic Acids Res. 2017;45(4):1889-901.
97. Gardner MJ, Hall N, Fung E, White O, Berriman M, Hyman RW, et al. Genome sequence of the human malaria parasite *Plasmodium falciparum*. Nature. 2002;419(6906):498-511.
98. Ararat-Sarria M, Patarroyo MA, Curtidor H. Parasite-Related Genetic and Epigenetic Aspects and Host Factors Influencing Plasmodium falciparum Invasion of Erythrocytes. Front Cell Infect Microbiol. 2018;8:454.
99. Lovett ST. Encoded errors: mutations and rearrangements mediated by misalignment at repetitive DNA sequences. Mol Microbiol. 2004;52(5):1243-53.
100. Foth BJ, Zhang N, Chaal BK, Sze SK, Preiser PR, Bozdech Z. Quantitative time-course profiling of parasite and host cell proteins in the human malaria parasite *Plasmodium falciparum*. Mol Cell Proteomics. 2011;10(8):M110 006411.
101. Latchman DS. Transcription by RNA poylmerases. In: Owen E, editor. Gene Control. New York: Garland Science; 2010. p. 98-9.

102. Callebaut I, Prat K, Meurice E, Mornon JP, Tomavo S. Prediction of the general transcription factors associated with RNA polymerase II in *Plasmodium falciparum*: conserved features and differences relative to other eukaryotes. BMC Genomics. 2005;6:100.
103. Carninci P, Sandelin A, Lenhard B, Katayama S, Shimokawa K, Ponjavic J, et al. Genome-wide analysis of mammalian promoter architecture and evolution. Nat Genet. 2006;38(6):626-35.
104. Horrocks P, Wong E, Russell K, Emes RD. Control of gene expression in *Plasmodium falciparum* - ten years on. Mol Biochem Parasitol. 2009;164(1):9-25.
105. Adjalley SH, Chabbert CD, Klaus B, Pelechano V, Steinmetz LM. Landscape and Dynamics of Transcription Initiation in the Malaria Parasite *Plasmodium falciparum*. Cell Rep. 2016;14(10):2463-75.
106. Painter HJ, Carrasquilla M, Llinas M. Capturing *in vivo* RNA transcriptional dynamics from the malaria parasite *Plasmodium falciparum*. Genome Res. 2017;27(6):1074-86.
107. Russell K, Emes R, Horrocks P. Triaging informative cis-regulatory elements for the combinatorial control of temporal gene expression during *Plasmodium falciparum* intraerythrocytic development. Parasit Vectors. 2015;8:81.
108. Young JA, Johnson JR, Benner C, Yan SF, Chen K, Le Roch KG, et al. *In silico* discovery of transcription regulatory elements in *Plasmodium falciparum*. BMC Genomics. 2008;9:70.
109. Aravind L, Iyer LM, Wellems TE, Miller LH. *Plasmodium* biology: genomic gleanings. Cell. 2003;115(7):771-85.
110. Komaki-Yasuda K, Okuwaki M, Nagata K, Kawazu S, Kano S. Identification of a novel and unique transcription factor in the intraerythrocytic stage of *Plasmodium falciparum*. PLoS One. 2013;8(9):e74701.
111. Gissot M, Ting LM, Daly TM, Bergman LW, Sinnis P, Kim K. High mobility group protein HMGB2 is a critical regulator of *Plasmodium* oocyst development. J Biol Chem. 2008;283(25):17030-8.
112. Coulson RM, Hall N, Ouzounis CA. Comparative genomics of transcriptional control in the human malaria parasite *Plasmodium falciparum*. Genome Res. 2004;14(8):1548-54.
113. Templeton TJ, Iyer LM, Anantharaman V, Enomoto S, Abrahante JE, Subramanian GM, et al. Comparative analysis of apicomplexa and genomic diversity in eukaryotes. Genome Res. 2004;14(9):1686-95.
114. Gissot M, Briquet S, Refour P, Boschet C, Vaquero C. PfMyb1, a *Plasmodium falciparum* transcription factor, is required for intra-erythrocytic growth and controls key genes for cell cycle regulation. J Mol Biol. 2005;346(1):29-42.
115. Boschet C, Gissot M, Briquet S, Hamid Z, Claudel-Renard C, Vaquero C. Characterization of PfMyb1 transcription factor during erythrocytic development of 3D7 and F12 *Plasmodium falciparum* clones. Mol Biochem Parasitol. 2004;138(1):159-63.
116. Campbell TL, De Silva EK, Olszewski KL, Elemento O, Llinas M. Identification and genome-wide prediction of DNA binding specificities for the ApiAP2 family of regulators from the malaria parasite. PLoS Pathog. 2010;6(10):e1001165.
117. Llora-Batlle O, Michel-Todo L, Witmer K, Toda H, Fernandez-Becerra C, Baum J, et al. Conditional expression of PfAP2-G for controlled massive sexual conversion in *Plasmodium falciparum*. Sci Adv. 2020;6(24):eaaz5057.
118. Modrzynska K, Pfander C, Chappell L, Yu L, Suarez C, Dundas K, et al. A Knockout Screen of ApiAP2 Genes Reveals Networks of Interacting Transcriptional Regulators Controlling the *Plasmodium* Life Cycle. Cell Host Microbe. 2017;21(1):11-22.
119. Santos JM, Josling G, Ross P, Joshi P, Orchard L, Campbell T, et al. Red Blood Cell Invasion by the Malaria Parasite Is Coordinated by the PfAP2-I Transcription Factor. Cell Host Microbe. 2017;21(6):731-41 e10.
120. Yamasaki K, Kigawa T, Seki M, Shinozaki K, Yokoyama S. DNA-binding domains of plant-specific transcription factors: structure, function, and evolution. Trends Plant Sci. 2013;18(5):267-76.

121. Hollin T, Le Roch KG. From Genes to Transcripts, a Tightly Regulated Journey in *Plasmodium*. Front Cell Infect Microbiol. 2020;10:618454.
122. Le Roch KG, Johnson JR, Florens L, Zhou Y, Santrosyan A, Grainger M, et al. Global analysis of transcript and protein levels across the *Plasmodium falciparum* life cycle. Genome Res. 2004;14(11):2308-18.
123. Bunnik EM, Batugedara G, Saraf A, Prudhomme J, Florens L, Le Roch KG. The mRNA-bound proteome of the human malaria parasite *Plasmodium falciparum*. Genome Biol. 2016;17(1):147.
124. Reddy BP, Shrestha S, Hart KJ, Liang X, Kemirembe K, Cui L, et al. A bioinformatic survey of RNA-binding proteins in *Plasmodium*. BMC Genomics. 2015;16:890.
125. Lasonder E, Rijpma SR, van Schaijk BC, Hoeijmakers WA, Kensche PR, Gresnigt MS, et al. Integrated transcriptomic and proteomic analyses of *P. falciparum* gametocytes: molecular insight into sex-specific processes and translational repression. Nucleic Acids Res. 2016;44(13):6087-101.
126. Miao J, Fan Q, Parker D, Li X, Li J, Cui L. Puf mediates translation repression of transmission-blocking vaccine candidates in malaria parasites. PLoS Pathog. 2013;9(4):e1003268.
127. Miao J, Li J, Fan Q, Li X, Li X, Cui L. The Puf-family RNA-binding protein PfPuf2 regulates sexual development and sex differentiation in the malaria parasite *Plasmodium falciparum*. J Cell Sci. 2010;123(Pt 7):1039-49.
128. Marchese FP, Raimondi I, Huarte M. The multidimensional mechanisms of long noncoding RNA function. Genome Biol. 2017;18(1):206.
129. Sierra-Miranda M, Delgadillo DM, Mancio-Silva L, Vargas M, Villegas-Sepulveda N, Martinez-Calvillo S, et al. Two long non-coding RNAs generated from subtelomeric regions accumulate in a novel perinuclear compartment in *Plasmodium falciparum*. Mol Biochem Parasitol. 2012;185(1):36-47.
130. Broadbent KM, Park D, Wolf AR, Van Tyne D, Sims JS, Ribacke U, et al. A global transcriptional analysis of *Plasmodium falciparum* malaria reveals a novel family of telomere-associated lncRNAs. Genome Biol. 2011;12(6):R56.
131. Hoeijmakers WA, Stunnenberg HG, Bartfai R. Placing the *Plasmodium falciparum* epigenome on the map. Trends Parasitol. 2012;28(11):486-95.
132. Bunnik EM, Cook KB, Varoquaux N, Batugedara G, Prudhomme J, Cort A, et al. Changes in genome organization of parasite-specific gene families during the *Plasmodium* transmission stages. Nat Commun. 2018;9(1):1910.
133. Coetzee N, Sidoli S, van Biljon R, Painter H, Llinas M, Garcia BA, et al. Quantitative chromatin proteomics reveals a dynamic histone post-translational modification landscape that defines asexual and sexual *Plasmodium falciparum* parasites. Sci Rep. 2017;7(1):607.
134. Coleman BI, Skillman KM, Jiang RHY, Childs LM, Altenhofen LM, Ganter M, et al. A *Plasmodium falciparum* histone deacetylase regulates antigenic variation and gametocyte conversion. Cell Host Microbe. 2014;16(2):177-86.
135. Fraschka SA, Filarsky M, Hoo R, Niederwieser I, Yam XY, Brancucci NMB, et al. Comparative Heterochromatin Profiling Reveals Conserved and Unique Epigenome Signatures Linked to Adaptation and Development of Malaria Parasites. Cell Host Microbe. 2018;23(3):407-20 e8.
136. Waddington CH. The epigenotype. 1942. Int J Epidemiol. 2012;41(1):10-3.
137. Park M, Keung AJ, Khalil AS. The epigenome: the next substrate for engineering. Genome Biol. 2016;17(1):183.
138. Smith DW, Garland AM, Herman G, Enns RE, Baker TA, Zyskind JW. Importance of state of methylation of oriC GATC sites in initiation of DNA replication in *Escherichia coli*. EMBO J. 1985;4(5):1319-26.
139. Bogan JA, Helmstetter CE. DNA sequestration and transcription in the oriC region of *Escherichia coli*. Mol Microbiol. 1997;26(5):889-96.

140. Au KG, Welsh K, Modrich P. Initiation of methyl-directed mismatch repair. J Biol Chem. 1992;267(17):12142-8.
141. Willbanks A, Leary M, Greenshields M, Tyminski C, Heerboth S, Lapinska K, et al. The Evolution of Epigenetics: From Prokaryotes to Humans and Its Biological Consequences. Genet Epigenet. 2016;8:25-36.
142. Moore LD, Le T, Fan G. DNA methylation and its basic function. Neuropsychopharmacology. 2013;38(1):23-38.
143. Latchman DS. Role of chromatin structure in gene control. In: Owen E, editor. Gene Control. New York: Garland Science; 2010. p. 66-73.
144. Kouzarides T. Chromatin modifications and their function. Cell. 2007;128(4):693-705.
145. Latchman DS. Structure of Chromatin. In: Owen E, editor. Gene Control. New Work: Garland Science; 2010. p. 29-54.
146. Hergeth SP, Schneider R. The H1 linker histones: multifunctional proteins beyond the nucleosomal core particle. EMBO Rep. 2015;16(11):1439-53.
147. Bhattacharjee RN, Banks GC, Trotter KW, Lee HL, Archer TK. Histone H1 phosphorylation by Cdk2 selectively modulates mouse mammary tumor virus transcription through chromatin remodeling. Mol Cell Biol. 2001;21(16):5417-25.
148. Belikov S, Astrand C, Wrange O. Mechanism of histone H1-stimulated glucocorticoid receptor DNA binding *in vivo*. Mol Cell Biol. 2007;27(6):2398-410.
149. Radman-Livaja M, Rando OJ. Nucleosome positioning: how is it established, and why does it matter? Dev Biol. 2010;339(2):258-66.
150. Jiang C, Pugh BF. Nucleosome positioning and gene regulation: advances through genomics. Nat Rev Genet. 2009;10(3):161-72.
151. Miao J, Fan Q, Cui L, Li J, Li J, Cui L. The malaria parasite *Plasmodium falciparum* histones: organization, expression, and acetylation. Gene. 2006;369:53-65.
152. Bannister AJ, Kouzarides T. Regulation of chromatin by histone modifications. Cell Res. 2011;21(3):381-95.
153. Tan M, Luo H, Lee S, Jin F, Yang JS, Montellier E, et al. Identification of 67 histone marks and histone lysine crotonylation as a new type of histone modification. Cell. 2011;146(6):1016-28.
154. Kuo AJ, Song J, Cheung P, Ishibe-Murakami S, Yamazoe S, Chen JK, et al. The BAH domain of ORC1 links H4K20me2 to DNA replication licensing and Meier-Gorlin syndrome. Nature. 2012;484(7392):115-9.
155. Schotta G, Sengupta R, Kubicek S, Malin S, Kauer M, Callen E, et al. A chromatin-wide transition to H4K20 monomethylation impairs genome integrity and programmed DNA rearrangements in the mouse. Genes Dev. 2008;22(15):2048-61.
156. Xhemalce B. DMA, Bannister A.J. . Histone modifications. In: R. M, editor. Encyclopedia of Molecular Cell Biology and Molecular Medicine: John Wiley and Sons; 2011.
157. Wang Z, Zang C, Rosenfeld JA, Schones DE, Barski A, Cuddapah S, et al. Combinatorial patterns of histone acetylations and methylations in the human genome. Nat Genet. 2008;40(7):897-903.
158. Oki M, Aihara H, Ito T. Role of histone phosphorylation in chromatin dynamics and its implications in diseases. Subcell Biochem. 2007;41:319-36.
159. Hu S, Xie Z, Onishi A, Yu X, Jiang L, Lin J, et al. Profiling the human protein-DNA interactome reveals ERK2 as a transcriptional repressor of interferon signaling. Cell. 2009;139(3):610-22.
160. Kim J, Guermah M, McGinty RK, Lee JS, Tang Z, Milne TA, et al. RAD6-Mediated transcription-coupled H2B ubiquitylation directly stimulates H3K4 methylation in human cells. Cell. 2009;137(3):459-71.

161. Lee JS, Shukla A, Schneider J, Swanson SK, Washburn MP, Florens L, et al. Histone crosstalk between H2B monoubiquitination and H3 methylation mediated by COMPASS. Cell. 2007;131(6):1084-96.
162. Wang H, Wang L, Erdjument-Bromage H, Vidal M, Tempst P, Jones RS, et al. Role of histone H2A ubiquitination in Polycomb silencing. Nature. 2004;431(7010):873-8.
163. Seeler JS, Dejean A. Nuclear and unclear functions of SUMO. Nat Rev Mol Cell Biol. 2003;4(9):690-9.
164. Nathan D, Ingvarsdottir K, Sterner DE, Bylebyl GR, Dokmanovic M, Dorsey JA, et al. Histone sumoylation is a negative regulator in Saccharomyces cerevisiae and shows dynamic interplay with positive-acting histone modifications. Genes Dev. 2006;20(8):966-76.
165. Shiio Y, Eisenman RN. Histone sumoylation is associated with transcriptional repression. Proc Natl Acad Sci U S A. 2003;100(23):13225-30.
166. Bell O, Wirbelauer C, Hild M, Scharf AN, Schwaiger M, MacAlpine DM, et al. Localized H3K36 methylation states define histone H4K16 acetylation during transcriptional elongation in *Drosophila*. EMBO J. 2007;26(24):4974-84.
167. Carrozza MJ, Li B, Florens L, Suganuma T, Swanson SK, Lee KK, et al. Histone H3 methylation by Set2 directs deacetylation of coding regions by Rpd3S to suppress spurious intragenic transcription. Cell. 2005;123(4):581-92.
168. Hahn MA, Wu X, Li AX, Hahn T, Pfeifer GP. Relationship between gene body DNA methylation and intragenic H3K9me3 and H3K36me3 chromatin marks. PLoS One. 2011;6(4):e18844.
169. Calo E, Wysocka J. Modification of enhancer chromatin: what, how, and why? Mol Cell. 2013;49(5):825-37.
170. Nady N, Lemak A, Walker JR, Avvakumov GV, Kareta MS, Achour M, et al. Recognition of multivalent histone states associated with heterochromatin by UHRF1 protein. J Biol Chem. 2011;286(27):24300-11.
171. Ooi SK, Qiu C, Bernstein E, Li K, Jia D, Yang Z, et al. DNMT3L connects unmethylated lysine 4 of histone H3 to *de novo* methylation of DNA. Nature. 2007;448(7154):714-7.
172. Taverna SD, Li H, Ruthenburg AJ, Allis CD, Patel DJ. How chromatin-binding modules interpret histone modifications: lessons from professional pocket pickers. Nat Struct Mol Biol. 2007;14(11):1025-40.
173. Hu Y, Lu Y, Zhao Y, Zhou DX. Histone Acetylation Dynamics Integrates Metabolic Activity to Regulate Plant Response to Stress. Front Plant Sci. 2019;10:1236.
174. Graff J, Tsai LH. Histone acetylation: molecular mnemonics on the chromatin. Nat Rev Neurosci. 2013;14(2):97-111.
175. Teperino R, Schoonjans K, Auwerx J. Histone methyl transferases and demethylases; can they link metabolism and transcription? Cell Metab. 2010;12(4):321-7.
176. Tong X, Zhao F, Thompson CB. The molecular determinants of *de novo* nucleotide biosynthesis in cancer cells. Curr Opin Genet Dev. 2009;19(1):32-7.
177. Bailey LB, Gregory JF, 3rd. Polymorphisms of methylenetetrahydrofolate reductase and other enzymes: metabolic significance, risks and impact on folate requirement. J Nutr. 1999;129(5):919-22.
178. Martin C, Zhang Y. The diverse functions of histone lysine methylation. Nat Rev Mol Cell Biol. 2005;6(11):838-49.
179. Strahl BD, Allis CD. The language of covalent histone modifications. Nature. 2000;403(6765):41-5.
180. Fischle W, Tseng BS, Dormann HL, Ueberheide BM, Garcia BA, Shabanowitz J, et al. Regulation of HP1-chromatin binding by histone H3 methylation and phosphorylation. Nature. 2005;438(7071):1116-22.

181. Ernst J, Kellis M. Discovery and characterization of chromatin states for systematic annotation of the human genome. Nat Biotechnol. 2010;28(8):817-25.
182. Abel S, Le Roch KG. The role of epigenetics and chromatin structure in transcriptional regulation in malaria parasites. Brief Funct Genomics. 2019;18(5):302-13.
183. Cortes A, Deitsch KW. Malaria Epigenetics. Cold Spring Harb Perspect Med. 2017;7(7).
184. Trelle MB, Salcedo-Amaya AM, Cohen AM, Stunnenberg HG, Jensen ON. Global histone analysis by mass spectrometry reveals a high content of acetylated lysine residues in the malaria parasite *Plasmodium falciparum*. J Proteome Res. 2009;8(7):3439-50.
185. Felsenfeld G, Groudine M. Controlling the double helix. Nature. 2003;421(6921):448-53.
186. Fang HT, El Farran CA, Xing QR, Zhang LF, Li H, Lim B, et al. Global H3.3 dynamic deposition defines its bimodal role in cell fate transition. Nat Commun. 2018;9(1):1537.
187. Petter M, Lee CC, Byrne TJ, Boysen KE, Volz J, Ralph SA, et al. Expression of *P. falciparum var* genes involves exchange of the histone variant H2A.Z at the promoter. PLoS Pathog. 2011;7(2):e1001292.
188. Bartfai R, Hoeijmakers WA, Salcedo-Amaya AM, Smits AH, Janssen-Megens E, Kaan A, et al. H2A.Z demarcates intergenic regions of the *Plasmodium falciparum* epigenome that are dynamically marked by H3K9ac and H3K4me3. PLoS Pathog. 2010;6(12):e1001223.
189. Dalmasso MC, Sullivan WJ, Jr., Angel SO. Canonical and variant histones of protozoan parasites. Front Biosci (Landmark Ed). 2011;16:2086-105.
190. Talbert PB, Ahmad K, Almouzni G, Ausio J, Berger F, Bhalla PL, et al. A unified phylogeny-based nomenclature for histone variants. Epigenetics Chromatin. 2012;5:7.
191. Petter M, Selvarajah SA, Lee CC, Chin WH, Gupta AP, Bozdech Z, et al. H2A.Z and H2B.Z double-variant nucleosomes define intergenic regions and dynamically occupy var gene promoters in the malaria parasite *Plasmodium falciparum*. Mol Microbiol. 2013;87(6):1167-82.
192. Gill J, Kumar A, Yogavel M, Belrhali H, Jain SK, Rug M, et al. Structure, localization and histone binding properties of nuclear-associated nucleosome assembly protein from *Plasmodium falciparum*. Malar J. 2010;9:90.
193. Sullivan WJ, Jr., Naguleswaran A, Angel SO. Histones and histone modifications in protozoan parasites. Cell Microbiol. 2006;8(12):1850-61.
194. Gerald N, Mahajan B, Kumar S. Mitosis in the human malaria parasite *Plasmodium falciparum*. Eukaryot Cell. 2011;10(4):474-82.
195. Bunnik EM, Polishko A, Prudhomme J, Ponts N, Gill SS, Lonardi S, et al. DNA-encoded nucleosome occupancy is associated with transcription levels in the human malaria parasite *Plasmodium falciparum*. BMC Genomics. 2014;15:347.
196. Ponts N, Harris EY, Lonardi S, Le Roch KG. Nucleosome occupancy at transcription start sites in the human malaria parasite: a hard-wired evolution of virulence? Infect Genet Evol. 2011;11(4):716-24.
197. Kensche PR, Hoeijmakers WA, Toenhake CG, Bras M, Chappell L, Berriman M, et al. The nucleosome landscape of Plasmodium falciparum reveals chromatin architecture and dynamics of regulatory sequences. Nucleic Acids Res. 2016;44(5):2110-24.
198. Ruiz JL, Tena JJ, Bancells C, Cortes A, Gomez-Skarmeta JL, Gomez-Diaz E. Characterization of the accessible genome in the human malaria parasite Plasmodium falciparum. Nucleic Acids Res. 2018;46(18):9414-31.
199. Read DF, Cook K, Lu YY, Le Roch KG, Noble WS. Predicting gene expression in the human malaria parasite Plasmodium falciparum using histone modification, nucleosome positioning, and 3D localization features. PLoS Comput Biol. 2019;15(9):e1007329.
200. Cui L, Fan Q, Cui L, Miao J. Histone lysine methyltransferases and demethylases in *Plasmodium falciparum*. Int J Parasitol. 2008;38(10):1083-97.

201. Annunziato AT. Assembling chromatin: the long and winding road. Biochim Biophys Acta. 2013;1819(3-4):196-210.
202. Nagarajan P, Ge Z, Sirbu B, Doughty C, Agudelo Garcia PA, Schlederer M, et al. Histone acetyl transferase 1 is essential for mammalian development, genome stability, and the processing of newly synthesized histones H3 and H4. PLoS Genet. 2013;9(6):e1003518.
203. Cui L, Miao J, Furuya T, Li X, Su XZ, Cui L. PfGCN5-mediated histone H3 acetylation plays a key role in gene expression in *Plasmodium falciparum*. Eukaryot Cell. 2007;6(7):1219-27.
204. Miao J, Fan Q, Cui L, Li X, Wang H, Ning G, et al. The MYST family histone acetyltransferase regulates gene expression and cell cycle in malaria parasite *Plasmodium falciparum*. Mol Microbiol. 2010;78(4):883-902.
205. Jiang L, Mu J, Zhang Q, Ni T, Srinivasan P, Rayavara K, et al. PfSETvs methylation of histone H3K36 represses virulence genes in *Plasmodium falciparum*. Nature. 2013;499(7457):223-7.
206. Ukaegbu UE, Kishore SP, Kwiatkowski DL, Pandarinath C, Dahan-Pasternak N, Dzikowski R, et al. Recruitment of PfSET2 by RNA polymerase II to variant antigen encoding loci contributes to antigenic variation in *P. falciparum*. PLoS Pathog. 2014;10(1):e1003854.
207. Kishore SP, Stiller JW, Deitsch KW. Horizontal gene transfer of epigenetic machinery and evolution of parasitism in the malaria parasite *Plasmodium falciparum* and other apicomplexans. BMC Evol Biol. 2013;13:37.
208. Volz J, Carvalho TG, Ralph SA, Gilson P, Thompson J, Tonkin CJ, et al. Potential epigenetic regulatory proteins localise to distinct nuclear sub-compartments in *Plasmodium falciparum*. Int J Parasitol. 2010;40(1):109-21.
209. Lopez-Rubio JJ, Mancio-Silva L, Scherf A. Genome-wide analysis of heterochromatin associates clonally variant gene regulation with perinuclear repressive centers in malaria parasites. Cell Host Microbe. 2009;5(2):179-90.
210. Chen PB, Ding S, Zanghi G, Soulard V, DiMaggio PA, Fuchter MJ, et al. *Plasmodium falciparum* PfSET7: enzymatic characterization and cellular localization of a novel protein methyltransferase in sporozoite, liver and erythrocytic stage parasites. Sci Rep. 2016;6:21802.
211. Volz JC, Bartfai R, Petter M, Langer C, Josling GA, Tsuboi T, et al. PfSET10, a *Plasmodium falciparum* methyltransferase, maintains the active var gene in a poised state during parasite division. Cell Host Microbe. 2012;11(1):7-18.
212. Matthews KA, Senagbe KM, Notzel C, Gonzales CA, Tong X, Rijo-Ferreira F, et al. Disruption of the *Plasmodium falciparum* Life Cycle through Transcriptional Reprogramming by Inhibitors of Jumonji Demethylases. ACS Infect Dis. 2020;6(5):1058-75.
213. Hoeijmakers WAM, Miao J, Schmidt S, Toenhake CG, Shrestha S, Venhuizen J, et al. Epigenetic reader complexes of the human malaria parasite, *Plasmodium falciparum*. Nucleic Acids Res. 2019;47(22):11574-88.
214. Josling GA, Petter M, Oehring SC, Gupta AP, Dietz O, Wilson DW, et al. A Plasmodium Falciparum Bromodomain Protein Regulates Invasion Gene Expression. Cell Host Microbe. 2015;17(6):741-51.
215. Toenhake CG, Fraschka SA, Vijayabaskar MS, Westhead DR, van Heeringen SJ, Bartfai R. Chromatin Accessibility-Based Characterization of the Gene Regulatory Network Underlying *Plasmodium falciparum* Blood-Stage Development. Cell Host Microbe. 2018;23(4):557-69 e9.
216. Dastidar EG, Dzeyk K, Krijgsveld J, Malmquist NA, Doerig C, Scherf A, et al. Comprehensive histone phosphorylation analysis and identification of Pf14-3-3 protein as a histone H3 phosphorylation reader in malaria parasites. PLoS One. 2013;8(1):e53179.
217. Vermeulen M, Eberl HC, Matarese F, Marks H, Denissov S, Butter F, et al. Quantitative interaction proteomics and genome-wide profiling of epigenetic histone marks and their readers. Cell. 2010;142(6):967-80.

218. Salcedo-Amaya AM, van Driel MA, Alako BT, Trelle MB, van den Elzen AM, Cohen AM, et al. Dynamic histone H3 epigenome marking during the intraerythrocytic cycle of *Plasmodium falciparum*. Proc Natl Acad Sci U S A. 2009;106(24):9655-60.
219. Saraf A, Cervantes S, Bunnik EM, Ponts N, Sardiu ME, Chung DW, et al. Dynamic and Combinatorial Landscape of Histone Modifications during the Intraerythrocytic Developmental Cycle of the Malaria Parasite. J Proteome Res. 2016;15(8):2787-801.
220. Gupta AP, Zhu L, Tripathi J, Kucharski M, Patra A, Bozdech Z. Histone 4 lysine 8 acetylation regulates proliferation and host-pathogen interaction in *Plasmodium falciparum*. Epigenetics Chromatin. 2017;10(1):40.
221. Issar N, Ralph SA, Mancio-Silva L, Keeling C, Scherf A. Differential sub-nuclear localisation of repressive and activating histone methyl modifications in *P. falciparum*. Microbes Infect. 2009;11(3):403-7.
222. Issar N, Roux E, Mattei D, Scherf A. Identification of a novel post-translational modification in *Plasmodium falciparum*: protein sumoylation in different cellular compartments. Cell Microbiol. 2008;10(10):1999-2011.
223. Lopez-Rubio JJ, Siegel TN, Scherf A. Genome-wide chromatin immunoprecipitation-sequencing in *Plasmodium*. Methods Mol Biol. 2013;923:321-33.
224. Treeck M, Sanders JL, Elias JE, Boothroyd JC. The phosphoproteomes of *Plasmodium falciparum* and *Toxoplasma gondii* reveal unusual adaptations within and beyond the parasites' boundaries. Cell Host Microbe. 2011;10(4):410-9.
225. Cobbold SA, Santos JM, Ochoa A, Perlman DH, Llinas M. Proteome-wide analysis reveals widespread lysine acetylation of major protein complexes in the malaria parasite. Sci Rep. 2016;6:19722.
226. Gupta AP, Chin WH, Zhu L, Mok S, Luah YH, Lim EH, et al. Dynamic epigenetic regulation of gene expression during the life cycle of malaria parasite *Plasmodium falciparum*. PLoS Pathog. 2013;9(2):e1003170.
227. Flueck C, Bartfai R, Volz J, Niederwieser I, Salcedo-Amaya AM, Alako BT, et al. *Plasmodium falciparum* heterochromatin protein 1 marks genomic loci linked to phenotypic variation of exported virulence factors. PLoS Pathog. 2009;5(9):e1000569.
228. Zanghi G, Vembar SS, Baumgarten S, Ding S, Guizetti J, Bryant JM, et al. A Specific PfEMP1 Is Expressed in P. falciparum Sporozoites and Plays a Role in Hepatocyte Infection. Cell Rep. 2018;22(11):2951-63.
229. Agger K, Cloos PA, Christensen J, Pasini D, Rose S, Rappsilber J, et al. UTX and JMJD3 are histone H3K27 demethylases involved in HOX gene regulation and development. Nature. 2007;449(7163):731-4.
230. He C, Chen X, Huang H, Xu L. Reprogramming of H3K27me3 is critical for acquisition of pluripotency from cultured *Arabidopsis* tissues. PLoS Genet. 2012;8(8):e1002911.
231. Juan AH, Wang S, Ko KD, Zare H, Tsai PF, Feng X, et al. Roles of H3K27me2 and H3K27me3 Examined during Fate Specification of Embryonic Stem Cells. Cell Rep. 2017;18(1):297.
232. Mansour AA, Gafni O, Weinberger L, Zviran A, Ayyash M, Rais Y, et al. The H3K27 demethylase Utx regulates somatic and germ cell epigenetic reprogramming. Nature. 2012;488(7411):409-13.
233. Streubel G, Watson A, Jammula SG, Scelfo A, Fitzpatrick DJ, Oliviero G, et al. The H3K36me2 Methyltransferase Nsd1 Demarcates PRC2-Mediated H3K27me2 and H3K27me3 Domains in Embryonic Stem Cells. Mol Cell. 2018;70(2):371-9 e5.
234. Waddington CH. The epigenome. Endeavour. 1942(1):18-20.
235. Berger SL, Kouzarides T, Shiekhattar R, Shilatifard A. An operational definition of epigenetics. Genes Dev. 2009;23(7):781-3.
236. Liu X, Wang C, Liu W, Li J, Li C, Kou X, et al. Distinct features of H3K4me3 and H3K27me3 chromatin domains in pre-implantation embryos. Nature. 2016;537(7621):558-62.

237. Pauler FM, Sloane MA, Huang R, Regha K, Koerner MV, Tamir I, et al. H3K27me3 forms BLOCs over silent genes and intergenic regions and specifies a histone banding pattern on a mouse autosomal chromosome. Genome Res. 2009;19(2):221-33.
238. Ferrari KJ, Scelfo A, Jammula S, Cuomo A, Barozzi I, Stutzer A, et al. Polycomb-dependent H3K27me1 and H3K27me2 regulate active transcription and enhancer fidelity. Mol Cell. 2014;53(1):49-62.
239. Pasini D, Malatesta M, Jung HR, Walfridsson J, Willer A, Olsson L, et al. Characterization of an antagonistic switch between histone H3 lysine 27 methylation and acetylation in the transcriptional regulation of Polycomb group target genes. Nucleic Acids Res. 2010;38(15):4958-69.
240. Lee TI, Jenner RG, Boyer LA, Guenther MG, Levine SS, Kumar RM, et al. Control of developmental regulators by Polycomb in human embryonic stem cells. Cell. 2006;125(2):301-13.
241. Boyer LA, Plath K, Zeitlinger J, Brambrink T, Medeiros LA, Lee TI, et al. Polycomb complexes repress developmental regulators in murine embryonic stem cells. Nature. 2006;441(7091):349-53.
242. Mikkelsen TS, Ku M, Jaffe DB, Issac B, Lieberman E, Giannoukos G, et al. Genome-wide maps of chromatin state in pluripotent and lineage-committed cells. Nature. 2007;448(7153):553-60.
243. Lavarone E, Barbieri CM, Pasini D. Dissecting the role of H3K27 acetylation and methylation in PRC2 mediated control of cellular identity. Nat Commun. 2019;10(1):1679.
244. Tie F, Banerjee R, Stratton CA, Prasad-Sinha J, Stepanik V, Zlobin A, et al. CBP-mediated acetylation of histone H3 lysine 27 antagonizes Drosophila Polycomb silencing. Development. 2009;136(18):3131-41.
245. Li X, Isono K, Yamada D, Endo TA, Endoh M, Shinga J, et al. Mammalian polycomb-like Pcl2/Mtf2 is a novel regulatory component of PRC2 that can differentially modulate polycomb activity both at the Hox gene cluster and at Cdkn2a genes. Mol Cell Biol. 2011;31(2):351-64.
246. Sen GL, Webster DE, Barragan DI, Chang HY, Khavari PA. Control of differentiation in a self-renewing mammalian tissue by the histone demethylase JMJD3. Genes Dev. 2008;22(14):1865-70.
247. Pellakuru LG, Iwata T, Gurel B, Schultz D, Hicks J, Bethel C, et al. Global levels of H3K27me3 track with differentiation in vivo and are deregulated by MYC in prostate cancer. Am J Pathol. 2012;181(2):560-9.
248. Roychoudhury S. Genome-wide alterations of epigenomic landscape in plants by engineered nanomaterial toxicants. Comprehensive Analytical Chemistry. 2019;84C:199-223.
249. Lund AH, van Lohuizen M. Polycomb complexes and silencing mechanisms. Curr Opin Cell Biol. 2004;16(3):239-46.
250. Levine SS, King IF, Kingston RE. Division of labor in polycomb group repression. Trends Biochem Sci. 2004;29(9):478-85.
251. Kennison JA. The Polycomb and trithorax group proteins of Drosophila: trans-regulators of homeotic gene function. Annu Rev Genet. 1995;29:289-303.
252. Xiang Y, Zhu Z, Han G, Lin H, Xu L, Chen CD. JMJD3 is a histone H3K27 demethylase. Cell Res. 2007;17(10):850-7.
253. Lan F, Bayliss PE, Rinn JL, Whetstine JR, Wang JK, Chen S, et al. A histone H3 lysine 27 demethylase regulates animal posterior development. Nature. 2007;449(7163):689-94.
254. Yun M, Wu J, Workman JL, Li B. Readers of histone modifications. Cell Res. 2011;21(4):564-78.
255. Rea S, Eisenhaber F, O'Carroll D, Strahl BD, Sun ZW, Schmid M, et al. Regulation of chromatin structure by site-specific histone H3 methyltransferases. Nature. 2000;406(6796):593-9.
256. Eissenberg JC. Structural biology of the chromodomain: form and function. Gene. 2012;496(2):69-78.
257. Laugesen A, Helin K. Chromatin repressive complexes in stem cells, development, and cancer. Cell Stem Cell. 2014;14(6):735-51.

258. Karmodiya K, Pradhan SJ, Joshi B, Jangid R, Reddy PC, Galande S. A comprehensive epigenome map of *Plasmodium falciparum* reveals unique mechanisms of transcriptional regulation and identifies H3K36me2 as a global mark of gene suppression. Epigenetics Chromatin. 2015;8:32.
259. Josling G, Venezia J, Orchard L, Russell TJ, Painter H, Llinas M. Regulation of sexual differentiation is linked to invasion in malaria parasites. bioRxiv. 2019.
260. Lopez-Rubio JJ, Gontijo AM, Nunes MC, Issar N, Hernandez Rivas R, Scherf A. 5' flanking region of var genes nucleate histone modification patterns linked to phenotypic inheritance of virulence traits in malaria parasites. Mol Microbiol. 2007;66(6):1296-305.
261. Becker JS, Nicetto D, Zaret KS. H3K9me3-Dependent Heterochromatin: Barrier to Cell Fate Changes. Trends Genet. 2016;32(1):29-41.
262. Chen J, Liu H, Liu J, Qi J, Wei B, Yang J, et al. H3K9 methylation is a barrier during somatic cell reprogramming into iPSCs. Nature Genetics. 2013;45(1):34-42.
263. Buganim Y, Faddah DA, Cheng AW, Itskovich E, Markoulaki S, Ganz K, et al. Single-cell expression analyses during cellular reprogramming reveal an early stochastic and a late hierarchic phase. Cell. 2012;150(6):1209-22.
264. Liu J, Magri L, Zhang F, Marsh NO, Albrecht S, Huynh JL, et al. Chromatin landscape defined by repressive histone methylation during oligodendrocyte differentiation. J Neurosci. 2015;35(1):352-65.
265. Soufi A, Donahue G, Zaret KS. Facilitators and impediments of the pluripotency reprogramming factors' initial engagement with the genome. Cell. 2012;151(5):994-1004.
266. Hawkins RD, Hon GC, Lee LK, Ngo Q, Lister R, Pelizzola M, et al. Distinct epigenomic landscapes of pluripotent and lineage-committed human cells. Cell Stem Cell. 2010;6(5):479-91.
267. Bernstein BE, Mikkelsen TS, Xie X, Kamal M, Huebert DJ, Cuff J, et al. A bivalent chromatin structure marks key developmental genes in embryonic stem cells. Cell. 2006;125(2):315-26.
268. Dellino GI, Schwartz YB, Farkas G, McCabe D, Elgin SC, Pirrotta V. Polycomb silencing blocks transcription initiation. Mol Cell. 2004;13(6):887-93.
269. Zhu J, Adli M, Zou JY, Verstappen G, Coyne M, Zhang X, et al. Genome-wide chromatin state transitions associated with developmental and environmental cues. Cell. 2013;152(3):642-54.
270. Xu CR, Li LC, Donahue G, Ying L, Zhang YW, Gadue P, et al. Dynamics of genomic H3K27me3 domains and role of EZH2 during pancreatic endocrine specification. EMBO J. 2014;33(19):2157-70.
271. Trager W, Jensen JB. Human malaria parasites in continuous culture. Science. 1976;193(4254):673-5.
272. Lambros C, Vanderberg JP. Synchronization of *Plasmodium falciparum* erythrocytic stages in culture. J Parasitol. 1979;65(3):418-20.
273. Carter R, Ranford-Cartwright L, Alano P. The culture and preparation of gametocytes of *Plasmodium falciparum* for immunochemical, molecular, and mosquito infectivity studies. Methods Mol Biol. 1993;21:67-88.
274. Reader J, Botha M, Theron A, Lauterbach SB, Rossouw C, Engelbrecht D, et al. Nowhere to hide: interrogating different metabolic parameters of *Plasmodium falciparum* gametocytes in a transmission blocking drug discovery pipeline towards malaria elimination. Malar J. 2015;14:213.
275. van Biljon R, Niemand J, van Wyk R, Clark K, Verlinden B, Abrie C, et al. Inducing controlled cell cycle arrest and re-entry during asexual proliferation of *Plasmodium falciparum* malaria parasites. Sci Rep. 2018;8(1):16581.
276. Schneider CA, Rasband WS, Eliceiri KW. NIH Image to ImageJ: 25 years of image analysis. Nat Methods. 2012;9(7):671-5.
277. D'Alessandro S, Silvestrini F, Dechering K, Corbett Y, Parapini S, Timmerman M, et al. A *Plasmodium falciparum* screening assay for anti-gametocyte drugs based on parasite lactate dehydrogenase detection. J Antimicrob Chemother. 2013;68(9):2048-58.

278. Bolscher JM, Koolen KM, van Gemert GJ, van de Vegte-Bolmer MG, Bousema T, Leroy D, et al. A combination of new screening assays for prioritization of transmission-blocking antimalarials reveals distinct dynamics of marketed and experimental drugs. J Antimicrob Chemother. 2015;70(5):1357-66.
279. Walker JM. The bicinchoninic acid (BCA) assay for protein quantitation. Methods Mol Biol. 1994;32:5-8.
280. Painter HJ, Altenhofen LM, Kafsack BF, Llinas M. Whole-genome analysis of *Plasmodium spp.* Utilizing a new agilent technologies DNA microarray platform. Methods Mol Biol. 2013;923:213-9.
281. Irwin JJ, Shoichet BK. ZINC--a free database of commercially available compounds for virtual screening. J Chem Inf Model. 2005;45(1):177-82.
282. Pettersen EF, Goddard TD, Huang CC, Couch GS, Greenblatt DM, Meng EC, et al. UCSF Chimera--a visualization system for exploratory research and analysis. J Comput Chem. 2004;25(13):1605-12.
283. Waterhouse A, Bertoni M, Bienert S, Studer G, Tauriello G, Gumienny R, et al. SWISS-MODEL: homology modelling of protein structures and complexes. Nucleic Acids Res. 2018;46(W1):W296-W303.
284. Jumper J, Evans R, Pritzel A, Green T, Figurnov M, Ronneberger O, et al. Highly accurate protein structure prediction with AlphaFold. Nature. 2021.
285. Grosdidier A, Zoete V, Michielin O. SwissDock, a protein-small molecule docking web service based on EADock DSS. Nucleic Acids Res. 2011;39(Web Server issue):W270-7.
286. Andrews S. FastQC: a quality control tool for high throughput sequence data 2010 [cited 2019. Available from: http://www.bioinformatics.babraham.ac.uk/projects/fastqc.
287. Bolger AM, Lohse M, Usadel B. Trimmomatic: a flexible trimmer for Illumina sequence data. Bioinformatics. 2014;30(15):2114-20.
288. Li H, Durbin R. Fast and accurate long-read alignment with Burrows-Wheeler transform. Bioinformatics. 2010;26(5):589-95.
289. Li H, Handsaker B, Wysoker A, Fennell T, Ruan J, Homer N, et al. The Sequence Alignment/Map format and SAMtools. Bioinformatics. 2009;25(16):2078-9.
290. Ramirez F, Dundar F, Diehl S, Gruning BA, Manke T. deepTools: a flexible platform for exploring deep-sequencing data. Nucleic Acids Res. 2014;42(Web Server issue):W187-91.
291. Thorvaldsdottir H, Robinson JT, Mesirov JP. Integrative Genomics Viewer (IGV): high-performance genomics data visualization and exploration. Brief Bioinform. 2013;14(2):178-92.
292. Zhang Y, Liu T, Meyer CA, Eeckhoute J, Johnson DS, Bernstein BE, et al. Model-based analysis of ChIP-Seq (MACS). Genome Biol. 2008;9(9):R137.
293. Zaidan NZ, Sridharan R. HP1gamma regulates H3K36 methylation and pluripotency in embryonic stem cells. Nucleic Acids Res. 2020;48(22):12660-74.
294. Quinlan AR, Hall IM. BEDTools: a flexible suite of utilities for comparing genomic features. Bioinformatics. 2010;26(6):841-2.
295. Wang J, Nygaard V, Smith-Sorensen B, Hovig E, Myklebost O. MArray: analysing single, replicated or reversed microarray experiments. Bioinformatics. 2002;18(8):1139-40.
296. Ritchie ME, Phipson B, Wu D, Hu Y, Law CW, Shi W, et al. limma powers differential expression analyses for RNA-sequencing and microarray studies. Nucleic Acids Res. 2015;43(7):e47.
297. Park PJ. ChIP-seq: advantages and challenges of a maturing technology. Nat Rev Genet. 2009;10(10):669-80.
298. Liu ET, Pott S, Huss M. Q&A: ChIP-seq technologies and the study of gene regulation. BMC Biol. 2010;8:56.
299. Nakato R, Sakata T. Methods for ChIP-seq analysis: A practical workflow and advanced applications. Methods. 2021;187:44-53.
300. Karoopongse E, Yeung C, Byon J, Ramakrishnan A, Holman ZJ, Jiang PY, et al. The KDM2B- let-7b -EZH2 axis in myelodysplastic syndromes as a target for combined epigenetic therapy. PLoS One. 2014;9(9):e107817.

301. Tilgner K, Atkinson SP, Yung S, Golebiewska A, Stojkovic M, Moreno R, et al. Expression of GFP under the control of the RNA helicase VASA permits fluorescence-activated cell sorting isolation of human primordial germ cells. Stem Cells. 2010;28(1):84-92.
302. Kelsey AD, Yang C, Leung D, Minks J, Dixon-McDougall T, Baldry SE, et al. Impact of flanking chromosomal sequences on localization and silencing by the human non-coding RNA XIST. Genome Biol. 2015;16:208.
303. Chen X, Liu X, Zhao Y, Zhou DX. Histone H3K4me3 and H3K27me3 regulatory genes control stable transmission of an epimutation in rice. Sci Rep. 2015;5:13251.
304. Gao R, Chen S, Kobayashi M, Yu H, Zhang Y, Wan Y, et al. Bmi1 promotes erythroid development through regulating ribosome biogenesis. Stem Cells. 2015;33(3):925-38.
305. van Rossum B, Fischle W, Selenko P. Asymmetrically modified nucleosomes expand the histone code. Nat Struct Mol Biol. 2012;19(11):1064-6.
306. Voigt P, LeRoy G, Drury WJ, 3rd, Zee BM, Son J, Beck DB, et al. Asymmetrically modified nucleosomes. Cell. 2012;151(1):181-93.
307. Baum J, Richard D, Healer J, Rug M, Krnajski Z, Gilberger TW, et al. A conserved molecular motor drives cell invasion and gliding motility across malaria life cycle stages and other apicomplexan parasites. J Biol Chem. 2006;281(8):5197-208.
308. De Niz M, Meibalan E, Mejia P, Ma S, Brancucci NMB, Agop-Nersesian C, et al. Plasmodium gametocytes display homing and vascular transmigration in the host bone marrow. Sci Adv. 2018;4(5):eaat3775.
309. Paul RE, Brey PT, Robert V. *Plasmodium* sex determination and transmission to mosquitoes. Trends Parasitol. 2002;18(1):32-8.
310. Gulati S, Ekland EH, Ruggles KV, Chan RB, Jayabalasingham B, Zhou B, et al. Profiling the Essential Nature of Lipid Metabolism in Asexual Blood and Gametocyte Stages of *Plasmodium falciparum*. Cell Host Microbe. 2015;18(3):371-81.
311. Maguire PA, Sherman IW. Phospholipid composition, cholesterol content and cholesterol exchange in *Plasmodium falciparum*-infected red cells. Mol Biochem Parasitol. 1990;38(1):105-12.
312. Tran PN, Brown SH, Rug M, Ridgway MC, Mitchell TW, Maier AG. Changes in lipid composition during sexual development of the malaria parasite *Plasmodium falciparum*. Malar J. 2016;15:73.
313. Lindroth AM, Shultis D, Jasencakova Z, Fuchs J, Johnson L, Schubert D, et al. Dual histone H3 methylation marks at lysines 9 and 27 required for interaction with CHROMOMETHYLASE3. EMBO J. 2004;23(21):4286-96.
314. Hyun K, Jeon J, Park K, Kim J. Writing, erasing and reading histone lysine methylations. Exp Mol Med. 2017;49(4):e324.
315. Cheung P, Lau P. Epigenetic regulation by histone methylation and histone variants. Mol Endocrinol. 2005;19(3):563-73.
316. Perez-Toledo K, Rojas-Meza AP, Mancio-Silva L, Hernandez-Cuevas NA, Delgadillo DM, Vargas M, et al. *Plasmodium falciparum* heterochromatin protein 1 binds to tri-methylated histone 3 lysine 9 and is linked to mutually exclusive expression of *var* genes. Nucleic Acids Res. 2009;37(8):2596-606.
317. Eksi S, Haile Y, Furuya T, Ma L, Su X, Williamson KC. Identification of a subtelomeric gene family expressed during the asexual-sexual stage transition in *Plasmodium falciparum*. Mol Biochem Parasitol. 2005;143(1):90-9.
318. Frapporti A, Miro Pina C, Arnaiz O, Holoch D, Kawaguchi T, Humbert A, et al. The Polycomb protein Ezl1 mediates H3K9 and H3K27 methylation to repress transposable elements in *Paramecium*. Nat Commun. 2019;10(1):2710.
319. Fei Q, Yang X, Jiang H, Wang Q, Yu Y, Yu Y, et al. SETDB1 modulates PRC2 activity at developmental genes independently of H3K9 trimethylation in mouse ES cells. Genome Res. 2015;25(9):1325-35.

320. Ringrose L, Ehret H, Paro R. Distinct contributions of histone H3 lysine 9 and 27 methylation to locus-specific stability of polycomb complexes. Mol Cell. 2004;16(4):641-53.
321. Alder O, Lavial F, Helness A, Brookes E, Pinho S, Chandrashekran A, et al. Ring1B and Suv39h1 delineate distinct chromatin states at bivalent genes during early mouse lineage commitment. Development. 2010;137(15):2483-92.
322. Boggs BA, Cheung P, Heard E, Spector DL, Chinault AC, Allis CD. Differentially methylated forms of histone H3 show unique association patterns with inactive human X chromosomes. Nat Genet. 2002;30(1):73-6.
323. Rougeulle C, Chaumeil J, Sarma K, Allis CD, Reinberg D, Avner P, et al. Differential histone H3 Lys-9 and Lys-27 methylation profiles on the X chromosome. Mol Cell Biol. 2004;24(12):5475-84.
324. Coetzee N. Sexual differentiation of malaria parasites is controlled by unique epigenomic and proteomic cascades as revealed by comparative functional genome analyses: University of Pretoria; 2017.
325. von Gruning H, Coradin, M., Mendoza, M., Reader, J., Sidoli, S., Garcia, B. A. and Birkholtz, L.M. A dynamic and combinatorial histone code drives malaria parasite asexual and sexual development. BioRxiv. 2021.
326. PlasmoDB: An integrative database of the Plasmodium falciparum genome. Tools for accessing and analyzing finished and unfinished sequence data. The Plasmodium Genome Database Collaborative. Nucleic Acids Res. 2001;29(1):66-9.
327. Wu H, Chen X, Xiong J, Li Y, Li H, Ding X, et al. Histone methyltransferase G9a contributes to H3K27 methylation *in vivo*. Cell Res. 2011;21(2):365-7.
328. Pasini D, Bracken AP, Jensen MR, Lazzerini Denchi E, Helin K. Suz12 is essential for mouse development and for EZH2 histone methyltransferase activity. EMBO J. 2004;23(20):4061-71.
329. Cao R, Zhang Y. SUZ12 is required for both the histone methyltransferase activity and the silencing function of the EED-EZH2 complex. Mol Cell. 2004;15(1):57-67.
330. Amatangelo MD, Garipov A, Li H, Conejo-Garcia JR, Speicher DW, Zhang R. Three-dimensional culture sensitizes epithelial ovarian cancer cells to EZH2 methyltransferase inhibition. Cell Cycle. 2013;12(13):2113-9.
331. Konze KD, Ma A, Li F, Barsyte-Lovejoy D, Parton T, Macnevin CJ, et al. An orally bioavailable chemical probe of the Lysine Methyltransferases EZH2 and EZH1. ACS Chem Biol. 2013;8(6):1324-34.
332. Hsieh YY, Lo HL, Yang PM. EZH2 inhibitors transcriptionally upregulate cytotoxic autophagy and cytoprotective unfolded protein response in human colorectal cancer cells. Am J Cancer Res. 2016;6(8):1661-80.
333. Liu TP, Lo HL, Wei LS, Hsiao HH, Yang PM. S-Adenosyl-L-methionine-competitive inhibitors of the histone methyltransferase EZH2 induce autophagy and enhance drug sensitivity in cancer cells. Anticancer Drugs. 2015;26(2):139-47.
334. McCabe MT, Ott HM, Ganji G, Korenchuk S, Thompson C, Van Aller GS, et al. EZH2 inhibition as a therapeutic strategy for lymphoma with EZH2-activating mutations. Nature. 2012;492(7427):108-12.
335. Verma SK, Tian X, LaFrance LV, Duquenne C, Suarez DP, Newlander KA, et al. Identification of Potent, Selective, Cell-Active Inhibitors of the Histone Lysine Methyltransferase EZH2. ACS Med Chem Lett. 2012;3(12):1091-6.
336. Zhang P, de Gooijer MC, Buil LC, Beijnen JH, Li G, van Tellingen O. ABCB1 and ABCG2 restrict the brain penetration of a panel of novel EZH2-Inhibitors. Int J Cancer. 2015;137(8):2007-18.
337. Liu F, Chen X, Allali-Hassani A, Quinn AM, Wasney GA, Dong A, et al. Discovery of a 2,4-diamino-7-aminoalkoxyquinazoline as a potent and selective inhibitor of histone lysine methyltransferase G9a. J Med Chem. 2009;52(24):7950-3.

338. Vedadi M, Barsyte-Lovejoy D, Liu F, Rival-Gervier S, Allali-Hassani A, Labrie V, et al. A chemical probe selectively inhibits G9a and GLP methyltransferase activity in cells. Nat Chem Biol. 2011;7(8):566-74.
339. Inaba M, Nagashima K, Tsukagoshi S, Sakurai Y. Biochemical mode of cytotoxic action of neplanocin A in L1210 leukemic cells. Cancer Res. 1986;46(3):1063-7.
340. Greiner D, Bonaldi T, Eskeland R, Roemer E, Imhof A. Identification of a specific inhibitor of the histone methyltransferase SU(VAR)3-9. Nat Chem Biol. 2005;1(3):143-5.
341. Tachibana M, Sugimoto K, Nozaki M, Ueda J, Ohta T, Ohki M, et al. G9a histone methyltransferase plays a dominant role in euchromatic histone H3 lysine 9 methylation and is essential for early embryogenesis. Genes Dev. 2002;16(14):1779-91.
342. Tachibana M, Sugimoto K, Fukushima T, Shinkai Y. Set domain-containing protein, G9a, is a novel lysine-preferring mammalian histone methyltransferase with hyperactivity and specific selectivity to lysines 9 and 27 of histone H3. J Biol Chem. 2001;276(27):25309-17.
343. Cui L, Lindner S, Miao J. Translational regulation during stage transitions in malaria parasites. Ann N Y Acad Sci. 2015;1342:1-9.
344. Birkholtz L, van Brummelen AC, Clark K, Niemand J, Marechal E, Llinas M, et al. Exploring functional genomics for drug target and therapeutics discovery in *Plasmodia*. Acta Trop. 2008;105(2):113-23.
345. Burrows JN, Burlot E, Campo B, Cherbuin S, Jeanneret S, Leroy D, et al. Antimalarial drug discovery - the path towards eradication. Parasitology. 2014;141(1):128-39.
346. Delves MJ. *Plasmodium* cell biology should inform strategies used in the development of antimalarial transmission-blocking drugs. Future Med Chem. 2012;4(18):2251-63.
347. Connacher J, Josling GA, Orchard LM, Reader J, Llinas M, Birkholtz LM. H3K36 methylation reprograms gene expression to drive early gametocyte development in *Plasmodium falciparum*. Epigenetics Chromatin. 2021;14(1):19.
348. Lee K, Park OS, Jung SJ, Seo PJ. Histone deacetylation-mediated cellular dedifferentiation in Arabidopsis. J Plant Physiol. 2016;191:95-100.
349. Boros J, Arnoult N, Stroobant V, Collet JF, Decottignies A. Polycomb repressive complex 2 and H3K27me3 cooperate with H3K9 methylation to maintain heterochromatin protein 1alpha at chromatin. Mol Cell Biol. 2014;34(19):3662-74.
350. Chen Z, Djekidel MN, Zhang Y. Distinct dynamics and functions of H2AK119ub1 and H3K27me3 in mouse preimplantation embryos. Nat Genet. 2021;53(4):551-63.
351. Miller SA, Damle M, Kim J, Kingston RE. Full methylation of H3K27 by PRC2 is dispensable for initial embryoid body formation but required to maintain differentiated cell identity. Development. 2021;148(7).
352. Wee S, Dhanak D, Li H, Armstrong SA, Copeland RA, Sims R, et al. Targeting epigenetic regulators for cancer therapy. Ann N Y Acad Sci. 2014;1309:30-6.
353. Buchi F, Masala E, Rossi A, Valencia A, Spinelli E, Sanna A, et al. Redistribution of H3K27me3 and acetylated histone H4 upon exposure to azacitidine and decitabine results in de-repression of the AML1/ETO target gene IL3. Epigenetics. 2014;9(3):387-95.
354. Huang Z, Li R, Tang T, Ling D, Wang M, Xu D, et al. A novel multistage antiplasmodial inhibitor targeting Plasmodium falciparum histone deacetylase 1. Cell Discov. 2020;6(1):93.
355. Chandar Charles MR, Li MC, Hsieh HP, Coumar MS. Mimicking H3 Substrate Arginine in the Design of G9a Lysine Methyltransferase Inhibitors for Cancer Therapy: A Computational Study for Structure-Based Drug Design. ACS Omega. 2021;6(9):6100-11.
356. Kaniskan HU, Jin J. Chemical probes of histone lysine methyltransferases. ACS Chem Biol. 2015;10(1):40-50.

357. Reader J, van der Watt ME, Taylor D, Le Manach C, Mittal N, Ottilie S, et al. Multistage and transmission-blocking targeted antimalarials discovered from the open-source MMV Pandemic Response Box. Nat Commun. 2021;12(1):269.
358. Feachem RGA, Chen I, Akbari O, Bertozzi-Villa A, Bhatt S, Binka F, et al. Malaria eradication within a generation: ambitious, achievable, and necessary. Lancet. 2019;394(10203):1056-112.
359. Josling GA, Williamson KC, Llinas M. Regulation of Sexual Commitment and Gametocytogenesis in Malaria Parasites. Annu Rev Microbiol. 2018;72:501-19.
360. Llinas M, Deitsch KW, Voss TS. *Plasmodium* gene regulation: far more to factor in. Trends Parasitol. 2008;24(12):551-6.
361. Duffy MF, Selvarajah SA, Josling GA, Petter M. Epigenetic regulation of the *Plasmodium falciparum* genome. Brief Funct Genomics. 2014;13(3):203-16.
362. Venkatesh S, Workman JL. Set2 mediated H3 lysine 36 methylation: regulation of transcription elongation and implications in organismal development. Wiley Interdiscip Rev Dev Biol. 2013;2(5):685-700.
363. Cheung V, Chua G, Batada NN, Landry CR, Michnick SW, Hughes TR, et al. Chromatin- and transcription-related factors repress transcription from within coding regions throughout the Saccharomyces cerevisiae genome. PLoS Biol. 2008;6(11):e277.
364. Strahl BD, Grant PA, Briggs SD, Sun ZW, Bone JR, Caldwell JA, et al. Set2 is a nucleosomal histone H3-selective methyltransferase that mediates transcriptional repression. Mol Cell Biol. 2002;22(5):1298-306.
365. Scherf A, Lopez-Rubio JJ, Riviere L. Antigenic variation in *Plasmodium falciparum*. Annu Rev Microbiol. 2008;62:445-70.
366. Wong MPM, Ng, R. K. Resetting Cell Fate by Epigenetic Reprogramming. In: Logie CaK, T. A., editor. Chromatin and Epigenetics: IntechOpen; 2020. p. 165-206.
367. Cui L, Miao J. Chromatin-mediated epigenetic regulation in the malaria parasite *Plasmodium falciparum*. Eukaryot Cell. 2010;9(8):1138-49.
368. Vanheer LN, Zhang H, Lin G, Kafsack BFC. Activity of Epigenetic Inhibitors against *Plasmodium falciparum* Asexual and Sexual Blood Stages. Antimicrob Agents Chemother. 2020;64(7).
369. DiFiore JV, Ptacek TS, Wang Y, Li B, Simon JM, Strahl BD. Unique and Shared Roles for Histone H3K36 Methylation States in Transcription Regulation Functions. Cell Rep. 2020;31(10):107751.
370. Huang Y, Gu L, Li GM. H3K36me3-mediated mismatch repair preferentially protects actively transcribed genes from mutation. J Biol Chem. 2018;293(20):7811-23.
371. Li L, Wang Y. Cross-talk between the H3K36me3 and H4K16ac histone epigenetic marks in DNA double-strand break repair. J Biol Chem. 2017;292(28):11951-9.
372. Liu B, Liu Y, Wang B, Luo Q, Shi J, Gan J, et al. The transcription factor OsSUF4 interacts with SDG725 in promoting H3K36me3 establishment. Nat Commun. 2019;10(1):2999.
373. Zhang M, Wang C, Otto TD, Oberstaller J, Liao X, Adapa SR, et al. Uncovering the essential genes of the human malaria parasite *Plasmodium falciparum* by saturation mutagenesis. Science. 2018;360(6388).
374. Ikadai H, Shaw Saliba K, Kanzok SM, McLean KJ, Tanaka TQ, Cao J, et al. Transposon mutagenesis identifies genes essential for *Plasmodium falciparum* gametocytogenesis. Proc Natl Acad Sci U S A. 2013;110(18):E1676-84.
375. Wang J, Lunyak VV, Jordan IK. BroadPeak: a novel algorithm for identifying broad peaks in diffuse ChIP-seq datasets. Bioinformatics. 2013;29(4):492-3.
376. Dukatz M, Holzer K, Choudalakis M, Emperle M, Lungu C, Bashtrykov P, et al. H3K36me2/3 Binding and DNA Binding of the DNA Methyltransferase DNMT3A PWWP Domain Both Contribute to its Chromatin Interaction. J Mol Biol. 2019;431(24):5063-74.

377. Mauser R, Kungulovski G, Keup C, Reinhardt R, Jeltsch A. Application of dual reading domains as novel reagents in chromatin biology reveals a new H3K9me3 and H3K36me2/3 bivalent chromatin state. Epigenetics Chromatin. 2017;10(1):45.
378. Sui P, Shi J, Gao X, Shen WH, Dong A. H3K36 methylation is involved in promoting rice flowering. Mol Plant. 2013;6(3):975-7.
379. Chantalat S, Depaux A, Hery P, Barral S, Thuret JY, Dimitrov S, et al. Histone H3 trimethylation at lysine 36 is associated with constitutive and facultative heterochromatin. Genome Res. 2011;21(9):1426-37.
380. Huang C, Zhu B. Roles of H3K36-specific histone methyltransferases in transcription: antagonizing silencing and safeguarding transcription fidelity. Biophys Rep. 2018;4(4):170-7.
381. Li B, Jackson J, Simon MD, Fleharty B, Gogol M, Seidel C, et al. Histone H3 lysine 36 dimethylation (H3K36me2) is sufficient to recruit the Rpd3s histone deacetylase complex and to repress spurious transcription. J Biol Chem. 2009;284(12):7970-6.
382. Pu M, Ni Z, Wang M, Wang X, Wood JG, Helfand SL, et al. Trimethylation of Lys36 on H3 restricts gene expression change during aging and impacts life span. Genes Dev. 2015;29(7):718-31.
383. Morahan BJ, Strobel C, Hasan U, Czesny B, Mantel PY, Marti M, et al. Functional analysis of the exported type IV HSP40 protein PfGECO in *Plasmodium falciparum* gametocytes. Eukaryot Cell. 2011;10(11):1492-503.
384. Contet A, Pihan E, Lavigne M, Wengelnik K, Maheshwari S, Vial H, et al. *Plasmodium falciparum* CTP:phosphocholine cytidylyltransferase possesses two functional catalytic domains and is inhibited by a CDP-choline analog selected from a virtual screening. FEBS Lett. 2015;589(9):992-1000.
385. Hopp CS, Balaban AE, Bushell ES, Billker O, Rayner JC, Sinnis P. Palmitoyl transferases have critical roles in the development of mosquito and liver stages of *Plasmodium*. Cell Microbiol. 2016;18(11):1625-41.
386. Santos JM, Duarte N, Kehrer J, Ramesar J, Avramut MC, Koster AJ, et al. Maternally supplied S-acyl-transferase is required for crystalloid organelle formation and transmission of the malaria parasite. Proc Natl Acad Sci U S A. 2016;113(26):7183-8.
387. Tay CL, Jones ML, Hodson N, Theron M, Choudhary JS, Rayner JC. Study of *Plasmodium falciparum* DHHC palmitoyl transferases identifies a role for PfDHHC9 in gametocytogenesis. Cell Microbiol. 2016;18(11):1596-610.
388. Barski A, Cuddapah S, Cui K, Roh TY, Schones DE, Wang Z, et al. High-resolution profiling of histone methylations in the human genome. Cell. 2007;129(4):823-37.
389. Coetzee N, von Gruning H, Opperman D, van der Watt M, Reader J, Birkholtz LM. Epigenetic inhibitors target multiple stages of *Plasmodium falciparum* parasites. Sci Rep. 2020;10(1):2355.
390. Perillo B, Tramontano A, Pezone A, Migliaccio A. LSD1: more than demethylation of histone lysine residues. Exp Mol Med. 2020;52(12):1936-47.
391. Schmidt DM, McCafferty DG. trans-2-Phenylcyclopropylamine is a mechanism-based inactivator of the histone demethylase LSD1. Biochemistry. 2007;46(14):4408-16.
392. Ngwa CJ, Kiesow MJ, Orchard LM, Farrukh A, Llinas M, Pradel G. The G9a Histone Methyltransferase Inhibitor BIX-01294 Modulates Gene Expression during *Plasmodium falciparum* Gametocyte Development and Transmission. Int J Mol Sci. 2019;20(20).
393. Ngwa CJ, Kiesow MJ, Papst O, Orchard LM, Filarsky M, Rosinski AN, et al. Transcriptional Profiling Defines Histone Acetylation as a Regulator of Gene Expression during Human-to-Mosquito Transmission of the Malaria Parasite *Plasmodium falciparum*. Front Cell Infect Microbiol. 2017;7:320.
394. Wang L, Chang J, Varghese D, Dellinger M, Kumar S, Best AM, et al. A small molecule modulates Jumonji histone demethylase activity and selectively inhibits cancer growth. Nat Commun. 2013;4:2035.

395. Yuan S, Natesan R, Sanchez-Rivera FJ, Li J, Bhanu NV, Yamazoe T, et al. Global Regulation of the Histone Mark H3K36me2 Underlies Epithelial Plasticity and Metastatic Progression. Cancer Discov. 2020;10(6):854-71.
396. Suzuki S, Kato H, Suzuki Y, Chikashige Y, Hiraoka Y, Kimura H, et al. Histone H3K36 trimethylation is essential for multiple silencing mechanisms in fission yeast. Nucleic Acids Res. 2016;44(9):4147-62.
397. Kuo AJ, Cheung P, Chen K, Zee BM, Kioi M, Lauring J, et al. NSD2 links dimethylation of histone H3 at lysine 36 to oncogenic programming. Mol Cell. 2011;44(4):609-20.
398. Pokholok DK, Harbison CT, Levine S, Cole M, Hannett NM, Lee TI, et al. Genome-wide map of nucleosome acetylation and methylation in yeast. Cell. 2005;122(4):517-27.
399. Rao B, Shibata Y, Strahl BD, Lieb JD. Dimethylation of histone H3 at lysine 36 demarcates regulatory and nonregulatory chromatin genome-wide. Mol Cell Biol. 2005;25(21):9447-59.
400. Sinha I, Buchanan L, Ronnerblad M, Bonilla C, Durand-Dubief M, Shevchenko A, et al. Genome-wide mapping of histone modifications and mass spectrometry reveal H4 acetylation bias and H3K36 methylation at gene promoters in fission yeast. Epigenomics. 2010;2(3):377-93.
401. Woo H, Dam Ha S, Lee SB, Buratowski S, Kim T. Modulation of gene expression dynamics by co-transcriptional histone methylations. Exp Mol Med. 2017;49(4):e326.
402. Wu SF, Zhang H, Cairns BR. Genes for embryo development are packaged in blocks of multivalent chromatin in zebrafish sperm. Genome Res. 2011;21(4):578-89.
403. Wagner EJ, Carpenter PB. Understanding the language of Lys36 methylation at histone H3. Nat Rev Mol Cell Biol. 2012;13(2):115-26.
404. Berr A, McCallum EJ, Menard R, Meyer D, Fuchs J, Dong A, et al. *Arabidopsis* SET DOMAIN GROUP2 is required for H3K4 trimethylation and is crucial for both sporophyte and gametophyte development. Plant Cell. 2010;22(10):3232-48.
405. Dhayalan A, Rajavelu A, Rathert P, Tamas R, Jurkowska RZ, Ragozin S, et al. The Dnmt3a PWWP domain reads histone 3 lysine 36 trimethylation and guides DNA methylation. J Biol Chem. 2010;285(34):26114-20.
406. Chen ES, Zhang K, Nicolas E, Cam HP, Zofall M, Grewal SI. Cell cycle control of centromeric repeat transcription and heterochromatin assembly. Nature. 2008;451(7179):734-7.
407. Allfrey VG, Faulkner, R and Mirsky, A.E. Acetylation and methylation of histones and their possible role in the regulation of RNA synthesis. Proc Natl Acad Sci U S A. 1964;51(5):786-94.
408. Zhao Y, Garcia BA. Comprehensive Catalog of Currently Documented Histone Modifications. Cold Spring Harb Perspect Biol. 2015;7(9):a025064.
409. Peter CJ, Akbarian S. Balancing histone methylation activities in psychiatric disorders. Trends Mol Med. 2011;17(7):372-9.
410. Zaware N, Zhou MM. Chemical modulators for epigenome reader domains as emerging epigenetic therapies for cancer and inflammation. Curr Opin Chem Biol. 2017;39:116-25.
411. Henikoff S. Histone modifications: combinatorial complexity or cumulative simplicity? Proc Natl Acad Sci U S A. 2005;102(15):5308-9.
412. Gillette TG, Hill JA. Readers, writers, and erasers: chromatin as the whiteboard of heart disease. Circ Res. 2015;116(7):1245-53.
413. Turner BM. Decoding the nucleosome. Cell. 1993;75(1):5-8.
414. Egelhofer TA, Minoda A, Klugman S, Lee K, Kolasinska-Zwierz P, Alekseyenko AA, et al. An assessment of histone-modification antibody quality. Nat Struct Mol Biol. 2011;18(1):91-3.
415. Fuchs SM, Krajewski K, Baker RW, Miller VL, Strahl BD. Influence of combinatorial histone modifications on antibody and effector protein recognition. Curr Biol. 2011;21(1):53-8.
416. Schwammle V, Sidoli S, Ruminowicz C, Wu X, Lee CF, Helin K, et al. Systems Level Analysis of Histone H3 Post-translational Modifications (PTMs) Reveals Features of PTM Crosstalk in Chromatin Regulation. Mol Cell Proteomics. 2016;15(8):2715-29.

417. Schmitges FW, Prusty AB, Faty M, Stutzer A, Lingaraju GM, Aiwazian J, et al. Histone methylation by PRC2 is inhibited by active chromatin marks. Mol Cell. 2011;42(3):330-41.
418. Yu Y, Chen J, Gao Y, Gao J, Liao R, Wang Y, et al. Quantitative Profiling of Combinational K27/K36 Modifications on Histone H3 Variants in Mouse Organs. J Proteome Res. 2016;15(3):1070-9.
419. Yuan W, Xu M, Huang C, Liu N, Chen S, Zhu B. H3K36 methylation antagonizes PRC2-mediated H3K27 methylation. J Biol Chem. 2011;286(10):7983-9.
420. Zheng Y, Sweet SM, Popovic R, Martinez-Garcia E, Tipton JD, Thomas PM, et al. Total kinetic analysis reveals how combinatorial methylation patterns are established on lysines 27 and 36 of histone H3. Proc Natl Acad Sci U S A. 2012;109(34):13549-54.
421. Saksouk N, Barth TK, Ziegler-Birling C, Olova N, Nowak A, Rey E, et al. Redundant mechanisms to form silent chromatin at pericentromeric regions rely on BEND3 and DNA methylation. Mol Cell. 2014;56(4):580-94.
422. Peters AH, Kubicek S, Mechtler K, O'Sullivan RJ, Derijck AA, Perez-Burgos L, et al. Partitioning and plasticity of repressive histone methylation states in mammalian chromatin. Mol Cell. 2003;12(6):1577-89.
423. Cooper S, Dienstbier M, Hassan R, Schermelleh L, Sharif J, Blackledge NP, et al. Targeting polycomb to pericentric heterochromatin in embryonic stem cells reveals a role for H2AK119u1 in PRC2 recruitment. Cell Rep. 2014;7(5):1456-70.
424. Puschendorf M, Terranova R, Boutsma E, Mao X, Isono K, Brykczynska U, et al. PRC1 and Suv39h specify parental asymmetry at constitutive heterochromatin in early mouse embryos. Nat Genet. 2008;40(4):411-20.
425. Zhang T, Cooper S, Brockdorff N. The interplay of histone modifications - writers that read. EMBO Rep. 2015;16(11):1467-81.
426. Gaydos LJ, Rechtsteiner A, Egelhofer TA, Carroll CR, Strome S. Antagonism between MES-4 and Polycomb repressive complex 2 promotes appropriate gene expression in *C. elegans* germ cells. Cell Rep. 2012;2(5):1169-77.
427. Nichol JN, Dupere-Richer D, Ezponda T, Licht JD, Miller WH, Jr. H3K27 Methylation: A Focal Point of Epigenetic Deregulation in Cancer. Adv Cancer Res. 2016;131:59-95.
428. Keiser AA, Wood MA. Examining the contribution of histone modification to sex differences in learning and memory. Learn Mem. 2019;26(9):318-31.
429. Tachibana M. Epigenetics of sex determination in mammals. Reprod Med Biol. 2016;15(2):59-67.
430. Bell O, Conrad T, Kind J, Wirbelauer C, Akhtar A, Schubeler D. Transcription-coupled methylation of histone H3 at lysine 36 regulates dosage compensation by enhancing recruitment of the MSL complex in *Drosophila melanogaster*. Mol Cell Biol. 2008;28(10):3401-9.
431. Steinmann-Zwicky M. Sex determination in *Drosophila*: the X-chromosomal gene liz is required for Sxl activity. EMBO J. 1988;7(12):3889-98.
432. Ge C, Ye J, Weber C, Sun W, Zhang H, Zhou Y, et al. The histone demethylase KDM6B regulates temperature-dependent sex determination in a turtle species. Science. 2018;360(6389):645-8.
433. Jung HR, Sidoli S, Haldbo S, Sprenger RR, Schwammle V, Pasini D, et al. Precision mapping of coexisting modifications in histone H3 tails from embryonic stem cells by ETD-MS/MS. Anal Chem. 2013;85(17):8232-9.
434. Zaghi M, Broccoli V, Sessa A. H3K36 Methylation in Neural Development and Associated Diseases. Front Genet. 2019;10:1291.
435. Zheng ZH, Sam TW, Zeng Y, Chu JJH, Loh YH. Chromatin Regulation in Development: Current Understanding and Approaches. Stem Cells Int. 2021;2021:8817581.
436. Wutz A. Epigenetic regulation of stem cells : the role of chromatin in cell differentiation. Adv Exp Med Biol. 2013;786:307-28.

437. Dixon JR, Jung I, Selvaraj S, Shen Y, Antosiewicz-Bourget JE, Lee AY, et al. Chromatin architecture reorganization during stem cell differentiation. Nature. 2015;518(7539):331-6.
438. Jain R, Dey P, Gupta S, Pati S, Bhattacherjee A, Munde M, et al. Molecular dynamics simulations and biochemical characterization of Pf14-3-3 and PfCDPK1 interaction towards its role in growth of human malaria parasite. Biochem J. 2020;477(12):2153-77.
439. Fan Q, An L, Cui L. PfADA2, a *Plasmodium falciparum* homologue of the transcriptional coactivator ADA2 and its *in vivo* association with the histone acetyltransferase PfGCN5. Gene. 2004;336(2):251-61.
440. Bryant JM, Baumgarten S, Dingli F, Loew D, Sinha A, Claes A, et al. Exploring the virulence gene interactome with CRISPR/dCas9 in the human malaria parasite. Mol Syst Biol. 2020;16(8):e9569.
441. Bischoff E, Vaquero C. *In silico* and biological survey of transcription-associated proteins implicated in the transcriptional machinery during the erythrocytic development of *Plasmodium falciparum*. BMC Genomics. 2010;11:34.
442. Ukaegbu UE, Zhang X, Heinberg AR, Wele M, Chen Q, Deitsch KW. A Unique Virulence Gene Occupies a Principal Position in Immune Evasion by the Malaria Parasite *Plasmodium falciparum*. PLoS Genet. 2015;11(5):e1005234.
443. LaCount DJ, Vignali M, Chettier R, Phansalkar A, Bell R, Hesselberth JR, et al. A protein interaction network of the malaria parasite *Plasmodium falciparum*. Nature. 2005;438(7064):103-7.
444. Oehring SC, Woodcroft BJ, Moes S, Wetzel J, Dietz O, Pulfer A, et al. Organellar proteomics reveals hundreds of novel nuclear proteins in the malaria parasite Plasmodium falciparum. Genome Biol. 2012;13(11):R108.
445. Chandra BR, Olivieri A, Silvestrini F, Alano P, Sharma A. Biochemical characterization of the two nucleosome assembly proteins from *Plasmodium falciparum*. Mol Biochem Parasitol. 2005;142(2):237-47.
446. Wang WF, Zhang YL. PfSWIB, a potential chromatin regulator for var gene regulation and parasite development in Plasmodium falciparum. Parasit Vectors. 2020;13(1):48.
447. Kim A, Popovici J, Menard D, Serre D. *Plasmodium vivax* transcriptomes reveal stage-specific chloroquine response and differential regulation of male and female gametocytes. Nat Commun. 2019;10(1):371.
448. Yeoh LM, Goodman CD, Mollard V, McFadden GI, Ralph SA. Comparative transcriptomics of female and male gametocytes in *Plasmodium berghei* and the evolution of sex in alveolates. BMC Genomics. 2017;18(1):734.
449. Walzer KA, Kubicki DM, Tang X, Chi JT. Single-Cell Analysis Reveals Distinct Gene Expression and Heterogeneity in Male and Female *Plasmodium falciparum* Gametocytes. mSphere. 2018;3(2).
450. Sinden RE. Sexual development of malarial parasites. Adv Parasitol. 1983;22:153-216.
451. Jaenisch R, Bird A. Epigenetic regulation of gene expression: how the genome integrates intrinsic and environmental signals. Nat Genet. 2003;33 Suppl:245-54.
452. Wiles ET, Selker EU. H3K27 methylation: a promiscuous repressive chromatin mark. Curr Opin Genet Dev. 2017;43:31-7.
453. Kolasinska-Zwierz P, Down T, Latorre I, Liu T, Liu XS, Ahringer J. Differential chromatin marking of introns and expressed exons by H3K36me3. Nat Genet. 2009;41(3):376-81.
454. Rodriguez-Navarro S. Insights into SAGA function during gene expression. EMBO Rep. 2009;10(8):843-50.
455. Johnsson AE, Wright AP. The role of specific HAT-HDAC interactions in transcriptional elongation. Cell Cycle. 2010;9(3):467-71.
456. Ali M, Hom RA, Blakeslee W, Ikenouye L, Kutateladze TG. Diverse functions of PHD fingers of the MLL/KMT2 subfamily. Biochim Biophys Acta. 2014;1843(2):366-71.

457. Klein BJ, Piao L, Xi Y, Rincon-Arano H, Rothbart SB, Peng D, et al. The histone-H3K4-specific demethylase KDM5B binds to its substrate and product through distinct PHD fingers. Cell Rep. 2014;6(2):325-35.
458. Zhang Y, Yang H, Guo X, Rong N, Song Y, Xu Y, et al. The PHD1 finger of KDM5B recognizes unmodified H3K4 during the demethylation of histone H3K4me2/3 by KDM5B. Protein Cell. 2014;5(11):837-50.
459. Alver BH, Kim KH, Lu P, Wang X, Manchester HE, Wang W, et al. The SWI/SNF chromatin remodelling complex is required for maintenance of lineage specific enhancers. Nat Commun. 2017;8:14648.
460. Tolstorukov MY, Sansam CG, Lu P, Koellhoffer EC, Helming KC, Alver BH, et al. Swi/Snf chromatin remodeling/tumor suppressor complex establishes nucleosome occupancy at target promoters. Proc Natl Acad Sci U S A. 2013;110(25):10165-70.
461. Bosch-Presegue L, Raurell-Vila H, Thackray JK, Gonzalez J, Casal C, Kane-Goldsmith N, et al. Mammalian HP1 Isoforms Have Specific Roles in Heterochromatin Structure and Organization. Cell Rep. 2017;21(8):2048-57.
462. Jamieson K, Wiles ET, McNaught KJ, Sidoli S, Leggett N, Shao Y, et al. Loss of HP1 causes depletion of H3K27me3 from facultative heterochromatin and gain of H3K27me2 at constitutive heterochromatin. Genome Res. 2016;26(1):97-107.
463. Shirane K, Miura F, Ito T, Lorincz MC. NSD1-deposited H3K36me2 directs *de novo* methylation in the mouse male germline and counteracts Polycomb-associated silencing. Nat Genet. 2020;52(10):1088-98.
464. Xu Q, Xiang Y, Wang Q, Wang L, Brind'Amour J, Bogutz AB, et al. SETD2 regulates the maternal epigenome, genomic imprinting and embryonic development. Nat Genet. 2019;51(5):844-56.
465. Shao R, Zhang Z, Xu Z, Ouyang H, Wang L, Ouyang H, et al. H3K36 methyltransferase NSD1 regulates chondrocyte differentiation for skeletal development and fracture repair. Bone Res. 2021;9(1):30.
466. Hawass Z, Gad YZ, Ismail S, Khairat R, Fathalla D, Hasan N, et al. Ancestry and pathology in King Tutankhamun's family. JAMA. 2010;303(7):638-47.
467. Ghebreyesus TA. The malaria eradication challenge. Lancet. 2019;394(10203):990-1.
468. An S, Camarillo JM, Huang TY, Li D, Morris JA, Zoltek MA, et al. Histone tail analysis reveals H3K36me2 and H4K16ac as epigenetic signatures of diffuse intrinsic pontine glioma. J Exp Clin Cancer Res. 2020;39(1):261.
469. Sims D, Sudbery I, Ilott NE, Heger A, Ponting CP. Sequencing depth and coverage: key considerations in genomic analyses. Nat Rev Genet. 2014;15(2):121-32.
470. Oyola SO, Otto TD, Gu Y, Maslen G, Manske M, Campino S, et al. Optimizing Illumina next-generation sequencing library preparation for extremely AT-biased genomes. BMC Genomics. 2012;13:1.
471. Jung YL, Luquette LJ, Ho JW, Ferrari F, Tolstorukov M, Minoda A, et al. Impact of sequencing depth in ChIP-seq experiments. Nucleic Acids Res. 2014;42(9):e74.
472. Reader J, Van der Watt ME, Taylor D, Le Manach C, Mittal N, Ottilie S, et al. Multistage and transmission-blocking trageted antimalarials discovered from the open-source MMV Pandemic Response Box. BioRxiv. 2020.